Proceedings of the Autrans seminar on

Modelling and simulation of biological processes in the context of genomics

Edited by: Patrick Amar, François Képès, Victor Norris & Philippe Tracqui

Cover design and book layout: Patrick Amar

"But biotechnology will ultimately and usefully be better served by following the spirit of Eddington, by attempting to provide enough time and intellectual space for those who want to invest themselves in exploration of levels beyond the genome independently of any quick promises for still quicker solutions to extremely complex problems."
Strohman RC (1997) Nature Biotech 15:199

FOREWORD

What are the salient features of the new scientific context within which biological modeling and simulation will evolve from now on ? The global project of high-throughput biology may be summarized as follows. After genome sequencing comes the annotation by 'classical' bioinformatics means. It then becomes important to interpret the annotations, to understand the interactions between biological functions, to predict the outcome of perturbations, while incorporating the results from post-genomics studies (of course, sequencing and annotation do not stop when simulation comes into the picture). At that stage, a tight interplay between model, simulation and bench experimentation is crucial.

This scientific development is necessarily a long-term trend for the following (non exhaustive) reasons.

1. (Post-) genomics is characterized by the massive accumulation of molecular data, allowing in principle to generate predictions of a more quantitative nature than before. Modeling / simulation is the priviledged tool to test quantitative predictions that involve a great number of objects and their interactions. Since we ultimately challenge our understanding of biological phenomena by prediction testing, simulation is going to play a major and increasing role in the progress of the biological sciences.
2. Simulation becomes irreplaceable when it is difficult or impossible to experiment on live material for economical, technical or ethical reasons. The predictive outcome of a successful simulation guides the *in vivo* experimentation, thus reducing its cost ; the *in vivo* experimental results validate or falsify the initial model : this is how the synergistic loop between these two types of experimentation can be primed.
3. Ambitious modeling / simulation attempts stumble on fundamental obstacles, including the lack of proper definitions for such basic biological notions like information, function, organization, and the difficulty of defining the domain of observability / falsifiability of a model. Overcoming these obstacles requires a long-term effort.
4. The now recognized relevance of mechanical processes in the control of biological functions at different levels (DNA accessibility, endomembrane morphogenesis, signal mechanotransduction, cytoskeletal and cell adhesion remodeling...) can hardly be analysed without considering physical models and associated simulations based on mathematical descriptions.

The undersigned are scientists from various (geographic and scientific) areas who started in January 2001 to face these challenges in a stimulating year-round workshop that was initiated and supported by genopole®. Some of us were initially more familiar with the field of modeling / simulation, while others were involved in various aspects of (post-) genomics. After 14 months of work, we held a small multidisciplinary seminar in Autrans, which was open to everybody. For us, it was an opportunity to listen to other viewpoints and to improve our work following suggestions, reactions and criticisms. In the course of, and beyond the scientific program, this seminar was a permanent (albeit mostly from 8 am to 1 am) forum for informally exchanging ideas.

We are glad to welcome to our year-round workshop several participants who expressed their interest in our endeavors.

Patrick Amar, Pascal Ballet, Gilles Bernot, Paul Bourgine, Alessandra Carbone, Franck Delaplace, Jean-Marc Delosme, Maurice Demarty, Jean-Louis Giavitto, Christophe Godin, Misha Gromov, Janine Guespin, Roberto Incitti, François Képès, Olivier Michel, Victor Norris, Alain Rambourg, Michel Thellier, Philippe Tracqui, Abdallah Zemirline.

Acknowledgments

We would like to thank the seminar participants, who have contributed in a way or another to this book. It gathers overviews of the talks, discussions and roundtables, original articles contributed by speakers, abstracts from attendees, and courses proposed by the epigenesis group to review or illustrate matters related to the scientific topics of the seminar.

Of course, the organization team would like to thank all the staff of *l'Escandille* for the very good conditions we have found during the seminar.

Special thanks go to Hélène Pollard and Paul Soler of Genopole who helped us a lot during the elaboration of this book.

We would also like to thank the sponsors of this seminar for making it possible for all the participants to share their enthusiasm and ideas in such a constructive way. They were IMPG, Genopole, EDIV, IMAG, and the SFBT.

The editors
Patrick Amar, François Képès, Vic Norris and Philippe Tracqui

List of attendees

(in alphabetic order)

Marie Aimar
Patrick Amar
Pierre Auger
Pascal Ballet
Vincent Bassano
Gilles Bernot
Bruno Bost
Yves Bouligand
Georgia Bralovatz-Meimon
David Campard
Christophe Chassagnole
Athel Cornish-Bowden
Arnaud Courtois
Gilles Curien
Vincent Danos
Laurent David
Jean-Paul Delahaye
Franck Delaplace
Jean-Marc Delosme
Maurice Demarty
Jacques Demongeot
Damien Eveillard
Sophie Féréol
Julie Fiévet
Jean-Baptiste Fournier
Vincent Fromion
Jean-Louis Giavitto
Christophe Godin
Janine Guespin-Michel
Roberto Incitti
Antoine Joulie
Daniel Kahn
Marcelline Kaufman
François Képès
Yannick Kergosien
Benjamin Leblanc
Michel Leborgne
Guillaume Legent
Jean-Pierre Mazat
Pierre Maziere
Aurélien Mazurie
Olivier Michel
Franck Molina
René Natowicz
Victor Norris
Elisabeth Pecou-Gambaudo
Emmanuelle Planus
Jacques Prost
Derek Raine
Nancie Reymond
Jacques Ricard
Camille Ripoll
Magali Roux-Rouquié
Vincent Schächter
Christophe Soulé
Michel Thellier
Hélène Touzet
Philippe Tracqui
Laurent Trilling
Bernard Vandenbunder
Jean-Claude Vincent
Adballah Zemirline

Contents

Hyperstructures

Synthesis proposed by Janine Guespin-Michel

I chose to present the discussions of this workshop, not as a report of the events but as a presentation of the topics, namely: what are hyperstructures? What is the aim of this concept? What is the use of simulating hyperstructues?
The drawback of this choice is that it does not show the evolution of the discussion during the 2 hours of the workshop, from a rather critical attitude toward a more positive one.

The propositions of the organisers of the workshop (Michel Thellier and Vic Norris) are in italics

I. What are hyperstructures ?

They appear during the operation of a particular cellular function (when this functioning requires association between macromolecules), and as a consequence of it, for instance as changes in affinity between the molecules that stabilise their association as long as the function is required.

They are most often of a heterogeneous nature and in addition to proteins and lipids may also involve DNA, RNA, ions etc..

Many of them are dissipative structures that only exist during active, energy-consuming functioning. But Vic Norris proposes that they include some of the stable cellular substructures

Examples:

-protein/protein: an enzymatic complex has been described by J. Ricard, the structure of which exists during its functioning but lasts a little longer

-proteins /lipids: the hyperstructure which consists in the PEP phsphorylating glucose permease, might also involve the glycolytic enzymes thus leading to channelling. The bacterial chemiotactic apparatus (Denniss Bray)

-protein/lipid/DNA : bacterial cell division structures

-Proteins/lipids/DNA/RNA: transertion structures in bacteria.

Structures that are more or less stable depending on the species: The Golgi apparatus.

Stable structures: mitochondrion (or more exactly, hyperstructures within the mitochonrion mediated for example by calcium binding to cardiolipin).

Discussion;

Some mathematicians wondered whether the word " structure " was really appropriate, since, in mathematics it was successfully replaced by the word " category". (A discussion ensued, that showed that so far this does not seem to be pertinent in biology where the word " structure " seems satisfactory)

Questions: Are hyperstructures purely material, or might they be virtual such as metabolic networks (*Spatial co-localisation is essential)*

Is there a level of generalisation?

Is there evidence for a glycolysis hyperstructure ?

Since these structures are often short-lived, could they include intermediate metabolic steps?

Is it the material aspect (structure) or their purpose (function) that is the pertinent level to characterise them? (*The interesting point is precisely that these two properties are interconnected, and cannot be dissociated*)

Do time constants impose hierarchies? How can you account for the existence of, say three time scales in chemiotactism? Were thermodynamic studies performed ?

Critics. This concept groups structures of much too widely different natures, it is too much heterogeneous (stable/unstable, different sizes, different time scales).

Proposals and agreements.

Wouldn't it be simpler to call them dissipative structures?

Cells from the immune system form aggregate through chemical reactions that mediate the scale change. They may be a new example of hyperstructures in which chemical modifications and not only affinity changes are involved in the formation of the structure.

Thermodynamic studies have been performed for the mitotic spindle, which is a very good example of a hyperstructure.

II. What is the aim of the hyperstructure concept ?

This notion allows us to :

- handle a biological level intermediate between the molecule and the cell

- focus on the importance of the function for the structure (in contrast to the general point of view that stresses the reverse relation).

- connect approaches most often dissociated, between fields in biology, (genome, proteins/lipid affinities, various networks) or even between biology and other scientific fields (liquid crystals, tensegrity ...)

Discussion:

Critics:

-There is a lack of experimental work in this field, mainly because experimental work is not even possible in most cases. *(A reply is given in the next section.*

-Too many unrelated ideas. (For instance the liquid crystals are only interesting in biology for studying DNA through very nice experimental devices. (*Vic Norris strongly advocated the broader interest of liquid crystals).*

Proposals and agreements

This concept emphasises several new and important aspects:

-The importance of taking into account three-dimensional space,

-The importance of the dynamics between construction and destruction.

-The importance of being aware of the possible multiplicity of functions for a single protein, which should have consequences in terms of evolution theory and of localisation.

-In addition it stresses the importance of working hypotheses, in contrast to more than 10 years of data accumulation without explicit hypotheses

The cell cycle in E.coli is a good example of what the hyperstructure concept can contribute. Although everything seems known concerning this bacterium, whose genome has been sequenced for some time, it is still impossible to understand the mechanisms underlying something of such paramount importance as the cell cycle. None of the explanations offered so far are satisfactory. Why is this? Couldn't it be that current explanations sought arise from

a quest for THE miracle protein? What if, instead, the explanation were in terms of an interaction between dynamical structures[1]?

A posteriori the author of the synthesis has taken advantage of her position to add one more argument: The chemiosmotic gradient was discovered by Mitchell when the whole community in the field was looking for the miracle protein. Mitchell showed that the answer was a proton flux (I do not know whether a hyperstructure can be involved). This explanation was only accepted after a long history of rejections, mainly from editorial boards. (Mitchell had to edit his own journal).

III What is the use of simulating hyperstructures?

As noticed before, the concept of hyperstructure is rather complicated and often not easily amenable to experimental testing. Therefore, in silico experiments are needed to allow investigation of some of their properties, and even to test whether the concept is coherent. An example is the 3D model created by Lois Le Sceller[2] which shows that it is possible to find simple general rules to generate hyperstructures whose existence and stability depend on a flux of material.
Models may also prompt new ideas. (Indeed the very idea of a level of hyperstructures arose from the combination of a biological enigma and a very simple simulation of structure generation by a multi-agents model)

Discussion.

-When the model is not amenable to experimental tests, one must be very cautious in choosing the formalism to avoid generating automatically the expected results.

-Multi-agent models may be best suited for the purpose of simulating hyperstructures.

Nowadays, hypotheses tend to be limited by the technology available. In the case where the hyperstructure postulated is not readily amenable to experimentation, simulation may permit the emergence of unexpected properties characteristic of the living system. Three steps may be proposed: formulation of the hypothesis (the hyperstructure); simulation, that allows the multiple consequences of the hypothesis to be revealed and that may suggest novel experiments; performing these experiments.

---

[1] NORRIS V, ALEXANDRE S, BOULIGAND Y, CELLIER D, DEMARTY M, GREHAN G, GOUESBET G, GUESPIN J, INSINNA E, LE SCELLER L, MAHEU B, MONNIER C, GRANT N, ONODA T, ORANGE N, OSHIMA A, PICTON L, POLAERT H, RIPOLL C, THELLIER M, VALLETON JM, VERDUS MC, VINCENT JC, WHITE G, WIGGINS P. Hypothesis: hyperstructures regulate bacterial structure and the cell cycle. Biochimie 81: 915-920.

[2] Le SCELLER, L., RIPOLLl, C., DEMARTY, M., CABIN-FLAMAND, A., NYSTROM, T.,SAIER Jnr, M. and NORRIS, V. Modelling bacterial hyperstructures with cellular automata. Interjournal of Complex Systems : MS 366.

Endomembranes

Synthesis proposed by Roberto Incitti

The starting point of the "endomembranes" session is a model for the morpho-genesis and the function of the Golgi apparatus, based on one experimental approach of A. Rambourg and F. Képès. The model was presented and discussed as a paradigm of a dynamical structure in the context of molecular cell biology. A molecular and a physico-chemical model was also presented to explain the tubulization and the vesiculation that is observed.

I. The morphological model

The structures making up the secretory pathway had, until recently, been observed only in a static way on two dimensional projections. Stereoscopic techniques, consisting in taking two micrographs of the object by two different angles and at different stages, allow a three dimensional and dynamical view of the structure. In the following, we summarize the observations that were made possible by this techniques, in two animal and one yeast cases, the former with regard to three mutants: at a first stage, the mammalian Golgi apparatus appears as consisting of a pile of 8/9 thin saccules. Those saccules undergo a fenestration, starting from the first one, which leads to the formation of a tubular network that finally breaks up to form vesicular granules containing the secretory cargo.

One further examination is allowed by the use of yeast temperature-sensitive mutants: when set at suitable temperatures, they loose the wild type phenotype, and accumulate various types of structures (small vesicles, membranous sheets, tubules, secretory granules, etc.) that do not follow the dynamics described above. In particular, the secretion of granules can be blocked. In one case one can also observe that the structure itself disappears, if no secretory cargo is transported. This suggests that the Golgi apparatus is not a permanent structure, but it is continuously renewed and that there is a causal link between content sorting and container formation. This defines the Golgi apparatus as a dissipative structure.

II. The molecular model

The molecular model is intended to explain the tubulization of the saccules which leads to vesiculation, and, ultimately, to secretion granules. Is is based on a cytoplasmic protein (Sar1), that is known to induce tubulization of membrances, and on a transmembrane protein (Sec12). The model proposes that by random fluctuation Sec12 gathers a hypercritical concentration at certain spots and then recruits Sar1, giving a complex capable of recruiting the secretory cargo on one side of the membrane and a cytoplasmic protein (COPII) on one other side. COPII polymerizes to form a coat which exerts a mechano-chemical bending force leading eventually to the breaking up of a vesicule.

III. Extensions

Some further study is proposed that could validate and extend the model:

1. In S. cerevisiae, the site of ER exit changes from one budding event to the other, unlike in Pichia pastoris, where one observes that the Golgi elements tend to pile up where they are formed. This may be explained by the sequestration of sec12 and by the viscosity of the cytoplasm.

2. Look for the possible existence of a matrix protein that gives to the Golgi apparatus some cohesiveness, as is suggested by the fact that, in plants, remnants of the Golgi apparatus are observed when the secretory function is prevented by various means, as in one of the observations on mutants described above.
3. A typical phenomenon of animal cell is the aggregation of many Golgi apparatus on a few giant ones. One possible explanation is that they stack around a microtubule.

Finally, an interpretation of those three phenomena can be given in terms of an evolution scenario.

IV. The physico-chemical model

The above molecular model is similar to the known mechanism of the clathrin-mediated vesciculation in endocytocis, with the dynamin playing the role of Sec12 and the clathrin that of COPII. The migration of the dynamin across the membranes under certain conditions has been modeled in the paper of J.-B. Fournier et al. that was presented by J.-B. Fournier at the conference.

The membrane is modelled by a plane surface, in which a sufficient amount of wedges are inserted, that locally exert an anisotropic (i.e. varying w.r.t. the direction) inclusion. The surface presents a budding invagination and the wedges are free to diffuse across the surface. The authors find that the local curvature induced by the wedges causes the exertion of long range elastic forces among the wedges. By carrying out the simulation, they find a regime in which the wedges form a ring around the budding invagination, which is reminiscent of the the process of vesicle scission. F. K\'ep\`es pointed out that this could be the case of Sar1, that has three hydrophobic legs that may help this protein to stay fixed on the membrane and preventing from crossing it. It seems verifiable whether this inclusion is anisotropic.

The above model is expected to capture the long-range elastic interactions among the membrane inclusions, and to yield accurate interactions for separations as small as about three times the particles size, and for protein host of a size comparable to the thickness of the membrane. This kind of simulation can also be carried out on spherical and a cylindrical surface. The authors also describe the simplifications made in the model.

The talk of J. Prost pointed out another possible mechanism for the vesiculation and the bending of the membranes. It is known that the latter can be caused not only by self-assembly of moleculat coats, as in the clathrin-mediated vesiculation, but also by the action of microtubules or that can pull the membranes. The latter may take place by the action of Sar1, which is capable of recruiting nanotubules, or by a molecular motor.

During the discussion at the conference, it was clearly stated that there are other possible mechanisms that may explain the morphogenesis observed in the Golgi apparatus. It is known, for example, that asymmetric bilayers can easily undergo a bending process, due to forces depending on local curvature. It those forces can accentuate the curvature, a sufficiently large random fluctuation can start a process of bending. Moreover, the morphogenesis can be explained by several mechanisms, each intervening at a specific time. To this effect, it would be interesting to know the time scale of the migration described in the physico-chemical model presented by J.-B. Fournier. J.-M. Delosme suggested that an order of magnitude may suffice to have an idea of the range of validity of this model in the morphogenesis of the Golgi apparatus.

On models and experiments in molecular biology

An account by Jean-Marc Delosme

During the discussion led by members of the workgroup on "observability", a key motivation for their endeavor appeared clearly. Some words, such as "epigenesis", cover different meanings within the community of biologists. To some, epigenesis involves DNA methylation and other chemical mechanisms, while, to others, it has a broader meaning. Thus, staying with the epigenesis illustration, a particular "epigenetic" hypothesis for the explanation of the transmission of a modification from a cell to its progeny should be stated in a formal way in order to be properly understood by the community as a whole. Indeed, the hypothesis would then be understood independently of the meaning of the word "epigenetic".

Another reason for getting out of empiricism and employing a formalism is the complexity of the hypothesis. Refering to the case study in the paper by Bernot, Guespin *et al.*., the hypothesis that there may be populations of *pseudomonas aeruginosa* bacteria that keep on producing mucus outside the lungs of patients because of an epigenetic mutation cannot be stated just that simply. A formalism must be selected and a model of the object under study must be constructed using that formalism.

A model with parameters varying continuously and that could be tweaked to fit observations does not appear appropriate for the study of epigenesis. Lack of numerical accuracy of observations, variability within populations, and, more fundamentally, genericity in a mathematical sense (*e.g.* in affine geometry, 3 points are in generic position if they do not lie on a straight line: a notion that applies *mutatis mutandis* to non-linear dynamical systems) are considerations that lead to considering models within a discrete formalism. Physicists have devised generic approaches, for instance by identifying the symmetries and the relevant variables (*e.g.* rules for identifying the slow variables in generalized hydrodynamics), such that the models constructed using these approaches capture the phenonena at a level that is not too fine (*e.g.* mesoscopic *vs.* microscopic) . The use of a generic approach is the physicist:s way of selecting the proper formalism within which to construct a model for the problem at hand.

The formalism (or underlying theory) used for the case study is the one presented by Marcelline Kaufman in her *Logical Analysis of Regulatory Networks in Terms of Feedback Circuits* paper. The formalism uses multivalued logical variables and, in addition, a simple temporal logic. It accounts for changes of values of variables in an asynchronous fashion so that, although the models constructed using it are not continuous, they still capture the essential phenomenon of hysteresis, hence the memory effect in dynamical systems with multiple stable states. The model constructed for the case study using this formalism is presented schematically in Fig. 1.b of the paper by Bernot, Guespin *et al.* The model may be viewed as a means of describing a complex hypothesis (of course the hypothesis is not very complex in this example but the approach employed has been devised so that it can handle complex hypotheses in a similar fashion).

A model consists in modes of operation, *i.e.* modes of interaction or relations between components or parameters whose number is typically sufficiently large that one cannot readily figure out its behaviors. The model is not the whole story, and one does not merely want to validate the model. Since the objective of this type of modeling is understanding, one actually wants to validate (or attempt to refute, following Karl Popper) not only the model but

also statements about model behavior. These statements (hypotheses) combined with the model make up a (complex) hypothesis; it is this pair that will be submitted to experiments. Separating model and statements about the model (such as feedback loops in the model for the case study and a statement about which loop is functional) makes things cleaner, albeit all are hypotheses and could be merged into the model.

The model proposes some explanations about behaviors—which come out of modes of operation—and statements about its behavior are expressed as properties (hypotheses about the model, *i.e.* about modes of operation). Formally, a model is a semantics, *i.e.* a mathematical description of some modes of operation, and properties about behavior coming out of modes of operation. belong to syntax, which indicates what one is allowed to write about a model. A well-formed property is a property that one is allowed to write. In addition a language enables to express the set of what can be asserted and a symbol links model—an interpretation of the language—and properties in order to express when a model satisfies a set of properties. A well-formed property may be false in that the model does not satisfy it.

In general there are experimental limits in that, even with an infinity of experiments, some formulas or properties cannot be refuted (or, consequently, validated). On one hand, one may not be able to bring the model in some desired state in order to test a property this is the notion of "operability" (basically the notion of "controllability" in systems theory). On the other hand, for a variety of reasons, one may not be able to observe enough about a biological system to conclude immediately if a property is true or false; this is the notion of "observability". To be able to refute a property, one must be able to construct experiments that provide enough information to be able to say if it is true or false. When this can be done, *i.e.* have both operability and observability of a property, the property is simply said to be observable.

Four sets may be distinguished:
P – the set of properties that are possible under the working hypotheses (a set that is restricted according to which problem one focusses on);
O – the set of properties directly observable—without reasoning—on the biological object that the model is supposed to model (a property for which an experiment that would allow its observation has not been devised yet does not belong to O);
M – the set of properties of the mathematical model itself, *i.e.* the properties that are true for the model, properties that may or may not belong to O;
S – the set of statements (formulas) about the behavior of the model that are to be validated, statements that may or may not be observable.
The model M itself may be incoherent, then any property may be proved to be true for the model and then M covers all of P. Of course only a coherent model is of any interest. Even for a coherent model some statements may not belong to M (*i.e.* M does not satisfy the property; the statement is false in M); these are internal contradictions.

Assume a property in S (a consequence of statements in S) that also belongs to O but does not belong to M. This provides a refutation, showing an incoherence between the statement and the model, since the property is directly observable by at least one experiment and is not a property of the model.
Assume there is no such property. There may remain some property in S that does not belong to M. Since the property does not belong to O, it is not possible to see by an experiment that it is incoherent with the model. Hence statements can be made about the model for which one will never be able to devise an experiment in order to show that they are

false in M (recall that, following Popper, in order to validate a model one tries as hard as possible to refute it). This is a sign that the formalism is too rich, that too many statements can be made about the model.

Continuing with the considerations about the four sets, three things about a model are to be considered:
- Do the observable properties of the model allow to imply (or falsify) the statements that are made? Otherwise, if one cannot devise an experiment to try to falsify a property of the model, that modeling activity should not be considered scientific. Note that to falsify a statement is not a bad news as far as the advancement of science is concerned since this enables one to improve the model.
- Do the observable properties of the model imply the properties of the model? Restating the question in Popper's way, if a property of the model is false is there an observable experiment that will show that indeed that property is false? If yes, this means that the formalism is not too rich.
- Does the model satisfy Occam's razor? In other words, is the model minimal with respect to the properties that can be expressed about the model? In general one obtains a model—within an equivalence class of models that have the same properties—that cannot be said to be minimal. However, using a proper definition of the observational equivalence of the models, one may be able to say that it is representative of the equivalence class.

Returning to the *pseudomonas aeruginosa* bacteria case study, a statement about a particular epigenetic modification is the hypothesis J. Guespin tries, following a Popperian approach, to falsify. Referring to the paper developing this example, although there is a positive feedback loop in the model this is only a necessary condition for the existence of a multistationarity that could result in that epigenetic modification, hence all the work remains to be done in order to devise an experiment, if not several, that could refute that hypothesis.
Formally, the statement to be validated is that if at some time $x = 2$, then, later, in a strict future, $x = 2$. This property is true within the mathematical model, as shown by M. Kaufman and J. Guespin, hence here S is included in M.
The only operability available is to boost x. The observability consists in checking if $z = 1$.
To validate the hypothesis, an experiment consists in boosting x until $x = 2$, waiting, and checking if $z = 1$ (because $x = 2$ is not directly observable). Where is Popper here? Imagine an experiment where $x = 0$ and look at what happens, first the result is known (standard bacteria outside the lung, stay in the [0 0] state), second, and more important, this experiment cannot possibly falsify the formula. Indeed, to succeed in falsifying a formula "A implies B", the precondition A must be true (and then one can try to falsify B), hence here we need to have $x = 2$ to have any chance to falsify the model. Thus Popper was here to show that we needed to have $x = 2$ in our experiment; hence that no other experiment than "$x = 2$" could have any interest.
Here only one experiment is needed to prove the property. This is because the precondition has no free variables; it is unique and only one experiment (if it succeeds) makes it true. If a precondition has some free variables that can take any value, an infinity of experiments could be needed to find all the cases for which the precondition is true—since it may be that one of them falsifies the formula—and thus one cannot prove that the formula is true. While one can prove when the number of experiments is finite that a formula is true, it is in the more general case, with free variables, that the proposed approach, inspired by methods in programming and software design, will show its real power. Indeed there exist strategies in software testing (such as "unfolding") that increase the probability of falsifying a formula through a finite number of experiments.

Organisation Group

Proposed by Franck Delaplace

The goal of the organisation group is to determine applied an theoretical tools for genomic analysis. Two kinds of direction has been shown : simulation and analysis. Simulation corresponds to a corpus of tools which simulate the behavior of biological process. Analysis corresponds to tools for the finding of structural and dynamical properties from a topological representation.

Members of the group have presented works achieved in the group.

- Jean Louis Giavitto has summarized the work of the group in his talk.
- Christophe Godin has presented tools for the simulation of plants growth.
- Franck Molina has presented work on the definition of a language dedicated to the design of ontologies.
- Franck Delaplace has presented works for the analysis of emergent properties applied to biological networks.

Talks and the discussion puts the emphasis on the relationships between models and computational frameworks.

- Nowadays, the definition of a biological model requires to represent a large amount of relationships between components. Finding appropriate languages to deal with biological complexity appear to be a challenging problem.
- Topological analysis of biological networks to find characteristic patterns also appear to be an important trend.

Conference synthesis

Proposed by Victor Norris.

The talks at the conference can be placed into one of four categories – physico-chemical approaches, metabolic modelling, interaction networks and miscellaneous – although of course no categorisation does them justice.

The talks of Jacques Prost, Jean-Baptiste Fournier, Camille Ripoll and Yves Bouligand had physico-chemical approaches to the dynamics of intracellular structures as a common theme. Different sorts of modelling and simulation also played a large part in their work. Prost brought together physics and biology in explaining how bacteria such as *Listeria monocytogenes* travel within and between human cells by locally polymerising actin using a bacterial protein, ActA. He showed how ActA-coated beads could move in a similar way and discussed symmetry-breaking, persistence-lengths and the squeezing of cherry-stones to make them fly. It would seem that *Listeria* has a lot to teach us about the operation of the actin cytoskeleton. On a different tack, he showed how motor proteins travelling along microtubules could tug tubes of lipids. One might imagine that this dynamic plumbing is crucial for intracellular transport.

Fournier has developed a physico-chemical model based on long-range elastic interactions to explore how the curvature of membranes by proteins influences their distribution. He applied this numerical model to the recruitment of dynamins by clathrin coats during endocytosis. There is a general principle here that may underpin the behaviour of many proteins that are integral or peripheral to the membrane and, in my view, the model may be relevant to other fundamental events involving membrane curvature such as cell division.

Ripoll applied physico-chemical theories about the condensation of counter-ions onto linear, negatively charged, cytoskeletal structures to explain a whole range of disparate findings about calcium control of cellular processes. He proposed that condensation and decondensation of ions orchestrate kinases and phosphatases which in turn feed back on structures. These structures might include hyperstructures (extended assemblies of different species of molecules that serve a cellular function) in which case the mechanism would be a powerful integrative one. I wonder if the model might be usefully married to tensegrity to relate mechanical deformations to gene expression or explain the dramatic transitions that occur during the eukaryotic cell cycle.

Bouligand took us through the history of liquid crystals in biology and showed us how cholesteric liquid crystals form *in vitro* and *in vivo*. He discussed how liquid crystals in DNA may affect the transcription of genes and the replication and partitioning of chromosomes. Planar twisted or cylindrical twisted cholesteric phases may be the equilibrium state of chromosomes on which DNA dynamics are based. One of the many questions his talk raised is whether genome sequences could be used to determine which regions are in a liquid crystalline state.

The take-home message from this group of speakers is that physico-chemical principles underpin intracellular events. In the theatre of the cell, these principles provide the script that a host of molecular actors have learnt over the aeons to interpret.

The next group, Athel Cornish-Bowden, Jean-Pierre Mazat, Christophe Chassagnole and Julie Fievret, focused on metabolism – and the necessity of using computer modelling. Metabolism is what cells do, Cornish-Bowden reminded us, and attempts to exploit genomic data that ignore

metabolism are doomed. African sleeping sickness is caused by *Trypanosoma brucei* which has its glycolytic enzymes compartmentalised in a glycosome. To identify targets for drug therapy, he used metabolic simulations to determine which of the glycosomal enzymes would be good candidates and which would be useless. (Since these enzymes are co-localised, it is conceivable that their structure-forming properties might also be targeted.)

Mazat showed how computer-modelling might be used in pursuit of the holy grail of a virtual mitochondrion. The first steps involve using the kinetic parameters of enzymes to predict metabolic fluxes within mitochondria which vary according to cell type. Like Cornish-Bowden, Mazat used metabolic control analysis to exploit experimental data by computer-modelling. This can only lead to a better understanding of mitochondrial diseases. Many mitochondrial DNAs have now been sequenced and he held out the prospect of deriving metabolic maps from genetic ones. (Perhaps a key step in this will turn out to be the self-association properties of the mitochondrial enzymes and the structuring properties of transcription and translation within the mitochondrion?)

Chassagnole also used metabolic control analysis in modelling how pollutants such as heavy metals affect the flux through the threonine pathway. He determined the control points and showed that the multiple effects of these pollutants can only be understood by modelling the whole pathway.

Fievret gave a different dimension to metabolism by introducing constraints due to molecular crowding and the cost of protein synthesis. She introduced the concept of combined response coefficient which takes into account the necessity for cells to evolve a particular distribution of enzymes to optimise the flux through a given pathway. An awareness of the evolutionary pressures on the entire system, in which a pathway is embedded, is clearly important. Perhaps, these pressures on enzymes are more than just to optimise flows?

In these presentations of metabolic modelling, there was little joy for proponents of the genome or proteome as the source of all wisdom – the emphasis was placed on control coefficients and on an integrative understanding of pathways. That said, there was not much joy either for *aficionados* of enzyme superstructures or hyperstructures. One possibility is that hyperstructures are important in the overall dynamics of the cell rather than simply in the maximisation of fluxes.

Cellular life is all about patterns of interactions. Interpretation of these patterns were proposed by Derek Raine, Jacques Ricard, Marcelline Kaufman and Jacques Demongeot. Raine gave us the history of power laws, self-organised criticality and small world networks in metabolism and gene regulation. He derived a parameter related to information entropy to assess the complexity of a network based on the ratio of the clustering or cliquishness to the average path-length between two elements. He examined gene expression during the cell cycle of *Caulobacter crescentus* in terms of this complexity parameter. He also speculated about how these concepts might lead to a reformulation of intensive and extensive variables.

Ricard told us more about information. He pointed out that metabolic networks may contain more information than genetic ones. He argued that in metabolic networks the nodes could usefully be considered to be the reactions themselves. Then, beginning with Shannon's theory of information, he derived expressions for metabolic networks in which the values correspond to either integrated systems or emergent systems.

Kaufman took us through the logical analysis method for determining the dynamics of regulatory networks that include gene-protein networks and protein-protein interaction networks. This essentially Boolean approach has been developed to allow asynchronous events in a network to be analysed. This approach permits multi-stationarity states and periodicity to be predicted relatively easily from complex experimental data.

Demongeot continued in the vein of logical analysis by discussing interaction matrices which represent how, for example, one gene regulates another. He reviewed Stuart Kauffman's work on the connectivity of systems of logic gates and its relevance to multi-stationarity and periodicity. He then raised the problem of the relationship between the number of steady states of the system and the number of regulatory circuits in the interaction matrix. Whilst these analytical techniques should prove suitable for interpreting the wealth of transcriptome data now available, Demongeot showed us that these data are far from perfect and presented a statistical method that helps improve them.

The preceding four talks were all of relevance to the interactions occurring in large intracellular networks, an understanding of which is critical if we are to exploit genome sequencing and the transcriptome. The next series of talks were more general. Pierre Auger began by arguing that a progression up through the levels in biology (starting with the atomic level and ending with the ecosystem) is accompanied by a reduction in the time required for the units to interact and by an increase in the size of the units. This allowed him to apply an aggregation method to hierarchical biological systems and so obtain a simple model in which only a few global variables are important.

Yannick Kergosien explored the relationship between adaptation and branching using a simple robust algorithm that is of general relevance to epigenesis or to other situations where multi-dimensional tree graphs are drawn. He showed us how repeated, abortive attempts at branching might precede a major branch point. (It might be wondered whether such branching occurs in the case of gene expression within a population of bacterial cells where divergent patterns of expression could favour survival of the population.)

Finally, Vincent Schachter gave us a salutary tour of the problems associated with trying to make sense of biological data. These ranged from serious problems with the quality of the experimental data to the inadequacy or limited applicability of models. What Schachter's talk highlighted the importance of developing better and more integrative models and simulation techniques. There was no shortage of candidate methods of simulation presented at the meeting on different occasions by the multi-disciplinary audience. These ranged from multi-agent systems and cellular automata to L-systems, P-systems, MGS and SiliCell.

I took away a couple of messages. Firstly, to be successful in exploiting the results offered by the investment in the genome, a truly integrative modelling has to take into account physical chemistry of the sort presented at the conference. Secondly, the gap between biological and physical approaches to complex systems is being bridged. New concepts are being generated and those interested in integrative simulation now have the exciting task of learning to exploit them.

Dynamin recruitment by clathrin coats: a physical step?

J.-B. Fournier* and P.-G. Dommersnes†

Laboratoire de Physico-Chimie Théorique and FR CNRS 2438 "Matière et Systèmes Complexes", ESPCI, 10 rue Vauquelin, F-75231 Paris cedex 05, France

P. Galatola

LBHP, Université Paris 7—Denis Diderot and FR CNRS 2438 "Matière et Systèmes Complexes", Case 7056, 2 place Jussieu, F-75251 Paris cedex 05, France

Abstract – Recent structural findings have shown that dynamin, a cytosol protein playing a key-role in clathrin-mediated endocytosis, inserts partly within the lipid bilayer and tends to self-assemble around lipid tubules. Taking into account these observations, we make the hypothesis that individual membrane inserted dynamins imprint a local cylindrical curvature to the membrane. This imprint may give rise to long-range mechanical forces mediated by the elasticity of the membrane. Calculating the resulting many-body interaction between a collection of inserted dynamins and a membrane bud, we find a regime in which the dynamins are elastically recruited by the bud to form a collar around its neck, which is reminiscent of the actual process preempting vesicle scission. This physical mechanism might therefore be implied in the recruitment of dynamins by clathrin coats.

endocytosis / clathrin / dynamin / membrane inclusions interactions

Résumé – **Une étape physique dans le recrutement des dynamines par les capsules de clathrine ?** Des donnés structurales récentes ont montré que la dynamine, une protéine du cytosol qui joue un rôle clé dans l'endocytose clathrine-dépendante, s'insère partiellement dans la bicouche membranaire et tend à s'auto-assembler autour de tubules lipidiques. En tenant compte de ces observations, nous faisons l'hypothèse que les dynamines impriment localement une courbure cylindrique dans la membrane. Cette empreinte peut engendrer des forces élastiques de longue portée. En calculant l'interaction multi-corps entre un ensemble de dynamines insérées dans la membrane et une capsule endocytotique, nous trouvons un régime dans lequel les dynamines sont recrutées élastiquement par la capsule pour former un collier autour de son cou, ce qui rappelle le processus précédant la scission des vésicules d'endocytose. Ce mécanisme physique pourrait donc être impliqué dans le recrutement des dynamines par les capsules de clathrine.

endocytose / clathrine / dynamine / interactions entre inclusions membranaires

* Author for correspondence (jbf@turner.pct.espci.fr)

† Present address: Institutt for fysikk, Kontor D-5 184. NTNU. N-7491 Trondheim. Norway.

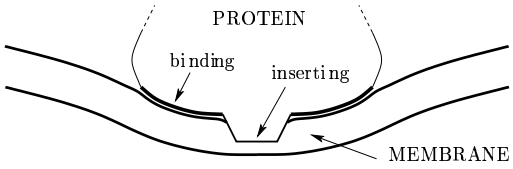

FIG. 1: Schematic representation of a cytosol protein partly inserting within a lipid bilayer and inducing a local membrane curvature via a binding region.

I. Introduction

In eukaryotic cells, membranes of different organelles are functionally connected to each other via vesicular transport. Formation of transport vesicles from invaginated buds of the plasma membrane is called *endocytosis* [1]. In clathrin-mediated vesiculation, vesicle formation starts with the assembly on the donor membrane of a highly organized "coat" of clathrins [2], which acts both to shape the membrane into a bud and to select cargo proteins [3–7]. The mechanism by which an invaginated clathrin-coated bud is converted to a vesicle (scission) involves the action of a cytoplasmic GTPase protein called *dynamin* [6, 8]. Dynamins form oligomeric rings at the neck of deeply invaginated membrane buds and induce scission [9, 10]. How exactly dynamin is recruited and how the scission actually occurs remains unclear [11, 12]. In this paper we propose that dynamin recruitment by clathrin coats could be driven by long-ranged *physical* forces mediated by the membrane curvature elasticity.

Cryo-electron microscopy has recently revealed the detailed structure of the clathrin coats at 21 Å resolution [2]. Clathrin units, also called "triskelions", have a star-like structure with three legs. Initially solubilized into the cytoplasmic fluid, they self-assemble onto the membrane surface into a curved, two-dimensional solid scaffold. The latter is a honeycomb made of hexagons and pentagons (geometrically providing the curvature) the sides of which are built by the overlapping legs of the clathrin triskelions. In the plasma membrane, clathrins usually interact with "adaptor" transmembrane proteins, which also serve to select cargo proteins. However it has been shown that clathrin coats can readily self-assemble onto protein-free liposomes [13, 14].

Dynamin is known to be solubilized in the cytosol as tetramers, and to aggregate in low-salt buffers into rings and spirals [9]. Dynamin also self-assembles onto lipid bilayers, forming helically striated tubules that resemble the necks of invaginated buds (tube diameter $\simeq 50\,\mathrm{nm}$) [10]. Addition of GTP induces morphological changes: either the tubules constrict and break [15], or the dynamin spiral elongates [16]. These findings suggest that the scission of clathrin-coated buds is produced by a mechanochemical action [16, 17].

At the earlier stages of the budding process, dynamins already strongly interact with bilayer membranes. Indeed, *in vivo* studies showed that dynamin binds acidic phospholipids in a way that is essential to its ability to form oligomeric rings on invaginated buds [18–22]. Using a model lipid monolayer spread at the air-water interface, it was shown that dynamins actually penetrate within the acyl region of the membrane lipids [23]. This finding was recently confirmed by the three-dimensional reconstruction of the dynamin structure by cryo-electron microscopy at 20 Å resolution [24]: dynamins form T-shaped dimers the "leg" of which inserts partly into the outer lipid leaflet.

It was long ago suggested [25, 26] that particles inserted within bilayers should feel long-range interactions mediated by the elasticity of the membrane. Indeed, a protein penetrating within a bilayer and binding its lipids—such as dynamin—may in general produce a local membrane curvature (see Fig. 1). Because of the very nature of the curvature elasticity of fluid membranes, this deformation

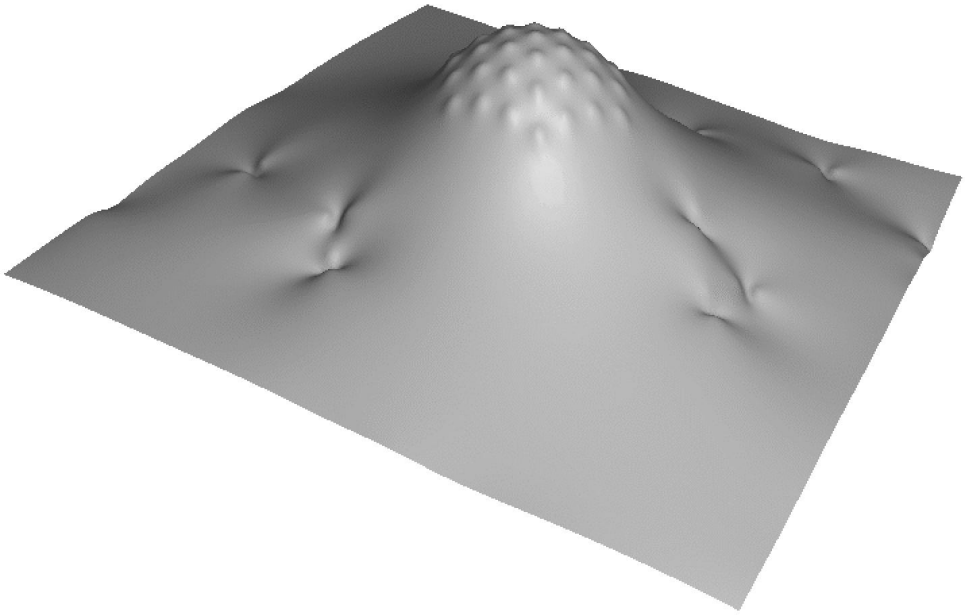

FIG. 2: Piece of a model membrane showing a clathrin coated bud and the imprints of inserted dynamins.

relaxes quite slowly away from its source, and the presence of another inserted particle produces an interference implying an interaction energy [25]. The first calculation of this effect was performed for two isotropic particles each locally inducing a *spherical* curvature [27–29]. The interaction was found to be repulsive, proportional to the rigidity κ of the membrane and to the sum of the squares of the imposed curvatures; it decays as R^{-4}, where R is the distance between the particles. The case of anisotropic particles producing non-spherical membrane deformations is even more interesting, since their collective action on the membrane is expected to have nontrivial morphological consequences [30–32]. The local deformation of a membrane actually involves *two* distinct curvatures, associated with two orthogonal directions (as in a saddle or in a cylinder). Recent calculations showed that the interaction between two anisotropic inclusions is very long-ranged and decays as R^{-2} [33–35]. It is always attractive at large separations and favors the orientation of the axis of minor curvature along the line joining the particles [34]. Note that these elastic interactions prevail at large separations, since they are of much longer range than other forces, such as van der Waals or screened electrostatic interactions.

II. Model

Among the above informations, let us outline the three points that are essential for our model. (i) Clathrin coats are solid scaffolds that rigidly shape extended parts of the membrane into spherical caps. (ii) Dynamins are solubilized proteins that partly insert within the membrane bilayer. (iii) Inserted membrane hosts that imprint a local membrane curvature interact with long-range forces of elastic origin.

We therefore build the following physical model. We describe a clathrin coated bud as an extended zone bearing a spherical curvature. Technically, this is done by placing point-like spherical curvature sources at the vertex of a hexagonal lattice patch (see Fig. 2). The precise physical realization of this

bud is not important as long as it is spherically curved and impenetrable by other membrane hosts. Because dynamins partly insert within the membrane and seem to accommodate cylindrical curvature, we model them as sources locally imprinting a cylindrical curvature. We place a large number of such "dynamins" on a membrane in the presence of an artificial bud as described above (Fig. 2), and we study whether the latter will recruit or not the dynamins through elastic long-range forces.

A. Long-range elastic interactions between many membrane inclusions

The elastic interaction between N isotropic or anisotropic membrane hosts can be calculated from first principles [34, 36]. The membrane is described as a surface which is weakly deformed with respect to a reference plane. Without this assumption, analytical calculations are virtually impossible. An obvious consequence is that we can accurately describe only weakly invaginated buds; nevertheless, we expect that our results will hold qualitatively for strongly invaginated buds. The membrane hosts are described as point-like sources bearing two curvatures c_1 and c_2, associated with two orthogonal directions. These values represent the two principal curvatures that the hosts imprint on the membrane through their binding with the membrane lipids (assuming the binding region is itself curved). For instance, a spherical impression corresponds to $c_1/c_2 = 1$, a cylindrical impression corresponds to $c_1/c_2 = 0$, and a saddle-like impression corresponds to $c_1/c_2 = -1$. This over-simplified model actually contains the essential ingredients responsible for the long-range elastic interactions between membrane inclusions: for protein hosts of a size comparable to the thickness of the membrane, it yields accurate interactions for separations as small as about three times the particles size. Note that the curvature actually impressed by a particle could be affected by the vicinity of another inclusion, we shall however neglect this effect for the sake of simplicity (strong binding hypothesis).

The point-like curvature sources describing the membrane hosts diffuse and rotate within the fluid membrane, because of the forces and torques exerted by the other membrane hosts and of the thermal agitation $k_{\mathrm{B}}T$. We parameterize the orientation of a particle by the angle θ that its axis of minor curvature, i.e., the axis associated with $\min(|c_1|, |c_2|)$, makes with the x-axis, in projection on the (x, y) reference plane. Given N inclusions with specified positions x_i and y_i, orientations θ_i, and curvatures c_{1i} and c_{2i}, for $i = 1 \ldots N$, we calculate the shape of the membrane satisfying the N imposed point-like curvatures and we determine the total elastic energy of the system. We thereby deduce the N-body interaction between the hosts $F_{\mathrm{int}}(\ldots, x_i, y_i, \theta_i, c_{1i}, c_{2i}, \ldots)$. The mathematical details of this procedure are sketched in Appendix A.

B. Pairwise interactions

Before studying the collective interaction between model dynamins and clathrin coats, let us describe how point-like spherical and cylindrical sources interact pairwise.

The membrane distortion produced by two inclusions modeled as point-like spherical curvature sources is shown in Fig. 3a. Each inclusion appears as a small spherical cap away from which the membrane relaxes to a flat shape. As evidenced by the plot of the interaction energy (see Fig. 3a), such spherical inclusions repel one another. Calling κ the bending rigidity of the membrane, a the thickness of the membrane (which is comparable to the size of the inclusions), c the curvature set by

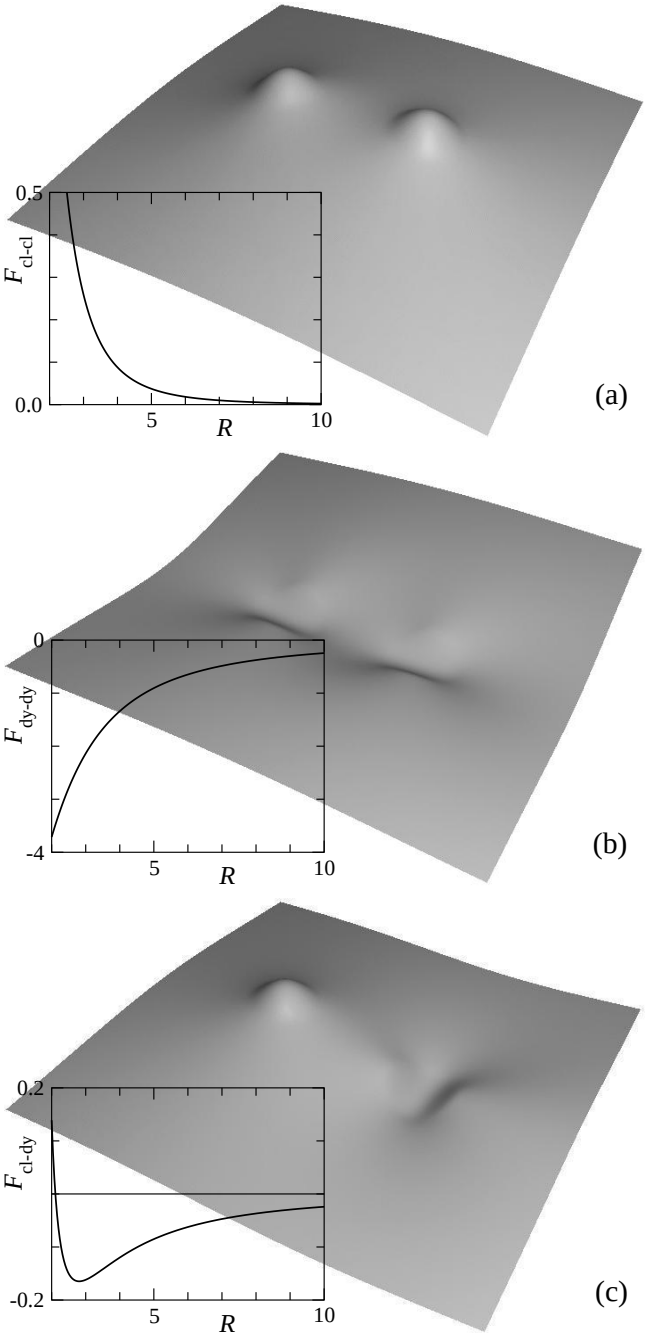

FIG. 3: Shape of a membrane distorted by two inclusions imprinting local curvatures and interaction energy as a function of separation. Distances are rescaled by the membrane thickness a and energies by $\kappa a^2 c^2$. (a) spherical inclusions of curvature c; (b) cylindrical inclusions of curvature c; (c) spherical inclusion of curvature c and cylindrical inclusion of curvature $0.2\,c$. The shapes are calculated from Eq. (A13), the interaction energies from Eq. (A12).

the inclusions and R their separation, our calculation gives (see Appendix A):

$$F_{\text{cl}-\text{cl}}(R) \simeq 8\pi\kappa\, a^2 c^2 \left(\frac{a}{R}\right)^4 \tag{1}$$

for the the asymptotic interaction at large separations, in agreement with previous works [27, 33, 34]. Note that the plot given in Fig. 3a corresponds to the exact interaction within our model, not to the

asymptotic expression (1).

The membrane distortion produced by two inclusions modeled as point-like cylindrical curvature sources is shown in Fig. 3b. Each inclusion appears as a small cylindrical cap away from which the membrane relaxes to a flat shape. The interaction between two such hosts depends on their relative orientation. The minimum energy is found when the axes of the cylinders are parallel to the line joining the inclusions. As evidenced by the plot of the interaction energy (see Fig. 3b), the interaction is then attractive. It therefore turns out that two such hosts produce a weaker membrane deformation when they are close to one another than when they are far apart. As described in Ref. [34], when their curvature is strong enough, such inclusions tend to aggregate and to form linear oligomers. Their asymptotic interaction energy is given by

$$F_{\mathrm{dy-dy}}(R) \simeq -8\pi\kappa\, a^2 c^2 \left(\frac{a}{R}\right)^2 . \tag{2}$$

It decays as R^{-2}, hence it is of longer range than (1).

Finally, we show in Fig. 3c the membrane distortion produced by the interaction between a spherical source and a cylindrical one. The latter is oriented in the direction that minimizes the energy. As evidenced by the plot of Fig. 3c, the interaction is attractive at large separations and repulsive at short separations, with a stable minimum configuration at a finite distance. Calling c the curvature set by the cylindrical inclusion and c' the one set by the spherical inclusion, our calculations give the asymptotic interaction

$$F_{\mathrm{cl-dy}}(R) \simeq -4\pi\kappa\, a^2 c\, c' \left(\frac{a}{R}\right)^2 . \tag{3}$$

We may therefore expect that dynamins will be attracted by clathrins coats; however, owing to the non-pairwise character of the interaction [34], it is necessary to actually perform the corresponding many-body calculation. It is also necessary to check whether thermal agitation will or will not disorder the inclusions.

III. Collective interactions between model dynamins and clathrin buds

As described in Sec. II, we build a model clathrin-coated bud by placing in a membrane N_{cl} point-like spherical inclusions of curvature c_{cl} on a hexagonal array with lattice constant b. Here, we have chosen $N_{\mathrm{cl}} = 37$ and $b = 3a$. By changing the curvature c_{cl}, we can adjust the overall curvature of the clathrin scaffold, thereby simulating the growth of a vesicular bud. We then add $N_{\mathrm{dy}} = 40$ point-like cylindrical sources of curvature c_{dy} modeling inserted dynamins.

To study the collective behavior of this system under the action of the multibody elastic interactions (see Sec. II A) and of thermal agitation, we perform a Monte Carlo simulation. The details of the simulations are given in Appendix B. To prevent unphysical divergences of the elastic interaction energy, it is necessary to introduce a hard-core steric repulsion preventing two inclusions to approach closer than a distance d. Since the size of the inclusions imprints is of the order of the membrane thickness a, we have chosen $d = 2a$. Actually, at such microscopic separations, other short-ranged interactions intervene, the details of which are still unknown. Here, we disregard them, since our interest lies in the mechanism by which the recruitment process and the formation of dynamin collars is driven. In a later stage, which we do not model here, dynamin rings are further stabilized by bio-chemical interactions [11].

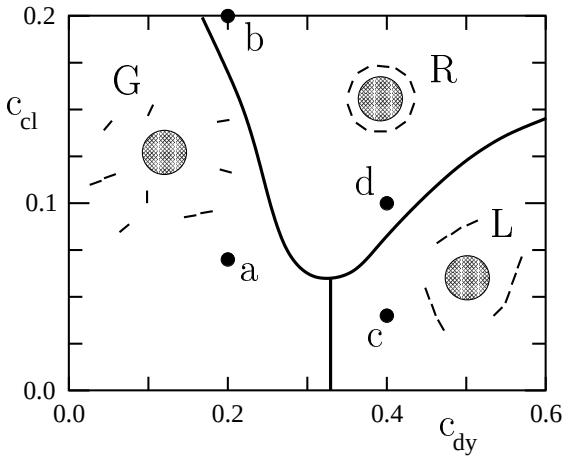

FIG. 4: Phase diagram representing the typical equilibrium configurations of a system of model dynamins in the vicinity of a curved clathrin scaffold. $c_{\rm dy}$ and $c_{\rm cl}$ are the curvatures associated with the dynamins and clathrins, respectively, in units of the inverse membrane thickness a. In region G, the dynamins form a "gas" non interacting with the clathrin scaffold. In region L, the dynamins form a system of linear oligomers non interacting with the clathrin scaffold. In region R, the dynamins form a ring around the clathrin scaffold, which is reminiscent of real endocytosis.

The results of the Monte Carlo simulations are summarized in the phase diagram of Fig. 4, in terms of the curvatures $c_{\rm cl}$ and $c_{\rm dy}$ of the clathrins and dynamins imprints, respectively. Here, we have chosen to span $c_{\rm cl}$ between 0 to $0.2\,a^{-1}$: for a lattice constant $b = 3a$ and assuming $a \simeq 40\,\text{Å}$, this corresponds for the clathrin-coated bud to a maximum curvature of radius $\rho \simeq b/(a\,c_{\rm cl}) \simeq 60\,\text{nm}$. Since our clathrin patch has 7 spherical sources on its diameter, the size of the bud is $7b \simeq 85\,\text{nm}$. These values are typical for clathrin-mediated endocytosis [6]. For the dynamins, we have spanned $c_{\rm dy}$ between $0.1\,a^{-1}$ and $0.4\,a^{-1}$, which corresponds to a maximum curvature of the imprint $\simeq 0.1\,\text{nm}^{-1}$. As for the membrane bending rigidity, we have taken $\kappa = 60\,k_{\rm B}T$, since for biological membranes at room temperature κ lies between 50 and $100\,k_{\rm B}T$ [37, 38].

The phase diagram displays three regimes (see Fig. 4): a state in which the dynamins are disordered in a gas-like fashion (G), a state in which the dynamins form linear oligomers that do not interact with the clathrin bud (L), and a state in which the dynamins form a ring around the clathrin bud (R). In region (R), due to the shallowness of the dynamin imprints, the system is disordered by thermal agitation. Increasing the curvature of the dynamin imprints increases the elastic attraction between the dynamins (see Fig 3b) and leads to the formation of linear oligomers (L). These oligomers wrap around the clathrin bud when the latter is sufficiently developed (R). Typical snapshots corresponding to the four points a, b, c, d in Fig. 4 are shown in Fig. 5. Note that in Fig. 5b the dynamin collar is rather "gaseous" due to the weakness of the dynamins' imprints, while in Fig. 5d the ring is tight and well-ordered.

IV. Conclusion

In this paper, we have shown that if membrane inserted dynamins produce cylindrical imprints and if the latter are sufficiently curved, then the resulting long-range forces mediated by the membrane elasticity are strong enough to overcome Brownian motion and bring them into a collar around the neck of a clathrin bud. Of course, simple diffusion could also bring dynamins around clathrin buds,

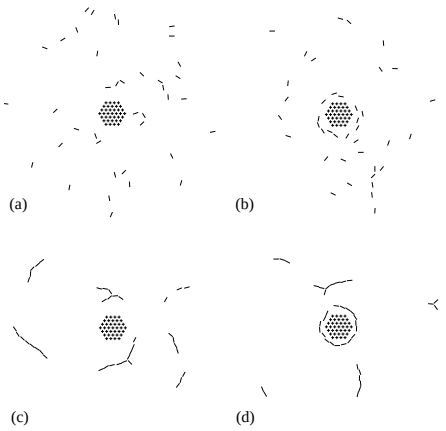

FIG. 5: Typical snapshots showing the equilibrium arrangement of model dynamins (bars) in the vicinity of the clathrin scaffold (hexagonal array). The figures (a), (b), (c) and (d) refer to the corresponding points in the phase diagram of Fig. 4.

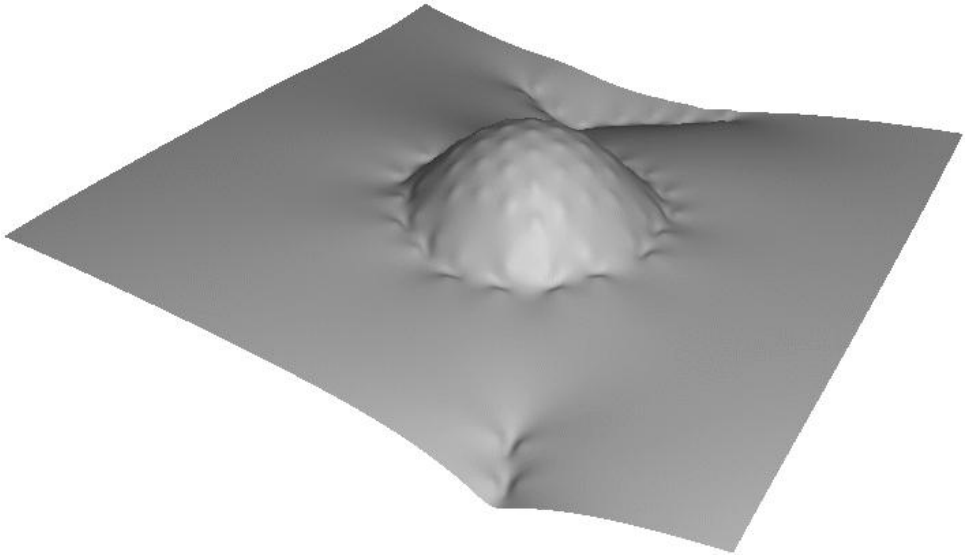

FIG. 6: Membrane shape corresponding to point (d) in Figs. 4 and 5, showing the self-assembly of a ring of dynamins around a clathrin bud.

and their binding into a ring could be the result of specific bio-chemical interactions. However, if a cylindrical imprint can speed up this process, then evolution may have selected it.

To test this model, one might look experimentally for linear oligomers of dynamins (see Fig. 5c). However, since "gaseous" rings are also possible (see Fig. 5b), the existence of such linear aggregates may not be necessary. It would be more interesting to directly check, e.g., by cryo-electron microscopy, the shape of the dynamin region that penetrates within the membrane.

Finally, note that our model is over-simplified since: i) many other integral proteins float around dynamins, ii) dynamins may interact with various lipidic domains within the bilayer, iii) the membrane may have a spontaneous curvature due to its asymmetry, and iv) fluctuations are not only thermal but also active, and hence could be larger than we estimate. Nonetheless, we hope that our model correctly captures the effects of the long-range elastic interactions.

Acknowledgments

We acknowledge fruitful discussions with R. Bruinsma, F. Jülicher, F. Képès, J.-M. Delosme, B. Goud, P. Chavrier, V. Norris, and J.-M. Valleton.

Appendix A: many-body interactions between point-like curvature sources

Let us outline the derivation of the interaction between N anisotropic point-like sources that locally imprint a curvature on the membrane. As explained in the text, such constraints modelize a wide class of membrane inclusions, including transmembrane and cytosol proteins partly inserted within the membrane.

For small deformations $u(x, y)$ with respect to the (x, y) plane, the free energy associated with the curvature elasticity of a membrane is given by [39]:

$$F_{\rm el} = \frac{\kappa}{2} \int dx\, dy \left(\nabla^2 u\right)^2 . \tag{A1}$$

Indeed, for small deformations, the Laplacian $\nabla^2 u(\mathbf{r})$ is equal to the sum of the membrane's principal curvatures at point $\mathbf{r} = (x, y)$. The material parameter κ is the bending rigidity.

Determining the shape of the membrane in the presence of inclusions at positions $\mathbf{r}_\alpha$ imprinting local curvatures requires minimizing the elastic energy (A1) with local constraints on the membrane curvature tensor. In the small deformation limit, the elements of the latter are given by the second spatial derivatives of the membrane shape: $u_{,xx}(\mathbf{r})$, $u_{,xy}(\mathbf{r})$ and $u_{,yy}(\mathbf{r})$. Introducing $3N$ Lagrange multipliers Λ^α_{ij} to enforce the curvature constraints, the Euler-Lagrange equation corresponding to the constrained minimization is

$$\begin{aligned} \nabla^2\nabla^2 u\,(\mathbf{r}) = \sum_{\alpha=1}^{N} \Big[& \Lambda^\alpha_{xx}\, \delta_{,xx}\,(\mathbf{r}-\mathbf{r}_\alpha) \\ & + \Lambda^\alpha_{xy}\, \delta_{,xy}\,(\mathbf{r}-\mathbf{r}_\alpha) + \Lambda^\alpha_{yy}\, \delta_{,yy}\,(\mathbf{r}-\mathbf{r}_\alpha) \Big], \end{aligned} \tag{A2}$$

where $\delta(\mathbf{r})$ is the two-dimensional Dirac's delta and a comma indicates derivation. By linearity, the solution of this equation is

$$u(\mathbf{r}) = \sum_{\mu=1}^{3N} \Lambda_\mu \Gamma_\mu(\mathbf{r}), \tag{A3}$$

where the Λ_μ's and Γ_μ's are the $3N$ components of the column matrices

$$\Lambda = \begin{pmatrix} \Lambda^1_{xx} \\ \Lambda^1_{xy} \\ \Lambda^1_{yy} \\ \Lambda^2_{xx} \\ \vdots \end{pmatrix}, \qquad \Gamma(\mathbf{r}) = \begin{pmatrix} G_{,xx}(\mathbf{r}-\mathbf{r}_1) \\ G_{,xy}(\mathbf{r}-\mathbf{r}_1) \\ G_{,yy}(\mathbf{r}-\mathbf{r}_1) \\ G_{,xx}(\mathbf{r}-\mathbf{r}_2) \\ \vdots \end{pmatrix}, \tag{A4}$$

and

$$G(\mathbf{r}) = \frac{1}{16\pi} r^2 \ln r^2 \tag{A5}$$

is the Green function of the operator $\nabla^2\nabla^2$, satisfying the equation $\nabla^2\nabla^2 G(\mathbf{r}) = \delta(\mathbf{r})$.

We introduce a column matrix K containing the values of the $3N$ constraints

$$\mathsf{K} = \begin{pmatrix} u_{,xx}(\mathbf{r}_1) \\ u_{,xy}(\mathbf{r}_1) \\ u_{,yy}(\mathbf{r}_1) \\ u_{,xx}(\mathbf{r}_2) \\ \vdots \end{pmatrix}. \tag{A6}$$

With $u(\mathbf{r})$ given by Eq. (A3), enforcing the constraints yields the following equation for the Lagrange multipliers:

$$\sum_{\nu=1}^{3N} M_{\mu\nu}\Lambda_\nu = K_\mu, \tag{A7}$$

where the $3N \times 3N$ matrix M is given by

$$\mathsf{M} = \begin{pmatrix} \mathsf{m}_{11} & \mathsf{m}_{12} & \dots & \mathsf{m}_{1N} \\ \mathsf{m}_{21} & \mathsf{m}_{22} & & \vdots \\ \vdots & & \ddots & \vdots \\ \mathsf{m}_{N1} & \dots & \dots & \mathsf{m}_{NN} \end{pmatrix}, \tag{A8}$$

in which the $\mathsf{m}_{\alpha\beta}$'s are N^2 matrices of size 3×3 defined by

$$\mathsf{m}_{\alpha\beta} = \begin{pmatrix} G_{,xxxx}(\mathbf{r}_{\beta\alpha}) & G_{,xxxy}(\mathbf{r}_{\beta\alpha}) & G_{,xxyy}(\mathbf{r}_{\beta\alpha}) \\ G_{,xxxy}(\mathbf{r}_{\beta\alpha}) & G_{,xxyy}(\mathbf{r}_{\beta\alpha}) & G_{,xyyy}(\mathbf{r}_{\beta\alpha}) \\ G_{,xxyy}(\mathbf{r}_{\beta\alpha}) & G_{,xyyy}(\mathbf{r}_{\beta\alpha}) & G_{,yyyy}(\mathbf{r}_{\beta\alpha}) \end{pmatrix}, \tag{A9}$$

where $\mathbf{r}_{\beta\alpha} = \mathbf{r}_\alpha - \mathbf{r}_\beta$. Setting

$$\mathbf{r}_\alpha - \mathbf{r}_\beta = r_{\beta\alpha}\left[\cos\theta_{\alpha\beta}\,\hat{\mathbf{x}} + \sin\theta_{\alpha\beta}\,\hat{\mathbf{y}}\right], \tag{A10}$$

yields explicitely

$$\mathsf{m}_{\alpha\beta} = \frac{1}{4\pi r_{\beta\alpha}^2} \begin{pmatrix} \cos(4\,\theta_{\alpha\beta}) - 2\cos(2\,\theta_{\alpha\beta}) & \sin(2\,\theta_{\alpha\beta})\left[2\cos(2\,\theta_{\alpha\beta}) - 1\right] & -\cos(4\,\theta_{\alpha\beta}) \\ \sin(2\,\theta_{\alpha\beta})\left[2\cos(2\,\theta_{\alpha\beta}) - 1\right] & -\cos(4\,\theta_{\alpha\beta}) & -\sin(4\,\theta_{\alpha\beta}) - \sin(2\,\theta_{\alpha\beta}) \\ -\cos(4\,\theta_{\alpha\beta}) & -\sin(4\,\theta_{\alpha\beta}) - \sin(2\,\theta_{\alpha\beta}) & \cos(4\,\theta_{\alpha\beta}) + 2\cos(2\,\theta_{\alpha\beta}) \end{pmatrix}. \tag{A11}$$

Integrating Eq. (A1) by parts and taking into account the constraints yields the elastic energy

$$F_{\rm el} = \frac{1}{2}\kappa\,\mathsf{K}^t\mathsf{M}^{-1}\mathsf{K}, \tag{A12}$$

where K^t is the transpose of K. From Eqs. (A3) and (A7), the equilibrium shape of the membrane is given by

$$u(\mathbf{r}) = \mathsf{K}^t\mathsf{M}^{-1}\mathsf{\Gamma}(\mathbf{r}). \tag{A13}$$

When $\alpha = \beta$, $\mathsf{m}_{\alpha\beta}$ as given by Eq. (A11) diverges: indeed Eq. (A1) correctly describes the membrane elastic energy only for distances $r \gtrsim r_0$, where r_0 is of the order of the membrane thickness. It

is therefore necessary to introduce a high wavevector cutoff r_0^{-1} in the theory. From the definition of the Green function $G(\mathbf{r})$, we deduce, in Fourier space

$$G_{,xxxx}(\mathbf{r}) = \int \frac{d^2q}{(2\pi)^2} \frac{q_x^4\, e^{i\mathbf{q}\cdot\mathbf{r}}}{q^4}. \tag{A14}$$

Hence, introducing the cutoff, we obtain

$$G_{,xxxx}(\mathbf{0}) = \int_0^{r_0^{-1}} \frac{q\, dq}{(2\pi)^2} \int_0^{2\pi} d\theta\, \cos^4\theta = \frac{3}{32\pi r_0^2}, \tag{A15}$$

and similarly for the other elements of the matrix (A9). With the above prescription, we obtain

$$\mathsf{m}_{\alpha\alpha} = \frac{1}{32\pi r_0^2} \begin{pmatrix} 3 & 0 & 1 \\ 0 & 1 & 0 \\ 1 & 0 & 3 \end{pmatrix}. \tag{A16}$$

As an illustration, let us consider the case of two identical isotropic inclusions, each prescribing the curvature c. Then

$$\mathsf{K}^t = (c, 0, c, c, 0, c)\,, \tag{A17}$$

and, from Eqs. (A12), (A8), (A11), and (A16), with $r_{12} = R$, the interaction energy is

$$F_{\rm el} = \frac{512\,\pi\kappa\,(r_0 c)^2}{\left(\dfrac{R}{r_0}\right)^4 + 8\left(\dfrac{R}{r_0}\right)^2 - 32}, \tag{A18}$$

in which we have discarded a constant term. Setting $r_0 = a/2$, we indeed obtain the leading asymptotic interaction (1). This special choice for r_0 allows to match the result of Goulian et al. (1993), which was obtained from multipolar expansions. It should be noted that the interaction given by Eq. (A18) is *exact* within the present formalism (for r larger than $\simeq a$), whereas multipolar expansions can only give in analytical form the leading asymptotic orders.

When many inclusions are present, the matrix M and its inverse, which determines the interaction energy through Eq. (A12), can be easily calculated numerically once the positions of the inclusions are defined.

Appendix B: Monte Carlo simulations

The Monte Carlo simulation that we perform employs the standard Metropolis algorithm [40]. For given positions and orientations of the particles representing the dynamins, the energy is numerically calculated from Eq. (A12). At each Monte Carlo step, we perform a Metropolis move consisting in either a translation or a rotation of one arbitrarily chosen dynamin particle. The amplitude of the moves is adjusted in order to keep an average acceptance rate of 50%. We confine the dynamins inside a circular box (of radius $80\,a$) centered around the clathrin lattice, which is kept fixed. To take into account the hard-core repulsion (see Sec. III), we simply reject any move bringing two particles closer than the minimum approach distance d (here $2a$). Note that in this simulation the membrane is not discretized: the interaction energy that we use fully takes into account the elasticity of the membrane.

[1] H. Lodish, A. Berk, S. L. Zipursky, P. Matsudaira, D. Baltimore, and J. E. Darnell, *Molecular Cell Biology, 4th ed.* (W H Freeman & Co, New York, 1999).

[2] C. J. Smith, N. Grigorieff, and B. M. Pearse, EMBO J. **17**, 4943 (1998).

[3] B. M. Pearse and M. S. Robinson, Annu. Rev. Cell. Biol. **6**, 151 (1990).

[4] J. E. Rothman, Nature **372**, 55 (1994).

[5] R. Schekman and L. Orci, Science **271**, 1526 (1996).

[6] M. Marsh and H. T. McMahon, Science **285**, 215 (1999).

[7] K. Takei and V. Haucke, Trends Cell Biol. **11**, 385 (2001).

[8] S. L. Schmid, M. A. McNiven, and P. D. Camilli, Curr. Opin. Cell Biol. **10**, 504 (1998).

[9] J. E. Hinshaw and S. L. Schmid, Nature **374**, 190 (1995).

[10] K. Takei, P. S. McPherson, S. L. Schmid, and P. D. Camilli, Nature **374**, 186 (1995).

[11] J. E. Hinshaw, Annu. Rev. Cell Dev. Biol. **16**, 483 (2000).

[12] D. Danino and J. E. Hinshaw, Cur. Opin. Cell Biol. **13**, 454 (2001).

[13] K. Takei, V. Haucke, V. Slepnev, K. Farsad, M. Salazar, H. Chen, and P. D. Camilli, Cell **94**, 131 (1998).

[14] K. M. Huang, K. D'Hondt, H. Riezman, and S. K. Lemmon, EMBO J. **18**, 3897 (1999).

[15] S. M. Sweitzer and J. E. Hinshaw, Cell **93**, 1021 (1998).

[16] M. H. B. Stowell, B. Marks, P. Wigge, and H. T. McMahon, Nature Cell Biol. **1**, 27 (1999).

[17] B. Marks, M. H. B. Stowell, Y. Vallis, I. G. Mills, A. Gibson, C. R. Hopkins, and H. T. McMahon, Nature **410**, 231 (2001).

[18] P. L. Tuma, M. C. Stachniak, and C. A. Collins, J. Biol. Chem. **268**, 17240 (1993).

[19] J. P. Liu, K. A. Powell, T. C. Sudhof, and P. J. Robinson, J. Biol. Chem. **269**, 21043 (1994).

[20] H. C. Lin, B. Barylko, M. Achiriloaie, and J. P. Albanesi, J. Biol. Chem. **272**, 25999 (1997).

[21] Y. Vallis, P. Wigge, B. Marks, P. R. Evans, and H. T. McMahon, Curr. Biol. **9**, 257 (1999).

[22] A. Lee, D. W. Frank, M. S. Marks, and M. A. Lemmon, Curr. Biol. **9**, 261 (1999).

[23] K. N. J. Burger, R. A. Demel, S. L. Schmid, and B. de Kruijff, Biochemistry **39**, 12485 (2000).

[24] P. Zhang and J. E. Hinshaw, Nature Cell Biol. **3**, 922 (2001).

[25] H. Gruler, Z. Naturforsch. **30 c**, 608 (1975).

[26] H. Gruler and E. Sackmann, Croat. Chem. Acta **49**, 379 (1977).

[27] M. Goulian, R. Bruinsma, and P. Pincus, Europhys. Lett. **22**, 145 (1993).

[28] M. Goulian, R. Bruinsma, and P. Pincus, Europhys. Lett. **23**, 155 (1993).

[29] J.-B. Fournier and P. G. Dommersnes, Europhys. Lett. **39**, 681 (1997).

[30] Y. Bouligand, in *Geometry in condensed matter physics*, edited by J.-F. Sadoc (World Scientific, Singapore) p. 225 (1990).

[31] J.-B. Fournier, Phys. Rev. Lett. **76**, 4436 (1996).

[32] V. Kralj-Iglič, V. Heinrich, S. Svetina, and B. Žekš, Eur. Phys. J. B **10**, 5 (1999).

[33] J. M. Park and T. C. Lubensky, J. Phys. I France **6**, 1217 (1996).

[34] P. G. Dommersnes and J.-B. Fournier, Eur. Phys. J. B **12**, 9 (1999).

[35] T. Chou, K. S. Kim, and G. Oster, Biophys. J. **80**, 1075 (2001).

[36] P. G. Dommersnes and J.-B. Fournier, To be published (2001).

[37] J. B. Song and R. E. Waugh, Biophys. J. **64**, 1967 (1993).

[38] H. Strey and M. Peterson, Biophys. J. **69**, 478 (1995).

[39] W. Helfrich, Z. Naturforsch. **28c**, 693 (1973).

[40] N. Metropolis, A. W. Rosenbluth, M. N. Rosenbluth, A. H. Teller, and E. Teller, J. Chem. Phys. **21**, 1087 (1953).

Virtual Mitochondria And Their Control

Marie Aimar[1], Bernard Korzeniewski[3], Jean-Pierre Mazat[1] and Christine Nazaret[2] (alphabetic order)

[1]Inserm EMI 9929, and [2]ESTBB, Université de Bordeaux 2, 146 rue Léo-Saignat, F 33076, Bordeaux-cedex France.
[3] Jagiellonian University, ul. Gronostajowa 7, 30-387 Krakow, Poland

Résumé
Dans la cellule eucaryote, les mitochondries sont des organelles responsable de la fourniture en énergie sous forme d'ATP. Le contrôle de la production d'ATP mitochondrial est un problème complexe avec différentes expression dans différents tissus et organes.
Notre but est de continuer la modélisation des oxydations phosphorylantes mitochondriales, d'y ajouter le reste du métabolisme mitochondrial et d'intégrer cette mitochondrie virtuelle dans une cellule virtuelle.
Pour construire les cartes du métabolisme mitochondrial, on se servira des séquences connues des génomes eucaryotes (10 à 15% du génome de la levure concerne les mitochondries).

Abstract
Inside the eukaryotic cell, mitochondria are internal organelles of prokaryotic origin, responsible for energy supply in the cell. The control of the mitochondrial ATP production is a complex problem with different patterns according to different tissues and organs.
Our aim is to continue to develop the modelling of oxidative phosphorylation in different tissues, to model other parts of mitochondrial metabolism and to include this virtual mitochondria in a virtual cell.
In constructing the complete metabolic map of mitochondria, we will take advantage of the sequenced genomes of eukaryotic organism, (10-15% of the yeast genome concerns mitochondria).

Introduction
Mitochondria are internal organelles inside the eukaryotic cell; it is the place of oxidative phosphorylation (OXPHOS), i.e. of an ATP synthesis coupled to respiratory chain functioning (Fig. 1). The respiratory chain itself is a series of oxido-reduction reactions linking the oxidation of a respiratory substrate (glucose, fatty acids, pyruvate etc.) to the reduction of oxygen in water, by an electron transfer through a succession of proteinous complexes, correctly arranged in the inner mitochondrial membrane. These complexes are made of polypeptides encoded both by nuclear and mitochondrial DNA.
Mitochondria possess their own DNA (mtDNA), circular, double stranded molecules, involving 1659 base pairs in human, sequenced by the group of Sanger in 1981 [1]. Each mitochondrium contains 2-10 mtDNA molecules. In man mitochondrial DNA codes for 13 mitochondrial proteins among approximately 70 in the respiratory chain [2-5]. Mitochondria play an important role not only in ATP synthesis but also (non-exhaustive list) in some specific metabolic pathways, in cell oxido-reduction ratio upholding, in cell calcium homeostasy and signalling, in apoptosis, etc. The mitochondrial metabolism is thus rich and varied and it is one of the aims of our work to understand how this metabolism can account for very different functions and behaviour of mitochondria in different tissues.

Moreover mitochondria, though performing the same general functions, are different in different organisms from plant to animals, including yeast and heterotrophic flagellate like *Reclinomonas americana*.
The first aim of our work is to continue the modelling of oxidative phosphorylation in different tissues in order to simulate their functioning and to understand the basis in their control differences.
In addition mitochondria hold a significant part of cellular metabolism : Krebs cycle, β-oxidation of fatty-acids, etc., and the second aim of our work will be to model this metabolism. In the third step we will include this virtual mitochondria in a virtual cell by modelling the exchanges of metabolites, energy and signals (calcium signals) between the cell and mitochondria.
In constructing the complete metabolic map of mitochondria, we will take advantage of the sequenced genomes of eukaryotic organism, from which a significant part (10-15% in yeast) concerns mitochondria. Our project will also lean on sequenced genomes of prokaryotic organisms which are ancestors of mitochondria. This should help to ascribe functions to unknown ORF, possibly involved in mitochondrial metabolism.
To sum it up, our work will consist in linking sequenced genomes to mitochondrial metabolism, in order to construct mitochondrial metabolic maps, to analyze the mitochondrial fluxes and their regulation.

Results

Experimental studies enabled a great progress in our understanging of the complex set of mitochondrial functions. Nevertheless, it is frequently not easy to integrate a great amount of qualitative and quantitative experimental data in an intuitive way. In such cases, different quantitative mathematical methods, especially computer kinetic models of particular metabolic pathways can be used.

Well-tested kinetic models can prove to be very useful research tools. Such models help to interpret, analyse and process a great number of quantitative and semiquantitative experimental data concerning a sophisticated metabolic system under consideration. They may be very useful for explaining the basis and nature of different complex phenomena. Computer modelling forces a researcher to formulate all the problems in an explicit and quantitative way, which is not always the case with intuitive considerations. Kinetic models allow one to investigate how the macroscopic level of the cell behaviour emerges from the interplay of particular elements at the microscopic level of enzymatic reactions. They also help to check in a quantitative way, if all known elements and their properties suffice to explain the entire behaviour of the investigated metabolic system in vivo, or else, if some new factors possessing properties determined by a model should be looked for. Human brain could not cope by itself with such a sophisticated, multi-factor analysis. Finally, quantitative models can be used to calculate variable values and to simulate different dynamic properties that have not been yet measured experimentally (e.g. because of technical difficulties) and to predict the existence of completely new phenomena that have not been discovered yet in the experimental way. Of course, all such predictions have to be verified (or falsified) by experimental studies. In other worlds, theoretical predictions obtained with the aid of a computer kinetic model can inspire and direct further experimental studies.

Oxidative phosphorylation is probably the mitochondrial metabolic pathway that was most frequently modelled in the quantitative way. The general scheme of oxidative phosphorylation is presented in Fig. 1. Several different kinetic (and thermodynamic) models of this process have been developed. They are shortly summarised in Table 1. Among these models, only the model developed by Korzeniewski and co-workers has been tested for a broad range of experimentally-measured parameter values and system properties. This model was used to predict new properties of the system and the existence of new phenomena.

One of the most important predictions was that only a direct activation of (almost) all oxidative phosphorylation steps, in parallel with the activation of ATP usage, by some (still unknown) cytosolic factor X, transmiting the signal of stimulation of a cell by neural excitation (skeletal muscle, heart) or hormones (liver) can explain the large changes in fluxes (respiration, ATP turnover) accompanied by only moderate changes in metabolite concentrations (ATP/ADP, $NADH/NAD^+$) in intact tissues [17,21,25]. Some other important predictions concern the effect of inborn enzyme deficiencies and the ethiology of mitochondrial diseases. First, it has been demonstrated in the theoretical way that the expression of enzyme deficiencies will depend on the origin of the mutation (nuclear or mitochondrial): mutations in mitochondrial genes encoding some subunits of oxidative phosphorylation complexes will generally tend to have a more harmful effect than mutations in nuclear genes encoding the remaining oxidative phosphorylation complexes/subunits [22]. Second, the effect of enzyme deficiencies will depend on the relative energy demand of a given tissue – the greater the energy demand, the stronger the impairment of oxidative phosphorylation [22]. This founding can help to explain the tissue specificity of mitochondrial diseases. Third, the above-mentioned direct activation of different steps in the ATP supply-demand system will essentially lessen the inhibitory effect of enzyme deficiencies on oxidative phosphorylation [23].

Computer models of other metabolic pathways located in mitochondria, for example of Krebs cycle, were also developed. These models also helped significantly to understand the control and regulation of mitochondrial metabolism.

Some of the results obtained experimentally or predicted with the help of a model are understandable in the framework of metabolic control analysis. In this theory [28-30] the sensitivity of the flux of a metabolic network as a function of a step perturbation is analyzed in the linear domain around a steady-state. This allows to define the so-called „control coefficients", which measure the fraction of a step perturbation transmitted to a whole flux (involving several steps including or not the perturbed one). The theoretical models of oxidative phosphorylation developed so far, allow more or less easily to calculate its control coefficients. The Korzeniewski et al. model was extensively used to this aim [17-20,31] . We are now adapting the model to different tissues in order to account for the differences in control coefficient we have measured in mitochondria isolated from different rat tissues [32, 33]. The values of control coefficients are of great interest in the prediction of the effects of a deficiency in mitochondrial diseases; they are also of interest in biotechnology, where some steps are amplified.

Conclusion

With the help of models of mitochondrial metabolism it is possible to analyse and to compare the metabolic organisation and functioning of different types of mitochondria. The basic knowledge (based on already studied enzymes and on reasonable hypotheses) of the kinetic parameters of enzymes or enzymatic complexes will enable us to predict the metabolic fluxes, their regulation and their control. In a sense our aim is to apply to mitochondria the method developed for whole cells in the post-genomic area, i.e. to construct and to analyse the metabolic maps from the genes. Due to the lower number of genes involved in mitochondria (10% of an eukaryotic genome, see table 2) this application could be easier than for whole cells and is, in any case, a compulsory step in cell metabolism modelling, because mitochondria are largely autonomous and independent units inside cells. This will impose to precisely recognise these sequences, involved in mitochondria.

Acknowledgements

This work was supported by the Association Française contre les Myopathies (A.F.M.), INSERM, the Université Bordeaux II and the Région Aquitaine. B.K. was supported by the KBN grant 0450/P04/2001/20.

References

[1] Anderson, S., Bankier, A.T., Barell, B.G., de Bruijn, M.H.L., Coulson, A.R., Drouin, J., Eperon, I.C., Nierlich, D.P., Roe, B.A., Sanger, F., Schreier, P.H., Smith, A.J.H., Staden, R., Young, I.G., Sequence and organisation of the human mitochondrial genome, Nature 290 (1981) 457-470.
[2] Attardi, G., Schatz, G., Biogenesis of mitochondria, Ann. Rev. Cell. Biol. 4 (1988) 289-333.
[3] Cann, R.L., Stoneking, M., Wilson, A.L., Mitochondrial DNA and Human Evolution, Nature 325 (1987) 31-36.
[4] Clayton, D.A.., Replication of animal mitochondrial DNA, Cell 28 (1982) 693-705.
[5] Fearnley, I.M., Walker, J.E., Two overlapping genes in bovine mitochondrial DNA encode membrane components of ATP synthetase, Embo J. 5 (1986) 2005-8.
[6] Chance, B., Williams, G.R., Respiration enzymes in oxidative phosphorylation. 1. Kinetics of oxygen utilization, J. Biol. Chem. 217 (1955) 383-393.
[7] Chance, B., Williams, G.R., The respiratory chain and oxidative phosphorylation, Adv. Enzymol. 17 (1956) 65-134.
[8] Rottenberg, H., Non-equilibrium thermodynamics of energy conversion in bioenergetics, Biochim. Biophys. Acta 549 (1979) 225-253.
[9] Westerhoff, H.V., van Dam, K., Thermodynamics and control of free-energy transduction, Elsevier, Amsterdam, 1987.
[10] Wilson, D.F., Owen, C.S, Erecińska, M., Quantitative dependence of mitochondrial oxidative phosphorylation on oxygen concentration: a mathematical model, Arch. Biochem. Biophys. 195 (1979) 494-504.
[11] Wilson, D.F., Owen, C.S. and Holian, A., Control of mitochondrial respiration: a quantitative evaluation of the roles of cytochrome c and oxygen, Arch. Biochem. Biophys. 182 (1977) 749-762.
[12] Bohnensack, R., Control of energy transformation of mitochondria. Analysis by a quantitative model, Biochim. Biophys. Acta 634 (1981) 203-218.
[13] Bohnensack, R., Küster, U., Letko, G., Rate-controlling steps of oxidative phosphorylation in rat liver mitochondria. A synoptic approach of model and experiment, Biochim. Biophys. Acta 680 (1982) 271-280.
[14] Gellerich, F.N., Bohnensack, R., Kunz, W., Control of mitochondrial respiration. The contribution of the adenine nucleotide translocator depends on the ATP- and ADP-consuming enzymes, Biochim. Biophys. Acta 722 (1983) 381-391.
[15] Holzhütter, H.-G., Henke, W., Dubiel, W., Gerber, G., A mathematical model to study short-term regulation of mitochondrial energy transduction, Biochim. Biophys. Acta 810 (1985) 252-268.
[16] Korzeniewski, B., Froncisz, W., An extended dynamic model of oxidative phosphorylation, Biochim. Biophys. Acta 1060 (1991) 210-223.
[17] Korzeniewski, B., Froncisz, W., Theoretical studies on the control of the oxidative phosphorylation system, Biochim. Biophys. Acta 1102 (1992) 67-75.
[18] Korzeniewski, B., Simulation of oxidative phosphorylation in hepatocytes, Biophys. Chem. 58 (1996) 215-224.

[19] Korzeniewski, B., Simulation of state 4 → state 3 transition in isolated mitochondria, Biophys. Chem. 57 (1996) 143-153.
[20] Korzeniewski, B., Mazat, J.-P., Theoretical studies of the control of oxidative phosphorylation in muscle mitochondria: application to mitochondrial deficiencies, Biochem. J. 319 (1996) 143-148.
[21] Korzeniewski, B., Regulation of ATP supply during muscle contraction: theoretical studies, Biochem. J. 330 (1998) 1189-1195.
[22] Korzeniewski, B., Malgat, M., Letellier, T. and Mazat, J.-P., Effect of binary mitochondria heteroplasmy on respiration and ATP synthesis: implications to mitochondrial diseases, Biochem. J. 357 (2001) 835-842.
[23] Korzeniewski, Parallel activation in the ATP supply-demand system lessens the effect of enzyme deficiencies, inhibitors, poisons and substrate shortage on oxidative phosphorylation, B., Biophys. Chem. (2002) in press.
[24] Korzeniewski, B., Zoladz, J.A., A model of oxidative phosphorylation in mammalian skeletal muscle, Biophys. Chem. 92 (2001) 17-34.
[25] Aliev, M.K., Saks, V.A., Compartmentalized energy transfer in cardiomyocytes: use of methematical modelling for analysis in vivo regulation of respiration, Biophys. J. 73 (1997) 428-445.
[26] Vendelin, M, Kongas, O., Saks, V., Regulation of mitochondrial respiration in heart cells analyzed by reaction-diffusion model of energy transfer, Am. J. Physiol. 278 (2000) C747-C764.
[27] Korzeniewski, B., Theoretical studies on the regulation of oxidative phosphorylation in intact tissues, Biochim. Biophys. Acta 1504 (2001) 31-45.
[28] Kacser, H., Burns, J.A., The control of flux, Symp. Soc. Exp. Biol. 32 (1973) 65-104.
[29] Heinrich, R., Rapoport, T.A., A linear steady-state treatment of enzymatic chains. General properties, control and effector strength, Eur. J. Biochem. 42 (1974), 89-95.
[30] Reder, C., Metabolic control theory: a structural approach, J. Theor. Biol. 135 (1988) 175-201.
[31] Korzeniewski, B., Mazat, J.-P., Theoretical studies on control of oxidative phosphorylation in muscle mitochondria at different energy demands and oxygen concentrations, Acta Biotheoretica 44 (1996) 263-269.
[32] Rossignol, R., Malgat, M., Mazat, J.-P., Letellier, T., Threshold effect and tissue specificity. Implication for mitochondrial cytopathies, J. Biol. Chem. 274 (1999) 33426-33432.
[33] Rossignol, R., Letellier, T., Malgat, M., Rocher, C., Mazat, J.-P., Tissue variation in the control of oxidative phosphorylation: Implication for mitochondrial diseases, Biochem. J. 347 (2000) 45-53.

Table 1. Quantitative models of oxidative phosphorylation available in the literature.

Authors	type of model	chatacteristics	references
Chance and Williams	one simple kinetic equation	for isolated mitochondria; Michaelis-Menten kinetic dependence of the respiration rate on [ADP]; black-box description	[6,7]
Rottenberg; Westerhoff and van Dam	NET – non-equilibrium thermodynamics	for isolated mitochondria; linear depencence of fluxes on thermodynamic forces; black-box description; limited range of application	[8,9]
Wilson, Erecińska and co-workers	static kinetic model of one rate-limiting step	for isolated mitochondria; kinetic description of cytochrome oxidase assumed to be the only rate-limiting step; depencence on external [ATP]/[ADP] instead of on Δp	[10,11]
Bohnensack and co-workers	static kinetic model involving many steps	for isolated mitochondria; kinetic description of many (but not all) complexes (phosphate carrier not included explicitly, respiratory chain described as one unit); tested for a limited set of system properties	[12-14]
Holzhütter and co-workers	dynamic kinetic model involving many steps	for isolated mitochondria; kinetic description of all complexes; several assumptions are not justified; developed for mitochondria working in non-physiological temperature (8 °C); tested for a limited set of system properties	[15]
Korzeniewski and co-workers	dynamic kinetic model involving many steps	for isolated mitochondria and intact tissues (liver, muscle); kinetic description of all complexes; tested for a broad set of system properties; used for a series of new theoretical predictions	[16-24]
Saks and co-workers	dynamic kinetic model involving many steps	for intact heart; creatine kinase assumed to be essentially displaced from thermodynamic equilibrium; P_i assumed to be the main metabolite regulating oxidative phosphorylation; contradicts several experimental data concerning the value of, and relative changes in, $[P_i]$	[25,26]

Table 2. Number of nuclear genes known for coding mitochondrial proteins :
SwissProt was used as a data bank. The interrogation was built with two kinds of keywords: different organism names (listed in the first column) and the prefix "mito"; the number of these occurrences is listed in the third column with the number of mtDNA uncoded proteins in brackets. The fourth column gives the percentage of the number of 'mito' occurences scaled by the total number of known proteins in the organisms under study (second column).

Organism	**Nb of known proteins**	**Nb of "mito"citations**	**%**
Arabidopsis thaliana	1513	101 (17)	6.67
Sacharomyces cerevisiae	4864	603 (18)	12.39
Drosophila melanogaster	1576	110 (13)	7.55
Caenorhabditis elegans	2214	112 (12)	5.05
Mus musculus	5070	397 (16)	7.83
Homo sapiens	7819	636 (13)	8.13

Figure legends

Fig. 1. Scheme of oxidative phosphorylation in mitochondria. SH, respiratory substrate; 1., substrate dehydeogenation; 2., complex I; 3., complex III; 4., complex IV; 5., proton leak; 6., ATP synthase, 7. ATP/ADP carrier; 8. phosphate carrier; 9., ATP usage

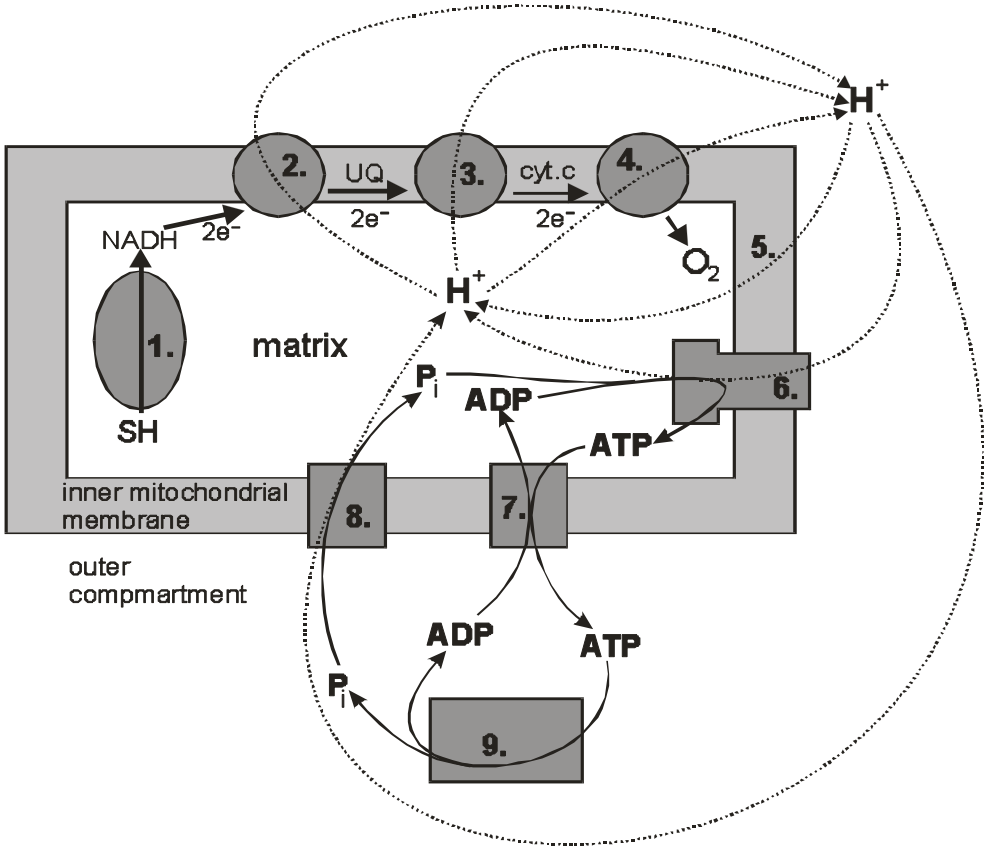

Dynamic Simulation Of Pollutant Effects On The Theonine Pathway In *Escherichia Coli*

Christophe Chassagnole[a1*], Eric Quentin[a2], David A. Fell[b], Pedro de Atauri[c] and Jean-Pierre Mazat[a]

[a] INSERM EMI 9929 and Université de Bordeaux II, 146 rue Léo-Saignat, 33076 Bordeaux Cedex, France.
[b] School of Biological and Molecular Sciences, Oxford Brookes University, Oxford OX3 0BP, U.K.
[c] Departement de Bioquimica I Biologia Molecular, Universitat de Barcelona, Marti I Franques 1, 08028 barcelona, Spain.
Present address: [1] INSA – dGBA 135 Av. de Rangueil F–31077 Toulouse Cedex, France. [2] DIOSYNTH France, BP 26, 60590 Eragny-sur-Epte France.
*Corresponding author: christophe.chassagnole@insa-tlse.fr, phone: +33 (0)5 61 55 94 18, fax: +33 (0)5 61 55 94 00

Abstract - The enzymatic activities of threonine pathway in *Escherichia coli* are sensitive to pollutants such as cadmium, copper and mercury which even at low concentration, can substantially decrease or even block the pathway at several steps. Our aim was to investigate the complex effects on a metabolic pathway of such general enzyme inhibitors with several sites of action, using a previously-developed computer simulation of the pathway. For this purpose, the inhibition parameters were experimentally determined and incorporated in the model. The calculation of the flux control coefficient distribution between the five steps of the threonine pathway showed that control remains shared between the three first steps under most inhibition conditions. Response coefficient analysis shows that the inhibition of aspartate semialdehyde dehydrogenase is quantitatively dominant in most circumstances.

***Keyword*:** Threonine, computer simulation, metabolic control analysis, biosynthetic pathway, pollutants.

Résumé – Les activités enzymatiques de la chaîne de biosynthèse de la thréonine d'*Escherichia coli* sont particulièrement sensibles a des polluants tels que le cadmium, le cuivre et le mercure, qui peuvent diminuer ou bloquer le métabolisme bactérien. Les paramètres cinétiques de ces inhibitions ont été déterminés expérimentalement, puis incorporé dans un modèle mathématique de la voie. Ce modèle a été utilisé pour simuler l'effets de ces inhibition sur le flux de biosynthèse de la thréonine et calculer la répartition des coefficients de contrôle entre les étapes de la voie. Ceci a montré que le contrôle est toujours reparti entre les trois première étapes.

***Mots clés*:** Thréonine, simulation du métabolisme, théorie du contrôle du métabolisme, voie de biosynthèse, polluants.

INTRODUCTION

The enzymatic activities of threonine pathway in *Escherichia coli* are sensitive to pollutants such as cadmium, copper and mercury which even at low concentration, can substantially decrease or even block the pathway at several steps. Such multiple sites of action must be taken into account when considering two important environmental roles of bacteria: in bioremediation of soils and as commensals of mammalian organisms.

Our aim was to evaluate the effects of enzyme inhibitions on threonine production using Metabolic Control Analysis (MCA) [1-5]. For this purpose, a computer simulation of the threonine pathway synthesis [6-8] was used. This model is based on kinetic functions developed from measurements on the pathway enzymes under near-physiological conditions. In order to represent the effects of the different pollutants on the threonine pathway, the model was extended with kinetic terms for the inhibition.

For this purpose, the kinetic parameters describing these inhibitions have been determined experimentally. In the first part of this experimental work, the more potent inhibitors were chosen by screening. Then the effects of these compounds on the different steps of the pathway were measured by titration of the enzyme activities.

The threonine pathway in *E. coli* involves 5 steps from aspartate (figure 1). The first step is important owing to its regulation. It is catalyzed by three isoenzymes: the aspartokinase I (AKI) inhibited by threonine, the synthesis of which is repressed by threonine plus isoleucine (an amino acid synthesized from threonine); aspartokinase III (AK III) inhibited by lysine (which is also synthesized from aspartate in *E. coli*), the synthesis of which is repressed by lysine; and aspartokinase II (AK II), the synthesis of which is repressed by methionine, the third amino-acid synthesized from aspartate in *E. coli* (for a review, see Cohen [9] and Neidhardt [10]). Aspartokinase I and aspartokinase II are bifunctional enzymes which also catalyze the third step, the homoserine dehydrogenase reaction (AKI-HDHI and AKII-HDHII). The amount of aspartokinase II-homoserine dehydrogenase II is low, so it may be omitted in an initial modelling approach.

MATERIALS AND METHODS

Cells

An E. *coli* strain K12 thiaisoleucine-resistant derivative (Tir-8) [11], de-repressed for the threonine operon [12], was used in the study. Bacteria were grown in a minimal medium at 37°C with 0.4 % (w/v) glucose as the carbon source. At the end of the exponential phase, the cells were harvested, washed and frozen at -80 °C in extraction buffer.

Chemicals

The different pollutants tested KNO_3, KNO_2, $CuCl_2$, $CdCl_2$, $HgCl_2$ and $ZnCl_2$ were from Sigma. The other chemicals were as described by Chassagnole et al. [6]

Enzyme Assays

The buffers and the crude extract preparation and the enzyme assays are described in a previous paper [6].

Initial screening

In order to study the pollutants' effects, we decided in the first instance to determine the potential

inhibitions by all of these compounds through a rough screening on all the enzymatic activities, at 5mM or the highest possible concentration given the solubility of the compound in the buffer. All the activities were measured at substrate concentrations around the Km value and the percentage inhibition calculated relative to controls.

IC_{50} and Hill coefficient determination

Each enzyme activity was measured as a function of the concentration of the inhibitory ion. The IC_{50} were calculated directly from the inhibition curves and the Hill coefficient by a classical Hill plot.

Threonine pathway model

The threonine pathway model used here is the culmination of a combined experimental and theoretical study, the details of this work can be found in [6-8]. In order to reproduce the *in vivo* steady-state of the pathway, the measured *in vivo* concentrations of the different substrates and effectors and the enzyme activities have been introduced into the model.

Incorporation of the effects of heavy metals in the model

In order to represent the effects of the different heavy metals on the different steps of the threonine pathway. A non-competitive inhibition term (eq. 1), with a Hill coefficient and a partial effect had been incorporated in each enzymatic rate equation (eq. 2), according to the experimental description of the inhibitions (Table II, III and IV).

$$\left(\frac{1+\left(\frac{I}{IC_{50}}\right)^{n}}{1+\left(\frac{100-\%inh}{100}\right)\left(\frac{I}{IC_{50}}\right)^{n}} \right) \quad \text{(eq. 1)}$$

$$v = \frac{V_m S}{(K_m + S)\left(\frac{1+\left(\frac{I}{IC_{50}}\right)^{n}}{1+\left(\frac{100-\%inh}{100}\right)\left(\frac{I}{IC_{50}}\right)^{n}} \right)} \quad \text{(eq. 2)}$$

where *%inh* represents the maximal limiting inhibition in the case of partial inhibitors.

Simulation

The dynamic modelling of the flux, the intermediates metabolites and the flux control coefficient determination have been done with the SCAMP (Simulation, Control Analysis, Modelling Package) software developed by Sauro and Fell [13-16]. With this software, the flux control coefficients and the overall flux response coefficient to an inhibitor are determined by numerical perturbations of the enzyme activities or inhibitor concentration respectively and recalculation of the corresponding steady state over a specified range of inhibitor concentrations. The program also allows calculation of enzyme elasticities with respect to the inhibitors, and partial response coefficients (the product of an enzyme's flux control coefficient and elasticity with respect to an inhibitor) [1] in order to assess the relative contribution of each enzyme to the total response to the inhibitor.

RESULTS AND DISCUSSION

Initial screening

The pollutants tested on the threonine pathway were nitrate, nitrite, copper, cadmium, mercury and zinc. The results of the initial screen of each of these are shown in table I.

We can see that neither nitrite nor nitrate inhibit the activities, except for weak inhibitions of AKI by nitrate and threonine synthase (TS) by nitrite. However we consider that these compounds will not inhibit the threonine pathway significantly at environmental concentrations. On the other hand, we can see that heavy metals inhibit all enzyme activities; moreover these inhibitions are strong and in some cases total. Hence we decided to study further three of these compounds: cadmium, copper and mercury.

Kinetic characterisation of the inhibition by heavy metals

Each enzyme activity was measured as a function of the concentration of the three toxic compounds cadmium, copper and mercury, at a constant concentration of substrate. Fig. 2 and 3 give some examples of these results. All the enzymes were inhibited by these heavy metals, particularly aspartate semi-aldehyde dehydrogenase (ASD) by cadmium, copper and mercury, TS by copper, AKI and homoserine kinase (HK) by mercury. Mercury is the most potent inhibitor of the whole threonine pathway, though the most sensitive enzyme varies with the metal. The IC50, Hill coefficients and the maximum percentage inhibition of these inhibitions are summarized in table II, III and IV.

Simulation of the effects of different pollutants

The mathematical model has been used to simulate the effects of the different heavy metals (cadmium, copper and mercury) on threonine pathway flux values (figure 4a, 4b, 4c). We can see that the IC_{50} for the pathway flux is always larger than the smallest IC_{50} for the individual steps (table II), in general by a factor of about four.

With the model it was also possible to calculate the flux control coefficient distribution between the different steps of the threonine pathway. In the "*in vivo*" steady-state conditions the control is shared between the three first steps 0.282, 0.249 and 0.466, respectively for the aspartokinase, the aspartic ß-semialdehyde dehydrogenase and the homoserine dehydrogenase. The homoserine kinase and the threonine synthase (respectively 0.005 and 0.000) flux control coefficients can be considered as negligible.

By increasing the cadmium concentration we observe (figure 5a) a transfer of the control from AK and HDH to ASD, reaching a maximum of 0.8 at 1.5 mM. This can be explained by the low IC_{50} for ASD. Up until 1.5 mM, inhibition of ASD makes the largest contribution to the response of threonine flux to cadmium, but above this, the flux control coefficients of AK and HDH rise and these two enzymes make the larger contribution to the continuing pathway response as the cadmium concentration is increased.

By increasing the copper concentration we also observe (figure 5b) in this case a transfer of the control from AK and HDH to the ASD, which attains a flux control coefficient of nearly 1.0. This means that all the control of the flux is shifted to the ASD. This is not just because ASD has the smallest IC_{50}, but because only the ASD can be 100% inhibited. So by increasing the copper concentration, the ASD becomes the only controlling step and the response of the pathway to copper is accounted for almost entirely by the response of ASD even though all the enzymes exhibit significant elasticities with respect to copper throughout the range.

When the mercury concentration increases, we once again observe (figure 5c) a transfer of the control from AK and HDH to the ASD, up to a maximum of 0.9. In this case, however, HK

becomes a dominant controlling step. The first part of the curve can be explained by two facts: firstly the ASD and the HDH can be 100% inhibited, which is not the case for the AK activity, and secondly the ASD IC_{50} (1.66 μM) <<HDH IC_{50} (0.51mM), so for this inhibitor concentration range (0-25 μM) the HDH inhibition is negligible.
In the second part of the curve, the transfer of control from ASD to HK, is explained by the high Hill coefficient (3.7) of this inhibition, reflected in the elasticitiy coefficient (-3.5). Furthermore, as HDH is inhibited, homoserine concentrations start to rise (see Fig. 6), causing further substrate inhibition of the enzyme. Hence at mercury concentrations above 0.025 mM, HDH makes the largets contribution to the pathway's response to mercury.

The variations of the intracellular concentrations of intermediate metabolite of the threonine pathway were also simulated with the model as a function of pollutant concentration. These concentrations: ß-aspartyl phosphate (ASPP), aspartic ß-semialdehyde (ASA), homoserine (HS) and *O*-phosphohomoserine (HSP) are represented as a function of the heavy metals in the figure 6. We can observe a slight increase of ASPP, the substrate of ASD, in all cases. In Figure 6c the rise in homoserine can be seen as HK becomes the more controlling step.

CONCLUSIONS

All these results show the necessity of a model to understand the effects of pollutants such as heavy metals. In fact, these compounds are responsible for multiple effects on the metabolic pathway. So it is not possible to simply correlate the IC_{50} of the individual steps to predict the global effect on the flux. Another motivation for modelling is the simulation of a steady state corresponding to the *in vivo* concentrations of the different substrates and effectors of the threonine pathway. A true steady state with these intracellular concentrations will be difficult to maintain long enough for an experimental flux determination, making direct dissection of the inhibitor effects too difficult by experiment.

ACKNOWLEDGEMENTS

The authors wish to thank the European Union for supporting this work through its Copernicus program.

REFERENCES

[1] Kacser H. and Burns J. A., The control of flux, Symp. Soc. Exp. Biol. 27 (1973) 65-104; reprinted in Biochem. Soc. Trans. 23 (1995) 341-366.
[2] Fell D. A., Metabolic control analysis: a survey of its theoretical and experimental developments, Biochem. J. 286 (1992) 313-330.
[3] Fell D. A., Understanding the Control of Metabolism, Portland Press, London, 1997.
[4] Heinrich R. and Rapoport T. A., A linear steady-state treatment of enzymatic chains; general properties, control and effector strength, Eur. J. Biochem. 42 (1974) 89-95.
[5] Reder C., Metabolic control theory : a structural approach, J. Theor. Biol. 135 (1988) 175-201.
[6] Chassagnole C., Raïs B., Quentin E., Fell D.A. and Mazat, J.P., An integrated study of threonine pathway enzyme kinetics *in Escherichia coli*, Biochem. J. 356 (2001) 415-423.
[7] Raïs B., Chassagnole C., Letellier T., Fell D.A. and Mazat J.P., Threonine synthesis from aspartate in *Escherichia coli* cell-free extracts: pathway dynamics, Biochem. J. 356 (2001) 425-432.

[8] Chassagnole C., Fell D.A., Raïs B., Kudla B., and Mazat J.P., Control of the threonine synthesis pathway in *Escherichia coli*: a theoretical and experimental approach. Biochem. J. 356 (2001) 433-444.
[9] Cohen G.N., Le métabolisme cellulaire et sa régulation, Hermann, Paris, 1967.
[10] Neidhardt F.C., *Escherichia coli* and *Salmonella typhimurium*. Cellular and molecular biology, American Society for Microbiology, Washington D.C, 1987.
[11] Szentirmai A., Szentirmai M. and Umbarger H. E., Isoleucine and valine metabolism properties of *Escherichia coli* XV. Biochemical properties of mutants resistant to thiaisoleucine, J. Bacteriol. 95 (1968) 1672-1679.
[12] Szczesiul M. and Wampler D. E., Regulation of a metabolic system in vitro: synthesis of threonine from aspartate, Biochemistry 15 (1976) 2236-2244.
[13] Sauro H.M., Control Analysis and simulation of metabolism, Ph.D. thesis, Oxford Polytechnic, 1986.
[14] Sauro H.M. and Fell D.A., SCAMP: A metabolic simulator and control analysis program, Math. Comput. Model. 15 (1991) 15-28.
[15] Sauro H.M, SCAMP: A general-purpose simulator and metabolic control analysis program, CABIOS 9 (1993) 441-450.
[16] Fell D.A. and. Sauro H.M., Metabolic control analysis by computer: Progress and prospects, Biomed. Biochim. Acta 49 (1990) 811-816.

LEGEND TO FIGURES

Figure 1: Threonine pathway from threonine in *E. coli*.
The different steps are catalyzed by aspartokinases I, II and III (AK I, AK II and AK III), aspartate semi-aldehyde dehydrogenase (ASD), homoserine dehydrogenase (HDH), homoserine kinase (HK) and threonine synthase (TS).
⊖ means retroinhibition.

Figure 2: Threonine synthase activity as a function of cadmium chloride concentration.
The activity is measured in the presence of homoserine-phosphate 1 mM

Figure 3: Homoserine kinase activity as a function of the mercury concentration.
The activity is assessed in the presence of homoserine 1 mM.

Figure 4: Threonine flux as a function of cadmium (a), copper (b) and mercury (c) concentrations

Figure 5: Flux control coefficient of the threonine pathway activities as a function of cadmium (a), copper (b) and mercury (c). — AK , ··· ASD, − − HDH and −·· HK. (NB: the TS flux control coefficient is not represented because its value is always near zero).

Figure 6: Intermediate metabolite concentrations of the threonine pathway as a function of cadmium (a), copper (b) and mercury (c). — ASPP , ··· ASA, − − HS and −·· HSP.

Figure 1

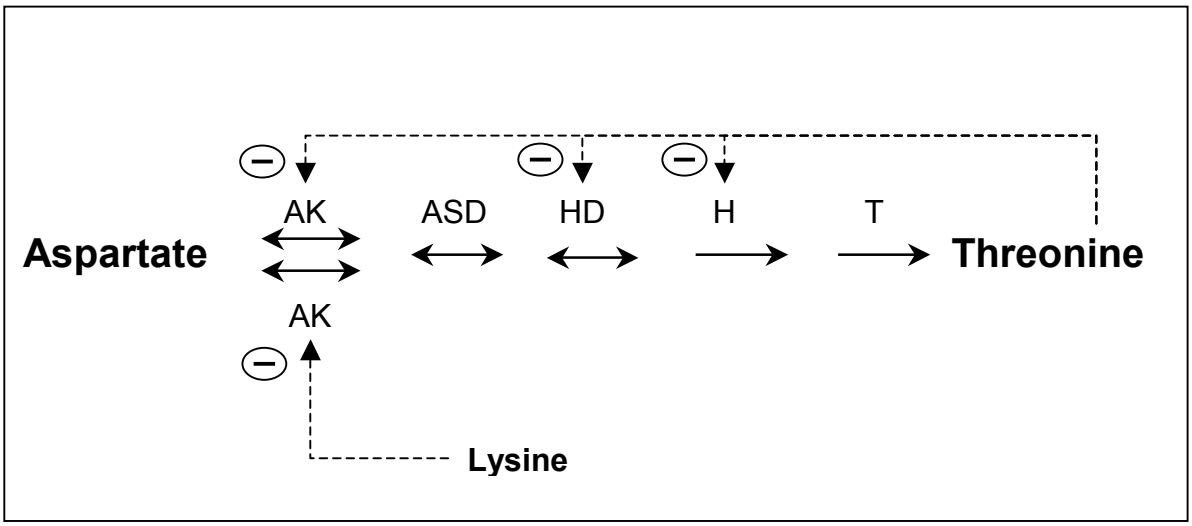

Figure 2

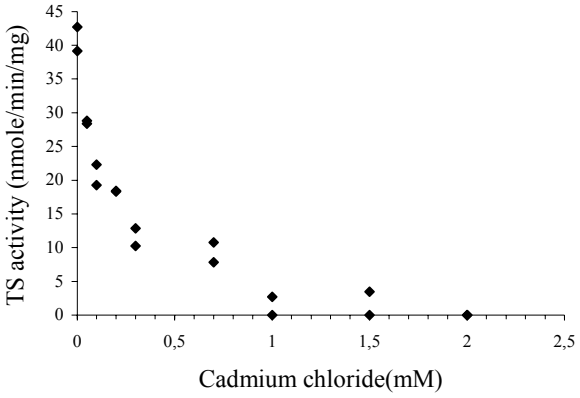

Figure 3

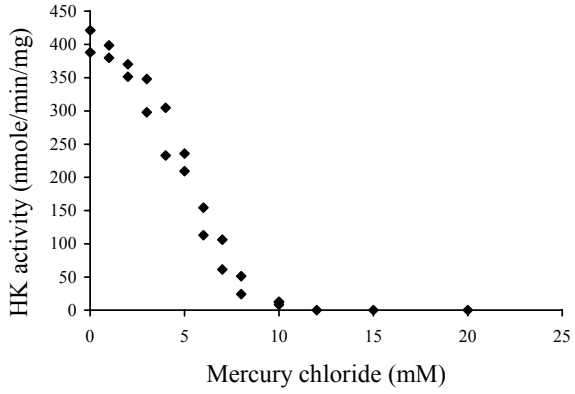

Figure 4

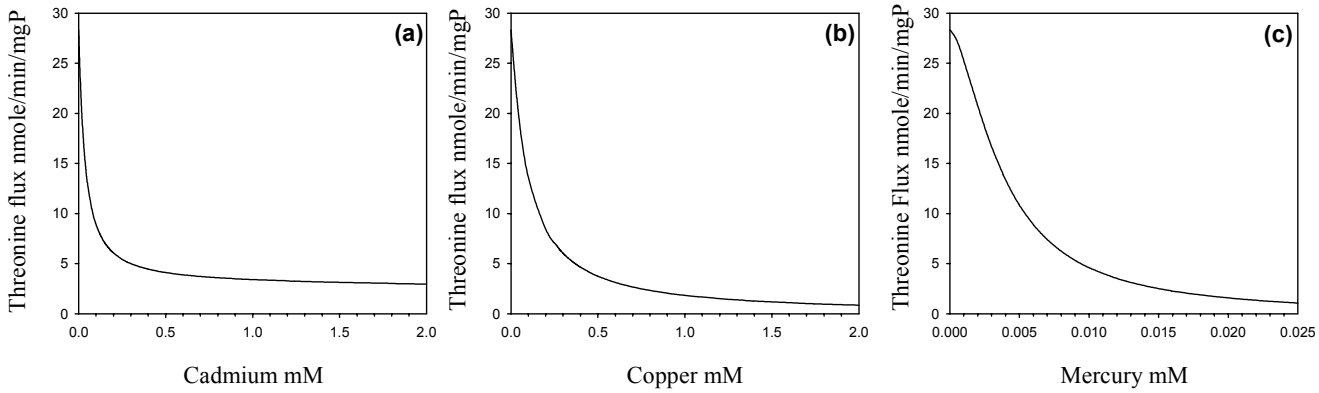

Figure 5

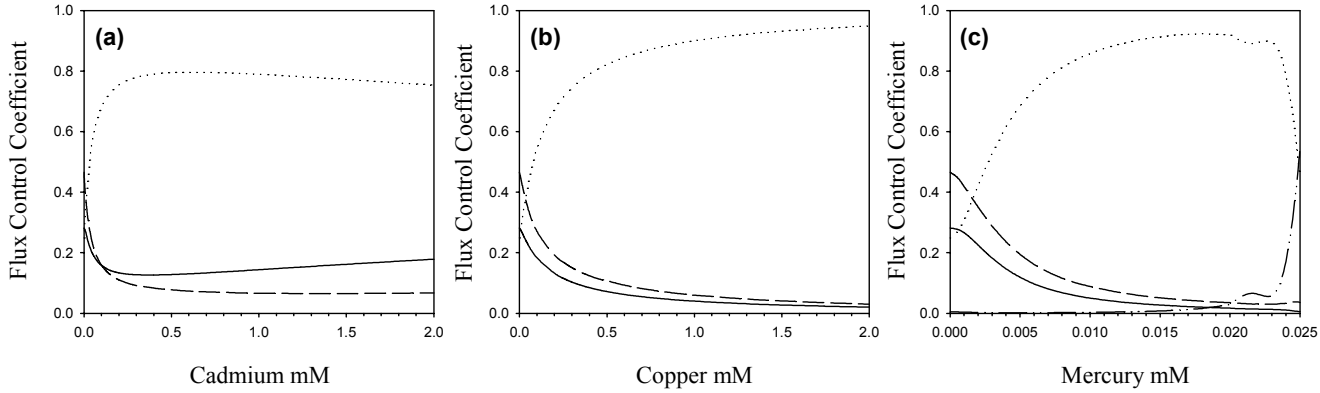

Figure 6

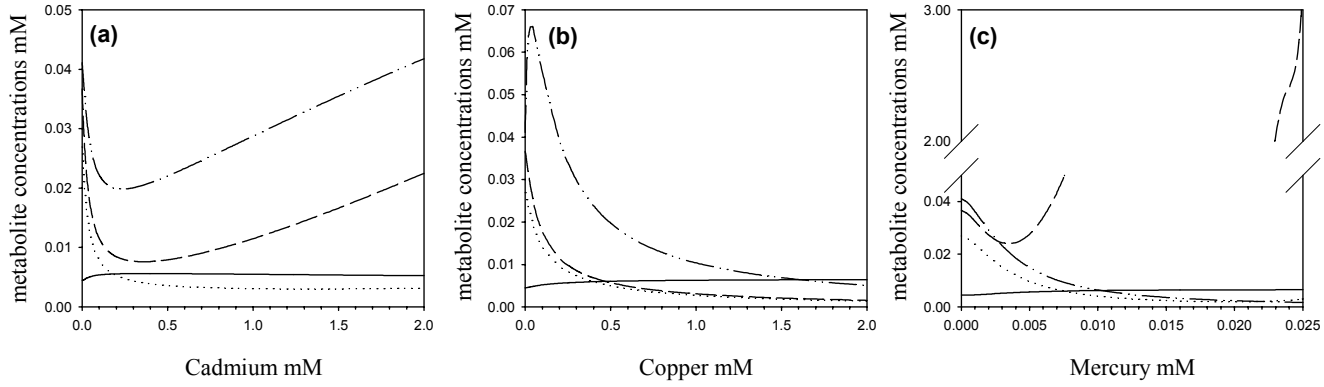

Table I: Percentage of inhibition of toxic compound on enzyme activities.

	mM	AK I	AK III	ASD	HDH I	HK	TS
Nitrate	5	14	n.I.	n.I.	n.I.	n.I.	n.I.
Nitrite	5	n.I.	n.I.	n.I.	n.I.	n.I.	32
Cadmium	5	79	100	97	60	98	100
Copper	0.2	85	63	100	50	36	80
Mercury	1	100	74	100	100	100	95
Zinc	5	100	99	78 (1)	88	100	99 (2)

n.I. : no inhibition (1) : 0.5 mM (2) : 1 mM

Table II : IC_{50} of different heavy metals on enzyme activities and threonine flux.

	AK I	AK III	ASD	HDH I	HK	TS	**Threonine Flux**
Cadmium	2 mM	0.1 mM	12.6 µM	2.76 mM	0.7 mM	0.13 mM	**43 µM**
Copper	62 µM	0.18 mM	33 µM	0.25 mM	0.47 mM	18 µM	**93 µM**
Mercury	0.95 µM	0.73 mM	1.66 µM	0.51 mM	5 µM	92 µM	**3.7 µM**

Table III : Hill number of different heavy metals on enzyme activities.

	AK I	AK III	ASD	HDH I	HK	TS
Cadmium	1.23	0.7	1.17	2.51	1.65	0.79
Copper	1.41	0.92	1.19	1.15	1.35	0.76
Mercury	1.93	1.17	1.71	1.96	3.7	1.25

Table IV: Maximum percentage of inhibition of toxic compound on enzyme activities.

	AK I	AK III	ASD	HDH I	HK	TS
Cadmium	100	100	97	85	100	100
Copper	100	80	100	60	90	100
Mercury	100	100	100	100	100	100

Metabolic analysis in drug design

Athel Cornish-Bowden* and María Luz Cárdenas

CNRS-BIP, 31 chemin Joseph-Aiguier, B.P. 71, 13402 Marseille Cedex 20, France
E-mail address: athel@ibsm.cnrs-mrs.fr

Abstract

Biotechnology is often presented as if progress in the past two decades represented a major success, but the reality is quite different. For example, ten major classes of antibiotics were discovered between 1935 and 1963, but after 1963 there has been just one, the oxazolidones. To illustrate the possibilities of doing better by taking account of the real behaviour of metabolic systems, we can examine how one might modify the activity of an enzyme in the cell (for example by genetic manipulation, or by the action of an inhibitor, etc.) to satisfy a technological aim. For example, if the objective is to eliminate a pest, one might suppose that the effect of an inhibitor could be to depress an essential flux to a level insufficient for life, or to raise the concentration of an intermediate to a toxic level. The former may seem the more obvious, but the latter is easier to achieve in practice, and there are some excellent examples of industrial products that work in that way, such as the herbicide 'Roundup' and antimalarials of the quinine class. A study of glycolysis in the parasite *Trypanosoma brucei* (which causes African sleeping sickness) indicates that for this approach to work the selected target enzyme must have a substrate with a concentration that is not limited by stoicheiometric constraints. That is not necessarily easy to find in a complicated system, and typically needs the metabolic network to be analysed in the computer.

Metabolic analysis / stoicheiometric analysis / uncompetitive inhibition / drug design

Résumé

La biotechnologie est souvent présentée comme si les nouvelles technologies des deux dernières décennies constituaient une réussite éclatante, mais la réalité est toute autre. Par exemple, entre 1935 et 1963 on a découvert dix classes majeures d'antibiotiques ; depuis 1963 on n'en a découvert qu'une seule, les oxazolidones. Pour illustrer les possibilités d'améliorer les résultats en tenant compte du comportement des systèmes métaboliques, nous pouvons examiner comment on peut modifier l'activité d'une enzyme dans la cellule (soit par manipulation génétique, soit par l'action d'un inhibiteur, etc.) pour satisfaire des objectifs biotechnologiques. Par exemple, si le but est d'éliminer une peste, on peut supposer que l'effet d'un inhibiteur puisse être d'abaisser un flux essentiel en-dessous d'un niveau indispensable à la vie, ou d'augmenter la concentration d'une métabolite à un niveau toxique. Le premier semble être le plus évident, mais le second est plus facile à réaliser dans la pratique, et on a d'excellents exemples de produits industriels très importants qui fonctionnent ainsi, comme le « Roundup » utilisé comme herbicide, ou la quinine comme médicament contre le paludisme. Une étude de la glycolyse dans le parasite *Trypanosoma brucei* (responsable de la maladie de sommeil) indique que, pour que cette approche soit efficace, il faut choisir comme cible une enzyme pour laquelle la concentration du substrat ne soit pas limitée par des relations stoechiométriques. Ceci n'est pas forcément facile à trouver dans un système compliqué, et nécessite typiquement une analyse métabolique par ordinateur.

Analyse métabolique / analyse stœchiométrique / inhibition incompétitive / conception de médicaments

Although the human genome project is yielding clues to thousands of new targets for drug development [1], selecting suitable targets is not easy, as we analyse here, and requires a systemic approach, i.e. one that recognizes that enzymes are organized into metabolic systems. Despite the triumphalism implicit in titles such as 'Intelligent drug design' [2] or 'Drug discovery' [3] for supplements in *Nature* and *Science,* there is now increasing recognition that intelligent drug design (or drug design *tout court)* remains something for the future, so that an industry analyst could recently write that 'any regular reader cannot avoid being impressed by the startling failure of the pharmaceutical research effort' [4]. Most currently prescribed antibiotics (and a good fraction of other drugs) are derivatives of agents in clinical use for 30 years or more [5], but this may appear less surprising when considered in the light of the low level of attention given to metabolism. The discovery of new classes of antibiotics has now virtually ceased—ten major classes discovered between 1935 and 1963; one class, the oxazolidones, since then—despite the urgent need for new antibiotics created by broad resistance to almost all existing ones by hospital-adapted pathogenic bacteria. In spite of genetic engineering, combinatorial chemistry, bioinformatics and so on, the impact of the human genome project on drug discovery has been disappointing.

Unfortunately 'intelligent drug design', at least as understood by authors who use the term, appears not to include the idea that what cells do is metabolism and a major thing drugs are supposed to do is to alter metabolism: of the 500 current targets 30% are enzymes and 45% are receptors [6]. To forget metabolism when discussing strategies for drug design [2] or drug discovery [3] (these two supplements barely mention metabolism) is a mistake.

Taking a broader view of biotechnology beyond the development of drugs, efforts to improve yields of industrial processes by overexpressing the enzymes thought to catalyse rate-limiting steps have been equally ineffective. As long ago as 1989 it was known from experiment that overexpressing phosphofructokinase in fermenting yeast by 250% had *no* perceptible effect on the flux to ethanol [7], a result subsequently confirmed in other organisms, but this knowledge did not prevent the investment of vast amounts of money in similarly fruitless quests. In 1989 one could perhaps have explained the absence of known examples of success in terms of commercial secrecy, but a decade later the only plausible explanation must be that no examples are known because no examples exist.

It is known from theoretical considerations [8] as well as experiments such as those in fermenting yeast [7] just mentioned, that increasing metabolic fluxes by significant amounts is very difficult. Decreasing them is easier, but still more difficult than one might hope. However, metabolite concentrations are much less stable than fluxes, and respond far more sensitively to perturbations in enzyme activities. This generalization is proving very helpful for probing the functions of supposedly silent genes [9] and it also suggests that pharmacological effects due to changes in metabolite concentration may be much easier to achieve than ones that require significant changes in fluxes. Significantly, 'Roundup' *(*N-phosphonomethylglycine), commercially by far the most successful of all herbicides, owes its effect to its capacity to raise the concentration of shikimate several hundredfold [10], and quinine, one of the more successful antimalarial drugs, likewise acts by increasing the concentration of haem in treated parasites to toxic levels [11]. Lithium, very effective in the treatment of manic depression, appears to exert its effect by decreasing the level of inositol [12]. Studying how such effects are brought about may offer a useful introduction to how intelligent drug design may one day become a reality. All three of the substances mentioned act by inhibiting enzymes, and all behave as uncompetitive inhibitors.

The common inhibition types are easily confused in experiments in the spectrophotometer, with the result that cases of mixed inhibition are frequently reported as competitive. However, steady-state experiments at substrate and product concentrations that are decided and fixed by the experimenter are very misleading as a model of inhibition *in vivo,* where

concentrations are not fixed at all, and certainly not by an external agent such as an experimenter. For a typical enzyme that catalyses a reaction in the middle of a metabolic pathway it is a better approximation (though still not exact) to consider that the rate is fixed and that the substrate and products are adjusted by the enzymes that use them to whatever values will sustain the appropriate flux. In these conditions competitive and uncompetitive inhibition become very different from one another [13] and the uncompetitive component becomes the main determinant of the response of the system to a mixed inhibitor.

These points are illustrated in *figure 1.* When the inhibition is competitive *(figure 1c),* effects on both flux and metabolite concentrations are very slight, but all become much larger when the inhibition is un-competitive *(figure 1d).* In the latter case the slopes are small at very low inhibitor concentrations, but the significant curvature causes the lines to become rapidly much steeper as the inhibitor concentration increases. The essential point is that a molecule that competes with a substrate is a molecule that a substrate can compete with, and so the effect of a competitive inhibitor can be nullified by relatively minor adjustments of the concentrations around the inhibited enzyme. By contrast, effects of uncompetitive inhibitor are potentiated by the variations in substrate that they generate, and fairly modest levels of inhibition may therefore produce huge changes in substrate concentration. It is essentially this kind of effect that is exploited by Roundup, which inhibits 3-phosphoshikimate 1-carboxyvinyltransferase, uncompetitively with respect to 3-phosphoshikimate [10].

Figure 1b shows the effects of varying enzyme activity without necessarily implying the presence of an inhibitor. In the basal state (point L on the curve), small variations in the activity of E 5 are almost without effect: in relative terms the effect of the flux is only 13% of the variation in enzyme activity. However, by the time the activity is decreased to about one-third (point M, corresponding approximately to the point in *figure 1d* where the steady state is lost) changes in flux are almost exactly proportional to changes in enzyme activity. On the other hand, if the basal activity had been twofold higher (point N), the system could stand quite large changes in activity in either direction with almost no effect on the flux. This type of curve explains why organisms can usually tolerate quite large losses of activity of many enzymes with almost no effect of phenotype, as studied for example in the context of mitochondrial diseases [14, 15].

Designing an inhibitor with significant uncompetitive character is a much more difficult task than designing a competitive inhibitor, because it cannot just be a substrate analogue. This difficulty is not an adequate reason for not attempting it, however, because solving a difficult task is likely to be more rewarding than solving an easy task if its solution is potentially useful and the solution to the easy problem potentially use-less. Nonetheless, the systemic context of the inhibition always needs to be considered because there are at least two circumstances where uncompetitive inhibition may not be much more effective than competitive.

The first of these is that some enzymes do act *in vivo* in environments resembling the constant-concentration conditions of the spectrophotometer: an enzyme that acts on glucose at the beginning of a minor pathway, for example, will have very little effect on the glucose concentration in any ordinary conditions, because that is determined by controls on the major glucose-using pathways like glycolysis and glycogen synthesis; such an enzyme can therefore be treated like an enzyme in a spectrophotometer, and will respond to competitive inhibition as readily as to uncompetitive inhibition, unless feedback loops ensure that its activity responds to demand for the product of the minor pathway, in which case it may largely ignore any kind of inhibitor.

The second point is that a metabolite concentration can only show a large response to changes in the activities of enzymes that consume it or produce it if it is largely free from stoicheiometric constraints. Some constraints are obvious from inspection: for example, in a cell with a fixed total NAD concentration the concentrations of neither reduced nor oxidized NAD

can exceed the fixed total. However, much more complicated constraints may also exist, and identifying these may require stoicheiometric analysis by computer.

Glycolysis in *Trypanosoma brucei (figure 2),* illustrates all of these points. It not only provides an example of a stoicheiometric relationship that one would be unlikely to discover by inspection, but it is also a very attractive system to model in the computer for several other reasons. *T. brucei* is responsible for a disease of major economic importance, African sleeping sickness, and is thus a major focus of research into tropical diseases. Its bloodstream form has possibly the simplest metabolism of any known organism, glycolysis accounting for nearly all of its metabolic activity, with glucose its only energy source [16, 17]. There is therefore some hope that it may be possible to model essentially the whole of its metabolism in the computer with experimentally deter-mined parameters for all the enzymes. Not only that, but most of the currently available kinetic data come from a single research group working to high standards, so variations due to arbitrary differences between the conditions used in different laboratories are largely avoided. All of this allowed the construction of a computer model [18, 19] that is about 60% complete, in the sense that it includes about 60% of the experimentally determined values that an ideal model would contain. With the possible exception of models of the human erythrocyte [20] no other metabolic model even approaches this degree of completeness.

Although at first sight the model in *figure 2* suggests numerous po-tential targets for drug design, metabolic simulations have shown that the real number of useful targets is much smaller. Computer analysis of the model in *figure 2* revealed four distinct stoicheiometric constraints on the metabolite concentrations. (The matrix algebra necessary to arrive at the stoicheiometric relationships systematically is explained elsewhere [21].) Three of these—oxidized and reduced NAD in the glycosome, adenine nucleotides in the glycosome, adenine nucleotides in the cytosol—are obvious from inspection, but the fourth, involving the metabolites marked by asterisks in the scheme, is not. It includes most of the transferable phospho groups in the glycosome, but not all of them: 3-phosphoglycerate is not involved, and 1,3-bisphosphoglycerate is counted only once even though it has two transferable phospho groups; it also includes cytosolic dihydroxyacetone phosphate and glycerol 3-phosphate (but not other cytosolic molecules, such as cyto-solic ATP). Once recognized, this relationship can be rationalized as representing that part of the glycosomal phosphate pool that is not accounted for by uptake of inorganic phosphate and export of 3-phos-phoglycerate.

The existence of the stoicheiometric constraints may appear to be of purely academic interest, but they have a practical importance as well, because they place severe restrictions on the possible targets of an inhibitor intended to destroy the trypanosome by acting in a similar way to Roundup in plants. As the four constraints involve nearly all of the metabolites in the glycosome, they rule out many of the enzymes as useful targets for uncompetitive inhibition. Of the few that remain, all but the pyruvate transporter are ruled out by other considerations [19], so that instead of the wealth of potential targets suggested by visual inspection of *figure 2* there is in reality just one. Until recently we overlooked a paper that bears directly on this point, and suggested the pyruvate transporter as a good target on the basis of theoretical analysis [19] without mentioning the experimental observation that inhibiting it *in vivo* does indeed cause the pyruvate concentration to rise, followed by osmotic Shock and, probably, death [22].

A frequent difficulty in simulations of metabolic pathways is the absence of experimentally determined kinetic parameters for reverse reactions, especially for reactions considered to be irreversible. Normal-ly the researcher has to choose between guessing the parameters for the reverse reaction from the equilibrium constant, or treating the reaction as irreversible. When the equilibrium constant is very high, as with pyruvate kinase, one may expect it not to matter one way or the other, but when simulating the *T. brucei* model we found that it did. The distribution of flux control was quite different in the two cases, with pyruvate transport, a step with no control at all with pyruvate kinase irreversible, becoming the second most

important step when pyruvate kinase was allowed to be reversible. This was a surprising result, and although resolving it was not very important for the *T. brucei* model as such, it was desirable to study the general implication that all metabolic models would need to be composed entirely of reversible steps if they were to give valid predictions.

The explanation [23] of this apparent anomaly proved to be quite simple, and relates more to the practices of biochemists than to the underlying biochemistry. There is no fundamental reason why an irreversible reaction should be insensitive to its product, as one may readily see from the reversible form of the Michaelis-Menten equation [24]:

$$v = \frac{k_A e_0 a - k_P e_0 p}{1 + \frac{a}{K_{mA}} + \frac{p}{K_{mP}}}$$

in which v is the rate, k_A, k_P, K_{mA} and $K_{mP}$are constants, e_0 is the total enzyme concentration, and a and p are the substrate and product concentrations respectively. Assuming irreversibility means assuming that the negative term in the numerator is negligible, but assuming insensitivity to product means assuming not only this but also that the term in p in the denominator is negligible. Many enzyme reactions are known that are irreversible for practical purposes but which are nonetheless inhibited by their products. In practice, however, over many years metabolic models have nearly always confused these two effects: enzymes that have been treated as irreversible have normally been exempt from product inhibition as well.

In the case of the model of glycolysis in *T. brucei,* making pyruvate kinase subject to inhibition by pyruvate (but still irreversible) proved sufficient to render the behaviour indistinguishable from that with a fullyreversible equation for this enzyme [23]. Thus the absence of product inhibition and not of reversibility was responsible for the anomaly noted earlier [19]. What is important is transfer through the pathway of information about the concentrations of metabolites: adequate regulation of any metabolic pathway requires mechanisms for enzymes early in the pathway to receive information about the concentrations of metabolites at the end [23]. The simplest mechanism is provided by serial product inhibition of all the enzymes in the system, but although this can regulate fluxes quite adequately it is very unsatisfactory for living systems because variations in flux are accompanied by huge variations in metabolite concentrations. In practice, therefore, living organisms virtually always obtain a more direct transfer of information by incorporating cooperative feedback inhibition [25].

The human genome project is suggesting as many as 30000 human gene products as research targets for drug development. Testing all these will be extremely expensive, with operation on a very large scale, and it will be essential to make efforts to restrict the number of targets to ones with a real chance of success. Metabolic simulation, as discussed here can help enormously to reduce the costs.

References

[1]Agnew, B., When pharma merges, R&D is the dowry, Science 288 (2000) 1952-1953.
[2] Supplement on Intelligent Drug Design, Nature 384 (suppl.) (1996) 1-26.
[3] Supplement on Drug Discovery, Science 288 (2000) 1951-1981
[4] Horrobin, D. F., Realism in drug discoveryÑcould Cassandrabe right? Nature Biotechnol. 19 (2001) 1099-1020.
[5] Rosamond, R., Allsop, A., Harnessing the power of the genomein the search for new antibiotics, Science 288 (2000) 1973-1976.
[6] Drews, J., Drug discovery: a historical perspective, Science 288 (2000) 1960-1964.

[7] Schaaff, I., Heinisch, J., Zimmermann, F. K., Overproduction of glycolytic enzymes in yeast, Yeast 5 (1989) 285-290.
[8] Kacser, H., Burns, J. A., Fell, D. A, The control of flux, Biochem. Soc. Trans. 23. (1995) 341-366.
[9] Cornish-Bowden, A., Cárdenas, M. L. Silent genes given voice, Nature 409 (2001) 571-572.
[10] Boocock, M. R., Coggins, J. R., Kinetics of inhibition of 5-*enol*pyruvylshikimate-3-phosphate synthase by glyphosate, FEBS Lett. 154 (1983) 127-133
[11] Enserink, M., Malaria researchers wait for industry to join fight, Science 288 (2000) 1956-1958.
[12] Berridge, M. J., Downes, C. P., Hanley, M. R, Neural and developmental actions of lithium: a unifying hypothesis, Cell.59 (1989) 411-419.
[13] Cornish-Bowden, A., Why is uncompetitive inhibition so rare? FEBS Lett.203 (1986) 3-6.
[14] Mazat, J.-P., Rossignol, R., Malgat, M., Rocher, C., Faustin,B., Letellier, T., What do mitochondrial diseases teach us about normal mitochondrial functions...that we already knew: threshold expression of mitochondrial defects, Biochim.Biophys. Acta 1504 (2001) 20-30
[15] Aimar, M., Korzeniewski, B. Mazat, J.-P., Nazaret, C.,Virtual mitochondria and their control, Comp. rend. Acad. Sci., (2002)
[16] Opperdoes, F. R., Compartmentation of carbohydrate metabolism in trypanosomes, Annu. Rev. Microbiol. 41 (1987) 127-151.
[17] Michels, P. A. M., Hannaert, V., Bringaud, F., Metabolic aspects of glycosomes in Trypanosomatidae-new data and views, Parasitol. Today16 (2000) 482-489.
[18] Bakker, B. M., Michels, P. A. M., Opperdoes, F. R., Westerhoff,H. V., Compartmentalized glycolysis in bloodstream form *Trypanosoma brucei* can be understood in terms of the kinetics of the glycolytic enzymes, J. Biol. Chem. 272 (1997) 3207-3215.
[19] Eisenthal, R., Cornish-Bowden, A. Prospects for antiparasitic drugs: the case of *Trypanosoma brucei,* the causative agent of African sleeping sickness, J. Biol. Chem. 273 (1998)5500-5505.
[20] Mulquiney, P. J., Kuchel, P. W., Model of 2,3-bisphosphoglyceratemetabolism in the human erythrocyte based on detailed enzymekinetic equations: equations and parameter treatment, Biochem. J. 342 (1999) 581-596.
[21] Cornish-Bowden, A., Hofmeyr, J.-H. S., The role of stoicheiometric analysis in studies of metabolism: an example, J. theor. Biol. (2002) in press
[22] Wiemer, E. A. C., Michels, P. A. M., Opperdoes, F. R., The inhibition of pyruvate transport across the plasma membrane of the bloodstream form of *Trypanosomabrucei* and its metabolic implications, Biochem. J. 312 (1995) 479-484.
[23] Cornish-Bowden, A., Cárdenas, M. L., Information transfer in metabolic pathways: effects of irreversible steps in computer models. Eur. J. Biochem. 268 (2001) 6616-6624
[24] Cornish-Bowden, A., Fundamentals of Enzyme Kinetics, 2nd edn., pp. 37-40, Portland Press, London, 1995.
[25] Cornish-Bowden, A., Hofmeyr, J.-H. S., Cárdenas, M. L., Strategies for manipulating metabolic fluxes in biotechnology, Bioorg. Chem. 23 (1995) 439-449

Figure Legends

Figure 1. Effects of inhibition on an enzyme in the middle of a long pathway. Panel(a) shows a pathway of ten reactions converting a starting material X_0 into as ink metabolite X_{10} via nine intermediates S_1, S_2 … S_9. The concentrations of X_0 and X_{10} are assumed to be10 and 0 arbitrary units) respectively, and those of the intermediates are those necessary to achieve a steady state. Each enzyme apart from E_5 is assumed to follow reversible Michaelis-Menten kinetics with limiting rate 10 in the forward direction, equilibrium constant 5 in favour of the forward direction, and Michaelis constants 1 and 5 for the forward and reverse reactions respectively. In the case of E_5, competitive inhibition was simulated by replacing the Michaelis constants for both directions by apparent values obtained by multiplying by a factor $(1 + [I]/K_{ic})$, where [I] is the inhibitor concentration and $K_{ic} = 1$; uncompetitive inhibition was simulated by replacing both limiting rates and Michaelis constants for both directions by apparent values obtained by multiplying by a factor $(1 + [I]/K_{iu})$, where [I]is the inhibitor concentration and $K_{iu} = 1$. Panel (b) shows the dependence of the flux through the pathway in the absence of inhibition on the activity of E_5 relative to the basal state (point **L**). The point **N** illustrates how the flux would depend on enzyme activity if the basal activity were twofold higher. Panel (c) shows the effect of a competitive inhibitor on the flux through the pathway and on the concentrations of the substrate (S_4) and product (S_5) of E_4. Metabolites earlier in the pathway behave like S_4,, and those later in the pathway like S_5, but in both cases with smaller slopes. Panel (d) shows the corresponding effect of an uncompetitive inhibitor. No steady state could be reached in the grey region at inhibitor concentrations above 1.7. The point labelled **L** refers to the same state as the point labelled **L** in panel (b); the point labelled **M** refers to a state similar to that of the point labelled **M** in panel (b). The labelling of the left-hand ordinate axis in panel (c) applies also to panel (d), and the labelling of the right-hand ordinate axis in panel (d) applies also to panel (c)

Figure 2. The glycolytic pathway in bloodstream form *Trypanosomabrucei.* There are four compartments, labelled Host blood, Cytosol, Glycosome and Mitochondrion. Dihydroxyacetone phosphate and glycerol 3-phosphate diffuse between the glycosome and the cytosol, but the two transport steps are not explicitly shown; glycerol 3-phosphate is reoxidized under aerobic conditions to dihydroxyacetone phosphate on the membrane of the mitochondrion.'GROWTH' represents all of the steps in the rest of metabolism that are driven by dephosphorylation of ATP. Each of the metabolites labelled * is counted once in the stoicheiometric constraint discussed in the text; each of those labelled ** is counted twice.

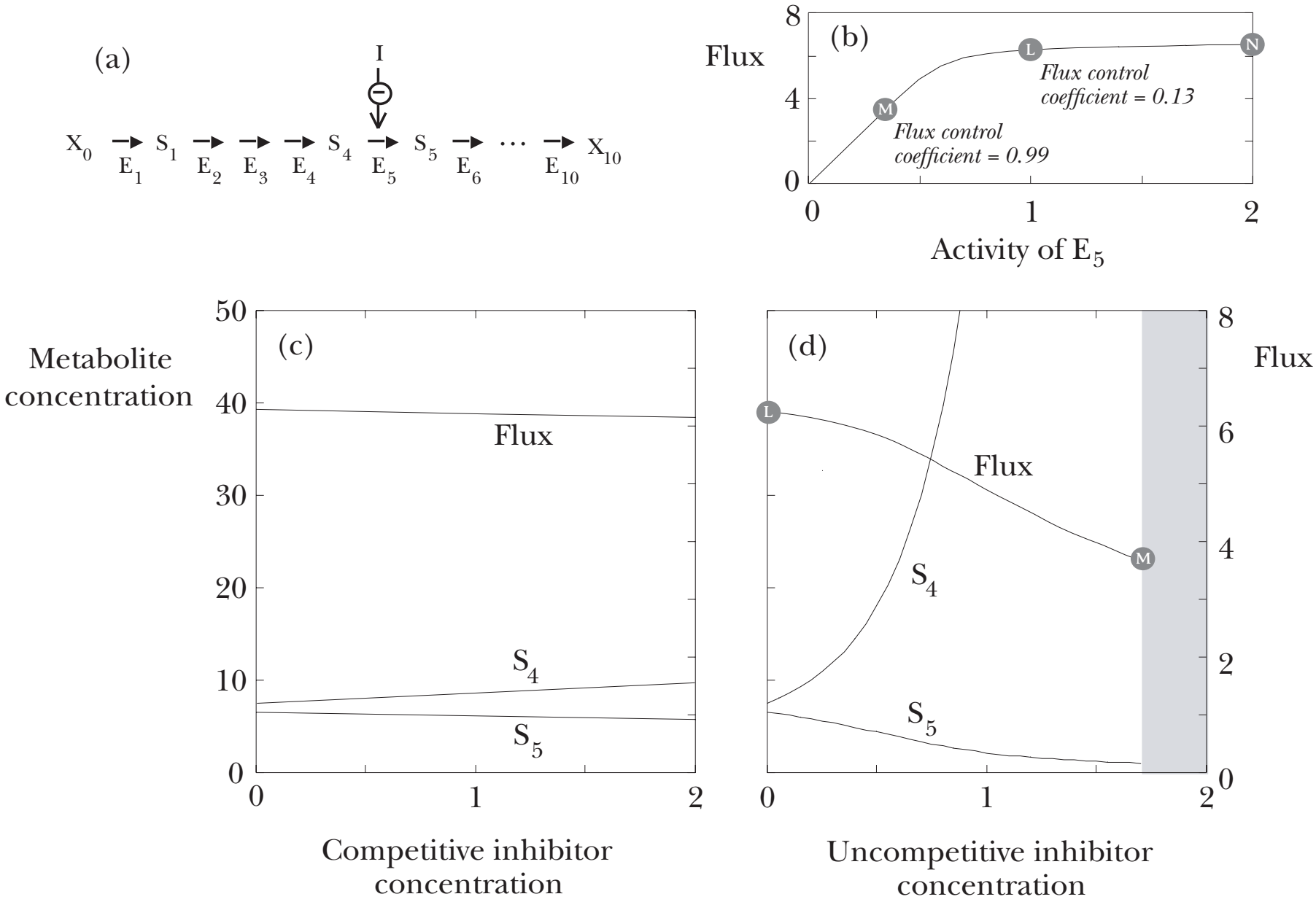

Athel Cornish-Bowden and María Luz Cárdenas: "Metabolic analysis in drug design", Fig. 1

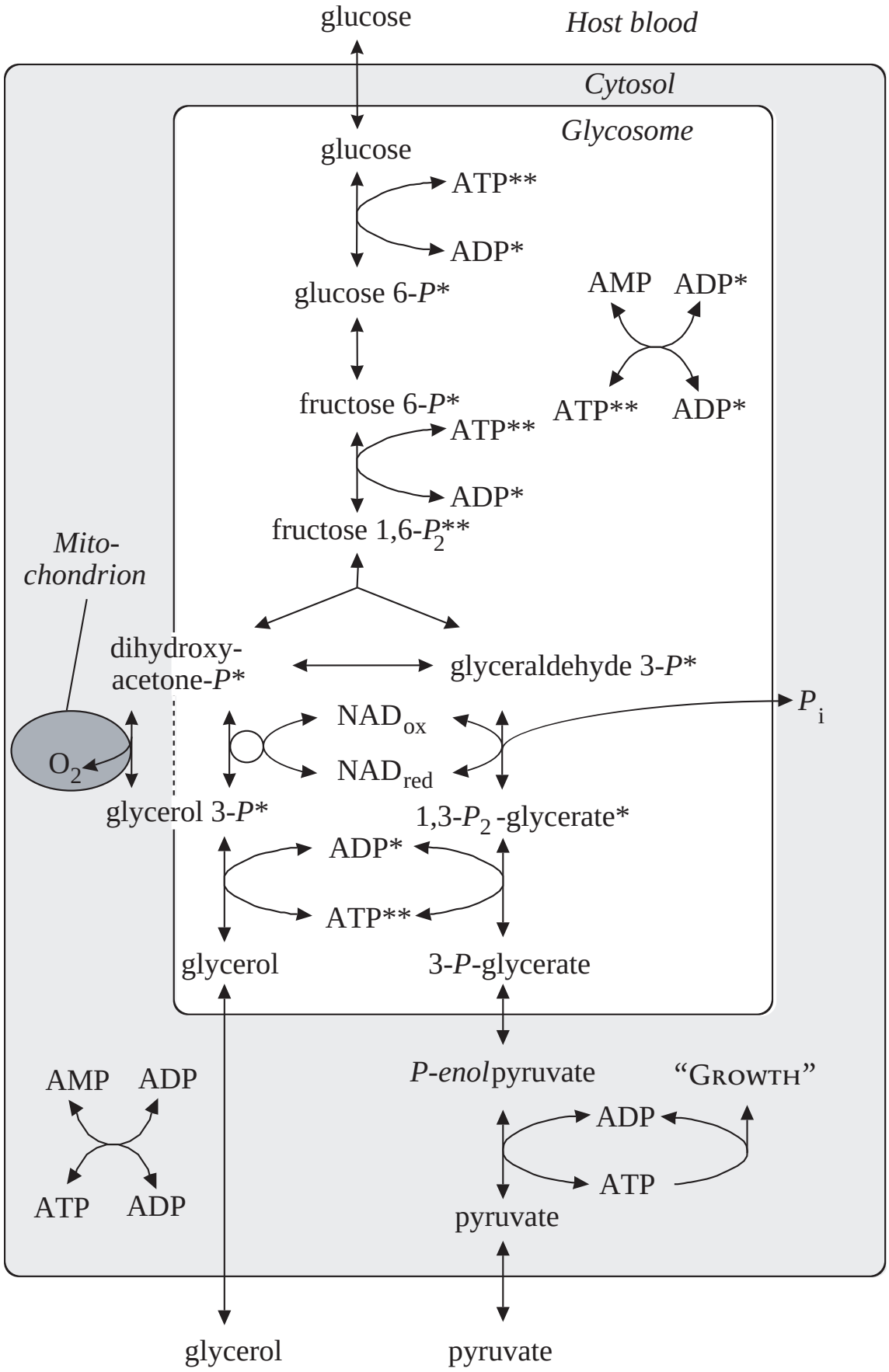

Athel Cornish-Bowden and María Luz Cárdenas: "Metabolic analysis in drug design", Fig. 2

Network Complexity

D J Raine* & V Norris+

*Department of Physics and Astronomy, University of Leicester, Leicester, LE1 7RH, UK
+Laboratoire des processus ioniques cellulaires UPRES A CNRS 6037, Faculté des Sciences et Techniques de Rouen , F76821 Mont Saint Aignan, France

Abstract

We discuss the background to the recent explosion of interest in the structure of homogeneous networks. We include a brief review of 'small worlds' and of the scale-free models that exhibit a power law distribution of nodes as a function of the number of links to or from them. The so-called standard canonical law of Mandelbrot is also considered and some examples from biology given. We then present the various ideas of the complexity of a network and introduce a measure that we call β-complexity. Finally we show how this notion might arise from a thermodynamics of stationary systems maintained far from equilibrium by constraints.

1. Prehistory

Until relatively recently it was widely believed that naturally occurring, homogeneous networks could be at least adequately modeled as random. Relational networks, such as food webs, which show a trophic structure [1], are consequently not homogeneous so are not counterexamples. Other relational graphs do however turn out to have interesting statistical properties and their structure may provide insights in many areas of science.

To set the scene we begin briefly with random graphs of N nodes, often called ER graphs [2]. These graphs are obtained by connecting randomly chosen pairs of nodes with probability p. Interesting questions that can be addressed usually involve the way in which properties scale with N or with p. For example, the smallest number of edges connecting randomly chosen nodes averaged over a random graph scales as log$N$. On the other hand, the appearance of a dominant connected subset sets in around $p = 1/N$. In the following we shall refer to networks and graphs virtually interchangeably, except that we shall regard networks always as connected.

Of most interest to us is the distribution of the degrees of the nodes, that is the probability $p(k)$ of picking a node having k edges, or, equivalently, the expected number of nodes of degree k, $Np(k)$. For the ER graphs this is given by a Poisson distribution

$$p(k) = \frac{\mu^k}{k!} e^{-\mu}$$

where $\mu = 2Np$ is the mean number of edges per node. (Strictly this is the distribution obtained by averaging over many realisations of the graph, but will hold to a good approximation for any particular realisation.) It is a simple matter to compare this with the distribution of node degrees in naturally occurring networks. Perhaps the most interesting feature of the distribution is how many networks in nature do not actually follow it. In fact, many recent investigations have shown power law distributions over much of the range of degrees. Examples range from metabolic networks [3, 4] and protein networks [5] to the internet, co-authorship, citations and the language structure (see the table in [6]). These networks have come to be called 'scale-free' [7].

It is obviously of interest to know how such networks can be constructed, since this may give insight into the evolution of these systems. We shall discuss various evolutionary models in section 2. It is also important to have some feel for the relevant properties of these networks. The most remarkable property turns out to be what has become known as the 'small worlds' structure. We shall discuss this also in section 2. We shall then introduce what we think of as a complexity parameter for these networks. Small worlds networks as originally constructed by Watts and Strogatz are not scale free. We shall extend the idea of a complexity parameter to a close relative of the power law distribution introduced by Mandlebrot in section 3. We shall then look at some examples of complexity in these networks applied to genetic expression. In section 4 we shall make some suggestions for the development of the theory of networks as models for a class of non-equilibrium self-organised structures.

2. Network models

The standard approach to the construction of network models has two key ingredients: growth of the number of nodes and a corresponding law of attachment, and reconnection. The original model of a 'small world' (SW) network is now widely known [8, 9] and makes use of the second of these only. We take a ring of nodes each initially connected to their k-nearest neighbours and, with probability p, rewire each connection randomly to a new node. The attraction of this network is that it interpolates between order and randomness in a very clear way. For $p = 0$ (no rewiring) the network is fully ordered; for $p = 1$, the network is fully random.

Two parameters turn out to be of particular interest: these are the clustering coefficient and the diameter, or characteristic path length.

The clustering coefficient C tells us what fraction of the nodes linked to a given vertex are, on average, themselves linked. For a random graph $C = \mu$ and for an ordered graph with each node connected to its μ nearest neighbours $C = 3(\mu - 2)/4(\mu - 1)$ [6]. For the small world, C can be computed numerically and is shown in figure 1.

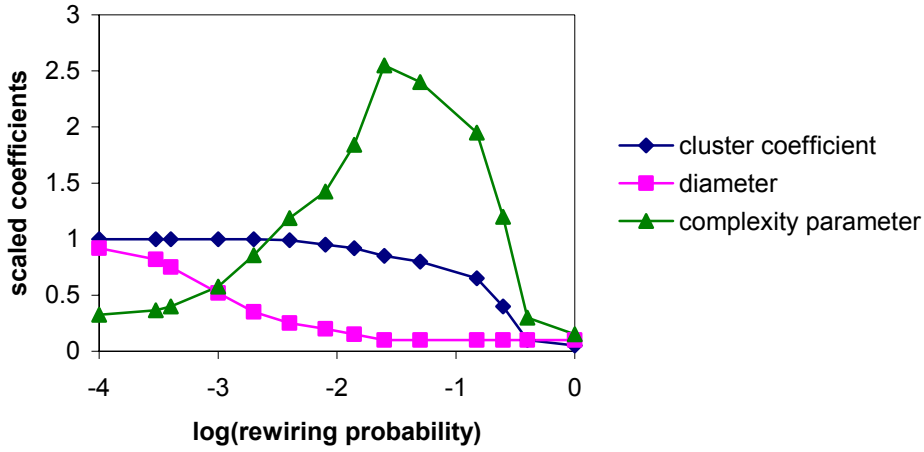

Figure 1. The ratio of clustering coefficient to characteristic length scale (or diameter) of the small world network of Watts and Strogatz [8] behaves as a complexity parameter.

Strictly we should distinguish between the diameter (the maximum number of edges in the shortest path between any pair of vertices) and the characteristic path length (the shortest distance between randomly chosen pairs of vertices averaged over the network). For convenience we shall use the term diameter even when we mean the latter of these, since in general they both scale in the same way. The diameter L of an ordered network scales as the number of nodes N; the diameter of a random network scales as $\log N$. Exact calculations (or even good analytical estimates) of L are notoriously difficult, so the diameter of the SW network as a function of the rewiring parameter p comes from numerical computation as shown schematically in figure 1. Note that C remains high even as L approaches the random regime. Many other networks are now known to exhibit this small worlds behaviour including the scale free networks to be discussed below.

A number of approaches have been proposed to define the complexity of a network. In graph theory the complexity $\kappa(G)$ of the network G is defined as the number of different spanning trees of the network, and can be related to algebraic properties of the incidence matrix (see below) of the graph [10]. Structural complexity [11] of a graph can be defined in terms of the number of parameters required to define it. Edge complexity [9] has been defined in terms of the averaged variability of the second shortest path between nodes. What all of these definitions have in common, and in contrast to the notion of algorithmic complexity in computer science, is that both ordered systems and random ones have zero complexity. From the graph of figure 1 we see that the parameter C/L has the form of a measure of network complexity. It is low for both ordered and random networks at the extremes ($p = 0$ and $p = 1$) and high in between. We shall adopt this as a measure of complexity, which we shall call β-complexity.

The degree distribution of the SW network is similar to a random graph, but with a somewhat smaller variance for a given mean number of edges per node, and hence is unlike the many examples of natural homogeneous networks. To obtain a power law distribution, as well as reconnection, we have to allow preferential attachment of the new nodes in a growing network,. In the absence of reconnection we can attach each of the μ edges of a new node to existing nodes of degree k_i with probability proportional to k_i [7]. This gives a power law $P(k) \propto k^{-3}$. Altering the probability of attachment from k_i to k_i^{α} does not give a power law distribution [12], but allowing for some rewiring of the growing network can give a power law [13]. Table III of [6] summarises some of the methods used to grow networks and the resulting distributions. These differ in the rules for growth, rewiring and reattachment and ageing of nodes and can be tuned to a range of power law indices.

3. The Standard Canonical Distribution and β-complexity

The power law distribution of word frequencies with rank, originally found by Zipf, was generalized by Mandelbrot [14] to what he called the standard canonical law (SCL), which gives the probability of occurrence of rank r as

$$p_r = \frac{P}{(r+\mu)^{\beta}},$$

where P and β are constants and μ is determined by $\Sigma p_r = 1$. For many purposes this is not only a more accurate representation of the data than a power law, but more convenient to work with. Examples of network degree distributions that fit this form include word frequencies [15], (where the network arises from by connecting words that occur together or in close proximity). The

movie actor collaboration network and co-authorship network of neuroscientists also appear to fit this form better than the power law showing the characteristic curvature for small r. Although not strictly networks, rates of protein expression [16], and company sizes [17] also follow this distribution. The average number of edges per node is $\Sigma r p_r \sim \mu/(\beta - 1)$.

The parameter β acts as an 'inverse temperature' [14] of the distribution. High values of β give a narrow range of degrees, equivalent to a small vocabulary; low values of β or high temperature correspond to a flatter distribution of nodes. The SCL distribution therefore interpolates between a random network with nodes of fixed degree and a random network with equal numbers of nodes of each degree (although such distributions which have $\beta < 1$ cannot be constructed). Obviously we expect the complexity of these networks to be related to β.

The question therefore arises as to whether we can estimate C/L for the SCL. Under certain assumptions about the absence of correlations in the network one can show that the SCL is approximately preserved for higher order neighbours with $\mu_2 \sim \mu^2$ for next-nearest neighbours and so on. We then introduce aliases for C and L [18], which we expect to have approximately the same temperature dependence as the exact quantities. We shall find that our definition of complexity does then indeed have the expected behaviour.

3.1 Matrix representation of graphs:

The adjacency matrix of a graph A is the matrix of which the i, j element is 1 if there is an edge between nodes i and j and is zero otherwise. An undirected graph is one for which $a_{ij} = a_{ji}$. Thus there is an edge connecting nodes i and j if $a_{ij} = 1$. Consider now the matrix A^2. There will be an edge connecting i and j via some node k if the $(i, j)^{\text{th}}$ element $a^{(2)}_{ij}$ of A^2 is non-zero.

An alternative representation of a graph, given by the incidence matrix (which we mentioned in connection with complexity based on spanning trees) is the matrix B with $b_{ij} = 1$ if the i^{th} edge is incident to the j^{th} node with $b_{ij} = 0$ otherwise.

3.2 Alias for *C* :

There will be a triangle connecting node i to itself if $a^{(3)}_{ii}$, the diagonal element of A^3, is non-zero. (In fact the value of the diagonal element is 6 times the number of such triangles.) Thus, defining the trace of a matrix as the sum of its diagonal elements, the number of triangles is

$$\Delta \propto \text{trace}(A^3).$$

If $P(a^{(3)}_{ii})$ is the probability that $a^{(3)}_{ii} \neq 0$ then the expectation value of the trace in a network of N nodes is $NP(a^{(3)}_{ii})$. But we know the distribution of non-zero entries in A^3 is given by the SCL distribution

$$P_3(k) = \frac{(2^{\beta-1/2}P)^3}{(k+\mu_3)^\beta};$$

i.e. $P_3(k)$ is the probability of finding a row of k non-zero entries in A^3. Now, assuming these entries are randomly distributed in the row, we get

$$P(a^{(3)}_{ii}) = \sum P_3(k)(k/N),$$

and hence $\Delta \propto P^3\mu_3$.

To obtain C we need to divide Δ by the possible number of triangles if all pairs of edges from a vertex were themselves joined, averaged over the network. The maximum number of triangles on average is

$$\int_0^\infty \tfrac{1}{2}k(k+1)P(k)dk = \frac{\mu^2}{2}\frac{\beta-1}{(\beta-2)(\beta-3)}$$

so, finally

$$C \propto \frac{\mu^{3\beta-3}}{(\beta-1)^3}\mu^{3(2-\beta)} \times \left[\frac{(\beta-2)(\beta-3)}{\mu^2(\beta-1)}\right] = \frac{\mu(\beta-2)(\beta-3)}{(\beta-1)^4}.$$

Note that the dependence on μ is the same as a random graph. This is because we have ignored correlations between vertices. (Edges from a particular node are not equally likely to be connected to nodes of any other degrees.) Nevertheless, we would argue that the β-dependence of the result is likely to be in the right direction. To simplify these expressions we consider large β for which we have $C \propto \mu/(\beta-1)^2$.

3.3 Alias for *L*:

We estimate the diameter of the graph by the number of steps L we need to take such that a node has a probability of 1/2 of being connected to itself. Thus

$$\sum P_L(k)k/N = 1/2$$

defines L. This gives constant or

$$\frac{\mu^{L(\beta-1)}}{(\beta-1)^L}\mu^{(2-\beta)L} = \frac{\mu^L}{(\beta-1)^L} = \text{constant},$$

and hence

$$C/L \sim C\log\beta C \sim -\frac{\log(\beta)}{(\beta-1)^2}.$$

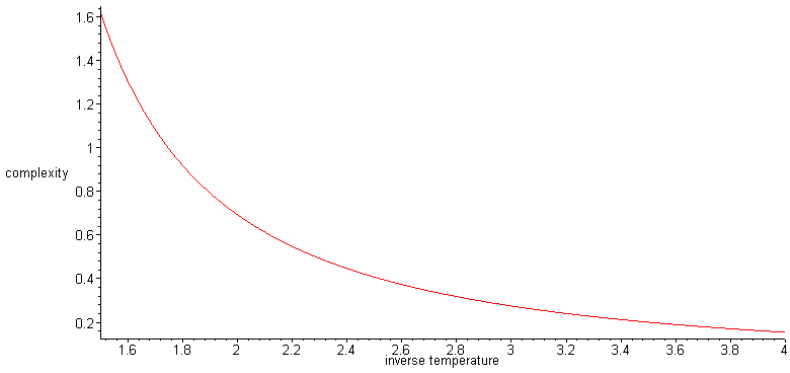

Figure 2 Complexity parameter *C/L* against inverse 'temperature' for the SCL distribution.

Figure 2 shows just what we would hope for from a complexity parameter. In order to have a way of distinguishing this measure from others we propose to call *C/L* the β-complexity of a graph. (We assume that *C/L* has been scaled appropriately to be independent of the number of nodes, or equivalently that the limit $N \to \infty$ is implied.)

The question naturally arises as to whether β-complexity provides any useful insight. We look at two examples where it might.

The first [16] comes from the synthesis rates of proteins during the development of *Streptomyces coelicolor*. These follow the SCL distribution with changes in β as the bacterium goes from

exponential to stationary phase. There is a transition from one developmental phase to another marked by a drop in β as the genomic resources are more fully utilised and a peak as resources are focused on the synthesis of a smaller number of essential proteins. The development therefore consists in a transition through high complexity and we would expect to find this mirrored in the protein network, or genetic regulatory network underlying the observed rates.

The second [19] involves the messenger RNA levels in the bacterium *Caulobacter crescentus* as a function of the cell cycle. The results here are not so clear-cut. There is a good fit of the original data from about 3000 genes to the SCL distribution for mRNA level versus rank. But the temperature of the fit does not vary during the cell cycle. The published data on the 533 genes that vary significantly provide a division into 9 ranks on the basis of relative variability. This is not sufficient to test for a fit to the SCL law. However, if we *assume* the data can be described in terms of an SCL temperature then the associated β-complexity of the cell shows a remarkable increase between initiation and division (Figure 3). We have previously predicted such an

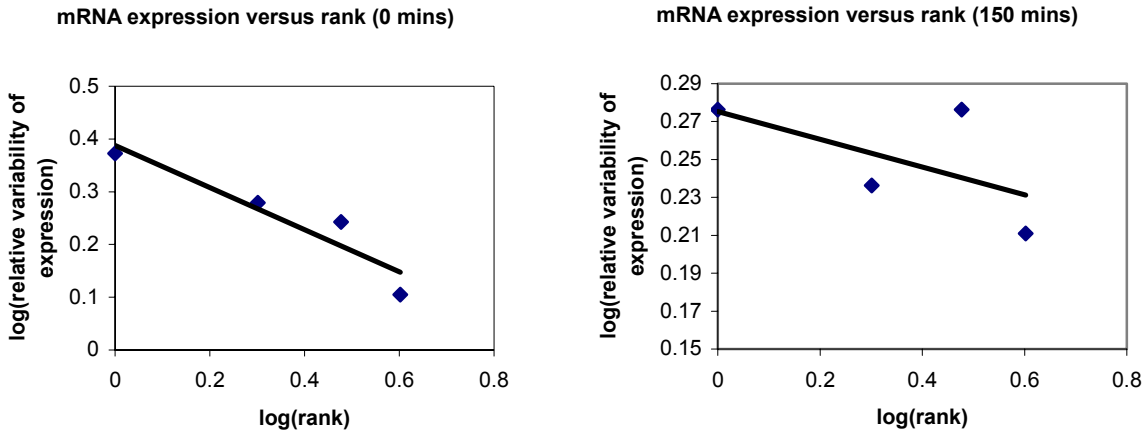

Figure 3. The relative variability of expression of 533 mRNAs in *Caulobacter crescentus* plotted as a function of rank at initiation (left panel) and division (right panel). The variability is defined as the percentage change from the average; the rank labels those that change the most to those that change the least.

increase in a model in which diversity of expression underpins cell cycle regulation.

4. Thermodynamic Complexity

Interesting though it is, the fitting of power laws or SCL distributions to network data provides limited insight into the origin and development of networks and the reason behind the structures. It also has apparently little predictive power. This is at least in part because the growth and rewiring modes of construction of networks are not uniquely determined by the few measurable parameters such as slope or 'temperature'. What we need are universal insights like the association of power laws with self-organisation [20]. Thus, in this final section we want to speculate about the possible role of networks as models of a (specially interesting) example of non-equilibrium thermodynamic behaviour.

First consider that many natural networks are not constructed systematically, but by stochastic processes. One thinks here of the evolutionary development of say a metabolic network by random evolutionary mutations. One can think therefore of a network exploring its environment by testing the efficacy of some random rewiring against some fitness landscape. It is then the

nature of the fitness landscape that provides the feedback by which structure is imposed on the network.

In the absence of any information from the environment the entropy $\sum_{r=1}^{R} p_r \log p_r$, (or relative information) [21] is maximised by a uniform distribution of node degrees $p_r = 1/R$ (where R is the maximum node degree). Such a network will have a low β-complexity since it encodes no information from the environment. Now let the network be in contact with a 'heat bath' which induces random rewiring subject to conservation of 'energy' $E = \Sigma r p_r$ = constant. This constraint on the system is communicated to the system by the environment via the energy cost of rewiring. The entropy $\log W = \sum p_r \log p_r + \beta \sum r p_r$ will be maximised for an exponential distribution of nodes, which is the distribution of a growing network without preferential attachment [6]. We expect this random network to have low β-complexity.

Now consider the constraint $\Sigma p_r \log(r + \mu) = \varepsilon$ = constant. This gives rise to the SCL distribution (or to a power law if $\mu = 0$). We should expect an arbitrary network, rewired to maximise the corresponding entropy, would have an SCL distribution of node degrees. Mandelbrot argues for this 'cost function' as appropriate to the transmission of information in words of length up to some fixed maximum. (The rank of a word must increase exponentially with its length for a fixed alphabet.) This is pertinent to metabolic networks since the links between metabolites are bought at the cost of the synthesis of enzymes up to some maximum number of linked amino acids. Alternatively, we can think of the constraint as the conservation of a quantity that is the geometric mean of the ranks. Whatever the rationale, the constraint is maintained by the interaction of the system with its environment. When the system has reached a stationary state, the entropy $\log W$ is less than the maximum (for $p_r = p$) because 'work' has been done on the system. Conversely, work - here a decrease in complexity - is the constrained release of energy.

Note that we do not have to refer explicitly to the dissipation required to maintain the system far from equilibrium: the subsystem of interest does not include the mechanism required to maintain the constraints which will in general be dissipative.

This leads to the following idea for a network model of a system maintained in a stationary state far from thermodynamic equilibrium by Mandelbrot type constraints. Introducing a constraint on the number of nodes N for completeness, we have, for the entropy S

$$S = \log W = \sum_{r=1}^{R} n_r \log n_r + \beta\varepsilon + \lambda N , \qquad (4.1)$$

where n_r is the number of nodes of degree r and

$$\varepsilon = \sum_{r=1}^{R} n_r \log(r + \mu) , \quad N = \sum_{r=1}^{R} n_r . \qquad (4.2)$$

The stationary distribution is, of course, the SCL

$$n_r = \frac{n_0}{(r+\mu)^{\beta}}$$

where $\log n_0 = -\lambda$. and λ is defined by the second of equations (4.2). We therefore have three extensive variables, ε, N and R. The corresponding intensive ones are

$$\beta = \frac{\partial S}{\partial \varepsilon} , \ \lambda = \frac{\partial S}{\partial N} , \text{ and } ? = \frac{\partial S}{\partial R} .$$

Clearly, from what we have said above, we should like to identify the question mark (?), or some function of it, with the complexity of the network. To us this makes sense: the complexity of the

network is related to the way in which it can perform useful 'work', and this arises from the way in which it is constrained. Note that the rank is a natural measure of (phase space) volume since it is related to word length.

We can illustrate this in the following table, which gives the parallels between conventional equilibrium thermodynamics and stationary, constrained, network thermodynamics.

Equilibrium Thermodynamics	Networks
Temperature	Information temperature
Pressure	Thermodynamic complexity
Volume	Rank
Equation of state	Complexity as a function of Information Temperature
Chemical potential	Cost of introducing an additional node
Total energy	Total cost

From the point of view of applications to biology this holds out the prospect that we may one day understand how (genetic regulatory, protein, metabolic) networks operate to the same extent that we understand steam engines [22].

Finally, let us turn to self-organisation. So far in this section we have thought of a network with given nodes exploring possible reconnections. We now think of the network also as growing by exploring a vast potential network space with feedback from the fitness landscape. To be specific, imagine a metabolic network evolving through mutations of enzymes. The addition of a node is irrelevant to the fitness of the network unless it leads to some consequential rearrangement of the network architecture to include the new metabolite in some functional way. (Of course, a single new product might be of use elsewhere in a cell, but that is outside the rules of this particular thought experiment.) Thus, sometimes a mutation will lead nowhere (although it might not be eliminated if it is not harmful) whereas on other occasions it will lead to a rearrangement of connections on various scales. The network has the potential to self-organise. Furthermore the tuning required for the classical sandpile [20, 23], namely a near zero rate of infall of sand, is met by genetic evolution, at least under some circumstances, for which the rate of mutation is sufficiently slow to allow an avalanche of reconnections to occur before the next mutation. We therefore have also the prospect that network evolution provides a nice model of a self-organised critical system.

Acknowledgements: We thank Camille Ripoll and Michel Thellier for discussions on intensive and extensive variables for complex systems that led to the ideas of section 4.

References

1. MacDonald N (1979) Simple aspects of food web complexity, J Theor. Biol. 80, 577-588
2. Erdos P and Renyi A (1960) Publ. Math. 5, 17
3. Raine D J. & Norris, V., (2000) Interjournal of Complex Systems B Article 361
4. Jeong H., Tombor B., Albert R., Oltvai Z. N., & Barabasi A.-L. (2000) Nature, 407, 651
5. Jeong H., Mason S.P., Oltvai Z. N., & Barabasi A.-L. (2001) Nature 411, 41
6. Albert R and Barabasi A-L (2002) *Statistical Mechanics of Complex Networks*, Rev. Mod. Phys. 74, 47-97.
7. Barabasi A. -L & Albert R., (1999) Science 286, 509
8. Watts D.J. & Strogatz S.H., (1998) Nature, 393, 440

9. Watts D.J. (1999) *Small Worlds: The Dynamics of Networks between Order and Randomness* (Princeton U.P.)
10. Andrásfai B. (1991) *Graph Theory: Flows, Matrices* (Adam Hilger, Bristol)
11. Crutchfield J. P. (1994) Physica D 75, 11-54
12. Krapivsky P. L., Redner S. & Leyvraz F., (2000) Phys nRev. Lett 85, 4629
13. Albert R. & Barabási A.-L., (2000) Phys. Rev. Lett. 85, 5234
14. Mandelbrot B., (1954) Word, 10, 1
15. Ferrer i Cancho R. & Solé R. V., (2001) Santa Fe Institute working paper 01-03-016
16. Vohradsky J & Ramsden J J., (2001) FASEB Journal article 10.1096/fj00-0889fje
17. Ramsden J.J. & Kiss-Haypál, Gy., (2000) Physica A 277, 220-227
18. Raine D. J. & Norris V., (2001) J. Biol. Phys. & Chem. 1, 89-94
19. Laub M. T., McAdams, H. H., Feldblyum T., Fraser C.M., Shapiro L., (2000) Science 290(5499), 2144-2148
20. Bak P. (1996) *How Nature Works: the Science of Self-Organised Criticality* (Copernicus. N.Y.)
21. Adami C., (1998) *Introduction to Artificial Life* (Springer, NY)
22. Norris, V., Demarty, M., Raine, D., Cabin-Flaman, A. and Le Sceller, L. (2002) *Hyperstructures regulate initiation in Escherichia coli. Biochimie* (in press)
23. Sornette D., Johansen A. & Dornic I., (1995) J. de Phys. I, 5, 325

Adaptive branching in Evolution and Epigenesis

Yannick L. Kergosien

Université de Cergy-Pontoise, Département d'Informatique
2, Avenue Adolphe Chauvin, Pontoise 95302 Cergy-Pontoise CEDEX, France
yannick.kergosien@libertysurf.fr

Abstract

We describe one of the simplest models which exhibit an adaptive branching behaviour. It is analyzed both experimentally and formally, and its successive bifurcations provide a good model of what R. Thom called "generalized catastrophes". Some theorems on the stochastic adaptability of the algorithm to very general shapes of target are given. The model further displays the phenomenon of abortive branching : each macroscopic branching appears after a burst of micoscopic branchings which stop growing after a very short time. The mathematical analysis of the model explains why and how this behaviour occurs. The applications of these models to Evolution (natural and artificial) and Epigenesis are discussed, and a higher dimensional version is applied to growing a tree in a space of shapes in the context of a database of medical images.

Keywords: branching, bifurcation, evolution, epigenesis, angiogenesis, tree, auto-organization, adaptive.

Résumé Ramification adaptative en Evolution et Epigénèse

Nous décrivons un des modèles mathématiques les plus simples qui soit capable de ramification adaptative et étudions sa pertinence biologique. Ayant défini dans un espace une probabilité chargeant une région appelée cible, et un ensemble appelé graine, état initial du réseau à faire croître, chaque tirage d'un point au sein de la cible définit un nouveau point à ajouter au réseau. On peut observer expérimentalement l'apparition d'arborescences qui adaptent progressivement la forme du réseau à celle de la cible. On peut aussi montrer plusieurs théorèmes d'adaptativité stochastique du réseau à des cibles très générales. L'étude plus fine des ramifications révèle l'existence du phénomène de ramifications abortives dont l'étude formelle s'apparente au concept de catastrophe généralisée. Ce modèle est applicable à l'espace tridimensionnel pour modéliser l'épigénèse, mais aussi à des espaces de dimension plus grande, comme des espaces de formes, dont nous discutons quelques applications dans le cadre de l'Evolution en Biologie, et pour des applications de bases de données de formes en imagerie médicale.

Mots-clés: ramification, bifurcation, evolution épigénèse, angiogénèse, adaptation, arbre, auto-organisation.

Introduction

The adaptive branching phenomenon in Biology

Branching phenomena are very common in Biology, and often related to some adaptation. They can take place in physical spaces when epigenetic morphogenesis is the question. There they can be com-

pared to or related to the morphological branching phenomena which rivers, sparks, or transportation networks display, where some variational or optimality principle can be recognized. It is tempting to look for some function being optimized as soon as some tree morphology is recognized, starting from plant biology! But one can also think of using trees when the objectives are given by humans and to be met by technology. Algorithmics has been such a fertile field of application. Even in Biology trees occur in more abstract spaces like those where phylogenetic trees are constructed. There also, one can either consider these trees as given and try to explain them from simpler principles, or use trees as a tool to explore and understand complex data spaces such as those which arise from the collaborative biological research.

The algorithm we are going to present can be used in both ways. We call it epigenetic, as opposed to preformationist algorithms, since it relies on adaptivity properties and environmental geometry rather than built-in information to evolve shape. We will study some of its features in a naturalist's way, so as to be able to look for similar patterns in biological phenomena and perhaps infer some interesting properties. On the other hand, its power can be used for more technologically oriented problems like the one we briefly mention at the end of this paper.

Some other simple models

Looking for the simplest models for adaptive branching, one has first to consider physical phenomena which can exhibit such behaviour. Among them, diffusion based models have been studied very early, for instance related to cristal growth. Diffusion can be coupled to reaction (since Turing) or other phenomena like accretion, and involve a number of diffusible species. The biologically oriented models of Gierer and Meinhard [1] used two diffusible species to obtain branching paterns. In [2,3] we described how to get branching with a single diffusible element, and moreover the adaptive properties of that model were experimentally demonstrated, especially the growth of the branching network toward preassigned targets, together with competition and target sharing phenomena. Such properties are important to model such epigenetic phenomena as angiogenesis towards tumors. However the interesting range of parameters with such a simple model is limited and the phenomenon rather unstable. In the sequel, we will rather consider a model less directly relevant to physical epigenesis but very robust and perhaps better adapted to the study of branching in abstract biological spaces. We insist on keeping an epigenetic approach in that we do not use any "preformation" and keep genetic information, i.e. the set of building rules, to a minimum.

A simple adaptive branching algorithm

Definitions, the algorithm

Here we introduce the algorithm in a simple setting which is not the most general one. The evolution takes place in the usual n-dimensional space $\mathbb{R}^n$. A fixed subset of it, finite or not, is called the target and noted C, with a probability defined on it. A second subset of R^n, which we call the network, is going to be modified (it will "grow") at each step of the algorithm. We shall note R_n the network after step n. Starting with an initial network R_0, each step will add a point to the network.

To start, one needs to define an initial network R_0, a target C with its probability distribution, and a real number $\epsilon \in]0,1[$. At each step, say i:

- randomly draw a point, say a_i, from the target (using the given probability distribution);
- look for b_i, the point of the network R_{i-1} which is closest to a_i;
- compute $b'_i = \epsilon.a_i + (1-\epsilon).b_i$;

- "graft" b'_i on the set R_{i-1} to get $R_i = R_{i-1} \cup \{b'_i\}$.

The stopping criterion can be the number of steps, or some condition on the network. The case of a tie for the choice of b_i formally calls for a procedure, either stochastic or deterministic, to choose b_i, but those cases are very unprobable (we will not develop that issue here). The formula to compute b'_i uses vector (or affine) algebra; typicaly ϵ is taken small, making b'_i close to b_i but slightly displaced in the direction of a_i.

Since each point added to the network is related to a definite point of the former network, the network has the structure of a finite tree. Branching points can thus be defined (more than one point grafted), besides "branch points" (one graft) and "tip points" (no graft). One could include in the definition of the network the line segments joining points to their grafted sons and compute closest points on this object, but we will not do it.

Experimental results

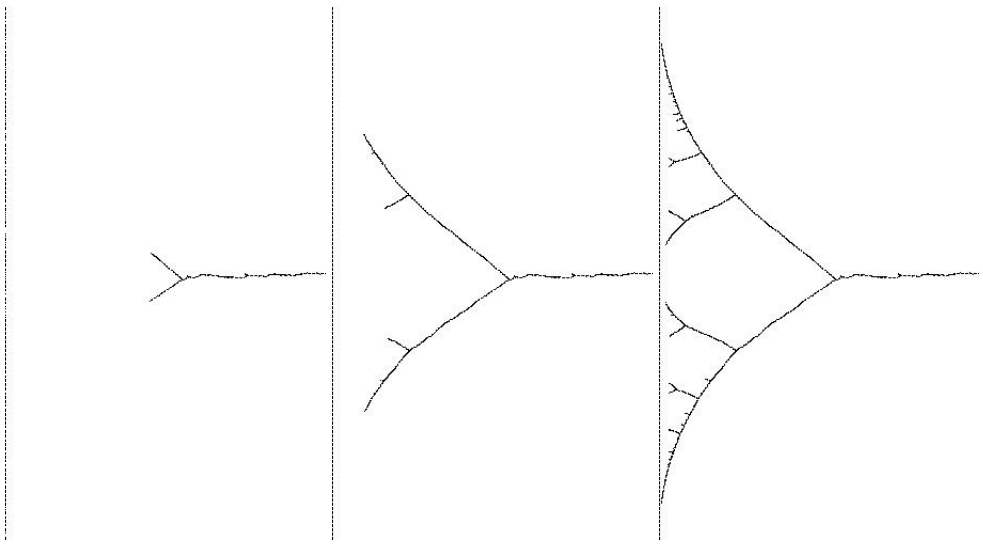

Figure 1: Linear target(left): network after 1000, 5000, 25000 steps

Figure 1 shows the result of the algorithm for a target being a line segment with uniform probability distribution, starting from a single point, and for $\epsilon = 0.001$. The network grows toward the target and branches several times in a way that looks adapted to the geometry of the target.

Starting from two points as the initial network can lead either to cooperation in a "market sharing" way or to a "winner takes all" competition, depending on the situation of the two seeds and the geometry of the target (figure 2).

Adaptation to more complex shapes of targets is also seen. In figure 3, the network adapts to two differents targets (i.e. two components of the target) the one on top being a circle with uniform probability and the bottom one being a disk with uniform probability, with the disk getting a total of four times more probability than the circle. On that figure the target have not been drawn. Notice the different morphologies of the network in the two cases.

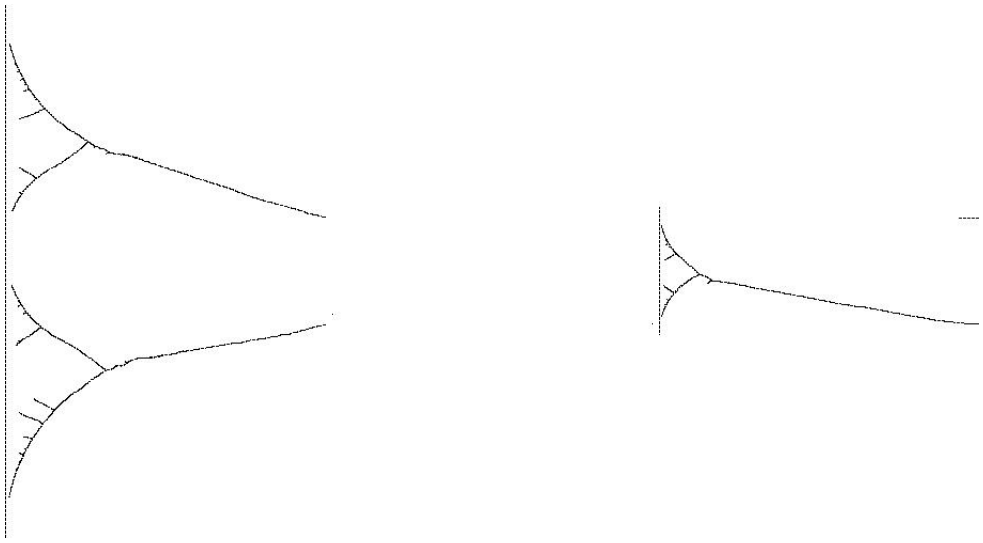

Figure 2: Two seeds either sharing the target (left)or competing for it (right)

Adaptativity theorems

The former experimental results are supported by the following two theorems which show the adaptive power of the algorithm. To state them we modify our definitions. Instead of defining first the target and second a probability on it, we start with a probability on R^n and define the target as the set of points of R^n for which any neighbourhood has positive (i.e. > 0) probability.

The first theorem states that for any ball we choose in the target and probability $1 - \eta$ as close to 1 as we wish, there is a definite number of steps after which the network willi, with the chosen probability, approach the ball to a distance we could choose in advance.

Theorem 1. $\forall \epsilon \in]0,1[,\ \forall \eta > 0, \forall x \in E, \forall r > 0\, s.t.\, P[B(x,r)] > 0, \forall r' > r, \exists N \in I\!N : \forall n > N, P[B(x,r') \cap R_n] > 1 - \eta$.

The second theorem states that, if the target is compact (here this means closed and bounded), for any distance r and any probability $1 - \epsilon$ we choose, there is a definite number of steps after which all the points of the target will be at a distance less than r.

Theorem 2. C being a compact target, $\forall \epsilon \in]0,1[,\ \forall \eta > 0, \forall r > 0, \exists N \in I\!N$ such that $\forall n > N, P[sup_{c \in C} d(c, R_n) < r] > 1 - \eta$.

Consequence. Let us define an active point of a network as a point which, for at least for one point of the target, is the closest among the network points: it is thus a point which still has a non-zero probability of being grafted. A consequence of the second theorem is that after the same number of steps, and with the same probability, no active point of the network remains further than r from the network. Whereas the network is an increasing set a part of which (the active set) approaches the target, the active set really tends to fit the target, leaving no point behind.

Abortive branchings

Decreasing ϵ usually makes branches straighter, and one could think that in the limit the algorithm tends to the clean branchings of a deterministic process. This does not happen because of a phenomenon which occurs repetitively in the vicinity of macroscopic branchings: many small branching appear but are soon inactivated by one of their branches winning over the other one. We called

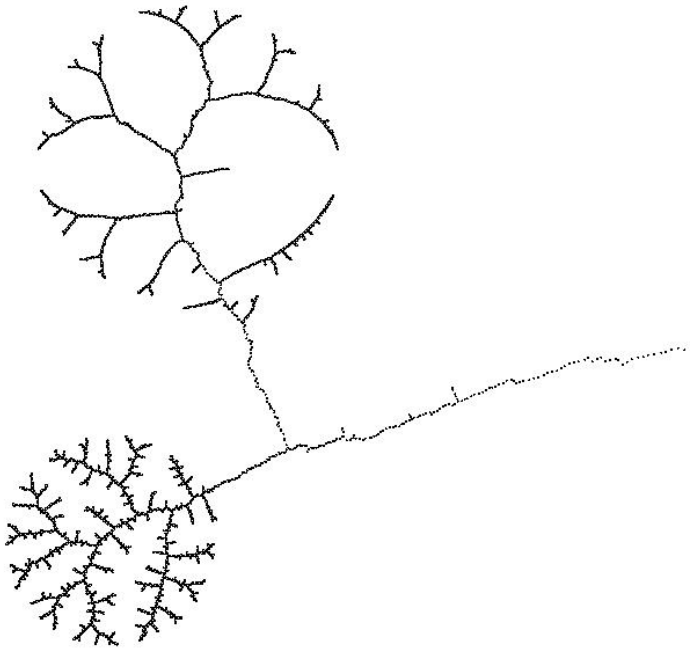

Figure 3: Evolution to a target (undrawn) made of a circle (top) and a disk (bottom)

"abortive bifurcations" this phenomenon. Analysing the 2-dimensional case leads to a good understanding of the phenomenon.

The geometry of branching

Branching occurs when some grafting takes place at a point of the network, say A, which is not a tip. This implies that A is closer to some point of the target than any point on the branch already grafted on A.

Demonstrating abortive bifurcations

Figure 4 shows an instance of successive abortive bifurcations before a macroscopic branching appears. To see them, one should use small ϵ and magnify the network at a distance from the target where a macroscopic branching is likely to occur. Notice the constant qualitative pattern of the network at each abortive bifurcation : after one of the branches wins over the other one, i.e. hides it from the target, the network bends back to the center of the target. In some contexts like Evolution, such repetition of abortive attempts of differentiation might probably be used to detect the imminence of a major branching.

Analysis of abortive branching

To understand why so abortive branching happens repetitively before a major branching can remain, one can restrict the study to the simple -dimensional case with a linear target. The evolution of the

Figure 4: Small abortive bifurcations slightly before a stable branching (going right to left)

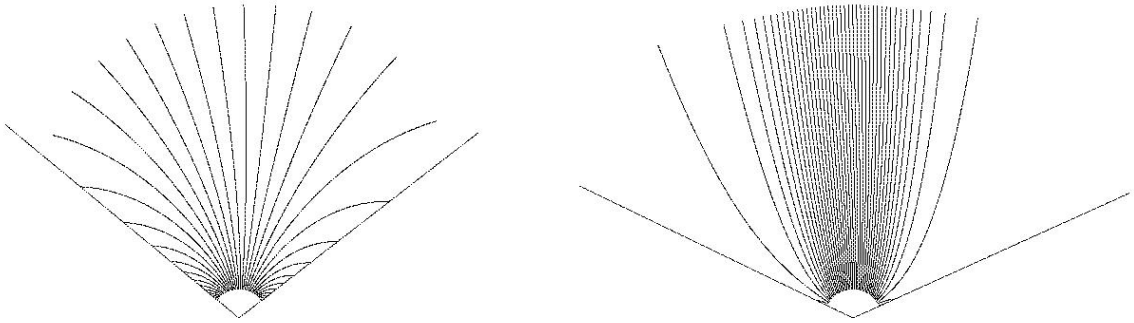

Figure 5: Phase portraits far from (left) and close to (right) target

two tips, say X and Y, that arise from a branching can be summarized by the evolution of the vector $Y - X$. Each of the two tips hides the other one and wins when the vector crosses some direction related to the ends of the target. The evolution of the vector is stochastic but the the expectation of the dynamical system which governs it can be computed easily from the target geometry and the position of the tips. Figure 5 shows the phse portraits of the dynamical system acting on the vector and the critical directions for two different distances to the target. When far from the target, all the trajectorie eventually cross one of the winning lines. Getting closer to the target modifies the picture, and a growing number of trajectories are able to make their way without hitting either of the critical lines. The real vector field that acts on the the couple of tips can be viewed as the sum of that deterministic (expected) field and a stochastic component which can be made small with ϵ small. The whole picture thus involves a bifurcation stochastically perturbed, the deterministic part of which depends on the position relative to the target. It fits with the idea of a "generalized catastrophe" proposed for study by Thom in [4].

Adaptive branching and evolution

Theories of biological evolution have given a major role to adaptation, especially through the concept of fitness. Branching is also essential in the classification of species and the building of phylogenetic trees. Such trees are not only a convenient classification of a set of past species but they account for the historic events that their branchings represent. It is tempting to try to relate branching and adaptivity for phylogenetic trees at the abstract level of the model we described and look for the possibility of some of the phenomena we observed, especially abortive branching. Let us consider the relevance of the former model to biological evolution as our problem : it should be discussed carefully elsewhere, but we shall outline some possible research directions toward intermediary models slightly closer to the biological reality of evolution.

The evolution of a specie in time can be represented by the trajectory of a representative point in some high dimensional parameter space. To account for a bifurcation into two species, there is a difficulty for classical deterministic modeling unless we study the evolution of sets like in our network formalism. Alternatively, an evolutionary tree can be seen as a union (in set theoretic terms) of deterministic trajectories. If we want species to adapt to environments, our target will represent some set of environments. Our next problem is to give some meaning to the distance from network to target and justify the model's rule for growth toward the target. We shall mainly adress the latter question, assuming for the moment, in still vague terms, that fitness improvement can be expressed by a the decrease of some distance.

Assume that a set of populations is distributed in a space where environmental characteristics may vary with location. If each population evolves and improves its fitness to its local environment, the union of all the trajectories representing the different populations will not, in general, follow the model we described. But if we also assume that some combination of a diffusion of individuals and a local competition, both at a faster time scale, results in the property for the system that, at any location and at any time, the globally fittest population is predominant, then any improvement of a population in the system towards its local environmental characteristics will follow the rule of our model (except for the exact direction and intensity of the improvement, to be discussed soon), i.e. will make smaller the distance from an environmental point to the fittest population. Of course, to arrive at this interpretation, we shifted from a rule where we draw points from the target to a rule where we draw points from the network and we should wonder whether this change still permits using the model. First of all, one may imagine the case of several locations having the same environmental characteristics. However, a genericity argument can be used: if the space of environmental characteristics is of a sufficient dimension, the mapping from the "location space" (2 or 3 dimensional) to the space of environments generically has no multiple points and should be an embedding under some natural hypotheses. Probability measures should also be examined : the correspondence between locations and mapped environments can serve to induce probability on the target from a probability measure on location space (e.g., related to population density, some rate of mutation, etc...) to establish model equivalence. As for the relation of the rule for computing grafted points ($b'_i = \epsilon.a_i + (1-\epsilon).b_i$, see section 2) and the exact directions and intensities of populations changes improving fitness, we should probably explore the assumption that the different changes which improve fitness average to a vector, like the gradient of fitness, the direction of which would correspond to the rule of our model, but that point should be examined further, together with the question of relating fitness and distance.

A modi ed algorithm

Some implementation issues

At each step of the algorithm, one has a closest point within the network. But most points are inactive and it is computationally more efficient to periodically detect and mark inactive points to avoid testing them for proximity (one can also maintain a list of active points: several variants and data structure can be used). A network point gets inactive when the other points of the network hide it from all the target points. In the of a linear target, it is easy to check that condition: one only needs checking the visibility of the end points of the target. In the case of a more complex target shape, however, no such simple rule is available. Another reason for modifying the algorithm is the number of comparisons to be performed, even if active points have been selected.

Avoiding garbage collection and using search trees

We experimented with success a modified version of the algorithm, where a binary search tree is used to locate the closest points, and where no garbage collection is needed. The new rule is that after some branching occurs, one definitively assigns a part of the target to the future growth of each of the two branches. After each target point has been drawn, one thus first locates the branch to be grown by successively comparing the distances to couples of sons of the former branchings points, starting from the root (a classical binary search in a tree). Such algorithm remains very efficient even with large trees in high dimensional spaces. It also behaves quite like the former one, with good adaptive properties, but of course with no abortive bifurcations since the subregions of the targets cannot move after each bifurcation.

Growing trees in shape spaces

Discrete trees are a data structure that has long been used in algorithms to organize comparisons. But there is also a need for continuous trees to organize morphogenetic or evolutive processes into continuous branching families of shapes. These viewpoints fuse in the technology of databases for continuously varying data like images or 3-dimensional protein shapes. We experimented the former algorithm to grow trees in a space of shapes extracted from medical images, but the technique can be extended to many problems of comparative morphology, possibly in the context of evolutionary studies.

The set used was the set of all the sections of a complex bone (human scapula). The original surface was reconstructed from a set of parallel sections acquired from CT-scanner, but considering any possible section in any direction leads to a very complex family where queries are still problematic. Each section is a set of polylines (some of the sections are not connected) but so far we kept only a single component so as to be able to use a simple matching procedure. Sections are thus points in a space the dimension of which is about 100. Randomly drawing sections from the set of all possible sections, and starting from simple shapes like a circle, we could grow a tree in the shape space and observe branchings that progressiveley led to the actual members of the set of sections. When searching for closest curves, prior matching was used, in order to focus on shape. Such methodology is close to some of the procedures used in exploratory statistics [6], but here we emphasized the construction of a continuous family with branchings that could be used in the comparison and study of complex biological objects.

Conclusion

A simple algorithm has been described which can adapt a finite subset with a tree structure to very general targets in $\mathbb{R}^n$. A major advantage of it is the small number of parameters to be chosen and the robustness of the adaptability property. The adaptability properties have been illustrated experimentally and supported by two theorems. The phenomenon of abortive bifurcations has been analysed and its pertinence to problems in biological evolution has been briefly sketched. As an application to databases of shapes, a tree is grown in a space of curves taken from medical images. Let us notice that whereas reconstructing putative family trees for species, languages, or myths, has been quite common, probably due to the lack of historical data, no theoretical morphogenesis seems to exist yet, that would study in a very general way how to organize the building of known structures under various constraints. Technology must already solve such problems in their instances, but some more abstract approach could be of interest.

Appendix: Proofs of the adaptativity theorems

We want to prove that $\forall \epsilon \in]0,1[,\ \forall \eta > 0, \forall x \in E, \forall r > 0\, s.t.\, P[B(x,r)] > 0, \forall r' > r, \exists N \in \mathbb{N} :$ $\forall n > N, P[B(x,r') \cap R_n] > 1-\eta$ where R_n is the network after the n-th accretion. A problem is that successive accretions due to points drawn from $B(x,r)$ may grow different branches of the network instead of adding their effects to the same tip. We thus choose a ball $B(y,\xi) \subset B(x,r)$ with $P[B(y,\xi)] > 0$ where ξ is a positive real number small enough (to be computed later). We know from elementary probability results that waiting long enough guarantees us to witness as many drawings from $B(y,\xi)$ as we wish, whatever the smallness of $P[B(y,\xi)]$. We will call $a_1, \ldots$ the points drawn from $B(y,\xi)$, $b_1, \ldots$ the corresponding closest network points, and $b'_1, \ldots$ the points consequently added to the network. We call b_0 the point of the initial network R_0 closest to $B(y,\xi)$, and $l_i = d(a_i, b'_i)$. If we can get a b'_i close enough to its a_i, it has to be in $B(x,r')$ and we are done. Let us compute how l_i decreases with i:

$$l_{i+1} = d(a_{i+1}, b'_{i+1}) = (1-\epsilon) d(a_{i+1}, b_{i+1})$$

$$\leq (1-\epsilon) d(a_{i+1}, b'_i)$$

(since otherwise b_{i+1} would not be closer to a_{i+1} than b'_i)

$$\leq (1-\epsilon)(d(a_{i+1}, a_i) + d(a_i, b'_i))$$

$$\leq (1-\epsilon)(2\xi + l_i)$$

If we took ξ such that, for all the l_i we need,

$$\xi \leq \frac{\epsilon\, l_i}{4(1-\epsilon)}$$

then

$$l_{i+1} \leq (1-\epsilon/2) l_i \leq (1-\epsilon/2)^{i+1} l_0$$

Just choose k big enough to get $l_k \leq (1-\epsilon/2)^k l_0 < r' - r$ and take ξ accordingly. After k points have been drawn from the $B(y,\xi)$ you chose, which happens with a probability greater than $1-\eta$ after a computable number N of steps of the algorithm, the network will have entered $B(x,r')$.

The second theorem states that $\forall \epsilon \in]0,1[,\ \forall \eta > 0, \forall r > 0, \exists N \in \mathbb{N}$ such that $\forall n > N, P[sup_{c \in C} d(c, R_n) < r] > 1-\eta$. Cover C with balls of radius $r/3$. Using the compacity of C, extract a finite covering

$(B(c_i, r/3))_{1 \leq i \leq M}$. Apply the former theorem and simultaneous inference to get N such that with a probability greater than $1 - \eta$:

$$\forall 1 \leq i \leq M \; \exists b_j \in R_n : b_j \in B(c_i, 2r/3).$$

Then with probability greater than $1 - \eta$:

$$\forall c \in C \; \exists j, \; 1 \leq j \leq M : \qquad d(c, R_n) \leq d(c, c_j) + d(c_j, b_j) < r/3 + 2r/3 = r$$

The consequence on the active set is obvious: if any point of the target is less than a distance r away from the network, then no point of the network can be active unless it is within that distance from the target.

References

[1] GIERER A., MEINHARDT H., A theory of biological pattern formation, Kybernetik 12 (1972), p. 30.

[2] KERGOSIEN Y. L., Adaptive ramification: comparing models for biological, economical, and conceptual organization. Acta Biotheoretica 38 (1990): 243-255.

[3] KERGOSIEN Y. L., Adaptive ramification and abortive concepts. Neural networks from models to applications (NEURO'88), I.D.S.E.T., Paris 1988, pp. 439-449.

[4] THOM R., Stabilité structurelle et morphogénèse: essai d'une théorie générale des modèles, Benjamin, Reading, 1972.

[5] BREIMAN L., FRIEDMAN J. H., OHLSEN R. A., STONE C. J., Classification and regression trees. Wadsworth, Belmont, 1984.

Bio-Array Images Processing And Genetic Networks Modelling

J. Demongeot, F. Berger*, T.P. Baum, F. Thuderoz & O. Cohen

TIMC-IMAG CNRS 5525 Faculty of Medicine 38 700 La Tronche France
*INSERM U 318 University Hospital of Grenoble 38 700 La Tronche France

Abstract

The new tools available for gene expression studies are essentially the bio-array methods using a large variety of physical detectors (isotopes, fluorescent markers, ultrasounds,…). Here we present an image processing method independent of the detector type, dealing with the noise and with the peaks overlapping, the peaks revealing the detector activity (isotopic in the presented example), correlated with the gene expression. After this first step of image processing, we can extract information about causal influence (activation or inhibition) a gene can exert on other genes, leading to clusters of co-expression in which we extract an interaction matrix explaining the dynamics of co-expression correlated to the studied tissue function.

Introduction

The total mRNA's of genes to test have been extracted from the studied tissue (in the present case a glioma tissue). Then DNA's are synthesized by reverse transcription from these mRNA's including bases labeled with the isotope P^{33}. Resulting DNA's are then tested against identified complementary DNA's (cDNA targets), previously amplified by PCR and fixed on a nylon gel. The hybridization results are revealed in a phospho-imager and yield a digital image coming from the radioactive hybridization plate, called the bio-array image or shortly the bio-image. cDNA hybridized with a P^{33}DNA means that the complementary sequence of the P^{33}DNA is present in the related mRNA proving that the corresponding gene is expressed in the studied tissue.

Peak segmentation

The first encountered problem is the fact that the bio-images are extremely noisy and that we have to low-pass them in order to suppress the high-frequency noise (see Figure 1).

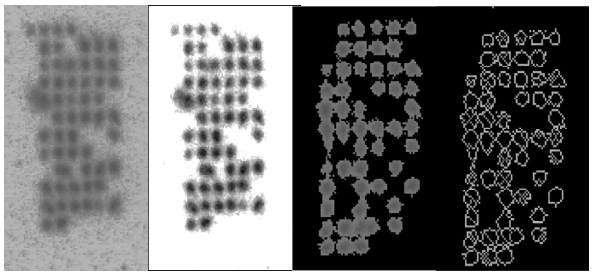

a) b) c) d)

Figure 1: a) raw data 1 b) low pass filtering bio-image 1 c) watershed segmenting and d) contouring bio-image 2

The result of this pre-treatment is a better separation of the isotopic activity peaks, allowing a watershed separation and contouring [1]. Then we will apply a more accurate segmentation and contouring method called the potential-hamiltonian method: let us remark than the peaks are about Gaussian, with a relatively weak kurtosis and skewness allowing in particular the respect of the conservation "law": 2/3 of the peak activity are concentrated into the set of points (x,y) where the Gaussian curvature C(x,y) vanishes, i.e. inside the maximum gradient line of the peak. By exploiting this property, it is possible to neglect the part of the peak outside the projection of this remarkable line, called in the following the characteristic line, its equation being:

$$C(x,y)=\partial^2 g/\partial x^2 \partial^2 g/\partial y^2 - (\partial^2 g/\partial x \partial y)^2 = 0,$$

g(x,y) denoting the gray function at the a pixel of coordinates (x,y).

G Gaussian peak H

H' p h

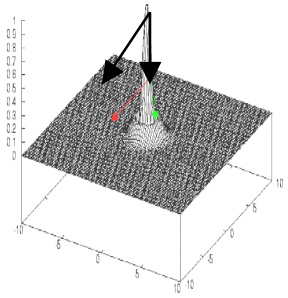

Figure 2: representation of g, H and H' (with indication of potential p and Hamiltonian h parts) for a Gaussian peak

We are thus led to consider the new height function H(x,y)=C(x,y) instead of the function g(x,y) and its level line H(x,y)=0. We display after a plane differential system of which the characteristic line is a limit cycle. Let H'(x,y) be the function defined by: $H'(x,y)=\left|H(x,y)\right|$. Vanishing of H'(x,y) occurs on the characteristic line (see Figure 2 for the visualization of g, H and H') and if we consider the following crude system:

$$dx/dt = -\alpha \partial H'/\partial x + \beta \partial H'/\partial y,\ dy/dt = -\alpha \partial H'/\partial y - \beta \partial H'/\partial x,$$

where α and β are real parameters, then the first part of this differential system is of steepest descent potential nature and along this flow, the orbits converge to the set of zeros of H'(x,y), on which the second part of convective Hamiltonian type becomes preponderant [2]. Parameters α and β are used to tune the speed of convergence to the limit cycle. To cope with random noise and numeric instabilities, we modify slightly the system into:

$$dx/dt=-\alpha\partial H'/\partial x[H(x,y)/G(x,y)]+\beta\partial H'/\partial y,$$
$$dy/dt= -\alpha\partial H'/\partial y\}\}[H(x,y)/G(x,y)]-\beta\partial H'/\partial x,$$

where $G(x,y)=||grad(g)||^2$.

The added term [H(x,y)/G(x,y)] speeds up the descent to the vanishing of H(x,y) and forces the stability. The usual discretization of Runge-Kutta yields ultimately the algorithm which is quite easy to implement. On each pixel (i,j) (boundary effects being neglected), the function H(i,j) reads:

$$H(i,j)=[g(i+2,j)-2g(i+1,j)+g(i,j)][g(i,j+2)-2g(i,j+1)+g(i,j)]-[g(i+1,j+1)-g(i,j+1)-g(i+1,j)+g(i,j)]^2.$$

We have seen that an important property of the characteristic line is that in the case of a Gaussian peak, it delimits a volume equal to 2/3 of the total volume of the peak. This property remains about exact in case of kurtosis and skewness of the peak. Hence by multiplying by 3/2 this volume, we get a good estimation of the gene activity and this value is better than those obtained by a watershed method due to over-segmentation (Figure 1). This approach is interesting because the lower part of the peak is often low-frequency noisy. The method seems particularly efficient when the mesas are well separated. If they are close (Figure 3), then we need to tune the parameters α and β (Figure 4). In further developments of the method, we look for a dynamical calculation of these parameters in terms of the data. Finally, we can standardize the estimated activity in terms of a bio-image with small squares symbolizing in gray levels the degree oh hybridization of the cDNA's (Figure 5). From such bio-images acquired at different times of the cell cycle in cells from the same tissue, we can study the interactions between genes by estimating an interaction matrix.

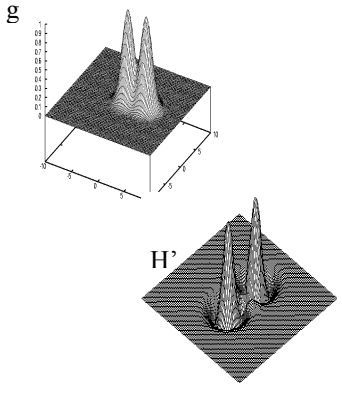

Figure 3: g (top) and H' (bottom) for close Gaussian peaks

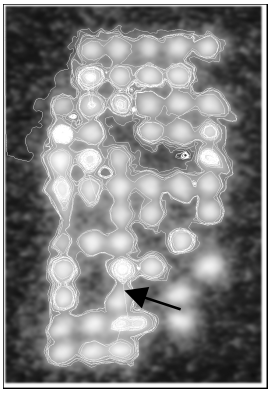

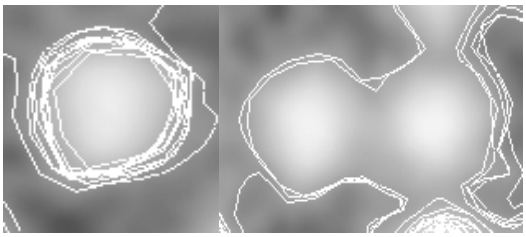

Figure 4: treated bio-image 2 (top), succeeding limit cycle (left bottom) and false contour (and right bottom)

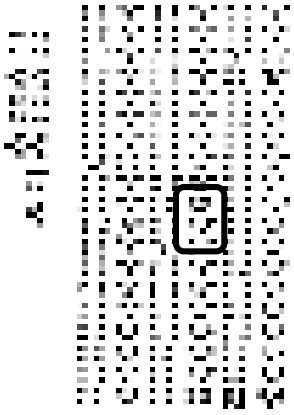

Figure 5: standardized bio-image 2

Interaction matrix

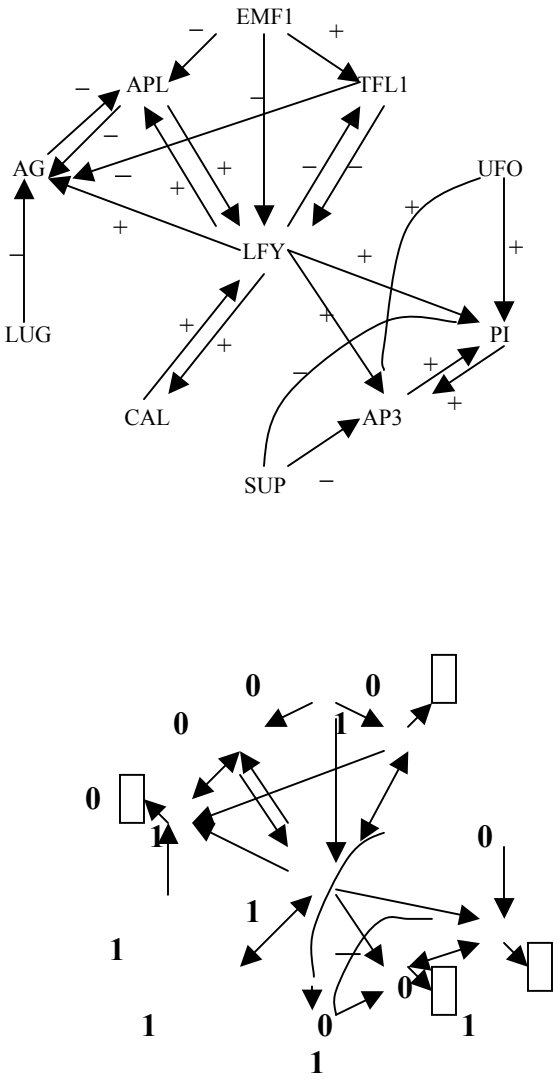

Figure 6: interaction graph of the flowering operon of *Arabidopsis* thaliana (top) and an attractor of its Boolean dynamics (bottom)

For each operon, we can define an interaction matrix M, which just expresses that if its coefficient m_{ij} is positive (resp. negative), the gene j is a promoter or activator (resp. repressor or inhibitor) of the gene i. If m_{ij} is null, then gene j has no influence on the expression of gene i. The interaction graph can be built from the interaction matrix M (Figure 6) by drawing an edge (j,i) + (resp. -) between the vertices representing the genes j and i, iff $m_{ij}>0$ (resp. <0). In order to calculate the m_{ij}'s, we can either determine the s-directional correlation $\rho_{ij}(s)$ between the state vector $\{x_j(t+s)\}_{t\in C}$ of gene j at times t+s and the state vector $\{x_i(t)\}_{t\in C}$ of gene i at times t, t varying during the cell cycle C, or identify the system with a Boolean neural network. We define the connectivity K(M) of the interaction matrix M by the ratio between the number m of edges of the interaction graph and its number n of vertices: in general, for known operons (lactose operon, Crow operon of the phage λ, lysogenic/lytic operon of the phage μ, gastrulation operon,…), K(M) is between 1.5 and 3. The observed induction proportion

(number of positive edges divided by m) is between 1/3 and 1/2. If some signs of the m_{ij}'s are unknown, then we can take it random by respecting the induction proportion.

Gemetic network dynamics

If we consider the interaction graph of the flowering operon of *Arabidopsis* thaliana (Figure 6 top) [3], then we can easily define from it a Boolean dynamics: the gene i has the state 1 if it is expressed and -1 if not. The change of state of gene i between t and t+1 obeys a threshold rule: $x_i(t+1)=H(\sum_{j=1,n}m_{ij}x_j(t)-b_i)$ or $x(t+1)=H(Mx(t))$, where H is the Heaviside step function and the b_i's are threshold values. When t is increasing, the genes states reach a stable set of configurations (a fixed configuration or a cycle of configurations) called attractor of the genetic network dynamics. In Figure 6 (bottom), an example of such attractor is given, with final states (in black boxes) different from the initial conditions.

We will present first some qualitative results from the human genome observation, and after some theoretical corresponding statements recently proved :

- in 1948, M. Delbrück [4] conjectured that the presence of positive loops (i.e. paths from a gene i to itself having an even number of inhibitions [5]) in the interaction graph was a necessary condition for the cell differentiation ; this conjecture has been written in the good mathematical context by R. Thomas in 1980 [6]
- in 1992, S. Kauffman [7] conjectured that the mean number of attractors for a Boolean genetic network with n genes and with connectivity 2, was equal to $\sqrt{n}$. This conjecture is supported by real observations: we have about 35 000 genes in the human genome and about 200 different tissues, which can be considered as different attractors of the same dynamics. For *Arabidopsis* thaliana, K(M)=22/11=2 and there is $4\approx\sqrt{11}$ different tissues (sepals, petals, stamens and carpels) [3] and for the Crow operon [8] of the phage λ, K(M)=14/5=2.8 and there is $2\approx\sqrt{5}$ observed (lytic and lysogenic) attractors.

Recently [9-15] the conjectures have been in part proved:

Proposition 1: if all loops of the interaction graph are positive, then there exists a state vector $x = (x_1 \ldots,x_n)$ in $\{-1,1\}^n$, such that x and $-x = (-x_1, \ldots, -x_n)$ are fixed configurations of the genetic network dynamics.

Proposition 2: if all loops of the interaction graph are negative, then there is no fixed configuration.

Proposition 3: let a genetic network having n genes and n interactions, then a necessary and sufficient condition of existence of a fixed configuration x is the existence of a positive loop and –x is also a fixed configuration.

Proposition 4: given a state vector x, the set of minimal matrices M having x as fixed configuration is given by the following conditions:

1) $m_{ij} = \square_{ij}\, x_i\, x_j$, where $\square_{ij}\geq 0$ and, for all i, there exists j(i) such that $\square_{ij(i)}>0$
2) $-|\square_{ij(i)}|<b_i\leq|\square_{ij(i)}|$, where the b_i's are the thresholds of the corresponding genetic network [14].

Proposition 5: if m is the number of positive loops L={(i,j)} made from edges (i,j)'s from i to j, then if F is the number of fixed configurations, then $F\leq 2^m$ and 2^m is reached iff: $\forall$ L, there does'nt exist (i,j) / $i\notin L$, $j\in L$.

Proposition 6: if the genetic network has n genes and Kn interactions, with K=2, then the expectation of the number of attractors is $\sqrt{n}$, if n is sufficiently large.

Open problems

An important open problem concerns the relationship between the number F of fixed configurations and the number S of interaction loops of the interaction matrix M: the problem is in fact to find the best upper bound for F for a given matrix M, which is the discrete translation of the famous XVIth Hilbert's problem of determining an efficient upper bound for the number of limit cycles of a polynomial differential system. Let us summarize the role of the architecture of positive and negative (with an odd number of inhibitions) loops of M on the occurrence of multiple stationary behaviors as obtained above: if the numbers of genes and interactions are the same, there is only one isolated loop (S=1) in M and either this loop is negative and the lowest bound (0) for F is reached, or this loop is positive and the upper bound (2^1) for F is reached. If the number of genes is n and the number of interactions is n+1, there is two interaction loops (S=2) with the following structure: if both loops are negative, F=0; if there is a positive loop and a negative loop disjoint, F=0; if there is a positive loop intersecting a negative loop, F=1; if there is a positive loop intersecting a positive loop, F=1; if there is two disjoint positive loops, $F=2^2$. If more generally the number S of loops of M is m, then: if all loops are negative (resp. positive), F=0 (resp. $2 \leq F \leq 2^m$) and iff all loops are positive and disjoint, $F=2^m$. An interesting open problem is now to make exhaustive the determination of F and S and in particular to find the circumstances (related to the loops structure) in which we can relate the number of intersecting and isolated loops to F. The approach for solving this open problem could consist first in finding coherent relationships between analogous properties discovered for continuous versions of the regulatory networks and for general Boolean networks.

Conclusion

A geneticist could exploit the results above in the following sense: we have shown that it would be possible to characterize the minimal interaction matrices having certain state vectors as fixed configurations. The determination of these matrices is not unique, but permits to focus on certain important equivalence classes in which the expected matrix has to belong. This considerably restricts the choice of the possible interaction matrices compatible with observed fixed configurations, when it is impossible to directly get from experiments all interaction coefficients, but possible to observe the phenomenology of fixed or cyclic configurations. This corresponds in genetics to the observation of stationary expression behaviors without experimental measure of the inhibitory and activatory coefficients of promoters and repressors. The possibility to obtain (even in an equivalence class) a sketch of the interaction matrix permits to construct (by randomizing the unknown coefficients of M) more complicated interaction matrices, then to test if they still have the observed states and keep or reject definitively these tested matrices and propose further experimental strategies using bio-arrays for refining knowledge about the interaction structure of the studied genetic networks.

Acknowledgements

We thank MENRT (Grant 00H0276) for supporting this work.

References

[1] J. Mattes, M. Richard, and J. Demongeot, "Tree representation for image matching and object recognition," *Lecture Notes in Comp. Sc.*, 1568, pp. 298-309, 1999.

[2] J. Demongeot, F. Estève, and P. Pachot, "Comportement asymptotique des systèmes : applications en biologie," *Rev. Int. Syst.*, 2, pp. 417-438, 1988.

[3] L. Mendoza, and E.R. Alvarez-Buylla, "Dynamics of the genetic regulatory network for Arabidopsis thaliana flower morphogenesis," *J. Theoret. Biology*, 193, pp. 307-319, 1998.

[4] M. Delbrück, "Unités biologiques douées de continuité génétique," *Colloques CNRS*, Paris, 8, pp. 33-35, 1949.

[5] J. Demongeot, M. Kaufmann, and R. Thomas, "Positive feedback circuit and memory," *C.R.A.S.*, 323, pp. 69-79, 2000.

[6] R. Thomas, "On the relation between the logical structure of systems and their ability to generate multiple steady states or sustained oscillations," *Synergetics*, 9, pp. 1-23, 1980.

[7] S. Kauffman, "The Origins of Order," *Oxford University Press*, Oxford, England, 1993.

[8] D. Thieffry, M. Colet, and R. Thomas, "Formalization of regulatory networks : a logical method and its automatization," *Math. Mod. Sc. Comp.*, 2, pp. 144-151, 1993.

[9] E. Plahte, T. Mestl, and S.W. Omholt, "Feedback loops and multi-stationarity," *J. Biol. Syst.*, 3, pp. 409-414, 1995.

[10] J. Demongeot, "Multi-stationarity and cell differentiation," *J. Biol. Syst.*, 6, pp. 1-2, 1998.

[11] E.H. Snoussi, "Necessary condition for multi-stationarity," *J. Biol. Syst.*, 6, pp. 3-10, 1998.

[12] J.L. Gouzé, "Positive and negative circuits in dynamical systems," *J. Biol. Syst.*, 6, pp. 11-16, 1998.

[13] J. Demongeot, J. Aracena, S. Ben Lamine, S. Meignen, A. Tonnelier, and R. Thomas, "Dynamical systems and biological regulations," *Complex systems*, E Goles & S Martinez eds., Kluwer, Amsterdam, pp. 107-151, 2001.

[14] J. Aracena, S. Ben Lamine, M.A. Mermet, O. Cohen, and J. Demongeot, "Mathematical modelling in genetic networks : relationships between the genetic expression and both chromosomic breakage and positive circuits," *BIBE 2000*, N. Bourbakis ed., IEEE Proc., pp. 141-149, 2000.

[15] O. Cinquin, and J. Demongeot, "Positive and negative feedback : striking a balance between necessary antagonists,"
J. Theoret. Biol., 214, to appear.

Simulations of Self-Organized Systems for Cellular and Intracellular Modeling

Pascal Ballet[1], Abdallah Zemirline[2] and Lionel Marcé[1]

[1] Laboratoire Langages et Interfaces pour Machines Intelligentes, EA2215 - University of Western Brittany Brest, France
[2] Laboratoire d'Informatique Fondamentale, EA2215 - University of Western Brittany Brest,France

Abstract

Many phenomenon occur in a living cell. Most of them are very complex and difficult to understand. However, several cell components seem to have simple interacting and behavioral rules. The aim of this paper is to show how complex phenomenon could appear with simple local rules by using a multi-agents simulator.

Introduction

A cell can be divided into numerous autonomous entities in interaction. Molecules, ions, membrane, and organelles can be seen as interacting reactive agents. A reactive agent is an abstraction or a simplification of a biological entity. It has sensors to get information from its local environment, a simple behavior to change its internal state and actuators to modify the environment [FER95].
We will see below computer examples that show how, complex phenomena can appear from simple behaviors and local interactions. Each example is then explained from a biological point of view.
Finally, we will try to extract the common points of these examples to determine the chacteristic of self-organization.

Simulator

A multi-agents simulator was developed to test self-organized systems. It allows to design agents with sensors to get information from the environment, with actuators to modify the environment and with a algorithmic behaviors to make decisions. Each agent has a 3 dimensional shape which can be controlled in the 3 directions (x, y, z) and in the 3 rotation axes (rx, ry, tz).
The agents live into an environment which is a set of 3D-grids. Each 3D-grid contains data shared by the agent. For example, an agent can read into the grid the identification of each agent to *decide* if they can bind together.
An important part is the visualization of the 3D-matrix containing the agents. That is why, a 3D viewer was designed to explore the in-silico environment. A classical 3D plotter is used to draw the simulation results and a basic simulation controller is included (play, pause, stop).
The next chapter will focus on different self-organized systems simulated using this simulator.

Simulations

Molecule transportation
This system shows how two types of agents can create complexes without any sense of density. The first type of agent is "static" and the second type is "transporter". A static agent can be moved by a transporter agent from one position to another. The rules are the following:
- A transporter moves at random (there is 26 neighbors for a cube in a 3D matrix)
- If a transporter is free and moves onto a static agent, it *gets* the static agent.
- If a transporter has a static agent and moves onto another static agent, first it moves and then it *drops* its own static agent (only if the place is free, that is if the place is not already occupied by a static agent).

These rules are inspired from [DEN91].
The two last rules are in opposition: get and drop could be seen as a $+z$ and $-z$ movements.
With these simple rules, transporter agents are able to make well-defined groups of static agents without definition of density. A simulation with 15 transporters and 50 statics into a 25x25x25 cubic environment, after 10 000 steps of simulation, shows the formation of groups of static agents (Figure 1).

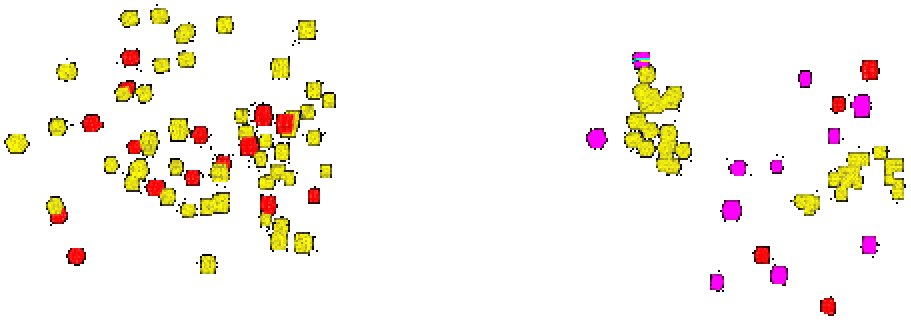

Figure 1: the left screenshot is the initial state of the system (time step = 0). The right image shows the formation of 2 groups of static agents after 10 000 time steps. Static agents are yellow (light), free transporters are red (dark) and filled transporters are magenta (light-dark). A free transporter does not have a static agent on it and a filled transporter has one.

This kind of system could represent the transportation of molecules by others. More precisely, when a molecule "transporter" meets a molecule "static", a complex of the two molecules is created . Then the complex moves at random and dissociates into its two constituents when it meets a "static" molecule. Static molecules could be viewed as nucleation centers.

Particles flow
This system shows how one type of agent that can avoid each other, creates a *linear structure* which minimize the agent collisions. An agent is a simple cube moving along the x-axis (if the way is free in front of it), or moving along the y-axis (if another agent is present -> collision). We design two *opposite* rules for this system: the first set of agents moves from $x-$ to $x+$ and the second set from $x+$ to $x-$. It represents two opposite particle flows that collide one with one another.
The environment is an $n.p$ matrix where agents evolves:

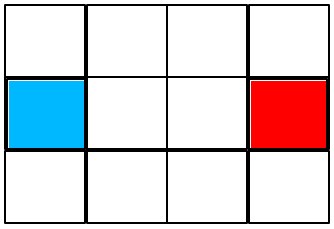

Simple Initial configuration
2 agents in opposition are going to meet.

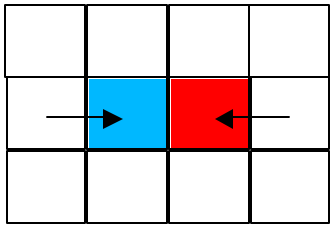

Step 1: agents are moving in opposite directions. They are going to collide.

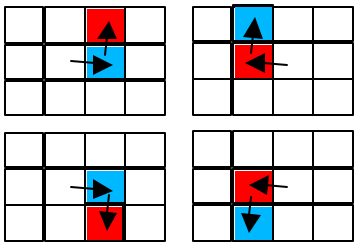

Step 2: agents collide and choose one of these 4 possible configurations with the same probability

Initially, we locate agents at random onto the matrix. Then, we simulate the system and observe the formation of a *linear structure* (Figure 2).

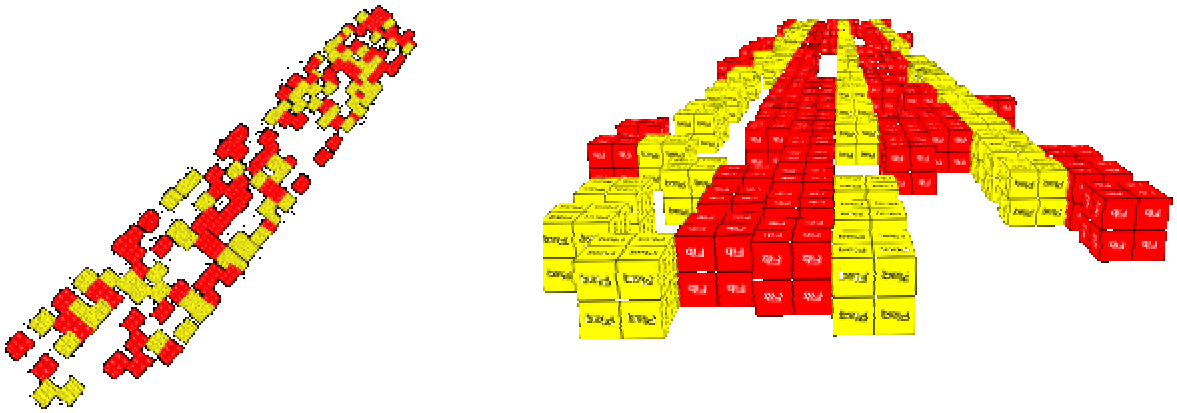

Figure 2: the left screenshot shows the initial state of the system, which is a set of agents located at random. The right image shows the formed a *linear structure* after 100 steps of simulation.

This system could be compared as two flows of particles or something like hydrophilic and hydrophobic molecules composing a membrane.

Membrane deformation

This system aims to reproduce a qualitative 2D cell membrane deformation. For this, we use a simple type of agent called unit membrane agent. An agent is linked to its two neighbors with elastic forces.

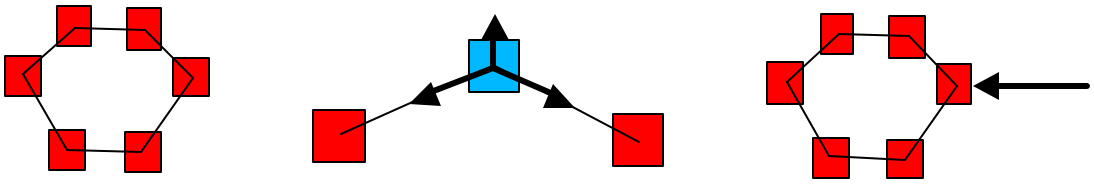

Figure 3: the membrane is compound by a set of agents (Figure 3-a) pair wise linked at the equilibrium state. An agent take into account three forces to calculate its movement. Two forces come from the elastic attraction between agents (E_1 and E_2) and the third is the osmotic pressure (O) which is radial (Figure 3-b). The next step consists in adding an external force applied onto one agent (Figure 3-c) to get a membrane deformation.

The simulation result can be seen in Figure 4.

The shape of the membrane is obtained by the local behaviors and interactions of each agent Ai when one of these agents, A_0, is submitted to a strong enough centripete external force:
A_0 attracts its two neighbors (right and left neighbors), then the right neighbor of A_0 attracts its own right neighbor and the left neighbor of A_0 attracts its own left neighbor and so on.
The duality at the equilibrium state (Figure 4-a) is the opposition between the elastic forces and the osmotic force. An external perturbation force produces a new equilibrium state (emergence) for the system (Figure 4-b) which expresses a qualitative cellular membrane deformation.

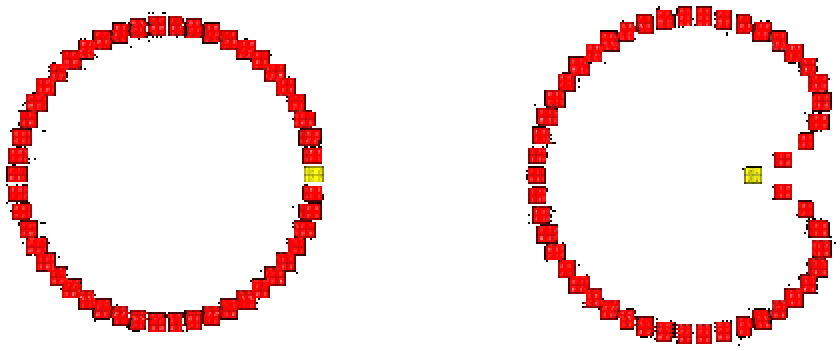

a b

Figure 4: the left image (a) is the initial state of the system (before applying an external force F) and the right image (b) shows the membrane deformation obtained after 100 time steps.

Cicatrisation

When a separation between fibroblast cells happen, the cells try to reduce the "hole" thanks to migration and proliferation. To reproduce such phenomenon, a fibroblast agent is designed. It can move in 8 directions according to its neighbors (adhesion *and* migration) and is able to create a clone of itself (proliferation *or* mitosis). A more accurate work can be found at [DOUG98]. The next figure shows how fibroblast agents will cicatrize (Figure 5).

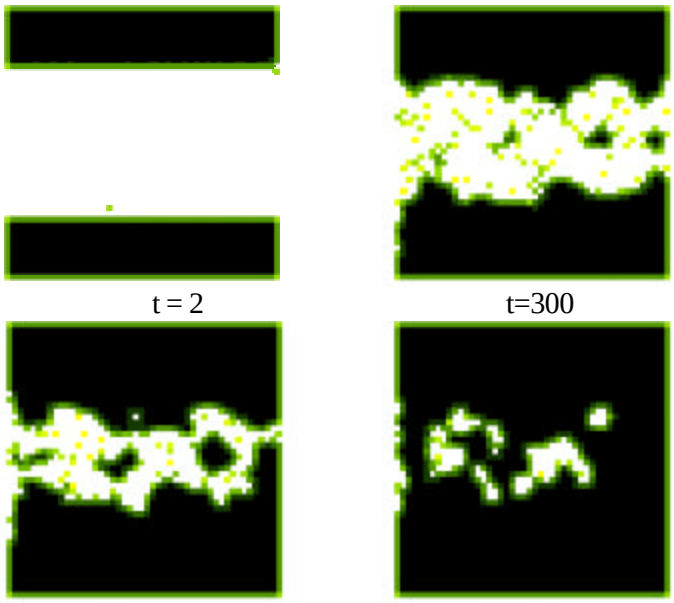

t = 2 t=300

t = 400 t = 500

Figure 5 : initially (t=2), two blocs of agents (in black) are placed face to face and are separated by a hole (in white). Agents are able to move and to clone themselves. Like this, the white hole is settled by the fibroblast agents (t=300, t=400 and t=500).

This system could be used to determine parameters like shape of hole for graft skin or rates of cell adhesion and proliferation during a cicatrisation.

Ring detection

In many biological phenomenon like trees cut or otolithes concretion, alternance of light and dark

structures is observed. The detection of such structure is difficult because

1. the rings are not well separated and the contrast is low
2. the rings have different thickness
3. there are “nods” where different rings are merged [BAL97a] [BAL97b].

A solution consists in defining two populations of agents working either on light rings, either on dark rings. An agent is able to follow dark or light rings and can increase the contrast between rings. Like this, there is a cooperation between the two populations. The increase of contrast could be viewed as a pheromone pathway. An example on an otolithe photo can be seen on the Figure 6.

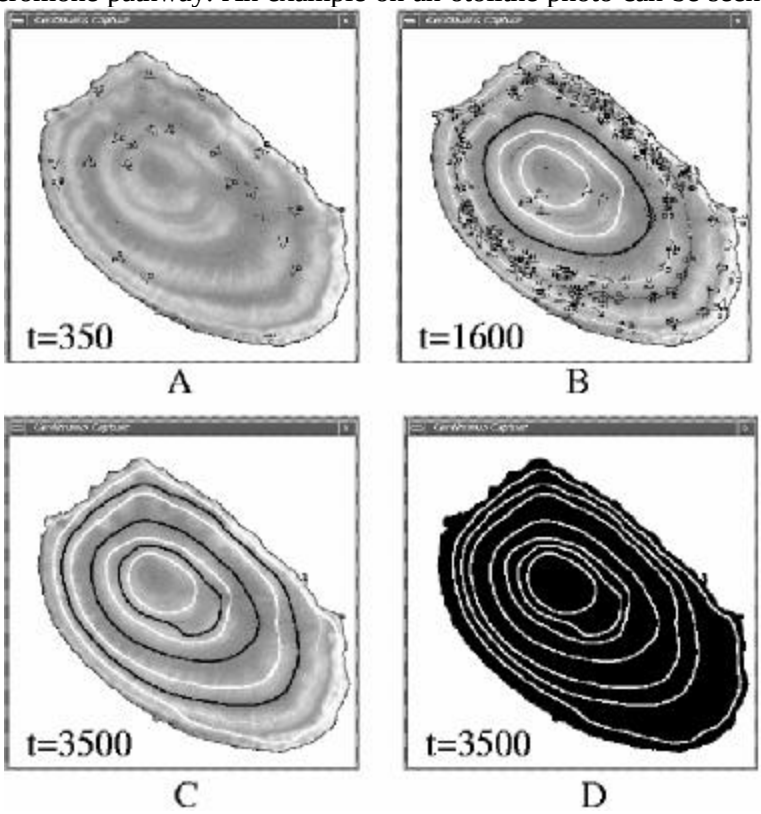

Figure 6: agents are placed at random on a noisy and few contrasted image with alternance of dark and light rings (A). Then they move around the rings according to their opposite behaviors (dark and light agents) (B). After all, they are able to detect the different rings (D) thanks to their dual enforcement behaviors (C).

This system is able to find a probalistic solution of the rings positions. There is an opposition (a competition and a cooperation) between the two types of agents: darks and lights. Biologically, this system could be viewed as an hyperstructure formation guided by an environment where the alternance between dark rings and light rings can be guaranty.

Discussion

Each system has at least 2 opposite rules (rule+ and rule-) which imply the emergence of specific patterns. For instance, for the molecule transportation system, the rule+ is “Get static agent” and the rule- is “Drop static agent” and for the particle flow simulation, the rule+ is “+x movement” and the rule- is “-x movement”. The different rules are summarized in Table 1.

Simulation	**Rule +**	**Rule -**	**Axe / Plan**	**Emergence**
Molecules transportation	Get (+z)	Drop (-z)	z	Group of molecules

Particle flow	+x	-x	x	Line of particules
Membrane deformation	radial	tangent	radial / tangent	Deformation
Cicatrisation	Adhesion	Movement	(x,y)	Group of organized fibroblast cells
Ring detection	+z (light agents)	-z (dark agents)	z	Dark and light pathways

Table 1: rules implied into the emergence of patterns. Remark that each opposite rule can be seen as a spatial opposition (axe).

For a given simulation, it is possible to attribute for the two opposite rules, a spatial opposition. These spatial oppositions, integrated into the agent behaviors, could be a mean to understand, to explain intracellular and cellular phenomenon and a mean to develop a computer model for an integrative cell simulator.

Conclusion

We have seen how simple rules allow to get complex organized systems. We think that such self-organized systems could be interesting for the understanding of intracellular and cellular phenomenon. Moreover, such systems could be easily simulated. Thus, the development of a virtual cell designer application, based on these concepts, should be a good alternative to more descriptive applications like E-Cell [ECE01] or Virtual Cell [VCE01].

References

[BAL97a] P. Ballet, V. Rodin et J. Tisseau, *Multiagent boundary detection system : a way to parallel image processing*, pages 316-323, SPIE's Optical Sciences, Engineering and Instrumentation'97, San Diego (USA), 27-31 July 1997.

[BAL97b] P. Ballet, V. Rodin et J. Tisseau, *A multiagent system for detecting concentric strias*, pages 659-666, SPIE's Optical Sciences, Engineering and Instrumentation'97, San Diego (USA), 27-31 July 1997.

[ECE01] Electronic Cell, http://www.e-cell.org

[DEN91] J-L. Deneubourg, S. Goss, A. Sendova-Franks, C. Detrain et L. Chretien, *The Dynamics of Collective Sorting Robot-like Ants and Ant-Like Robots*, From Animals to Animats, pages 356-363, MIT Press, 1991.

[DUG98] Dugnolle, P., Garbay, C. & Tracqui, P.: *A mechanical model to simulate cell reorganisation during in-vitro wound healing*, Proc ESM'98, 12th European Simulation Multiconference, pp. 343-347, SCS Europe, june 16-19 1998, Manchester.

[FER95] J. Ferber, *Les systèmes Multiagents*, InterEdition, Paris, 1995.

[VCE01] Virtual Cell, http://www.nrcam.uchc.edu

Modelling autocatalytic networks with artificial microbiology

Maurice Demarty[1], Bernard Gleyse[2], Derek Raine[3], Camille Ripoll[1] and Vic Norris[1]

[1]Laboratoire des Processus Integratifs Cellulaires, UPRESA CNRS 6037, Faculte des Sciences et Techniques de Rouen, F76821 Mont Saint Aigan, France
[2]INSA de Rouen, Madrillet, F76821 Mont Saint Aigan, France
[3]Department of Physics and Astronomy, University of Leicester, LE1 7RH, UK

Abstract

Hyperstructures or *modules* have been proposed to constitute an intermediate level of organisation within biological cells. Cells can usefully be equated to autocatalytic networks that increase in mass and then divide. To begin to model relationships between hyperstructures, autocatalytic networks and cell division, we have written a program of artificial chemistry that simulates a cell fed by monomers. These monomers are symbols that can be assembled into linear (unbranched) polymers to give different lengths. A reaction is catalysed by a particular polymer or 'enzyme' that may itself be a reactant of that reaction (autocatalysis). These reactions are only studied within the confines of the 'cell' or 'reaction chamber'. There is a flux of material through the cell since monomers and polymers may be both acquired by and lost from the cell. Eventually, the mass of polymers in the cell reaches a threshold at which, in this version of the program, we then analyse the cell. In the conditions studied (few types of monomers and short polymers), our results indicate that the most important enzymes are those that catalyse the addition of monomers; these enzymes may correspond to the precursors of ribosomes. Future development of the model will entail attributing increased probabilities of reactions to polymers that are colocalised so as to allow evaluation of the consequences of hyperstructure formation along with exploration of the consequences of cell division.

Introduction

The existence of a level of organisation in biology has been proposed intermediate between macromolecules and cells: this level is that of *modules* [1] or *hyperstructures* [2, 3]. Non-equilibrium hyperstructures result from the co-localisation of many different macromolecules in order to perform a particular function. For example, cell division in bacteria would be performed by a hyperstructure comprising division genes, their mRNA and enzymes, together with particular lipids and ions such as calcium, whilst the uptake and metabolisation of many carbohydrate sugars would involve a hyperstructure comprising the genes, mRNA and enzymes of both the phosphoenolpyruvate:carbohydrate phosphotransferase system and the glycolytic pathway [4].

Biological cells are autocatalytic networks [5] and several of their salient characteristics follow from this. For example, they take up nutrients and perform chemical reactions so as to gain mass, and then divide to form daughter cells. The evolution of autocatalytic networks within a self-contained system of artificial chemistry has been observed [6] and, in this context, the importance of simulating division has recently been shown [7].

To begin to model the formation and evolution of autocatalytic networks and their relationship with hyperstructures and cell division, we have written a program that can be approximated to a simulation of a cell that is fed by monomers which are the source of "energy" for the system. In this simulation, the monomers are labelled 1 to n. Different numbers of these monomers can be assembled into linear (unbranched) polymers to give different lengths. A polymer may be cleaved or added to another polymer or monomer in a reaction in which the order and total number of monomers are conserved. A reaction is catalysed by a particular polymer or 'enzyme' that may itself be a reactant of that reaction (autocatalysis). More than one variety of enzyme may separately catalyse the same reaction; a single variety of enzyme may catalyse more than one reaction; some polymers do not catalyse reactions. These reactions are only studied within the confines of the cell. The initial cell is created by the self-association of a random number of each monomer and a random number of a random selection of polymers formed outside the cell. The cell is then supplied with monomeric nutrients at regular or intermittent intervals. The cell is also supplied with enzymes but at a rate much lower than the rate of supply of nutrients. There is a flux of material through the cell since monomers and polymers may be lost from the cell (note that this facility is not used in the version described below). The dynamics of the system is described by representations of its state at discrete time steps. At each time step, a nutrient may or may not be incorporated into the cell depending on the availability of the nutrients outside the cell. At each time step, the cell is modified by calculating on the basis of concentrations whether each variety of enzyme catalyses its cognate reactions. Each variety of enzymes is examined. This results in changes in the numbers and types of monomers and polymers present in the cell. The time step is repeated until the mass of polymers in the cell reaches a threshold (corresponding to the size at which cell division would occur) and the cell is then analysed in terms of the number and nature of its polymers, reactions and their connectivity.

The model

1) We consider a set of monomeric molecules (monomers) of different nature labeled 1 to n.
2) These monomers are "nutrients" which are present outside a "reaction chamber" or "cell".
3) Different numbers PD (for Polymerisation Degree) of these monomers can be assembled in linear (unbranched) polymeric molecules (polymers) to give different lengths. The symbol $P_j(\{k\})$ represents a polymer containing PD=j monomeric units and {k} is an ordered set of j symbols each symbol being an element of the set of n monomeric units defined above. For example, if the polymer $P_j(\{k\})$ is the string 23112 then j=5 and {k}= {2,3,1,1,2}. Polymers containing PD=j monomeric units therefore exist in a maximum of n^j different permutations.
4) A polymer containing PD=p monomeric units may be cleaved or added to other polymers (PD=q) or monomers (PD=1) such that the order and total number of monomeric units is conserved in the reaction. Reactions between molecules are of the form, $P_p(\{k\}) \oplus P_q(\{l\}) = P_{p+q}(\{k\}\{l\})$ where {k} and {l} are ordered sets of the monomeric units and $(\{k\}\{l\})$ is the result of the addition of these sets in the order k to l. This reaction is reversible but is not commutative i.e. $P_q(\{l\}) \oplus P_p(\{k\}) = P_{p+q}(\{k\}\{l\})$ is a different reaction. It is therefore the equivalent of reactions of addition (left to right) or cleavage (right to left).
5) Reactions are catalysed by a particular polymer $P_p(\{k\})$ that may itself be a reactant (autocatalysis) and that we term "enzyme" for convenience. More than one variety of enzyme e.g. $P_p(\{k\})$ and $P_q(\{l\})$ may separately catalyse the same reaction. A single

variety of polymer may catalyse more than one reaction. No monomer may catalyse a reaction. Some polymers do not catalyse reactions.

6) Reactions of the above type are only studied in the confined volume of a cell or reaction chamber that, in its initial form, we regard as created by the self-association of a random number of each monomer and a random number of a random selection of polymers made outside the cell (by "abiotic" mechanisms that may be different from those in (5) and that we do not study).
7) Nutrients are then supplied to the cell at regular or intermittent intervals. The cell may also be supplied with polymers but at a rate much lower than the rate of supply of nutrients.
8) The dynamics of the system is described by representations of its state at discrete time steps. At each time step, nutrients may or may not be incorporated into the cell depending on the availability of the nutrients outside the cell. In principle, there could be an efflux of material through the cell since the possibility also exists of losing monomers and polymers from the cell (for example, the probability of a monomer or polymer being lost could be inversely proportional to the number of reactions in which it is involved). This possibility is not implemented in the version described here.
9) At each time step, two lists that describe the system are updated. The first list, the Moleculelist, contains a reference to each class of molecule present in the cell. Each class of molecules has a description comprising its label (name), the number of copies, whether it is a monomer or a polymer and in the latter case, whether it is an enzyme. The second list, the Enzymelist, contains a reference to each class of enzymes present in the cell. Each class of enzymes has a description comprising its label, the number of copies, its activity status (active or inactive) and the reaction(s) it catalyses. A reaction is defined by three molecules, corresponding to two substrates, $P_p(\{k\})$ and $P_q(\{l\})$, and one product, $P_{p+q}(\{k\}\{l\})$, and by the k_f and k_r for this reaction where k_f and k_r are the equivalent of the rate constants for the forward and reverse reactions, respectively. An enzyme can catalyse more than one reaction. Initially, the number of varieties of enzyme is chosen at random. Then the cell is fed in accord with (7).
10) At each time step, the system is updated by calculating whether each variety of enzyme catalyses its cognate reactions. Each variety of enzymes is examined. The forward reaction can take place if the enzyme $P_r(\{m\})$ is present and active and if $k_f * N(\{k\}) * N(\{l\}) > k_r * N(\{k\}\{l\}) * N_t$ where N_t is the total number of molecules in the cell and k_f and k_r are the rate constants for the particular reaction as catalysed by the enzyme. If the inequality is reversed, the reverse reaction occurs.
11) Iteration during the time step. A variety of enzyme is chosen from the Enzymelist either according to its concentration (as presented here) or at random (in the latter case, this choice is weighted by the number of copies, N_m, of the enzyme of a given variety, $P_r(\{m\})$, such that the probability of choosing this variety is proportional to N_m/N_{Et} where N_{Et} is the total number of enzymes).

The total increase and decrease in the number of copies of each molecule involved in a single catalysed reaction during the time step is obtained from:

$\Delta N(\{k\}\{l\}) = - \Delta N(\{k\}) = - \Delta N(\{l\})$

(note that in the version presented here the concentration of the enzyme determines how many times the same reaction occurs within the time step)

The set of molecules in the cell is therefore altered after every reaction. After one variety of enzyme has been treated as above, another variety is chosen and its cognate reaction

performed in the same way. Each variety of enzyme is chosen from the Enzymelist until all varieties have had the possibility of catalysing their reaction.

12) At the start of each time step, the cell is tested to see whether it has grown to a threshold at which cell division could occur. This test is based on the total number of polymers in the cell but alternatives include the number of monomers in the form of polymers as well as the number of copies of a specific polymer. In the present model, all reactions cease at this critical cell size and the program ends.

Method

The program was written in Pascal Object and run on a PC under Windows.

Results

Here, we present a typical run of the program using only three types of monomer (Table 1). The number of copies of these monomers present in the cell is given in column **CI**, for *concentration initiale*. The open circle symbol in column **O** indicates which of the polymers in column **ID**, for *identity*, were present in the cell at the start of the experiment. **CI** gives the number of copies at the start - note that this cell did *not* initially contain polymers of types ID 233 to ID 31321131212313211121. **CF** for *concentration finale* gives the number of copies of the polymer at the end of the experiment - note that if a polymer has an entry in neither **CI** nor **CF** it is because it was formed during the experiment but disappeared before the end. **Ns**, for *node as substrate*, indicates the number of different reactions in which a molecule was involved as a substrate; in other words, it is the node class of the molecule with respect to the reactions in which it has been consumed; **Np**, for *node as product*, indicates the number of different reactions in which a molecule was involved as a product; **Nt**, for *node total*, is the sum of **Ns** and **Np**. In this analysis, the cell can be regarded as a network of molecules that are connected by catalysed reactions; a molecule that can be made from 2 different molecules and made into 3 others has a node class of **Ns**=2, **Np**=3 and **Nt**=5. **Reaction** is the number of times the reaction occurred in the course of the experiment. The right arrow (**->**) is the number of times the molecule was consumed, the left arrow (**<-**) is the number of times the molecule was produced and **Net** is the difference between consumption and production.

The asterisks in column **E** (Table 1) indicate which of the polymers were enzymes. Polymers either start as enzymes or acquire activity later. This latter is simply a device to model the entry of a new enzyme by ascribing at random an activity to a polymer present in the original cell (Table 1); an alternative possibility not explored here is that acquisition of activity is due to a cofactor entering the cell.

The kinetics of the numbers of monomers and polymers (Figure 1) show that an event occurred at time step 360 when enzyme 11 'entered' the cell. The reaction catalysed by 11 is 2+3<==>23 and this led to a rapid increase in the numbers of 23 (Figure 2). There were no enzymes catalyzing the reaction 1+1<==>11 so catalytic closure did not occur [5]. Nevertheless, the system grew using its initial complement of polymer 11 until time step 688 when it had doubled the number of its polymers (from 68 to 136). 23 was also an enzyme and catalysed the reaction leading to another enzyme 33+21<==>3321; 3321 catalysed 2+33<==>233; 233 catalysed 11+31<==>1131, a reaction that consumes or generates 11 Table 2). Hence there is a cycle. (Note that the reactions of all enzymes are easily displayed although we do not show them here; many other reactions are indicated in Table 1).

The numbers of members of a particular node class (where the class is the sum of the reactions in which the molecule is either a substrate or product) reveals a distribution with a long tail (Figure 3). The molecules with the highest connectivities were 21 and 1121 and those with the next highest were 2, 313 and 31321 (Table 1). We have not analysed connectivity in terms of catalysts in a context where an enzyme could catalyse several reactions although this would be possible.

Discussion

Artificial chemistry offers a powerful possibility for both testing existing biological concepts and for deriving new ones [6]. We have used a variant that we term *artificial microbiology* to study how autocatalytic networks develop when they are confined to cells that are allowed to grow to a fixed size. For the limited range of monomers and polymers studied here, our results from a limited range of experiments, of which this is one, indicate that the most important enzymes are those that catalyse the addition of monomers. This is in fact obvious – as a network evolves, the first limiting step in the growth of the cell is the flow of monomers into the cell and the second limiting step is the addition of these monomers onto polymers or onto other monomers. The enzymes that add monomers may therefore correspond to the ancestral precursors of modern polymerases and ribosomes that also add monomers onto polymers.

Abstract networks or graphs consist of nodes and the connections or links between them. A particular node belongs to a node class which corresponds to the number of connections per node. By allocating a metabolite to a node class on the basis of its connections to other metabolites, we and, independently, others have found that real metabolic networks have a power law distribution of node classes characterized by a long tail [8, 9, 10]. Similar distributions have been found for proteins [11]. Artificial microbiology permits the origin and properties of real metabolic distributions to be investigated. For example, what confers robustness to fluctuations in nutrition? Where should the highest node classes be located so as to assure a maximum use of inputs and a steady output? What allows the network to be regenerated after starvation?

In the version presented here, the program ends when the cell attains a size at which division might occur. The importance of cell division in the evolution of autocatalytic networks has recently been described [7, 12]. Our program offers the possibility of exploring how competing autocatalytic networks within the mother cell may be separated by cell division into individual ones. By selecting the faster growing daughter cell, the role of cell division in the evolution of networks can then be studied. It seems likely that formation of hyperstructures [2] may make this role of division much more efficient. Future development of the model will therefore entail attributing increased probabilities of reactions to polymers that are colocalised so as to allow evaluation of the consequences of hyperstructure formation. Finally, artificial microbiology may be extended to study what happens when other types of reactions are introduced [13], when the cell shifts from a growing to a non-growing state, when inactive enzymes are preferentially inhibited, and when a coding polymer (DNA/RNA) is present.

Acknowledgements

We thank Dick D'Ari, and the members of the epigenesis atelier for helpful discussions.

References

1. L. H. Hartwell, J. J. Hopfield, S. Leibler and A. W. Murray. (1999). From molecular to modular cell biology. *Nature,* **402**(6761 Suppl), C47-52.
2. V. Norris, S. Alexandre, Y. Bouligand, D. Cellier, M. Demarty, G. Grehan, G. Gouesbet, J. Guespin, E. Insinna, L. Le Sceller, B. Maheu, C. Monnier, N. Grant, T. Onoda, N. Orange, A. Oshima, L. Picton, H. Polaert, C. Ripoll, M. Thellier, J.-M. Valleton, M.-C. Verdus, J.-C. Vincent, G. White and P. Wiggins. (1999). Hypothesis: hyperstructures regulate bacterial structure and the cell cycle. *Biochimie,* **81**, 915-920.
3. V. Norris, J. Fralick and A. Danchin. (2000). A SeqA hyperstructure and its interactions direct the replication and sequestration of DNA. *Mol. Microbiol.,* **37**, 696-702.
4. V. Norris, P. Gascuel, J. Guespin-Michel, C. Ripoll and M. H. Saier Jr. (1999). Metabolite-induced metabolons: the activation of transporter-enzyme complexes by substrate binding. *Mol. Microbiol.,* **31**, 1592-1595.
5. S. Kauffman. (1996). *At home in the Universe, the search for the laws of complexity.*, Penguin, London.
6. P. Dittrich and W. Banzhaf. (1998). Self-evolution in a constructive binary string system. *Artificial Life,* **4**, 203-220.
7. D. Segre, D. Ben-Eli and D. Lancet. (2000). Compositional genomes: prebiotic information transfer in mutually catalytic noncovalent assemblies. *Proc. Nat. Acad. Sci., U.S.A.,* **97**, 4112-4117.
8. D. J. Raine and V. Norris. (2000). Self-Organisation in Metabolic Pathways. *InterJournal,* Paper **361**, http://www.interjournal.org.
9. D. J. Raine and V. Norris. (2001). Network Structure of Metabolic Pathways. *J. Biol. Phys. Chem.,* **1**, 89-94.
10. H. Jeong, B. Tombor, R. Albert, Z. N. Oltvai and A.-L. Barabási. (2000). The large-scale organization of metabolic networks. *Nature,* **407**, 651-654.
11. J. J. Ramsden and J. Vohradsky. (1998). Zipf-like behavior in procaryotic protein expression. *Phys. Rev. E,* **58**, 7777-7780.
12. V. Norris and I. Fishov. (2001). Division in bacteria is determined by hyperstructure dynamics and membrane domains. *J. Biol. Phys. Chem.,* **1**, 29-37.
13. V. Norris and L. Le Sceller. (2001). *International Conference of Systemics, Cybernetics and Informatics, Orlando, Florida, USA*.

Table 1 Summary of the cell

O	E	ID	CI	CF	Food	Nt	Ns	Np	Reaction	->	<-	Net
°		1	53	107	54	1	1	0	0	0	0	0
°		2	54	0	54	6	6	0	1946	919	1027	-108
°		3	97	58	64	3	3	0	1307	602	705	-103
			204	**165**	**172**	**10**	**10**	**0**	**3253**	**1521**	**1732**	**-211**
°	*	11	14	6		5		5	1960	976	984	-8
°	*	12	2			4		4	2		2	-2
°	*	13	6			3		3	286	140	146	-6
°	*	21	13			7		7	1481	734	747	-13
°	*	22	3	3		1		1				
°	*	23	3	100		2		2	1021	559	462	97
°	*	31	6	3		2		2	1639	818	821	-3
°	*	32	15	1		3		3	14		14	-14
°	*	33	6			3		3	786	390	396	-6
	*	233		5		2	1	1	215	110	105	5
	*	312		3		2	1	1	443	223	220	3
	*	313				6	5	1	566	283	283	
	*	1121				7	5	2	1198	599	599	
	*	1131				1		1	1196	598	598	
	*	1212				2	1	1				
		3131				1		1				
	*	3232		6		3	2	1	10	8	2	6
	*	3321				4	2	2	618	309	309	
	*	21121				4	3	1	248	124	124	
		22233				1		1				
	*	23321				3	2	1	48	24	24	
	*	31321				6	5	1	162	81	81	
	*	323232				1		1				
	*	1123321		1		1		1	1	1		1
	*	1221121				1		1				
	*	2112112		2		3	2	1	24	13	11	2
	*	3131121				3	2	1	152	76	76	
	*	3133232		1		1		1	3	2	1	1
		112131321				1		1				
		132112112				3	2	1				
	*	211211121				2	1	1	26	13	13	
	*	212112112				2	1	1	22	11	11	
	*	313211121		5		2	1	1	37	21	16	5
	*	332131321				1		1				
	*	11132112112				1		1				
	*	21132112112				1		1				
	*	211211121313				1		1				
	*	2121121123 12				2	1	1				
	*	313213131121				1		1				
	*	1212313211121				3	2	1				
	*	1312123132 11121				2	1	1				
	*	23321212112112312				1		1				
	*	121231321112131311 21				1		1				
		313211312123132111 21				1		1				
		Total	**68**	**136**		**107**	**68**	**39**	**12158**	**6113**	**6045**	**68**

Table 2 A reaction network

	Id	Formation Step	Reaction	kf	kr
a	11	360	2 + 3 <==> 23	20	222
b	23	0	33 + 21 <==> 3321	74	426
c	3321	60	2 + 33 <==> 233	43	823
d	233	80	11 + 31 <==> 1131	1	102
e	1131	100	313 + 21 <==> 31321	15	168

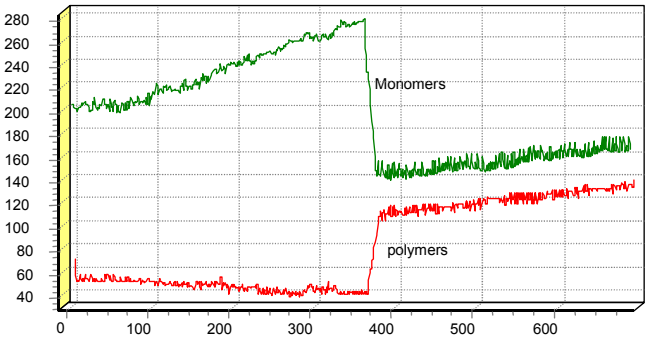

Fig 1 Numbers of monomers and polymers vs timestep

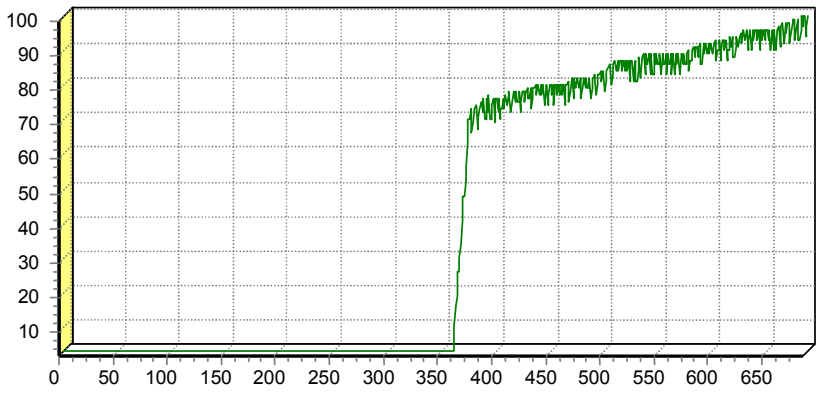

Fig 2 Number of copies of polymer 23 vs timestep.

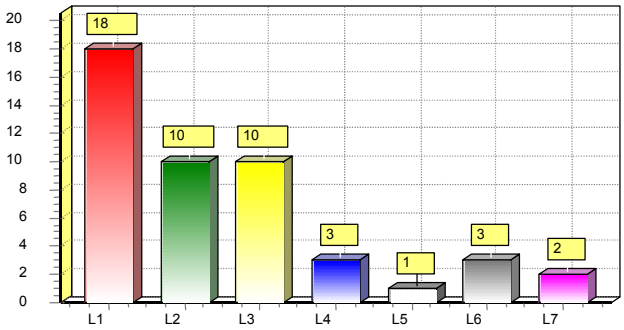

Fig. 3 Distribution of node classes. Number in Node Class vs Node Class

Planning du séminaire

Date	8:30 => 12:30 **Présentations**	12:30 => 17:15	17:15 => 19:15 **Ateliers**	19:30 => 20:30	20:30 => 22:30
18	Jacques PROST Jean-Baptiste FOURNIER Vincent SCHACHTER	Déjeuner + temps libre	Membranes	Diner	Discussions informelles Démonstrations Affiches
19	Jacques RICARD Jean-Pierre MAZAT Christophe CHASSAGNOLE Athel CORNISH-BOWDEN		Hyperstructures		
20	Pierre AUGER Derek RAINE Marcelline KAUFMAN Julie FIÉVET		Observabilité		
21	Yves BOULIGAND Camille RIPOLL Jacques DEMONGEOT Yannick KERGOSIEN		Organisation		

Programme détaillé

Lundi 18	9:00	Accueil, organisation matérielle	
	9:30	Jacques PROST	Listeria mobility: what do we learn for genomics?
	10:30	Pause café	
	11:00	Jean-Baptiste FOURNIER	Dynamin Recruitment by Clathrin Coats: a physical step?
	12:00	Vincent SCHACHTER	Quelques problèmes de représentation des réseaux biologiques
	12:30	déjeuner	
	17:15	Atelier: Membranes	
Mardi 19	8:30	Jacques RICARD	Information of metabolic networks
	9:30	Jean-Pierre MAZAT	Virtual mitochondria and their control
	10:30	Pause café	

	11:00	Christophe CHASSAGNOLE	Dynamic simulation of pollutant effects on the theonine pathway in Escherichia Coli
	11:30	Athel CORNISH-BOWDEN	Metabolic analysis in drug design
	12:30	déjeuner	
	17:15	Atelier: Hyperstructures	
Mercredi 20	8:30	Pierre AUGER	Une approche intégrative de la biologie : les changements de niveaux d'organisation
	9:30	Derek RAINE	The Complexity Of Canonical Power Law Networks
	10:30	Pause café	
	11:00	Marcelline KAUFMAN	Logical Analysis of Regulatory Networks in Terms of Feedback Circuits
	12:00	Julie FIÉVET	Optimisation des systèmes métaboliques contraints
	12:30	déjeuner	
	17:15	Atelier: Observabilité	
Jeudi 21	8:30	Yves BOULIGAND	Aspects *cristaux liquides et polymères* de L'ADN. le cas particulier des procaryotes et les perspectives d'applications
	9:30	Camille RIPOLL	Hypothesis: the condensation of counter-ions is an intracellular integrating process
	10:30	Pause café	
	11:00	Jacques DEMONGEOT	Bio-array images processing and genetic networks modelling
	12:00	Yannick KERGOSIEN	Adaptive Branching in Evolution and Epigenesis
	12:30	déjeuner	
	14:15	Atelier: Organisation	

Presentation abstracts

Listeria motility: what do we learn for genomics?

Jacques Prost

Institut Jacques Monod, CNRS, Universités Paris 6 et Paris 7

In this talk we will bring together physics and biology to explain how bacteria such as *Listeria monocytogenes* travel within and between human cells by locally polymerising actin using a bacterial protein, ActA. We will show how ActA-coated beads could move in a similar way and discuss symmetry-breaking, persistence-lengths and the squeezing of cherry-stones to make them fly.

Dynamin recruitment by clathrin coats: a physical step?

J.-B. Fournier* and P.-G. Dommersnes†

Laboratoire de Physico-Chimie Théorique and FR CNRS 2438 "Matière et Systèmes Complexes", ESPCI, 10 rue Vauquelin, F-75231 Paris cedex 05, France

P. Galatola

LBHP, Université Paris 7—Denis Diderot and FR CNRS 2438 "Matière et Systèmes Complexes", Case 7056, 2 place Jussieu, F-75251 Paris cedex 05, France

Abstract – Recent structural findings have shown that dynamin, a cytosol protein playing a key-role in clathrin-mediated endocytosis, inserts partly within the lipid bilayer and tends to self-assemble around lipid tubules. Taking into account these observations, we make the hypothesis that individual membrane inserted dynamins imprint a local cylindrical curvature to the membrane. This imprint may give rise to long-range mechanical forces mediated by the elasticity of the membrane. Calculating the resulting many-body interaction between a collection of inserted dynamins and a membrane bud, we find a regime in which the dynamins are elastically recruited by the bud to form a collar around its neck, which is reminiscent of the actual process preempting vesicle scission. This physical mechanism might therefore be implied in the recruitment of dynamins by clathrin coats.

endocytosis / clathrin / dynamin / membrane inclusions interactions

Résumé – **Une étape physique dans le recrutement des dynamines par les capsules de clathrine ?** Des donnés structurales récentes ont montré que la dynamine, une protéine du cytosol qui joue un rôle clé dans l'endocytose clathrine-dépendante, s'insère partiellement dans la bicouche membranaire et tend à s'auto-assembler autour de tubules lipidiques. En tenant compte de ces observations, nous faisons l'hypothèse que les dynamines impriment localement une courbure cylindrique dans la membrane. Cette empreinte peut engendrer des forces élastiques de longue portée. En calculant l'interaction multi-corps entre un ensemble de dynamines insérées dans la membrane et une capsule endocytotique, nous trouvons un régime dans lequel les dynamines sont recrutées élastiquement par la capsule pour former un collier autour de son cou, ce qui rappelle le processus précédant la scission des vésicules d'endocytose. Ce mécanisme physique pourrait donc être impliqué dans le recrutement des dynamines par les capsules de clathrine.

endocytose / clathrine / dynamine / interactions entre inclusions membranaires

* Author for correspondence (jbf@turner.pct.espci.fr)

† Present address: Institutt for fysikk, Kontor D-5 184. NTNU. N-7491 Trondheim. Norway.

Quelques problèmes de représentation des réseaux biologiques

Vincent Schächter

HYBRIGENICS - 3-5 impasse Reille, 75014 Paris

Les travaux récents dans le domaine de la reconstruction des réseaux biologiques et de la simulation des processus correspondants s'appuient sur des choix de représentation plus ou moins explicite -- souvent présentés sous la forme d'un modèle de données, exprimé dans un certain formalisme, ce dernier comprenant ou pas des aspects dynamiques. Ces couples formalisme/modèles de données sont souvent conçus pour des applications précises. A partir d'une revue comparative, nous tenterons de mettre en évidence les avantages et les limitations des représentations discrètes existantes, et de pointer vers les problèmes ouverts correspondants.

Information of metabolic networks

Jacques Ricard

Institut Jacques Monod, CNRS, Universités Paris 6 et Paris 7

As most enzyme reactions associate two, or three, reagents, metabolic networks may possibly contain an information which can be large relative to standard genetic information. Network information is adaptive as a response to several signals. A peculiarity of metabolic networks is that they may well not conform to the subadditivity principle of Shannon's information theory. This means that network information can be positive, nil or even negative. In that case, the system does not act as an information channel, but generates an information of its own and displays emergent properties.

Virtual Mitochondria And Their Control

Marie Aimar[1], Bernard Korzeniewski[3], Jean-Pierre Mazat[1] and Christine Nazaret[2] (alphabetic order)

[1]Inserm EMI 9929, and [2]ESTBB, Université de Bordeaux 2, 146 rue Léo-Saignat, F 33076, Bordeaux-cedex France.
[3] Jagiellonian University, ul. Gronostajowa 7, 30-387 Krakow, Poland

Résumé

Dans la cellule eucaryote, les mitochondries sont des organelles responsable de la fourniture en énergie sous forme d'ATP. Le contrôle de la production d'ATP mitochondrial est un problème complexe avec différentes expression dans différents tissus et organes.
Notre but est de continuer la modélisation des oxydations phosphorylantes mitochondriales, d'y ajouter le reste du métabolisme mitochondrial et d'intégrer cette mitochondrie virtuelle dans une cellule virtuelle.
Pour construire les cartes du métabolisme mitochondrial, on se servira des séquences connues des génomes eucaryotes (10 à 15% du génome de la levure concerne les mitochondries).

Abstract

Inside the eukaryotic cell, mitochondria are internal organelles of prokaryotic origin, responsible for energy supply in the cell. The control of the mitochondrial ATP production is a complex problem with different patterns according to different tissues and organs.
Our aim is to continue to develop the modelling of oxidative phosphorylation in different tissues, to model other parts of mitochondrial metabolism and to include this virtual mitochondria in a virtual cell.
In constructing the complete metabolic map of mitochondria, we will take advantage of the sequenced genomes of eukaryotic organism, (10-15% of the yeast genome concerns mitochondria).

Dynamic Simulation Of Pollutant Effects On The Theonine Pathway In *Escherichia Coli*

Christophe Chassagnole[a1*], Eric Quentin[a2], David A. Fell[b], Pedro de Atauri[c] and Jean-Pierre Mazat[a]

[a] INSERM EMI 9929 and Université de Bordeaux II, 146 rue Léo-Saignat, 33076 Bordeaux Cedex, France.
[b] School of Biological and Molecular Sciences, Oxford Brookes University, Oxford OX3 0BP, U.K.
[c] Departement de Bioquimica I Biologia Molecular, Universitat de Barcelona, Marti I Franques 1, 08028 barcelona, Spain.
Present address: [1] INSA – dGBA 135 Av. de Rangueil F–31077 Toulouse Cedex, France. [2] DIOSYNTH France, BP 26, 60590 Eragny-sur-Epte France.
*Corresponding author: christophe.chassagnole@insa-tlse.fr, phone: +33 (0)5 61 55 94 18, fax: +33 (0)5 61 55 94 00

Abstract - The enzymatic activities of threonine pathway in *Escherichia coli* are sensitive to pollutants such as cadmium, copper and mercury which even at low concentration, can substantially decrease or even block the pathway at several steps. Our aim was to investigate the complex effects on a metabolic pathway of such general enzyme inhibitors with several sites of action, using a previously-developed computer simulation of the pathway. For this purpose, the inhibition parameters were experimentally determined and incorporated in the model. The calculation of the flux control coefficient distribution between the five steps of the threonine pathway showed that control remains shared between the three first steps under most inhibition conditions. Response coefficient analysis shows that the inhibition of aspartate semialdehyde dehydrogenase is quantitatively dominant in most circumstances.

***Keyword*:** Threonine, computer simulation, metabolic control analysis, biosynthetic pathway, pollutants.

Résumé – Les activités enzymatiques de la chaîne de biosynthèse de la thréonine d'*Escherichia coli* sont particulièrement sensibles a des polluants tels que le cadmium, le cuivre et le mercure, qui peuvent diminuer ou bloquer le métabolisme bactérien. Les paramètres cinétiques de ces inhibitions ont été déterminés expérimentalement, puis incorporé dans un modèle mathématique de la voie. Ce modèle a été utilisé pour simuler l'effets de ces inhibition sur le flux de biosynthèse de la thréonine et calculer la répartition des coefficients de contrôle entre les étapes de la voie. Ceci a montré que le contrôle est toujours reparti entre les trois première étapes.

***Mots clés*:** Thréonine, simulation du métabolisme, théorie du contrôle du métabolisme, voie de biosynthèse, polluants.

Metabolic analysis in drug design

Athel Cornish-Bowden* and María Luz Cárdenas

CNRS-BIP, 31 chemin Joseph-Aiguier, B.P. 71, 13402 Marseille Cedex 20, France
E-mail address: athel@ibsm.cnrs-mrs.fr

Abstract

Biotechnology is often presented as if progress in the past two decades represented a major success, but the reality is quite different. For example, ten major classes of antibiotics were discovered between 1935 and 1963, but after 1963 there has been just one, the oxazolidones. To illustrate the possibilities of doing better by taking account of the real behaviour of metabolic systems, we can examine how one might modify the activity of an enzyme in the cell (for example by genetic manipulation, or by the action of an inhibitor, etc.) to satisfy a technological aim. For example, if the objective is to eliminate a pest, one might suppose that the effect of an inhibitor could be to depress an essential flux to a level insufficient for life, or to raise the concentration of an intermediate to a toxic level. The former may seem the more obvious, but the latter is easier to achieve in practice, and there are some excellent examples of industrial products that work in that way, such as the herbicide 'Roundup' and antimalarials of the quinine class. A study of glycolysis in the parasite *Trypanosoma brucei* (which causes African sleeping sickness) indicates that for this approach to work the selected target enzyme must have a substrate with a concentration that is not limited by stoicheiometric constraints. That is not necessarily easy to find in a complicated system, and typically needs the metabolic network to be analysed in the computer.

Metabolic analysis / stoicheiometric analysis / uncompetitive inhibition / drug design

Résumé

La biotechnologie est souvent présentée comme si les nouvelles technologies des deux dernières décennies constituaient une réussite éclatante, mais la réalité est toute autre. Par exemple, entre 1935 et 1963 on a découvert dix classes majeures d'antibiotiques ; depuis 1963 on n'en a découvert qu'une seule, les oxazolidones. Pour illustrer les possibilités d'améliorer les résultats en tenant compte du comportement des systèmes métaboliques, nous pouvons examiner comment on peut modifier l'activité d'une enzyme dans la cellule (soit par manipulation génétique, soit par l'action d'un inhibiteur, etc.) pour satisfaire des objectifs biotechnologiques. Par exemple, si le but est d'éliminer une peste, on peut supposer que l'effet d'un inhibiteur puisse être d'abaisser un flux essentiel en-dessous d'un niveau indispensable à la vie, ou d'augmenter la concentration d'une métabolite à un niveau toxique. Le premier semble être le plus évident, mais le second est plus facile à réaliser dans la pratique, et on a d'excellents exemples de produits industriels très importants qui fonctionnent ainsi, comme le « Roundup » utilisé comme herbicide, ou la quinine comme médicament contre le paludisme. Une étude de la glycolyse dans le parasite *Trypanosoma brucei* (responsable de la maladie de sommeil) indique que, pour que cette approche soit efficace, il faut choisir comme cible une enzyme pour laquelle la concentration du substrat ne soit pas limitée par des relations stoechiométriques. Ceci n'est pas forcément facile à trouver dans un système compliqué, et nécessite typiquement une analyse métabolique par ordinateur.

Analyse métabolique / analyse stœchiométrique / inhibition incompétitive / conception de médicaments

Une approche intégrative de la biologie : les changements de niveaux d'organisation

Pierre Auger & Christophe Lett

UMR CNRS 5558, Université Claude Bernard Lyon 1, 43 boulevard du 11 novembre 1918,
69622 Villeurbanne cedex.

Résumé

Les systèmes biologiques sont composés de différents niveaux d'organisation. Habituellement, les niveaux de l'atome, de la molécule, de la cellule, de l'individu, de la population, de la communauté et de l'écosystème sont considérés. Ces niveaux d'organisation correspondent en fait à des niveaux d'observation différents, c'est-à-dire à des échelles d'espace et de temps différentes: les niveaux plus microscopiques correspondent à des échelles de temps plus rapides et à des échelles d'espace plus petites. Ainsi, la dynamique globale d'un système biologique est le résultat des dynamiques couplées de chacun de ses niveaux d'organisation, dynamiques qui se déroulent à différentes échelles de temps. Les méthodes d'agrégation de variables tirent partie de l'existence de ces différentes échelles de temps afin de réduire la dimension des modèles mathématiques comme les systèmes d'équations différentielles ordinaires. Nous étudierons la dynamique d'un système présentant une structure hiérarchique, c'est-à-dire composée de groupes d'éléments, eux-même constitués de sous-groupes qui peuvent à leur tour être structurés en parties plus petites et ainsi de suite. La structure hiérarchique du système provient du fait que l'on suppose que les interactions intra-groupe sont rapides par rapport aux interactions de type inter-groupe. Nous présenterons la méthode d'agrégation qui permet de construire un modèle global gouvernant la dynamique de quelques variables macroscopiques à une échelle de temps lente.

Abstract

Biological systems are composed of different levels of organization. Usually, one considers the atomic, molecular, cellular, individual, population, community and ecosystem levels. These levels of organization also correspond to different levels of observation of the system, from microscopic to macroscopic, i.e., to different time and space scales. The more microscopic the level is, the faster the time scale and the smaller the space scale are. The dynamics of the complete system is the result of the coupled dynamical processes that take place in each of its levels of organization at different time scales. Variables aggregation methods take advantage of these different time scales to reduce the dimension of mathematical models such as a system of ordinary differential equations. We are going to study the dynamics of a system which is hierarchically organized in the sense that it is composed of groups of elements that can be themselves divided into further smaller sub-groups and so on. The hierarchical structure of the system results from the fact that the intra-group interactions are assumed to be larger than inter-group ones. We present aggregation methods that allow one to build a reduced model that governs a few global variables at the slow time scale.

Logical Analysis of Regulatory Networks in Terms of Feedback Circuits

Marcelline Kaufman

Université Libre de Bruxelles, Centre for Nonlinear Phenomena and Complex Systems, Campus Plaine U.L.B., CP 231, Boulevard du Triomphe, 1050 Bruxelles, Belgique

This presentation deals with a logical method for describing and analysing the dynamics of regulatory networks in terms of feedback circuits. The most distinctive feature of this logical method is its fully asynchronous character: while the variables that are associated with the relevant components of a network are discrete, time is continuous. We first describe the method in its "naïve" Boolean form and use it to illustrate the major laws of circuitry (namely, the involvement of positive circuits in multistationarity and of negative circuits in periodicity). We then present more refined versions of our logical description by introducing successively multivalued logical variables, logical parameters and logical values ascribed to the thresholds. Finally, we illustrate on simple examples the inductive use of the logical method. This reverse approach aims to proceed rationally from experimental facts towards the elaboration of a model.

Optimisation des systèmes métaboliques contraints

Julie Fiévet[1], Frédéric Gabriel[1], Bruno Bost[1], Christine Dillmann[2], Dominique de Vienne[2]

[1]Station de Génétique Végétale INRA/UPS/CNRS/INA-PG, Ferme du Moulon. 91190 Gif-sur-Yvette
[2]Institut de Génétique et Microbiologie, Université de Paris XI, 91405 Orsay

Le coût de la synthèse protéique et l'encombrement moléculaire imposent une contrainte globale sur la concentration totale d'enzymes dans une cellule, contrainte qui relie négativement entre elles les variations de concentration des enzymes. Pour un système métabolique donné, il existe une répartition optimale des concentrations d'enzymes, *i.e.* une répartition qui maximise les flux de ce système. L'interdépendance des concentrations et leurs relations avec les flux nous ont conduit à la notion de « coefficient de réponse combinée », $R_i^J = \frac{\partial J}{J} \Big/ \frac{\partial Q_i}{Q_i}$, qui mesure la sensibilité du flux J vis-à-vis de la variation de concentration Q_i de l'enzyme i. Comme cette variation affecte les concentrations d'autres enzymes de la voie, l'expression de R_i^J est différente de celle d'un coefficient de contrôle. Sauf au flux maximum, une valeur donnée de J peut être obtenue avec deux valeurs de Q_i, l'une inférieure, l'autre supérieure à la valeur optimale. Une approche analytique a montré que la valeur absolue de R_i^J était toujours plus élevée au-delà qu'en deçà de l'optimum, et ce quelle que soit la règle de redistribution de la concentration de l'enzyme. Du point de vue évolutif, ceci signifie que la sélection pour augmenter un flux sera toujours plus forte lorsqu'il s'agira de faire diminuer une concentration d'enzyme trop élevée que de faire augmenter celle d'une enzyme trop peu abondante. Ce résultat peut expliquer l'existence des mécanismes destinés à limiter la synthèse protéique. Une approche expérimentale a été initiée sur la glycolyse chez *S. cerevisiae*, afin de vérifier différentes prédictions liées aux contraintes.

Aspects «cristaux liquides et polymères» de l'ADN. Le cas particulier des procaryotes et les perspectives

Yves Boulgand[1], Vic Norris[2]

[1]Histophysique & Cytophysique. Ecole Pratique des Hautes Etudes. INSERM ERIT M 0104, 10 rue A.-Bocquel, 49100 Angers
[2]Laboratoire des Processus Intégratifs Cellulaires UMR CNRS 6037, Faculté des Sciences de Rouen, F76821 Mont Saint Aignan, France

Les acides nucléiques bicaténaires en double hélice donnent des cristaux liquides d'un type bien particulier, appelés « cholestériques », parce que cet état un peu singulier de la matière fut décrit initialement pour de nombreux dérivés du cholestérol. Il est connu aujourd'hui pour de nombreux polysaccharides et polypeptides, naturels ou de synthèse. Cet état cristallin liquide est obtenu pour des concentrations très élevées de l'ADN dans l'eau, entre 5 et 20%, comparables à celles que l'on trouve dans les chromosomes et beaucoup de noyaux cellulaires. C'est surtout chez certains procaryotes (bactéries et dinoflagellés) que ces états cristallins liquides furent observés *in vivo*, mais nous pensons qu'ils interviennent également chez les eucaryotes.

Chaque chromosome ne comporte qu'une seule molécule d'ADN (éventuellement en cours de duplication) et cela vaut en particulier pour le nucléoïde bactérien, comme pour l'un quelconque des chromosomes du noyau des dinoflagellés. C'est ce filament très long, mesuré en millimètres, qui est replié sur lui-même un grand nombre de fois en constituant une minuscule goutelette cristalline liquide, plus ou moins étirée, avec des boucles d'ADN qui s'étendent plus ou moins loin à l'extérieur du cristal liquide. Nous pensons que l'ordre de l'ADN au sein de la phase cristalline liquide, ainsi que sa fluidité, facilitent de nombreux aspects du fonctionnement du chromosome, dans sa duplication, comme dans sa participation à la synthèse des protéines.

Les progrès concernant la préparation des phases cristallines liquides de l'ADN conduisent à de nombreuses perspectives d'applications, dont beaucoup sont encore fort spéculatives, mais méritent discussion, notamment les problèmes de production de certains peptides à grande échelle en milieu acellulaire.

Hypothesis: the condensation of counter-ions is an intracellular integrating process

Camille Ripoll, Michel Thellier, Vic Norris

Laboratoire des Processus Intégratifs Cellulaires UMR CNRS 6037, Faculté des Sciences de Rouen, F76821 Mont Saint Aignan, France

One of the many problems in biology is to understand how a multitude of dynamic processes are integrated to assure the organisation and functioning of the cell. We propose that the condensation of counter-ions plays a major role in this integration. This condensation is based on the phenomenon of the confinement of counter-ions in the immediate vicinity of a macromolecule at a critical charge density. We review this phenomenon and discuss briefly the theoretical and experimental implications in the context of the cell considered as a dynamic continuum of charged structures. These structures create an intracellular network that extends from the membrane to the nucleus and that condenses ions. Our hypothesis is that the local level of condensed calcium modulates the activity of many kinases and phosphatases to generate short- or long-term changes in the phosphorylation status and in the stability of the network of structures via positive and negative feedback loops. We further propose that the ability of cells to discriminate between signals and to respond appropriately is a global or collective property of the network as mediated by counter-ion condensation. Evidence consistent with this hypothesis is based on calcium changes in plants subjected to abiotic stimuli. Further investigation will require the quantitative imaging of the distribution of free, bound and condensed ions and extensive mathematical modelling. Finally, we suggest that the network of structures may actually be a network of *hyperstructures* each comprising different species of molecules and macromolecules.

Bio-Array Images Processing And Genetic Networks Modelling

J. Demongeot, F. Berger*, T.P. Baum, F. Thuderoz & O. Cohen

TIMC-IMAG CNRS 5525 Faculty of Medicine 38 700 La Tronche France
*INSERM U 318 University Hospital of Grenoble 38 700 La Tronche France

Abstract

The new tools available for gene expression studies are essentially the bio-array methods using a large variety of physical detectors (isotopes, fluorescent markers, ultrasounds,…). Here we present an image processing method independent of the detector type, dealing with the noise and with the peaks overlapping, the peaks revealing the detector activity (isotopic in the presented example), correlated with the gene expression. After this first step of image processing, we can extract information about causal influence (activation or inhibition) a gene can exert on other genes, leading to clusters of co-expression in which we extract an interaction matrix explaining the dynamics of co-expression correlated to the studied tissue function.

Adaptive branching in Evolution and Epigenesis

Yannick L. Kergosien

Université de Cergy-Pontoise, Département d'Informatique
2, Avenue Adolphe Chauvin, Pontoise 95302 Cergy-Pontoise CEDEX, France
yannick.kergosien@libertysurf.fr

Abstract

We describe one of the simplest models which exhibit an adaptive branching behaviour. It is analyzed both experimentally and formally, and its successive bifurcations provide a good model of what R. Thom called "generalized catastrophes". Some theorems on the stochastic adaptability of the algorithm to very general shapes of target are given. The model further displays the phenomenon of abortive branching : each macroscopic branching appears after a burst of micoscopic branchings which stop growing after a very short time. The mathematical analysis of the model explains why and how this behaviour occurs. The applications of these models to Evolution (natural and artificial) and Epigenesis are discussed, and a higher dimensional version is applied to growing a tree in a space of shapes in the context of a database of medical images.

Keywords: branching, bifurcation, evolution, epigenesis, angiogenesis, tree, auto-organization, adaptive.

Résumé Ramification adaptative en Evolution et Epigénèse

Nous décrivons un des modèles mathématiques les plus simples qui soit capable de ramification adaptative et étudions sa pertinence biologique. Ayant défini dans un espace une probabilité chargeant une région appelée cible, et un ensemble appelé graine, état initial du réseau à faire croître, chaque tirage d'un point au sein de la cible définit un nouveau point à ajouter au réseau. On peut observer expérimentalement l'apparition d'arborescences qui adaptent progressivement la forme du réseau à celle de la cible. On peut aussi montrer plusieurs théorèmes d'adaptativité stochastique du réseau à des cibles très générales. L'étude plus fine des ramifications révèle l'existence du phénomène de ramifications abortives dont l'étude formelle s'apparente au concept de catastrophe généralisée. Ce modèle est applicable à l'espace tridimensionnel pour modéliser l'épigénèse, mais aussi à des espaces de dimension plus grande, comme des espaces de formes, dont nous discutons quelques applications dans le cadre de l'Evolution en Biologie, et pour des applications de bases de données de formes en imagerie médicale.

Mots-clés: ramification, bifurcation, evolution épigénèse, angiogénèse, adaptation, arbre, auto-organisation.

High Level Courses

Modeling the dynamics of secretory compartments

Alain Rambourg[1], Jean-Marc Delosme[2], Roberto Incitti[3], Béatrice Satiat-Jeunemaître[4], Philippe Tracqui[5] & François Képès[4, 6]

[1] Département de Biologie Cellulaire et Moléculaire, CEA / Saclay, France
[2] Laboratoire de Méthodes Informatiques, CNRS / genopole®, Evry, France
[3] Institut des Hautes Études Scientifiques, Bures, France & genopole®, Evry, France
[4] Dynamique de la Compartimentation Cellulaire, Institut des Sciences du Végétal, CNRS UPR2355, Gif, France
[5] DynaCell, TIMC-IMAG, CNRS UMR5525, Faculté de Médecine, La Tronche, France
[6] ATelier de Génomique Cognitive, CNRS ESA8071 / genopole®, Evry, France

A. The dynamics of secretory compartments

1. Introduction

One of the major challenges facing modeling and simulation for the coming decades is to deal with dynamical systems whose structures are not fixed, but evolve as a result of the system's internal dynamics. Most biological and sociological objects are indeed such systems. Interactions among their components specifically generate other components or, at least, modify their internal structure. As pointed out by Fontana & Buss (1994), these objects may be considered as "constructive dynamical systems". In cell biology, the secretory process in eukaryotic cells corresponds to this type of system, as it appears to generate new structures as a result of its internal dynamics.

Eukaryotic cells have built up a highly specific way to excrete some of their proteins. All proteins are synthesized in the cytoplasm, but those proteins destined to the extracellular space are transported through a series of membrane-bounded compartments making up the secretory pathway. They cross the membrane of the endoplasmic reticulum (ER). They subsequently undergo successive chemical modifications as they are transported by membrane fusion / fission events through a series of membrane-bounded compartments: ER, Golgi apparatus (GA), secretory granules (SG). The latter finally fuse with the plasma membrane to deliver their content outside the cell (exocytosis). Eukaryotic cells are also able to internalize material from the extracellular space (endocytosis) through compartments, some of which are shared with exocytosis. Internalized material is often degraded in the vacuole.

Until recently the structures making up the secretory pathway had only been observed in a static way on two dimensional projections. Many of the controversies that arose during the last decades about the exact structure and functioning of secretory compartments may be attributed to the difficulty of retaining simultaneously the required spatial resolution and a kinetic view of the secretory process. It is the purpose of this chapter to present data on the structure of the secretory pathway obtained at the ultrastructural level with stereoscopic techniques, to pinpoint structural modifications along this membranous system, and to propose a discursive model dealing with the autonomous creation of new structures.

2. Three-dimensional configuration of the secretory pathway

To obtain accurate and detailed information on the architecture of cell compartments, their three-dimensional features should be investigated in sections of various thicknesses stained with

heavy metals, examined with both standard and high voltage electron microscopes (EM). However, images observed on the fluorescent screen of the EM or conventional photographs of such images are not true representations of the reality but only shadows, projections of three-dimensional objects. As a result, serial sections examined or photographed under the EM screen to reconstruct a tridimensional object are in fact, serial projections which, when added together, may lead to erroneous interpretations of the structure of this object.

Thus, as seen in Figure 1, the projection (vertical arrow) of the tridimensional statue on the snow will be interpreted as that of …a running wolf !!! and not as that of a human being, Mr. McGill, the founder of McGill University in Montreal (Canada).

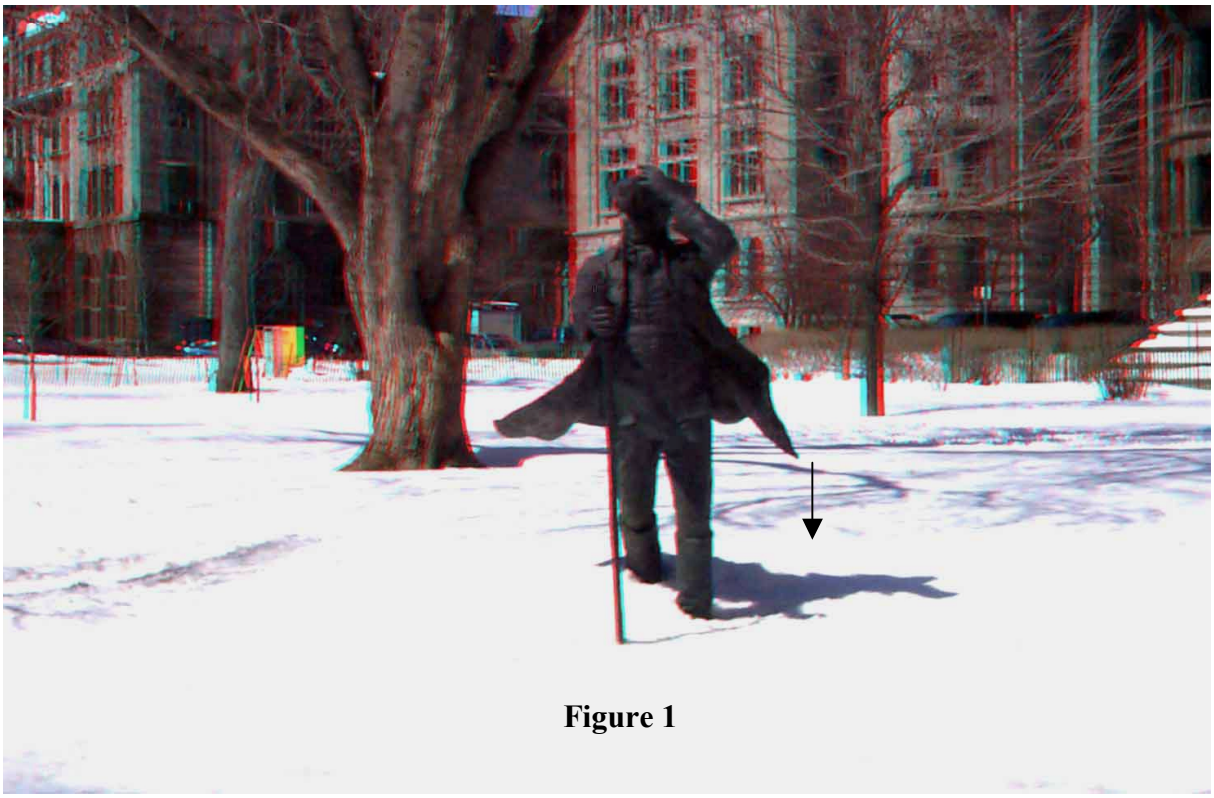

Figure 1

Stereoscopic picture of the statue of McGill on the McGill university campus in Montreal. Two pictures were taken in succession after moving the camera along an horizontal axis. The distance between the two pictures corresponded approximately to the interocular distance (60 mm). One of the photographs corresponding to the field viewed by the left eye was masked with a red filter and the other one, viewed by the right eye, with a cyan filter . The two pictures were then fused together to form a stereoscopic picture which, when examined with colored glasses, allows a three dimensional restitution of the scenery. The shape of the projection (shadow) of the statue is indicated by the vertical arrow. (see **plate 1** at the end of the book)

To avoid these projection artefacts, electron micrographs should always be examined with stereoscopic techniques which allow the brain to reconstruct a given object in three dimensions from the projections on each retina of this object, viewed by each eye from a different angle. In practice, two photographs of the same field are taken with the EM by tilting the object at two different angles. These two pictures correspond to two projection images of the same structure but photographed from two different angles. A three-dimensional view of the structure or the field under study may then be obtained by looking at properly adjusted pairs of such photographs either with a stereoscope or, as for the figure above, with colored glasses, the red lens being placed over the left eye. In this case, as in ordinary binocular vision, the three-dimensional structure of the objects can be directly observed and permits the observer to avoid laborious and problematic recontructions from serial sections.

3. secretory The pathway in animal cells

Two cases will now be examined to illustrate the two morphogenetic paths of Golgi maturation in animal cells.

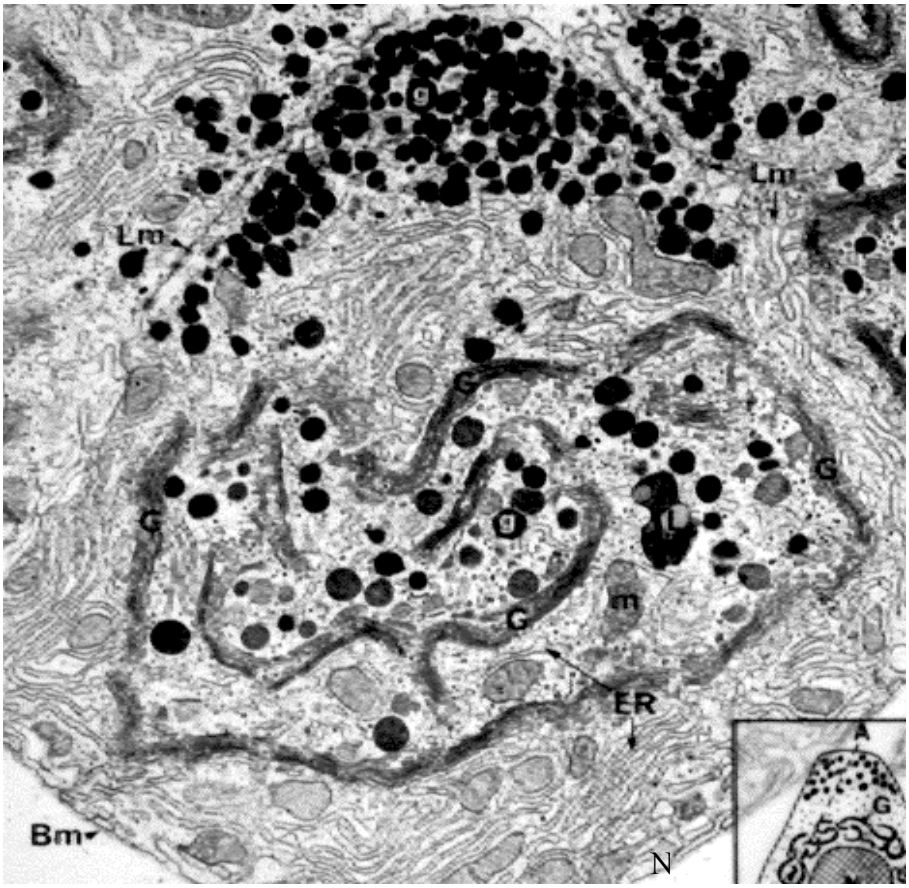

Low-power electron micrograph of the Golgi ribbon (G) in a mucous secretory cell of the Brünner's gland. The nucleus is not included in the section plane which is shown (B-A) in the inset at the lower right. Piles of cisternae of the endoplasmic reticulum (ER) are seen to surround the Golgi region. Secretion granules (g) are interspersed at close proximity of the twisted Golgi ribbon and accumulate at the apex of the cell. The lateral (Lm) and basal (Bm) plasma membrane delineates the roughly conical shape of the cell. x 10,000

3.1. Mucus producing cells of the Brünner's gland

Figure 2 shows an electron micrograph of an ultra-thin section through a secreting cell from a Brünner's gland, a mucus producing gland in the wall of the mouse small intestine. The specimen was fixed in glutaraldehyde and postfixed with reduced osmium in order to selectively stain membrane-bounded compartments. A staining gradient is observed along the membrane compartments of the secretory pathway. As indicated in the inset at the bottom right, a diagram showing the morphology of the cell as observed with the light microscope, it is a pyramidal cell with a basal nucleus (N) and an apical (A) region filled with secretion granules. In the mid-region of the cytoplasm, the Golgi apparatus (G) appears as a continuous twisted ribbon-like element that caps the apical pole of the nucleus. In the cell observed with the EM, roughly parallel elongated and interconnected cavities form at the base of the cell and around the Golgi ribbon (**G**) a continuous network : the endoplasmic reticulum (**ER**). Secretion granules (**g**) are observed in the Golgi region and accumulate at the apex of the cell. Mitochondria (**m**) are interspersed throughout the cytoplasm. Biochemical as well as cytochemical studies indicate that secretory proteins are synthesized in the cytoplasm and cross the membranes of the cavities making up the endoplasmic reticulum. They are then transported in the GA where they are modified and packed within prosecretory granules. After

their release from the GA, these prosecretory granules are further modified and transformed into fully mature secretion granules which, in most secretory cells, accumulate at the secretory pole of the cell.

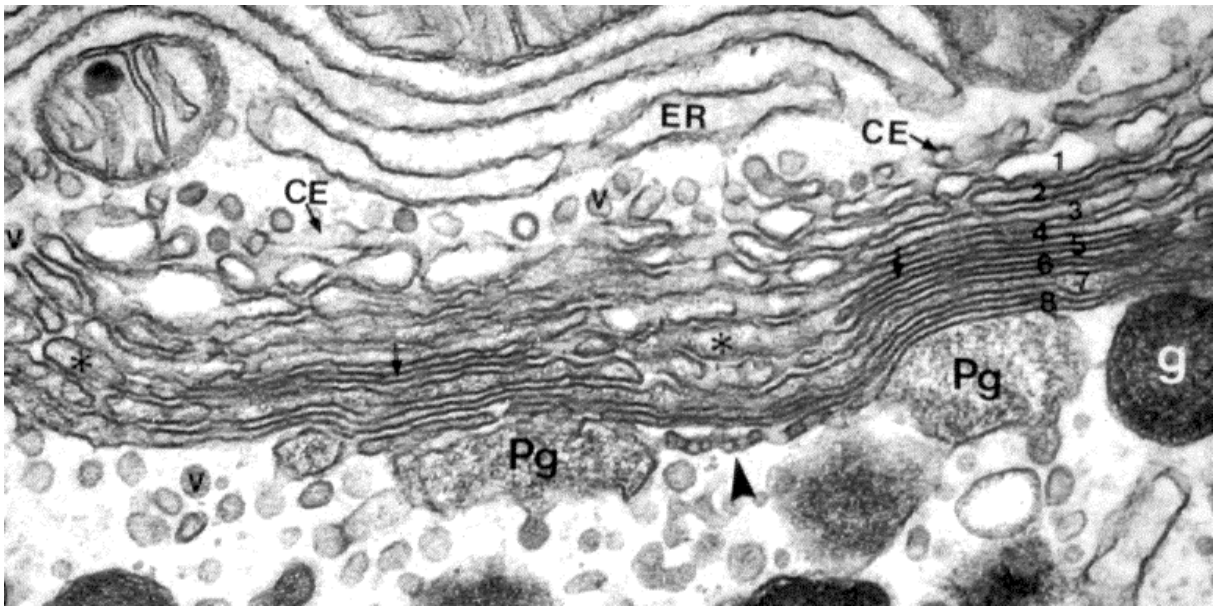

Figure 3

Higher magnification of the Golgi ribbon in a region similar to that delineated by the rectangle in Fig.2. Underlying the *cis*-element (CE), several elements numbered 1 to 8 are seen in side views and display flattened (arrows) and dilated (*) portions. On the *trans*-aspect of the Golgi ribbon, prosecretory granules Pg are interconnected by relatively shrunken tubular elements (arrowhead). ER : endoplasmic reticulum cisterna. g : secretion granule. x 80,000

When a portion of the Golgi ribbon such as the one delineated by a rectangle in Figure 2 is examined at a higher magnification, its appears to consist of several (8 to 9) parallel elements (Figure 3). On one face of the ribbon, referred to as the *trans*-face of the GA, prosecretory granules (Pg) are still connected by thin interconnected tubules indicated by the arrowhead. At the opposite face : the *cis*-face, a tubular network the *cis*-element (CE) or *cis*-Golgi network is facing the endoplasmic reticulum (ER) from which it remains separated by a clear space containing small vesicles (v) or interconnected tubules. Such tubular vesicular elements are thought by some authors

to form a separate structural compartment : the endoplasmic reticulum-Golgi intermediate compartment usually designed by the acronym : ERGIC.

Diagram illustrating a small portion of the Golgi ribbon in a mucous secreting cell of the

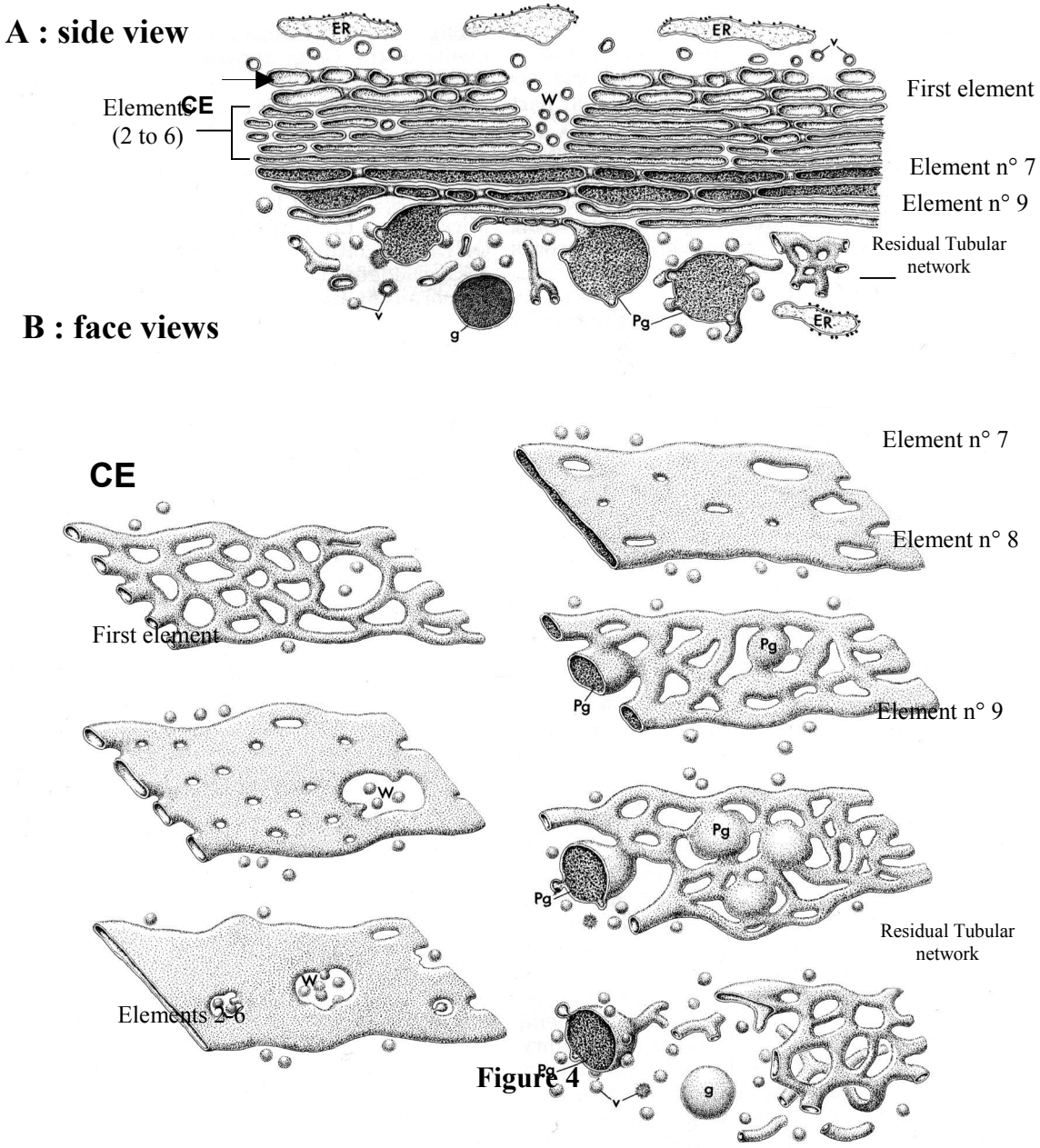

Figure 4

Brünner's gland. The various elements making up the Golgi ribbon observed in side view (A) are shown in front views in the B part of the diagram. ER : endoplasmic reticulum. CE : *cis*-element ; Pg : prosecretory granule ; g : secretion granule.

The tridimensional structure of the various elements of the Golgi ribbon seen in in Fig. 3 or in the upper part (A) of the diagram in Fig. 4 is illustrated in front views in the B part of the same figure. As indicated above, when seen in front view with a stereoscope, the *cis*-element (CE) is exclusively tubular and forms a *cis*-tubular network. Subjacent to this tubular network, more or less flattened elements, (elements 1-8 on the right side of Figure 3, or elements 1-9 in the diagram) are strictly parallel and close to each other to form «stacks of saccules», usually thought to characterize the GA in eukaryotic cells. The diameter of the fenestrations perforating the first element is approximately half that of the meshes of the *cis*-tubular network. The next elements (2-6) are poorly fenestrated. Yet, wide perforations interrupt in register two or more elements to form pan-shaped

cavities or « wells » (W) with a wide mouth opened on the *cis*-face of the stacked elements and a narrower bottom located in their lower half. The element 7 displays a few round or ovoid fenestrations. Its lumen contains an electron opaque secretory material which, as seen in side views (asterisk in Figure 3) may accumulate in dilated portions. The subjacent element 8, perforated with numerous pores, takes a fenestrated appearance and presents a few distensions which correspond to early prosecretory granules (Pg). The number of such prosecretory granules increases in element 9 while the areas separating them are more and more fenestrated and become tubular. The tubular elements making up such intermediate areas are relatively shrunken (arrowhead, Figure 3) and deprived of secretory material. Finally, on the trans side of the stack, free prosecretory granules, a few residual tubular networks as well as small tubular or vesicular profiles appear to result from the fragmentation of the superjacent tubulo-nodular (Figure 3, #8 or Figure 4, #9) element. Smaller mature secretion granules (g) are seemingly formed by transformation of prosecretory granules with emission by the latter of numerous small vesicles which may be observed at their periphery or in their immediate surroundings.

3.2. Prolactin secreting cells of the pituitary gland

As in the mucous secreting cell of the Brünner's gland, the segregation of prosecretory granules in other glandular cells appears to be concomitant with a progressive perforation of Golgi elements and their transformation into tubular networks when their three-dimensional structure is examined along a *cis-trans* axis from the *cis* to the *trans* aspect of the Golgi ribbon. Yet, in some glandular cells, remodeling of the free prosecretory granules into mature secretion granules may occur without emission of vesicles as seen in most cells. Thus, in prolactin cells of the pituitary gland (Figure 5), early prosecretory granules segregated in highly perforated elements on the

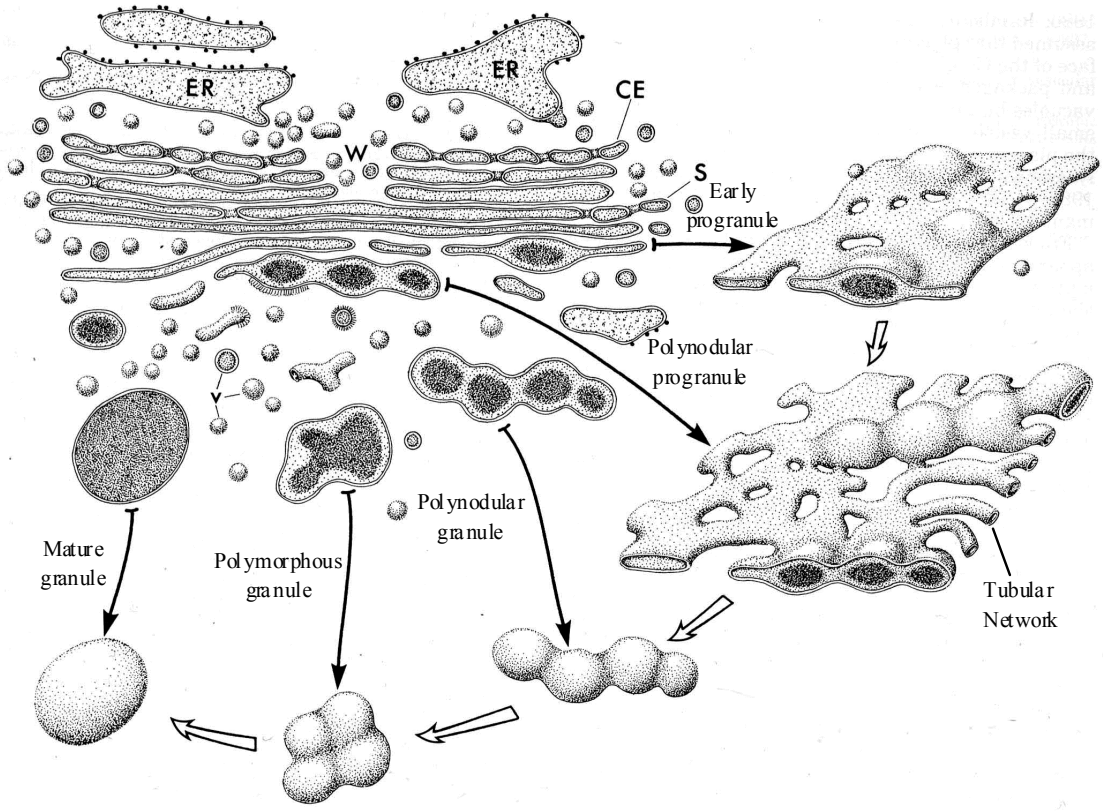

Figure 5

Diagram showing a small portion of the Golgi ribbon of the prolactin cell and the proposed mode of formation of secretory granules. The drawing at the upper left shows the stack of Golgi elements and granules in a perpendicular thin section through the stack. The various elements of the face of the stack implicated in granule formation as well as the elements seen at a short distance from it are shown in three dimensions in the surrounding drawings.

trans-face of the Golgi ribbon seem to aggregate to give rise in the next element to polynodular prosecretory granules separated from each other by tubular networks. Once liberated within the cytoplasm, seemingly by breaking of the tubular networks, they give rise to polynodular granules, closely apposed and usually parallel to the *trans*-face of the Golgi ribbon. Subsequently, these progranules migrate at some distance from the Golgi stacks and transform into more compact polymorphous granules which, in turn, give rise to the mature granules.

The breaking of the trans-tubular networks to liberate secretion granules in the cytoplasm implies that the various elements of the Golgi ribbon are permanently renewed from the endoplasmic reticulum in order to maintain their structural integrity. However, the structural complexity of the GA and its relative stability has prevented so far an exhaustive description of the kinetics of this compartment in cells maintained in their normal, *in situ*, environmental conditions.

Thus, recent biochemical and genetic investigations have made use of the baker's yeast *Saccharomyces cerevisiae* to analyse various cell biological processes and in particular those related to the secretory pathway which, in these cells as in mammalian cells, involves the GA (Figure 6). Temperature-sensitive mutants have been isolated that block protein traffic at various stages. When grown at a low temperature where the mutation is not expressed ("permissive" temperature), they display a phenotype resembling that of the wild-type (non-mutated) strain. Upon shifting to a higher temperature where the mutation is expressed ("restrictive" temperature), they gradually accumulate various types of structures (e.g. small vesicles, membranous sheets, tubules, secretory granules etc…), depending of the position of the block along the secretory pathway. Upon returning the cells to a permissive temperature, the phenotype of the wild-type cell is progressively restored. By examining the cells at various time intervals after a block or release of the block, it is possible to monitor the modifications of the tridimensional configuration of the membranous systems (e.g. ER, GA, etc…), which reflects their internal dynamics.

4. The secretory pathway in yeasts

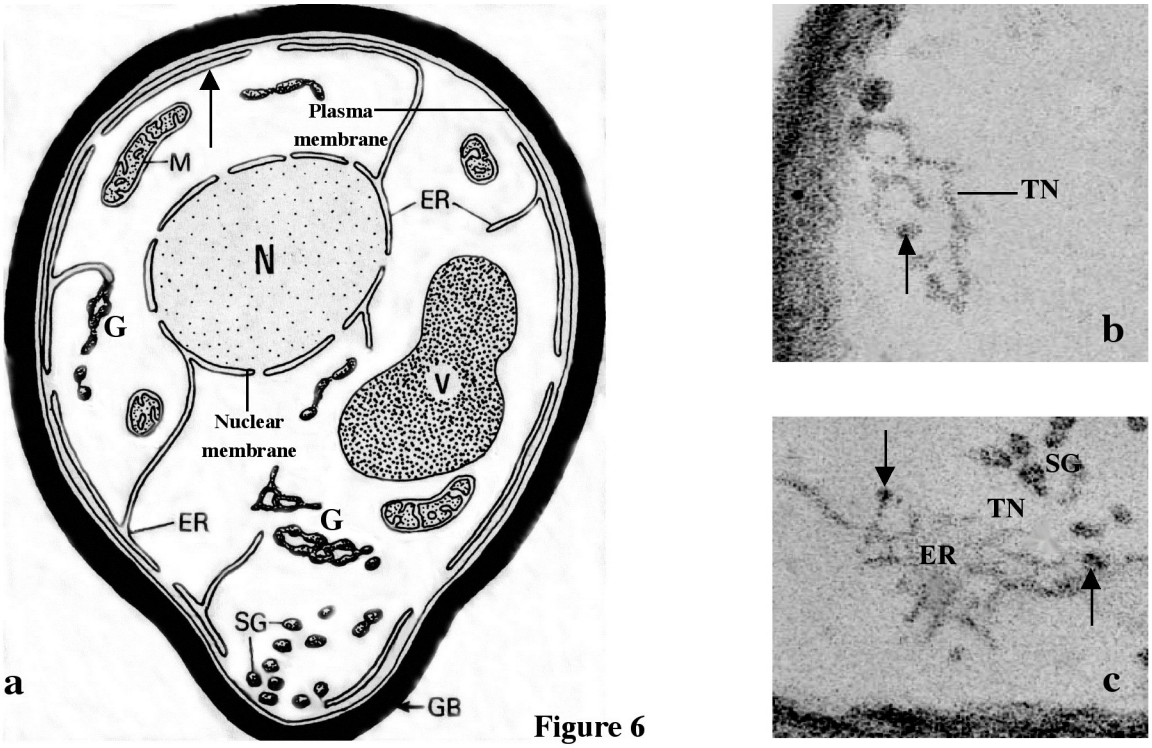

Figure 6

a) Diagram illustrating the structure of cell organelles in the yeast *Saccharomyces cerevisiae*. N : nucleus ; ER : endoplasmic reticulum ; M ; mitochondrion ; G : Golgi tubular networks ; SG : secretion granules. The vertical arrow points to the subplasmalemal ER which may be continuous with some Golgi networks such as the one (G) seen left of

the nucleus. b) A tubular network (TN), presumably Golgi in nature, contains dilations (vertical arrow) and is seemingly continuous with the subplasmalemmal endoplasmic reticulum (ER).
b) High power magnification of a Golgi tubular network (TN) at the periphery of a yeast cell. A dilated zone of a tubule, presumably a prosecretory granule is indicated by the vertical arrow. x 73,000.
c) A non perforated sheet of endoplasmic reticulum (ER) seen in face view is continuous at its periphery with interconnected membranous tubules forming a wide-meshed tubular network (TN). Dilations along these tubules are indicated by vertical arrows. x 63,000.

In wild type strains of yeasts fixed in glutaraldehyde and postfixed with reduced osmium in order to selectively stain membrane-bounded compartments, there is a staining gradient along the membrane compartments of the secretory pathway. The endoplasmic reticulum, the content of which is usually faintly stained, consists of poorly fenestrated sheets (**ER**, Figure 6c) interconnecting the nuclear membrane with cisternae located beneath the plasma membrane (Figure 6a, arrow). The GA consists of discrete separate units distributed throughout the cytoplasm (G, Figure 6a). They appear as small tubular networks with a stained material accumulating in dilations located at the junctions of membranous tubules. Some of these distensions are filled with an intensely stained material (Figure 6c, arrows) and are similar in size to nearby secretory granules (**SG**), suggesting that, as in animal cells, the latter are segregated by a progressive fenestration of membranous sheets and liberated in the cytoplasm by fragmentation of tubular networks (**TN**, Figure 6bc). Occasionally, as seen in Figure 6, tubular networks with stained dilations may be directly continuous with an ER cisterna beneath the plasma membrane (Figure 6b; Figure 7, "tER") or form the tubular periphery of an unperforated ER sheet (Figure 6c). Figure 7 exposes these features *in situ*.

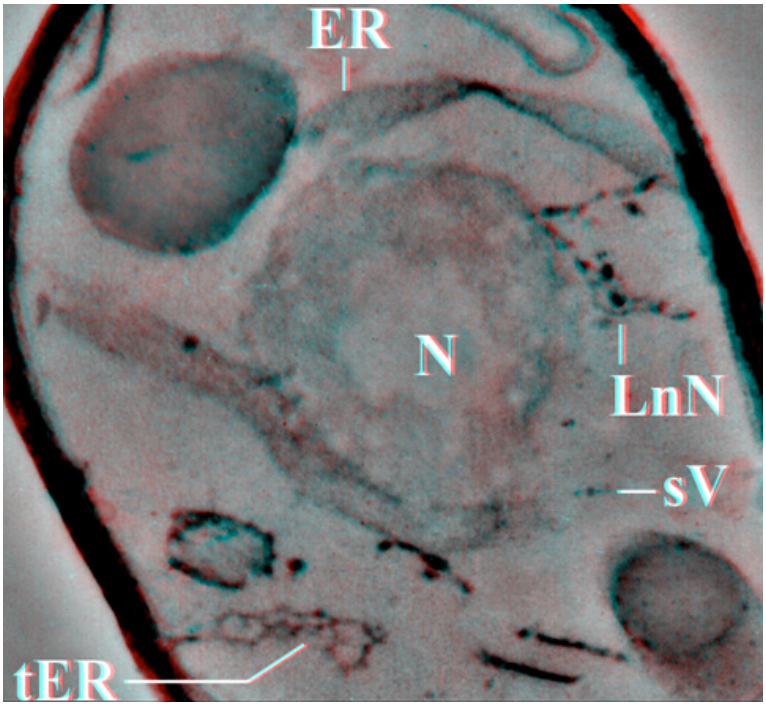

Figure 7
Anaglyph image of a 0.25-µm thick section of a wildtype yeast cell. A stereoscopic, more focused, view may be obtained with anaglyph glasses. The cell is surrounded by a thick and heavily stained wall. The plasma membrane corresponds to the innermost dark line of the wall. Beneath the plasma membrane, cisternal ER (ER) appears as a lighter, discontinuous line. Long ER cisternae bridge the nuclear envelope to subplasmalemmal ER. A polygonal network of pale-stained tubules is connected to subplasmalemmal ER (tER, tubular ER). The unstained nucleoplasm (N) is surrounded by the pale-stained nuclear envelope, pierced with nuclear pores. Top left and bottom right, the grey spheroidal masses correspond to vacuoles. A few pale-stained vesicles, 20-50 nm in diameter, are visible (sV). A network shows nodules (LnN), some of which have the size and staining properties of secretory granules. Magnification 10,000x. (see **plate 2** at the end of the book)

4.1. The sec7 mutant : a continuous membrane flow ?

When *sec7* mutants of the yeast *Saccharomyces cerevisiae* were maintained at the non-permissive temperature (37°C) for various time intervals, the secretion granules (Sg, Figure 8, 0 min) observed at permissive temperature (**SG**, Figure 6) progressively decreased in number and soon disappeared. Concomitantly, the networks of Golgi tubules increased in size and lost their distensions (Figure 8, 5 min). After 15 minutes, these tubules which formerly were interconnected in all directions of space formed arrays of tubular networks parallel to each other (Figure 8, 15 min). Between 15 and 30 minutes, these parallel elements were less and less perforated and finally transformed into stacks of five to eight flattened elements resembling those observed in the Golgi ribbon of animal cells (G, Figure 8, 30 min). At later time intervals, the size of the stacks did not increase but ER membranes started to accumulate on one side of the stacks and formed large reticulated bodies (ER, Figure 8, 60 min) made up of interconnected membranous tubules. Thus, in this mutant, segregation of secretory granules was blocked at the end of the secretory pathway. As a result, Golgi membranes accumulated to form a continuous system of stacked and interconnected flattened elements which on one side was itself continuous with accumulated ER membranous tubules. It was therefore postulated that membranes were continuously flowing down and accumulated as a result of a block at the distal extremity of the secretory pathway. The accumulation of interconnected tubules on one side of the stacked elements further suggested that the transition between ER and Golgi was operated by tubulization of usually poorly or non-fenestrated ER cisternae.

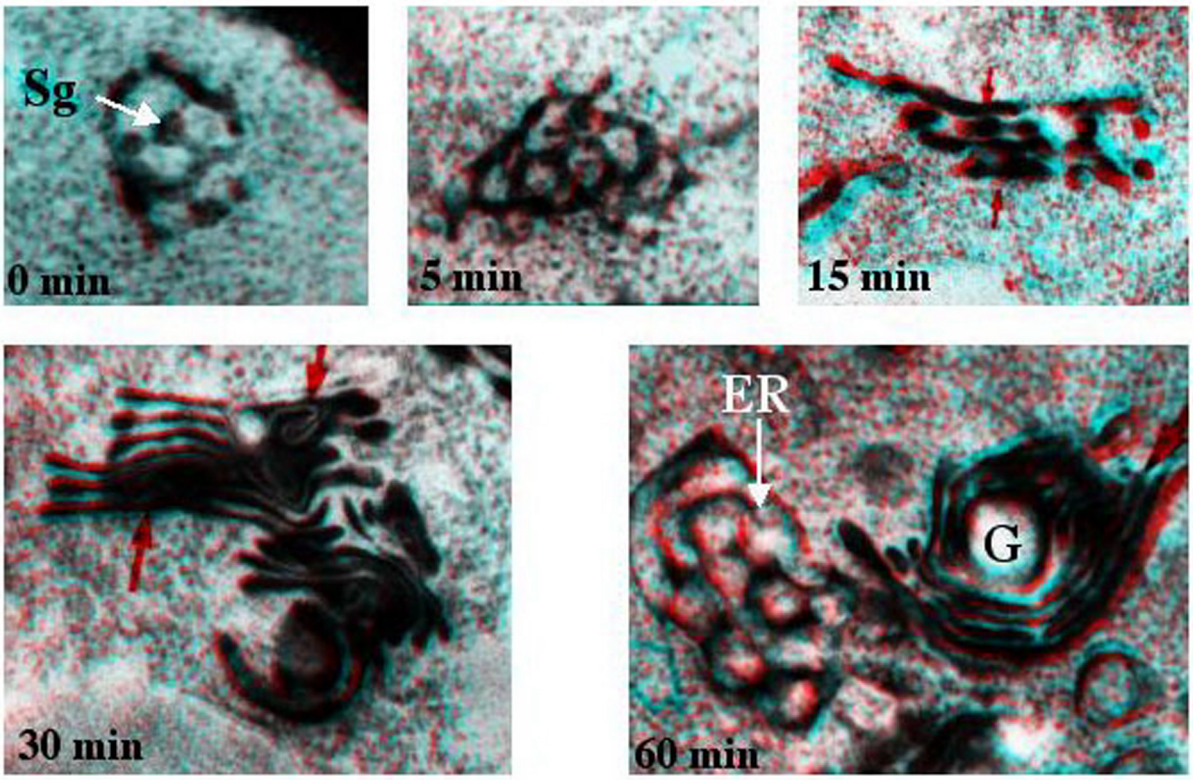

Figure 8

A series of electron micrographs illustrating the modifications of the Golgi networks in a *S. cerevisiae sec7* mutant at various time intervals following a shift to the nonpermissive temperature of 37°C. Sg : secretion granule ; G : Golgi stack of unfenestrated elements . At 60 min, the diameter of the meshes of the endoplasmic reticulum (ER) tubular network is almost similar to that of the Golgi network shown at 0 min . x 70,000. (see **plate 3** at the end of the book)

4.2 The sec18 and sec23 mutants : tubes or vesicles ?

After over one century of work, the morphogenesis and dynamics of the GA are still matters of bitter disputes, although a good description of its biochemical functions has become available in the meantime. As stated in the introduction, part of this problem may be attributed to the difficulty of retaining simultaneously the required spatial resolution and a kinetic view of the secretory process. While EM allows proper spatial resolution, the biological specimen is dead. Live cell imaging can be achieved by photon microscopy, whose resolution is however insufficient to address the controversy.

To work around this difficulty, secretion was synchronized in a large population of yeast cells by inhibiting protein synthesis and/or by subjecting temperature-sensitive secretory mutants (*sec18* or *sec23*) to double temperature shifts. The synchronized secretory events were kinetically monitored at the EM by categorizing and counting all membrane-bounded compartments on a significant number of cell sections selected at random. Five membrane-bounded structures orderly disappeared or reappeared at about the rate of secretory protein flow (Figure 9). 1/ Next to ER, very short-lived Clusters of Small Vesicles were the first detectable post-ER intermediates. 2/ Their constituent small vesicles were rapidly bridged by membrane tubules in a process that depended on the *SEC18* gene, giving short-lived tubular Clusters of Small Vesicles. 3/ Fine and 4/ Large nodular Networks. 5/ Secretory Granules. Upon relieving a secretory block, each structure successively reappeared, seemingly by transformation of the previous one. When no secretory cargo was to be transported, these structures were not renewed. They disappeared at least 5 times faster than enzymes residing at the Golgi membrane, implying that these enzymes are recycled.

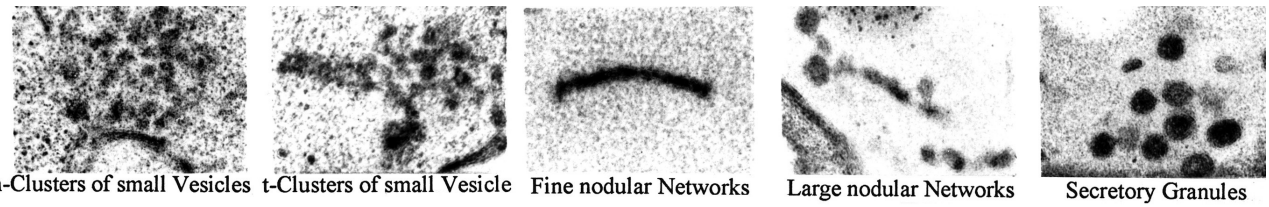

Figure 9

A gallery of yeast secretory membrane-bounded structures. The *sec23* mutant strain was shifted for 10 min to the restrictive temperature, and returned for 15 min to the permissive one. Cells were fixed and processed for EM. Micrographs from 0.1-µm thick sections. Magnification 30,000x.

This study demonstrated that the yeast GA is at steady-state a continuously renewed set of transitory membrane-bounded structures, rather than a permanent entity (Figure 10). The post-ER *SEC18*-mediated fusion event lays the foundation for each element of the apparatus. This element then progressively self-transforms, ultimately into a set of secretory granules destined for fusion at the plasma membrane. Its birth and death are two fusion events separated by a relatively constant amount of time, presumably required to achieve its sequential functions. It is proposed that self-maturation, among these sequential functions, provides the clock for this constant lifespan. The features and the very existence of this GA now appear as consequences of a dynamic equilibrium between production and consumption. Perturbing this dynamic equilibrium can reversibly cause morphological and kinetic changes. Perturbations thus reveal a rather flexible morphogenesis that contrasts with the constancies of the overall lifespan and function. Ultimately, experimental suppression of the flow of secretory cargo leads to the total disappearance of the GA, which in a way defines it as a dissipative structure. Like many biological structures however, this dissipative structure changes with time and even dies, as a consequence of its own internal dynamics. As such, it offers a challenging case study for modeling attempts.

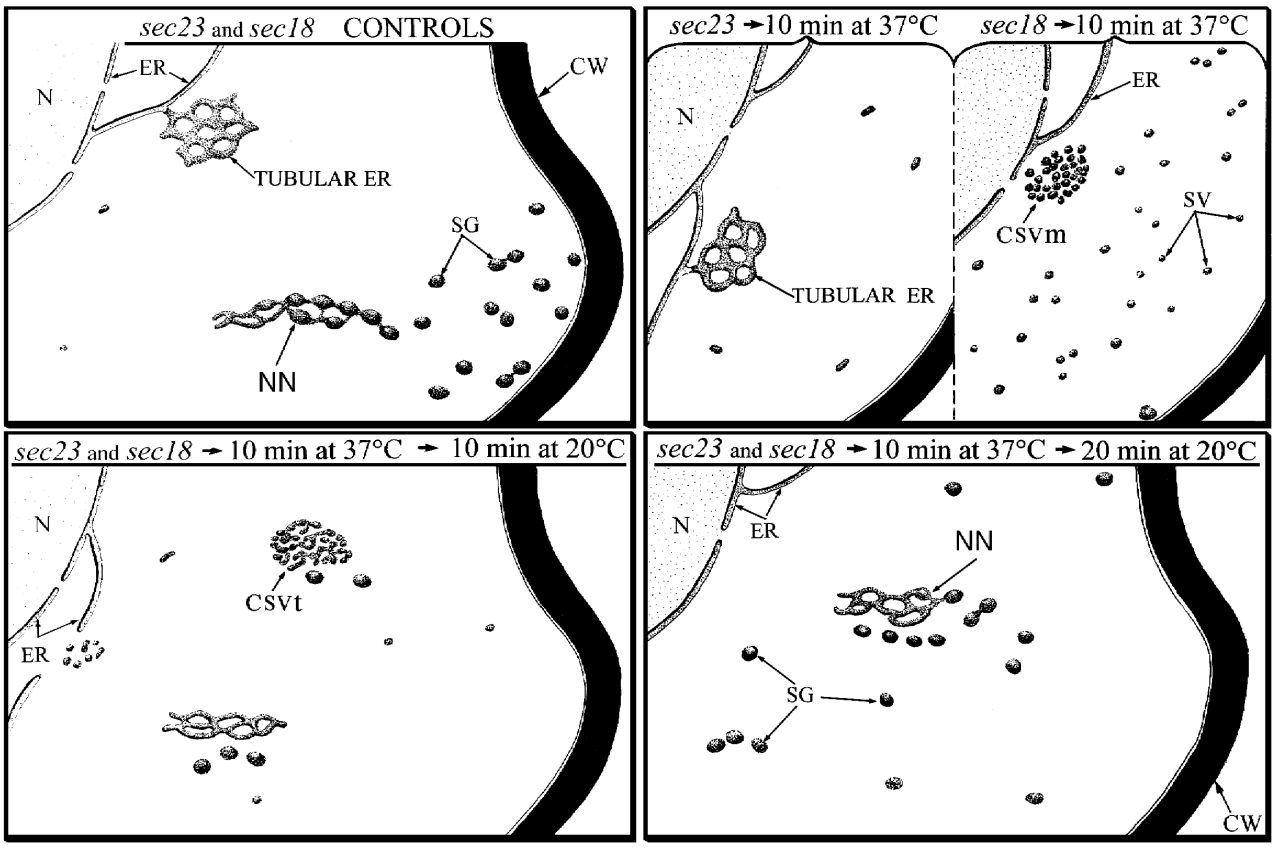

Figure 10

Diagram representing the phenotypes of *sec18* and *sec23* mutant *Saccharomyces cerevisiae* cells.
These drawings are supported by stereo electron micrographs and are meant to reflect the concentrations of some endomembrane structures in mutant cells following temperature shifts. Upper left/ Controls grown at the permissive temperature of 20°C. There are very few small vesicles. A Golgi element is represented with varying calibers (NN). Secretory granules, some still interconnected by tethers, are often located next to the plasma membrane. Upper right/ Mutant cells maintained 10 min at the restrictive temperature of 37°C. Nodular networks have disappeared and secretory granules are scarce. On the left (*sec23*), there is a limited increase in the number of small vesicles, most of which actually appear as short tubes. On the right (*sec18*), there is a large increase of small - generally round - vesicles (SV), and of clusters of unconnected small vesicles (CSVm) near ER cisternae. Lower left/ Cells have been shifted for 10 min at 37°C and 10 min at 20°C. A group of small vesicles emerge from an ER cisterna (left). Small vesicles within clusters are generally connected by tubules (CSVt). Nodular networks of the fine caliber are reforming (bottom). Secretory granules are observed near clusters or networks. Lower right/ Ten min later, nodular networks are more elaborate. Secretory granules accumulate in the cytoplasm (SG). Other abbreviations: ER, endoplasmic reticulum; N, nucleus; NN, nodular networks; CW, cell wall.

B. Content sorting coupled to container formation in cell biology: a model

Although the morphodynamical aspects of the secretory processes have been emphasized so far, minimal molecular aspects will now be introduced, that represent the internal dynamics counterpart of the early Golgi morphogenesis.

1. Scope

The present model is described with specific reference to protein sorting from the Endoplasmic Reticulum (ER) to the ER-to-Golgi Intermediate Compartment (ERGIC), en route to the Golgi apparatus (GA) in the yeast secretory pathway (Figure 11). However, its validity extends far past that particular case. Firstly, it extends to all eukaryotic cells: in yeast, plant and animal cells, the molecular machineries described below are conserved. Secondly, content sorting coupled to container formation is a central and ubiquitous process in cell biology. In fact, it is with a

different coat (clathrin) that the mechanochemical issues of the upcoming story have been best worked out so far. However, it is on the early secretory events described here that the intimate relation between the internal dynamics and the global form have been most strikingly demonstrated on live material (see above the *sec18/sec23* experiments). It means that the exact protein and compartment names given below should be considered as indicative, while the molecular interplay is essential.

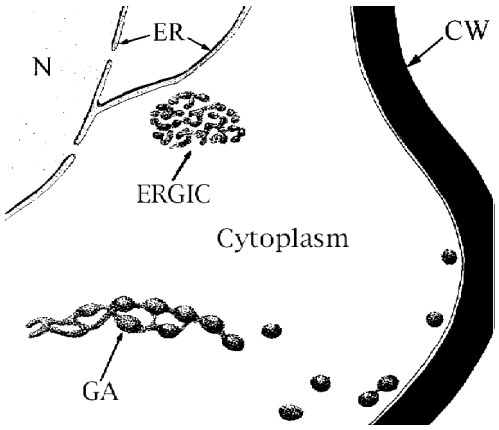

Figure 11

Main secretory compartments in yeast. ER, ERGIC and GA are membrane-bounded compartments within the cytoplasm. CW, cell wall; ER, Endoplasmic Reticulum : first compartment along the eukaryotic secretory pathway; ERGIC, ER-to-Golgi Intermediate Compartment : second compartment; GA, Golgi Apparatus : third compartment, includes the isolated secretory granules. Further details may be found in earlier sections.

2. Model

2.1. Molecules

2.1.1. alpha-factor : prototype of the secretory protein. It is a soluble protein that traverses the entire secretory pathway before being delivered to the outside medium. It must therefore be sorted away from the other ER components in order to move on to the GA. □-factor bears a signal for its sorting off the ER.

2.1.2. BiP : prototype of the resident protein. It is an abundant soluble protein that resides in the ER. It must therefore be retained in the ER and sorted away from continuing cargo such as □-factor. BiP does not bear a sorting signal.

2.1.3. Sar1p : prototype of the regulator. It is a cytoplasmic protein that can bind a Guanosine nucleotide (GDP or GTP [1]) and hydrolyze, albeit inefficiently, GTP into GDP (plus one phosphate). It is a "GTPase" that alternates between a GDP- and a GTP-bound form. Sar1p is mostly associated with the ER membrane.

2.1.4. Sec12p : prototype of the nucleator. It is a transmembrane protein that resides in the ER membrane, where it serves to initiate the events leading to protein sorting off the ER. Sec12p recruits Sar1p on the cytoplasmic side of the ER membrane. Sec12p catalyzes the exchange of a bound GDP for a bound GTP on the GTPase Sar1p; i.e. it is a "GDP/GTP exchange factor" for Sar1p.

2.1.5. COPII : prototype of the coat. It is a cytoplasmic protein that is partly associated with the ER and ERGIC membranes. It coats these membranes and can exert mechanochemical effects on them. COPII can dramatically increase the GTP hydrolysis capability of Sar1p; i.e. it is a GTPase Activating Protein ("GAP") for Sar1p.

2.2. Compartments

2.2.1. ER lumen : soluble compartment in ER, bordered by 2.2.2. □-factor traverses it, BiP resides there.

2.2.2. ER membrane : border of ER. Location for Sec12p. One portion of this membrane is where Sec12p is retained: this is the ER export site. The same site is where Sar1p and COPII are recruited onto the cytoplasmic face, and where a-factor is recruited on the lumenal side.

2.2.3. ERGIC lumen : soluble compartment of ERGIC, bordered by 2.2.4. □-factor traverses it.

2.2.4. ERGIC membrane : border of ERGIC.

2.2.5. Cytoplasm : soluble compartment of the cell, where ER, ERGIC and GA belong. Another location for Sar1p and COPII.

[1] GDP, Guanosine DiPhosphate; GTP, Guanosine TriPhosphate

2.3. Successive events

2.3.1. Random fluctuations will at a certain moment gather a hypercritical concentration of Sec12p at a certain spot on the ER membrane (Figure 12, step 1).

2.3.2. This will allow for the recruitment of a corresponding amount of Sar1p-GDP from the cytoplasm onto these Sec12p (Figure 12, step 2).

2.3.3. These Sec12p catalyze the exchange of a GDP for a GTP on each of the recruited Sar1p (Figure 12, step 3).

2.3.4. Sar1p-GTP activity alone leads to the formation of ER-derived tubular domains ("tubular ER"; Figure 13, step3, & Figure 14) and selectively mobilizes secretory proteins such as □-factor into this tubular ER [2] (Figure 12, step 3).

2.3.5. *Hypothesis*: additional Sar1p is recruited on the cytoplasmic side of the ER membrane selectively at the spot where □-factor is enriched on the other side.

2.3.6. Sar1p-GTP then recruits cytoplasmic COPII onto the cytoplasmic face of the tubular ER membrane, thus forming a coat on this surface (Figure 12, step 4).

[2] What was exactly observed *in vitro* was the Sar1p-dependent tubulation of saccular ER from animal cells (tubules emanating from ER). However, our *in vivo* data on yeast suggest that ER cisternae first fenestrate into polygonal networks, "tubular ER", which later fragment: a COPII mutant such as *sec23*, i.e. blocked right after Sar1p action, readily accumulates unfragmented tubular ER.

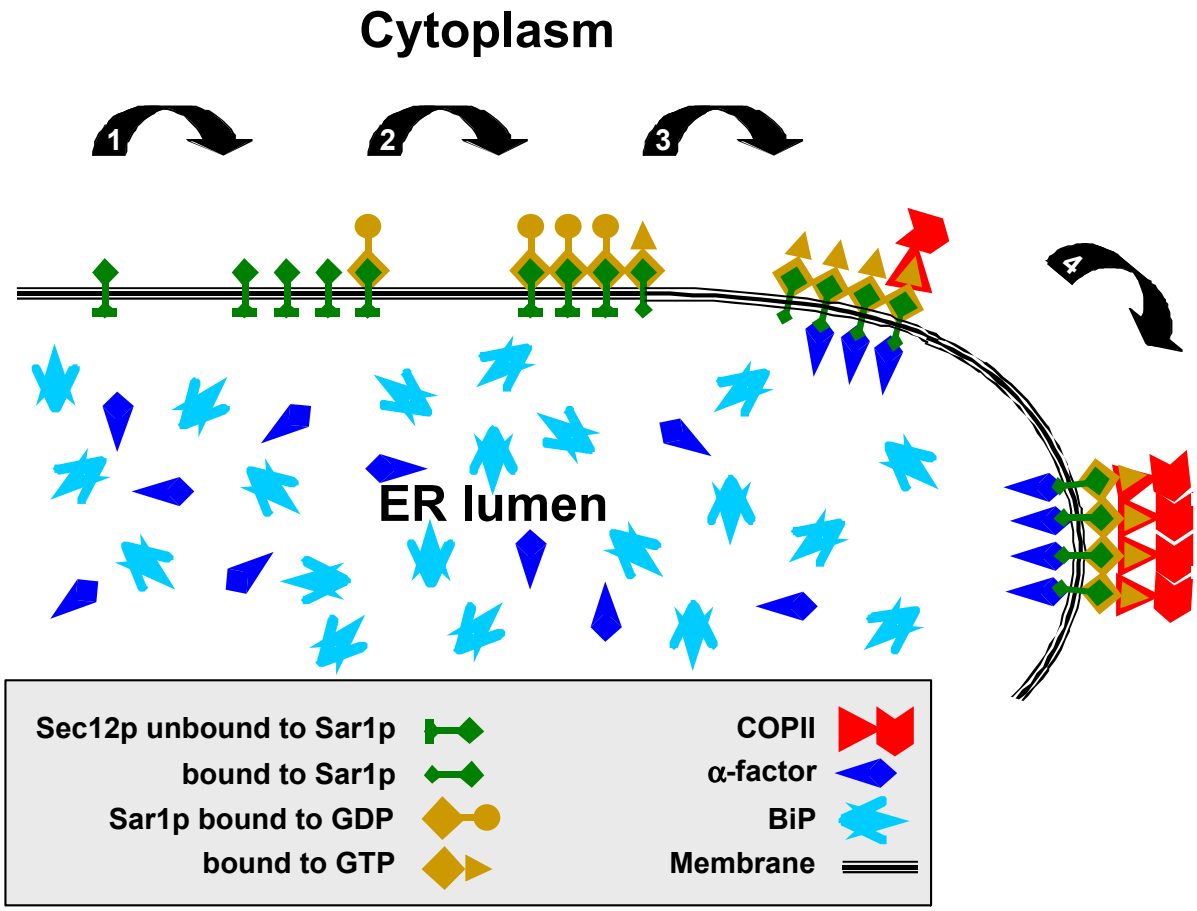

Figure 12

Successive molecular events of α-factor segregation into a coated area. α-factor and BiP are initially mixed in the ER lumen. Step 1: Sec12p molecules gather, thus nucleating an ER export site. Step 2: Sec12ps recruit Sar1p-GDP and start exchanging their GDP for GTP. Step 3: Sec12p/Sar1ps recruit α-factor and start recruiting COPII. They induce membrane tubulation, symbolized by limited bending. Step 4: COPII has been fully recruited and self-polymerizes into a membrane coat. The latter induces scission of the membrane tubules, symbolized by strong bending. (see **plate 4** at the end of the book)

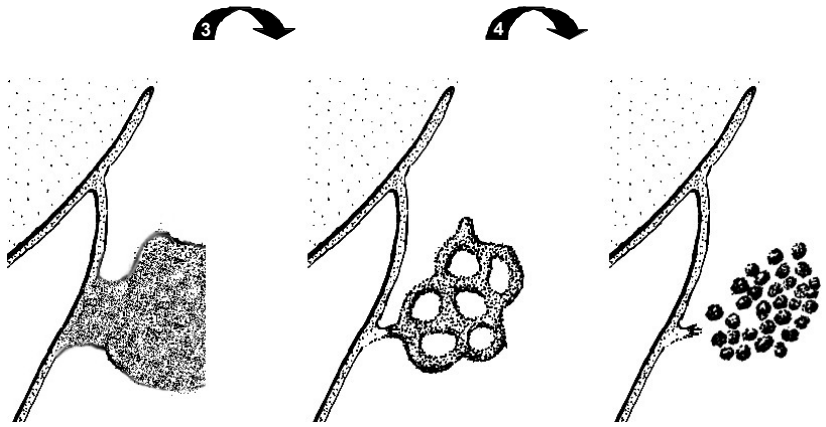

Figure 13

Successive morphological events from an ER saccule (left) to a fenestrated network of tubules (middle) to a cluster of vesicles and short tubes (vesiculo-tubular cluster, right). The arrow numbers roughly correspond with those of Figure 12.

2.3.7. COPII self-polymerizes into a curved coat, thereby confering a local curvature to this particular membrane spot. This results in sectioning the membrane-bounded tubes of the tubular ER into a set of shortened, disconnected tubes (Figures 12 & 13, step 4).

2.3.8. At that stage, □-factor has been tremendously enriched in the resulting new compartment by the above process. BiP has not been enriched.

2.3.9. At a later stage — not within the scope of the present model — the GAP activity of COPII will favor the GTP hydrolysis by Sar1p, thereby inducing the uncoating of COPII off the newly formed membrane-bounded compartment, ERGIC. One round of coating/uncoating is thought to be controlled by one cycle of Sar1p through a GDP- and a GTP-bound form.

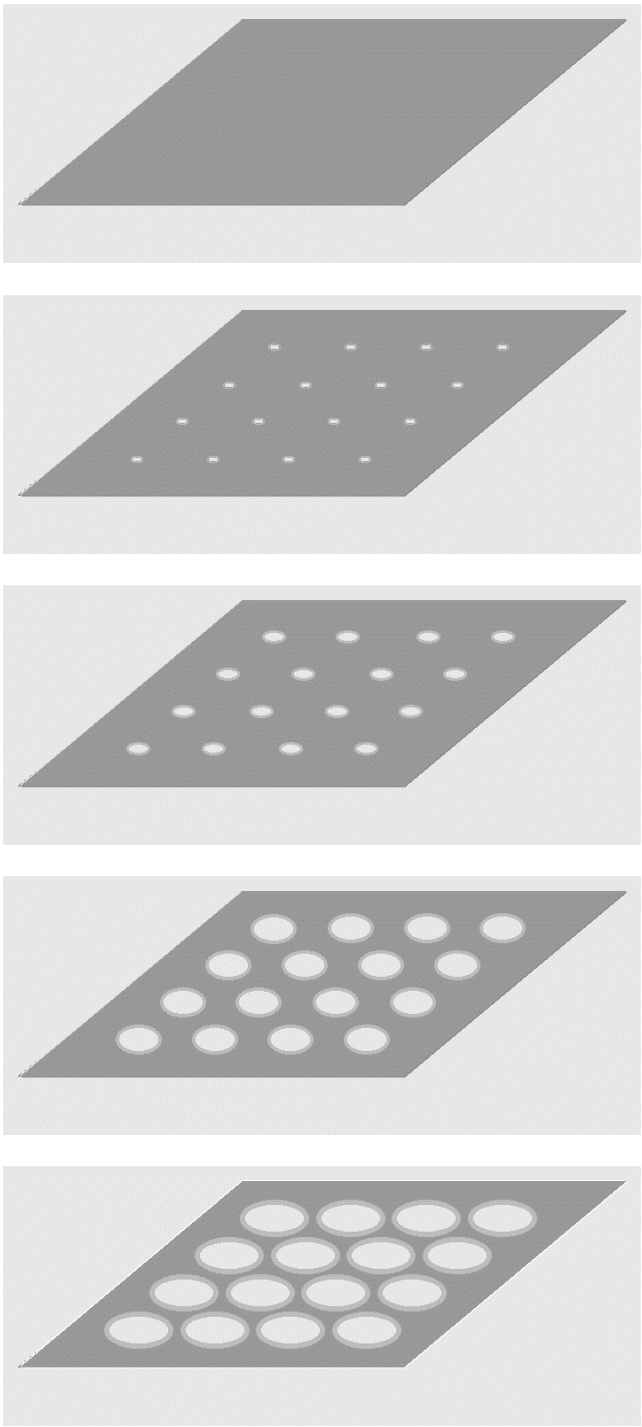

Figure 14

Construction of a tubular network (dark grey) from a planar saccule by progressive fenestration. Background is light grey. This fenestration corresponds to step 3 of the Figures 12 and 13.

3. Crucial point

The symmetrical statements 2.3.4 & 2.3.5 are crucial because they provide the causal link between content sorting (α-factor) and container formation (Sar1p and its morphogenetic effects). Together, they constitute a kind of positive feed-back loop, a virtuous cycle. The exact relevance of this positive loop to the causal link is very hard to test at the bench, and could much more easily be explored through modeling and simulation.

4. Significance

4.1. for the biologist

The paradigm of segregating two proteins, initially mixed, into two different compartments, sweeps across the entire field of cellular and molecular biology because it is a basic sorting process that is involved at all steps in compartmental traffic, secretory or otherwise: for instance in endocytosis, with clathrin playing the role of the coat, and membrane receptors playing that of the specific content. This topic traditionally drains many bench scientists, and it undergoes a conceptual revolution since 1997.

In biochemical terms, the question brought about by the symmetrical statements 2.3.4 & 2.3.5 is that of an auto-catalytic mutual recruitment between secretory protein and coat. As stated above, it is very difficult to test this question at the bench. The relevance to the whole process of some of the interrelations (described in 2.3) is also questionable. Some of the extensions proposed below also bear on controversial questions that modeling/simulation would enlighten too. Membrane lipids are not among the actors proposed here, although they likely play a role. However, no precise data are available on their role in the described process.

4.2. for the morphodynamicist

The basic model already includes the notion of a membrane curvature, i.e. a dynamic structural change. Numerous extensions to the basic model may be considered, including pathological (*sec7* mutation, Brefeldin A drug, …) or cross-species (see Extension 5.1) variations.

4.3. for the mathematician or the computer scientist

This discursive model provides a good opportunity to work out the interplay between models based on differential equations and discrete models based on sufficiently many local actors.

It encompasses a possible case of emergence: the local actors (proteins, membrane) are endowed with minimal properties, while a global behavior may be observed to emerge (e.g. auto-catalytic mutual recruitment between content and coat).

This model permits to conceptually separate the object (the object is open, one sees its internal dynamics) and its interactions with its environment (the object is closed, it is a "black box" that interacts).

5. Extensions

The general principle of three possible and successive extensions will briefly be outlined below, and then commented with respect to evolution.

5.1. Stacking

In *S. cerevisiae*, the site of ER exit, as defined by the positioning of Sec12p, changes from one budding event to the next one. Consequently, the Golgi element that forms is remote from other Golgi elements. In contrast, in another budding yeast called *Pichia pastoris*, the sites of ER export are fixed at sites where Sec12p appears to be sequestered (this modifies only statement 2.3.1). Hence, consecutive Golgi elements are pushed away from the same site in rapid sequence. As they

cannot diffuse fast in the very viscous cytoplasm, they consequently tend to pile up where they are formed, thus yielding the characteristic stack of Golgi elements.

5.2. Stabilizing

In yeasts, as described earlier, stopping secretory function results in full consumption and consequent loss of the Golgi elements. This is not the case in plant and animal cells, where GA remnants are observed when secretory function is prevented by various means. The discrepancy may be ascribed to the existence in plant and animal GA of matrix proteins that play a role in the assembly of Golgi elements and confer to the GA some cohesiveness. In principle, there should exist both an inner (lumenal) "glue" to make the lumen a saccule with parallel membranes, and an outer (cytoplasmic) "glue" to assemble these saccules in parallel arrays. Both glues may be the same molecule, this is irrelevant for our purposes. The essential demonstrated fact is that when the animal GA is disrupted, its matrix proteins are still associated to the remnants, whereas its secretory content and its membrane enzymes are gone. These matrix proteins would constitute an addition to the basic molecular model. They would be activated after the last stage described within the basic model, as Golgi elements successively join a stack.

5.3. Aggregating

While plant cells contain a few hundred small GA stacks, an animal cell typically contains one (or very few) giant GA. This discrepancy may principally be ascribed to the tethering of the animal GA to one type of directed intracellular skeleton called microtubules. This tethering is achieved via a microtubule motor that drags the attached membrane along the directed microtubule towards the MicroTubule Organizing Center, near one pole of the nucleus. All the small stacks aggregate there, which facilitates their fusion into a giant GA [3]. Some recent data suggest that the stage of Sar1p-coated ER-derived tubules (2.3.4) is already proficient for attachment of the membrane to microtubules.

5.4. Comments

As stated above, only animal cells display feature 5.3; animal and plant cells display feature 5.2; animal, plant and some yeast cells display feature 5.1, while some other yeast species do not. These extensions to the model may thus be considered as three successive "inventions" during the course of evolution. The first invention of a simple way to stack up the GA precursors paves the way to the second invention that stabilizes partially the little stacks. This second invention, in turn, opens the possibility of the third invention: gathering the little stacks into a single (or very few) GA. In a simplified view, *S. cerevisiae*, *P. pastoris*, plants and animals may be considered as representing each of these evolutionary levels [4].

It is still not clear what process exactly is optimized by these inventions. For instance, fragmenting the single GA in animal cells with microtubule-disrupting drugs usually has no detectable effect on the secretory kinetics.

The second invention is interesting also from an evolutionary viewpoint on hyperstructures (see companion Course by Norris et al.). It may be interpreted as the advent of a structural protein

[3] The recruitment of microtubules for chromosome segregation during cell division makes them unavailable for the GA, which consequently regresses into smaller and inactive fragments. This fragmentation facilitates proper segregation of the GA in daughter cells, and is followed by reconstruction of a functional giant GA per cell. Drugs that disrupt microtubules also fragment the GA, albeit it remains functional. Thus, GA inactivation during cell division involves a further layer of regulation, beyond microtubular interaction and beyond our scope.

[4] This is of course an oversimplification. For instance, plant and yeast cells make use of a different cytoskeleton than animal cells to optimize some of their membrane traffic, but they do not use it to aggregate a single GA.

(the "glue") to stabilize an existing non-equilibrium hyperstructure (*Pichia*'s informal stack) into an equilibrium one (plant's stack).

6. Appendices for the biologist

6.1. Other known facts

6.1.1. Grafting the "pro" region of □-factor on ER resident proteins make them leave the ER and follow the secretory pathway.

6.1.2. ER tubule formation is blocked by *in vitro* incubation with the dominant-negative Sar1p-GDP.

6.1.3. Inhibiting GTP hydrolysis by Sar1p *in vitro* causes the accumulation of vesicles which are functional intermediates of ER-to-GA transport.

6.1.4. Sec12p fails to be retained in the ER in the absence of Rer1p.

6.1.5. A yeast *sar1* mutant accumulates excess ER membranes.

6.1.6. *SAR1* overexpression suppresses the phenotypic effects of the *sec12* mutation and results in increasing the soluble cytoplasmic pool of Sar1p.

6.1.7. *SEC12* overexpression results *in vitro* in making Sar1p dispensable for forming post-ER vesicles which contain □-factor !

6.2. Other extensions

6.2.1. Distinguish within COPII the individual roles of its components, Sec23p/Sec24p, and Sec13p/Sec31p.

6.2.2. Bring into the picture additional players: Sec16p and Sed4p; Bet1p, Bos1p, Sed5p and other SNARES; NSF (Sec18p) and SNAP (Sec17p); p24.

6.2.3. Consider the recycling of resident ER membrane proteins (Wbp1) and non-membrane proteins (BiP) that have escaped from the ER.

6.2.4. Take into account the overlapping localization of GA membrane enzymes.

6.2.5. Bring into the picture the retrograde transport and COPI coat.

6.2.6. Model the whole lifespan of a yeast GA, beyond its birth !

Acknowledgments

Some of the diagrams shown here have been modified from original pen drawings by Dr. Yves Clermont, McGill University, Montreal. Special thanks to Hervé Delacroix, Janine Guespin, Jennifer Lippincott-Schwartz, Vic Norris and to the members of the workgroup CELLIA at the university of Évry, for fruitful discussions.

References

Aridor, M., K.N. Fish, S. Bannykh, J. Weissman, T.H. Roberts, J. Lippincott-Schwartz and W.E. Balch (2001). The Sar1 GTPase coordinates biosynthetic cargo selection with endoplasmic reticulum export site assembly. Journal of Cell Biology 152: 213-229.

Bonfanti, L., A.A. Mironov Jr., J.A. Martinez-Menarguez, O. Martella, A. Fusella, M. Baldassarre, R. Buccione, H.J. Geuze, A.A. Mironov and A. Luini (1998). Procollagen traverses the Golgi stack without leaving the lumen of cisternae: evidence for cisternal maturation. Cell 95: 993-1003.

Fontana, W. and L.W. Buss (1994). "The arrival of the fittest": toward a theory of biological organization. Bulletin of Mathematical Biology 56: 1-64.

Herrmann, J.M., P. Malkus and R. Schekman (1999). Out of the ER - outfitters, escorts and guides. Trends in Cell Biology 9: 5-7.

Képès, F. (2001). Simulation of biological processes in the genomic context. Biology International 41: 29-38.

Kuehn, M.J., J.M. Herrmann and R. Schekman (1998). COPII-cargo interactions direct protein sorting into ER-derived transport vesicles. Nature 391: 187-190.

Morin-Ganet, M.N., A. Rambourg, Y. Clermont and F. Képès (1998). Role of ER-derived vesicles in the formation of Golgi elements in *sec23* and *sec18 Saccharomyces cerevisiae* mutants. The Anatomical Record 251: 256-264.

Morin-Ganet, M.N., A. Rambourg, S.B. Deitz, A. Franzusoff and F. Képès (2000). Morphogenesis and dynamics of the yeast Golgi apparatus. Traffic 1: 56-68.

Novick, P., C. Field and R. Schekman (1980). Identification of 23 complementation groups required for post-translational events in the yeast secretory pathway. Cell 21: 205-215.

Presley, J.F., N.B. Cole, T.A. Schroer, K. Hirschberg, K.J. Zaal and J. Lippincott-Schwartz (1997). ER-to-Golgi transport visualized in living cells. Nature 389: 81-85.

Presley, J.F., T.H. Ward, A.C. Pfeifer, E.D. Siggia, R.D. Phair and J. Lippincott-Schwartz (2002). In vivo dissection of COPI and Arf1 dynamics and role in Golgi membrane transport. Nature, in press.

Rambourg, A., Y. Clermont and F. Képès (1993). Modulation of the Golgi apparatus in *Saccharomyces cerevisiae sec7* mutants as seen by three-dimensional electron microscopy. The Anatomical Record 237: 441-452.

Rossanese, O.W. et al. (1999). Golgi structure correlates with transitional ER organization in *P. pastoris* and *S. cerevisiae*. Journal of Cell Biology 145: 69-81.

Satiat-Jeunemaître, B., L. Cole, T. Bourett, R. Howard and C. Hawes (1996). Brefeldin A effects in plant and fungal cells: something new about vesicle trafficking? Journal of Microscopy 181: 162-177.

Seemann, J., E. Jokitalo, M. Pypaert and G. Warren (2000) Matrix proteins can generate the higher order architecture of the Golgi apparatus. Nature 407: 1022-1026.

Takei, K. and V. Haucke (2001). Clathrin-mediated endocytosis: membrane factors pull the trigger. Trends in Cell Biology 11: 385-391.

Hyperstructures

Vic Norris[1], Patrick Amar[2,4], Pascal Ballet[3], Gilles Bernot[2], Franck Delaplace[2], Maurice Demarty[1], Jean-Louis Giavitto[2], Camille Ripoll[1], Michel Thellier[1] and Abdallah Zemirline[3]

[1]Laboratoire des Processus Intégratifs Cellulaires, UPRESA CNRS 6037, Faculté des Sciences & Techniques , Université de Rouen, 76821, Mont-Saint-Aignan, France
[2]Laboratoire de Méthodes Informatiques, CNRS UMR 8042, Université d'Evry, 91025 Evry cedex, France
[3]Laboratoire des Interfaces Machines Intelligente, Université de Bretagne Occidentale, Brest, France
[4]Laboratoire de Recherche en Informatique, CNRS UMR 8623, Université Paris-Sud, Orsay, France

Contents

Abstract

New concepts may prove necessary to profit from the avalanche of sequence data on the genome, transcriptome and proteome and to relate this information to cell physiology. Here, we focus on the concept of hyperstructures in which a variety of types of molecules are brought together to perform a function. The processes responsible for hyperstructure formation include changes in enzyme affinities due to metabolite-induction, transertion, and elevated local concentrations of proteins and their binding sites on DNA and RNA. We review the evidence for the existence of hyperstructures responsible for the initiation of DNA replication, the sequestration of newly replicated origins and for cell division. We interpret cell cycle progression in terms of hyperstructure dynamics. Finally, we speculate on how a variety of *in silico* approaches could be combined to develop new concepts in the form of an *Integrated* or *Imaginary* cell – *I-cell* – which would undergo selection for growth and survival in a world of artificial microbiology.

1 Introduction

Molecular biology and biochemistry have provided a wealth of information about how RNA polymerases transcribe DNA into RNA and how ribosomes then translate mRNA into proteins, about the nature of those proteins and lipids and form membranes, and about other important molecules. Model organisms such as the bacterium *Escherichia coli* are invaluable in making sense of this information. The 4.6 Mb genome of *E. coli* has been sequenced (Blattner *et al*., 1997) and was found, at the time, to have 4288 protein-coding genes (cf 5885 in the eukaryote *Saccharomyces cerevisiae*) of which 38% had no attributed function. But even when all genes are ascribed functions, how are we to interpret this information and use it to predict phenotypes? The challenge is to understand how cells organise their myriad constituents and processes. To explain how the concept of hyperstructures may help us, here, we briefly review the bacterial cell cycle, focussing on the problem of division, and then discuss hyperstructures. We do this in the light of different questions: Why might a hyperstructure language be useful? What are hyperstructures? How do they form? How do they interact? How might they guide cells through state space to control growth, adaptation, differentiation and the cell cycle? We then discuss how the hyperstructure concept may help in exploiting the information provided by genome sequencing and how it may be tested. Finally, we advocate the construction of an integrated cell, I-cell, as a new approach to the study of biological complexity.

2 The bacterial cell cycle

The principal events in the bacterial cell cycle include:

- *Initiation of chromosome replication from a single origin of replication*
- *The sequestration of newly replicated origins of replication*
- *Chromosome separation*
- *Chromosome segregation*
- *Cell division*
- *Inactivation of the division site*

In the case of cell division, it is still not clear how this event is timed, positioned and coupled to other events. The earliest known protein to act in *E. coli* is the tubulin-like FtsZ which migrates from the cytoplasm to a mid-cell location on the membrane where it assembles into a ring-like structure and where it recruits other division proteins. What lies upstream of FtsZ? Is it yet

another protein or is it something else? We have shown that FtsZ can interact directly with phospholipid membranes in the absence of other proteins (Alexandre *et al* ., 2001). This is consistent with a major role for membrane dynamics in the regulation of the cell cycle as is the finding that membrane domains around the chromosomes differ from the domain at the future site of division (Fishov & Woldringh, 1999), this latter presumably being related to the large domains of cardiolipin observed at the division sites and poles (Mileykovskaya & Dowhan, 2000).

The constraints on a solution to the division problem for *E. coli* are that the division site must be:

• *in the right place – midcell – to give daughters of similar sizes*
• *between chromosomes to avoid producing a DNA-less cell*
• *formed at the right time in the cycle – perhaps to give the right DNA/mass ratio?*
• *formed at the right rate – to avoid, for example, cells getting bigger and bigger*
• *of the right nature – to allow membranes to curve and fuse whilst controlling ion and lipid fluxes*

It is in the context of trying to find a solution to this problem that we present hyperstructures.

3. Why invoke a hyperstructure language?

Cells survive and sometimes grow by somehow orchestrating millions of molecules of thousands of types to adapt to the environment and to proceed through the cell cycle. This entails cells solving the combinatorial problem of negotiating the immensity of state space since if each gene in *E. coli* were in either an on (transcribed) or an off (untranscribed) state, there would be 2^{4000} or 10^{1200} on-off patterns of gene expression (Kauffman, 1996). But there is more than this, there is also the epigenetic trap – cells in a population should not all have the same phenotype (else, for example, a single catastrophe would be more likely to wipe them all out). Exploring state space effectively boils down to: How can cells be both efficient and robust? We argue that the answer is that cells rely on an intermediate level of organisation – *hyperstructures.*

4. What are hyperstructures?

There are two sorts of hyperstructures:

• Non-equilibrium hyperstructures are large structures of diverse molecules – genes, mRNAs, proteins, ions, lipids – that depend on a flow of energy/material for their existence. These hyperstructures are assembled to serve a specific function and are disassembled when no longer functional (Figure 1).
• Equilibrium or quasi-equilibrium hyperstructures are large structures that are not dependent on a flow of energy for their existence. They are not assembled or disassembled according to whether they are required to serve a function. Our discussion of equilibrium hyperstructures will be very limited here.

Examples of possible non-equilibrium hyperstructures include:

An initiation hyperstructure responsible for starting the initiation of replication of the chromosome. This hyperstructure contains the DnaA protein and certain of the sites on DNA to which it binds (Norris *et al*., 2001). DnaA is the key protein in initiation in *E. coli* and binds to 9mer TTA/TTNCACA and 6mer AGATCT sites present in the origin of replication and in

certain replication-related genes (Speck *et al*., 1999). DnaA polymerisation (Weigel *et al*., 1999) and a fluid, acidic, membrane domain (Castuma *et al*., 1993; Fralick & Lark, 1973) are required for DnaA to be active in initiation.

A replication hyperstructure comprising the protein SeqA plus the key enzymes in DNA replication along with the genes that encode them (Norris *et al*., 2000). SeqA sequesters newly replicated origins of replication and prevents them from being used more than once within a substantial portion of the cell cycle (hence preventing a flurry of initiations when a single initiation signal is given). SeqA is found in clusters (Onogi *et al*., 1999). It binds to GATC sequences and it polymerises.
A cell division hyperstructure comprising the 10 or so division proteins (including FtsZ) plus enzymes involved in peptidoglycan synthesis together with the genes that encode them, many located together in the *dcw* cluster at the 2 min position on the chromosome (Buddelmeijer *et al*., 1998; Norris & Fishov, 2001).

Other hyperstructures include a DNA compaction hyperstructure possibly involving MukB which can form foci (Ohsumi *et al*., 2001); a nucleolus-like hyperstructure responsible for ribosome synthesis and assembly (Lewis *et al*., 2000; Woldringh & Nanninga, 1985); a chemotaxis hyperstructure comprising chemotactic receptors such as Tsr with the kinase CheA and the transducing protein CheA (Bray *et al*., 1998; Stock & Levit, 2000) plus, we propose, the genes encoding these proteins. Factors in the formation of possible hyperstructures for transport and glycolysis (Mitchell, 1996; Norris *et al*., 1999; Velot *et al*., 1997) are discussed below.
Examples of possible equilibrium hyperstructures:

These include immiscible domains within the condensed chromosome. This immiscibility occurs in the context of an ordered liquid, with the DNA closely layered by a regular twist (Bouligand & Norris, 2001), a situation that may minimize entangling and facilitate co-expression of the genes within a domain. Our discussion of equilibrium hyperstructures will be very limited here.

5. How do non-equilibrium hyperstructures form?

There are several complementary possibilities:

5.1 Metabolite-induction

The idea is that:

• Non-equilibrium hyperstructures form when the cell is actively engaged in processing substrates and disappear when they are not
• These hyperstructures include enzymes in the same pathway and their genes
• Formation of certain of these hyperstructures may involve an interplay between diffusion in 2-D and 3-D in the sense that enzymes confined to domains in the 2-D membrane interact with other enzymes or groups of enzymes diffusing in the 3-D cytoplasm (Figure 1)

The evidence consistent with this scenario has been advanced for the existence of metabolons which are assemblies of the enzymes that act in succession in a pathway (Velot et al., 1997). Of course, such metabolons may themselves associate into larger hyperstructures. In the case of secretion, substrate binding promotes assembly of the 3 components of the ABC exporters of Gram negative bacteria e.g. in *Erwinia chrysanthemi* the substrate (protease) binds to PrtD (an ABC protein) which then binds to PrtE (membrane fusion protein) and which binds to PrtF (outer

membrane protein) (Letoffe *et al*., 1996). In the case of glycolysis, the glycolytic pathway can be extracted as an equimolar complex of 1.65 megaDa that reveals compartmentation of substrates (Mowbray & Moses, 1976). In the case of import, sugar-specific phosphotransferase system permeases consist of EIIC and EIID in the membrane and EIIA and EIIB in the cytoplasm; EIIA is phosphorylated by HPr in a reaction catalysed by EI with phosphate from phosphoenolpyruvate; E2s+E1+HPr probably form a complex (Norris et al., 1999). The idea here is that successive enzymes in the same pathway can be activated to bind to one another in a *vertical* organisation. A complementary idea is that a single species of enzyme can be activated to oligomerize by substrate (Torshin, 1999); indeed, the full enzymatic activity of glyceraldehyde-3-phosphate dehydrogenase, phosphoglycerate mutase and enolase – all glycolytic enzymes – results from their association. Again, this *horizontal* organisation could help nucleate and stabilise hyperstructures (Figure 2).

5.2 Local concentrations

The phenomenon of oligomeric proteins binding to specific sites on DNA has been invoked to explain the operation of the *lac* and lambda repressors (Revet *et al*., 1999). It might also be invoked to explain the sequestering of newly replicated origins of replication by the protein SeqA (Onogi et al., 1999). There are variations of this theme with, for example, the possibility that proteins such as the histone-like protein HU, which binds to both RNA and DNA (Balandina *et al*., 2001), could play important roles (see below and Figure 3).

5.3 Transertion

Transertion is the coupled transcription, translation and insertion into and through membranes of proteins. The cytoplasmic membrane is composed of a wide variety of lipids and proteins so, if these proteins have lipid affinities, small proteolipid domains form. High rates of transertion may create a critical density of inserted nascent proteins that is sufficient for small proteolipid domains to fuse into large ones and so nucleate hyperstructure assembly (Norris, 1995) (Figure 4). For example, it might be supposed that the high density of transertion of the ATP synthetase components, which have lipid affinities (Arechaga *et al*., 2000; Ksenzenko & Brusilow, 1993), should result in assembly of an ATP synthesis hyperstructure.

5.4 Translated mRNA is protected from RNases and enzymes in metabolons are protected from proteases

It has been suggested that enzymes in complexes are more likely to escape the attention of proteases than when those enzymes are not in complexes (Miller, 1996). An extension of this idea is that the partitioning of enzymes into a hyperstructure protects them from proteases (providing the latter are excluded from the hyperstructure). Hence an enzyme which has been assembled into a hyperstructure *because* of its activity is thereby preserved (i.e. active enzymes are preferentially protected). A similar argument is that mRNA translated within a hyperstructure could be preferentially protected from RNases on the outside of the hyperstructure.

6. How do hyperstructures interact?

6.1 Shared lipid affinities creates shared membrane domains

It can be argued that proteins with lipid preferences may congregate with those lipids in a positive feedback fashion to form the membrane domain part of a hyperstructure (see *5.3 Transertion*). Similarly, it might be expected that hyperstructures characterised by enrichment for a particular lipid would also tend to associate.

6.2 Shared binding proteins create shared cytoplasmic compartments

The idea is that certain abundant proteins may participate in the assembly of several different types of hyperstructures. This would enable a synergy whereby the progressive formation of a group of hyperstructures responsible for a set of functions would aid the recruitment of other related hyperstructures fulfilling complementary functions. Candidates for these proteins include the DNA-binding proteins IHF, FIS, and HU (for references see (Ussery *et al*., 2001)). IHF can modulate the transcriptional activity of promoters by influencing the looping of upstream DNA; the consensus site of IHF binding, YAACTTNTTGATTTW, lies within many repetitive extragenic palindromic sequences. FIS binding to upstream regions can enhance the transcription of highly expressed genes; the consensus for the FIS binding site is weak with estimates of its numbers ranging from 6 to 68000. HU binds to DNA with no evident sequence preference and, in so doing, influences the interaction of regulatory proteins with their specific sites on the DNA (Bonnefoy & Rouviere-Yaniv, 1992); HU also recognizes certain specific structures of both DNA and RNA with very high affinity and, for example, binds to the mRNA for RpoS (Balandina et al., 2001; Kamashev & Rouviere-Yaniv, 2000). In addition, there are over a 100 known activators and repressors of transcription in *E. coli* (Ouzounis *et al*., 1996) and it may be expected that these will control the synthesis of certain oligomeric proteins important in the assembly of different – but complementary – hyperstructures.

6.3 Shared codon preferences

There are strong compositional asymmetries in codon and amino acid usage depending on the orientation of the genes with respect to DNA replication and on the nature of the proteins encoded. This has led to predictions of different compartments for the syntheses of different proteins (Danchin & Henaut, 1997).

6.4 Water preferences

Water exists as species with different structures and chemical properties that affect the distribution and activity of cellular constituents (Robinson *et al*., 1999; Wiggins, 1990). An important but difficult question is the extent to which the water preferences of the constituents of hyperstructures might determine hyperstructure formation and interaction.

6.5 Oscillations/vibrations

The Min system, which is involved in the selection or inactivation of the division site, oscillates with a periodicity of around 1 minute in *E. coli* (Raskin & de Boer, 1999). There are numerous oscillatory processes in eukaryotes of which the oscillation of protons and of NAD(P)H in neutrophils is particularly exciting (Petty & Kindzelskii, 2001). Such oscillations are candidates for playing global as opposed to local organising roles. Relating them to the dynamics of hyperstructures is a problem that has still to be addressed.

7. Cell division

The regulation of cell division can now be considered in terms of the dynamics of hyperstructures. It has been argued that one of the functions of the bacterial cell cycle is to generate daughter cells with different phenotypes since this would allow the population to both explore all the possibilities for growth offered by the environment and be ready for a sudden catastrophic change (Norris et al., 2001; Segre *et al*., 2000). In this scenario, during the run-up to

initiation, the mass to DNA ratio increases and certain hyperstructures become 'stronger' by attracting ever more of the cell's resources (such as the transcriptional and translational apparatus) whilst other hyperstructures are weakened and disappear (Norris et al., 2001)(Figure 5). This results in a drop in the diversity of hyperstructures, some of which release DnaA as they dissociate, a DnaA-initiation hyperstructure forms, and replication of the chromosome begins. Now suppose that short FtsZ polymers are associated with glycolytic and other hyperstructures so that FtsZ is effectively sequestered (noting that, at least in eukaryotes, tubulin is associated with glycolytic enzymes (Lloyd & Hardin, 1999)). This leads us to consider two possibilities. One is that the FtsZ-sequestering hyperstructures are temporarily disrupted by chromosome replication to release FtsZ which can then participate in division. The other, complementary, possibility is that the changing activity of the phosphotransferase system/glycolytic hyperstructure directly leads to its own disassembly (for example, its capacity might exceed demand and lead to feedback inhibition) and releases FtsZ. This would be consistent with the advance in divisions in synchronous cultures of *E. coli* induced by addition of the non-metabolisable, glucose analogue α-methylglucoside (Fishov, 1994) and the delay in divisions induced by transfer to a rich growth medium (Kepes & Kepes, 1985).

Before trying to put it all together, we should bear in mind that, all else being equal, the rates of transcription of two copies of the same gene diverge if this gene is –vely regulated *in trans* but +vely *in cis* (Norris & Madsen, 1995). The –ve regulation *in trans* could result from a repressor diffusing through the cytoplasm to each separate stretch of DNA whilst the +ve regulation *in cis* could result from an RNA polymerase transcribing a gene making this particular stretch of DNA accessible to another polymerase. This leads to the conclusion, surprising for many microbiologists, that two identical chromosomes in the same cytoplasm (which contain many such genes) *therefore* have different patterns of gene expression. The same argument can be made in terms of hyperstructures: a set of genes is expressed from one chromosome to form part of a hyperstructure; this assembly involves positive feedback between the constituent ions, lipids, proteins and nucleic acids since as the density of one constituent in a region increases, the probability increases that the density of another constituent will also increase. In the context of a cell in which hyperstructures compete for existence (that is, negative regulation *in trans*), the result is a highly structured, asymmetric cell in which each future daughter cell has a different set of hyperstructures associated with it and these sets differ in their composition of lipids, ions, water structures, proteins, mRNA and expressed genes (Figure 6). At present, it is difficult to discriminate between the different ways in which the principal proteolipid domains around the chromosomes could create a division site (red, dotted arrows in Figure 6). In one scenario, the site would simply consist of the *interface* between the two domains whilst in the other scenario, the site would consist of a distinct *domain* between the principle two domains. There are, of course, permutations of these possibilities. The essence of our proposal is that hyperstructure dynamics could achieve:

- separation of chromosomes during replication
- differentiation of both chromosomes and membrane
- the right place for a site to attract and activate division enzymes (between the chromosomes)
- the right time for the creation of a division site (after chromosome segregation)
- the right nature for a division site - a potential non-bilayer
- coupling between replication, segregation and cell division
- a calcium flux (down the concentration gradient)
- orchestration of membrane-activated kinases, proteases *etc.*

8. The advantage of organisation at the level of hyperstructures

It has been observed that the difficulty of administering a laboratory is proportional to the square of the number of members of the laboratory, N^2 (Bok, 1983). This difficulty, D, is reduced if the individuals are put into N_1 groups such that D equals the square of the number of groups (to reflect group interactions) plus the square of the number of individuals in each group N_0^2 (to reflect interactions within groups) times the number of groups:

$D = N_1^2+(N_0^2)N_1$

Hence $D = (N/N_0)^2+(N_0^2)N/N_0$

And $D = N^2/N_0^2+N_0N$

To minimise D,

$\delta D/\delta N_0 = -2N^2/N_0^3+N$

Hence the difficulty is at a minimum when

$N_0 = (2N)^{1/3}$

This formula helps to give us a feel for the numbers of hyperstructures that may exist in a cell. Just considering proteins, for example, a bacterium containing of the order of a million interacting proteins would be expected to have around a hundred hyperstructures. The existence of this intermediate level of organisation therefore means that the problem of generating a limited number of coherent phenotypes that are adapted to survival and/or growth is greatly simplified. Navigation through the immensity of state space becomes a choice between 100 or so hyperstructures rather than 4000 plus genes – 2^{100} on-off combinations rather than2^{4000}. To generate a coherent phenotype, for example, enzymes appropriate for growth in cold oxygenated conditions should not be synthesized in the same cell at the same time as those for growth in hot anaerobic conditions. Coherence can be achieved because cells can manage the relatively few common factors required to bring together a particular set of hyperstructures. The existence of hyperstructures also allows, we speculate, bacterial cells to regulate DNA replication and cell division so as to create heterogeneous populations that can both grow and survive unexpected challenges.

9. Using the hyperstructure concept to exploit sequence data

Of the numerous *in silico* approaches possible, we focus here on cellular automata which are used to model many physical and biological phenomena (Vichniac, 1984). Once the units that constitute the automata have been assigned initial states, the evolution of these states can then depend on both the previous history of the state and on the state of neighboring units. Hence, cellular automata can be particularly suitable for modeling the dynamics of interactions between molecules in 3 dimensions. We now use cellular automata to illustrate how they might be used to model the effects on hyperstructure assembly of the following:

9.1 Metabolite-induction

To determine the values of the parameters governing the formation of hyperstructures in bacteria, we have constructed a preliminary version of a cellular automaton program (with features of multi-agent systems) that simulates the dynamics of the localization of the PTS and glycolytic enzymes in both a 2 dimensional membrane and a 3 dimensional cytoplasm (Le Sceller *et al*., 2000). Each unit volume represents a 10nm*10nm*10nm cube in a cell that can have a maximum volume of 200*200*200 unit volumes or $8\mu m^3$. This is more than sufficient to represent *E. coli* which in certain growth conditions has a volume of 2 cubic microns. Each cubic unit volume in the membrane is surrounded by 8 other unit volumes and each unit volume in the cytoplasm is surrounded by 26 others. At each time step, all enzymes are considered in a random order. Each can move into a free neighboring unit volume. In this preliminary study, there was a structuring of both membrane and adjacent cytoplasm and hyperstructures were generated containing up to 500 enzymes.

9.2 Transertion

To model the anchoring effect of transertion on nascent proteins (Figure 4), a proportion of the PTS Enzymes II (for example) could be permanently confined *in silico* to a patch of the membrane. An important parameter may therefore be the *area* over which these proteins are inserted. It is not easy to obtain this area experimentally with current techniques (but see the NanoSIMS below). However, this may be an instance when the simulation reveals whether hyperstructure formation is very sensitive to the area of transertion and therefore whether energy should be invested in performing the relevant experiments.

9.3 Lipid preferences

The cosegregation of proteins with the lipids for which they have pronounced affinities is a potent way to produce domains. This process may be simulated in the 'membrane' of cellular automata given these affinities. Below (*10.3*), we suggest a series of experiments that could lead to consensus sequences for lipid binding and hence a way, ultimately, to convert sequence information into the 'lipidome' and facilitate the simulation of the distribution of all membrane proteins.

9.4 Local concentrations

Using cellular automata to model local concentrations might exploit knowledge of DNA-binding proteins and their sites providing DNA can also be introduced into the model. One way to achieve this would be to divide the chromosome into chunks comparable in size to proteins. Each chunk would be constrained in its diffusion by a function inversely proportional to the distance between the chunk in question and another chunk. It may also prove necessary to make efforts to model reptation, the constrained movement of polymers in a crowded solution.

9.5 DNA distribution

DNA curvature, flexibility and stability have been analysed for 18 fully sequenced bacterial genomes (Pedersen *et al*., 2000). This reveals many significant structural features including a set of 20 regions with identical and extreme structural properties that are proposed to function as topological domain boundaries. These features are presumably related to the properties of proteins such as HU (see *6.2*) which binds preferentially to unusual structures such as kinked or cruciform DNA (Bonnefoy *et al*., 1994; Kamashev & Rouviere-Yaniv, 2000). The challenge is to translate this information into a dynamic 3-D model taking into account that much of the DNA

is probably in a cholesteric form. One model that might be tested *via* cellular automata (as in *9.4*) is that HU both binds to these curved regions and self-associates such that curved regions are stacked at the edges of twisted liquid crystalline regions. In such a model, the terminus region, which has high curvature, low flexibility and low helix stability (Pedersen et al., 2000), might be expected to exhibit a distinctive packing.

9.6 Parallel approaches

In an activity-based vision of the cell, only a subset of its constituents is important in determining the phenotype of the cell at any one time (Norris, 1998). This subset comprises those constituents that are *active* where *active* is considered to mean being transcribed for a gene, being translated for a mRNA, and catalysing a reaction for an enzyme. Belonging to this active subset requires a competition between constituents that were active in the previous time period (the *status quo* factor) and constituents that act in synergy with one another (the coherence factor).

In this section, we describe a new implementation of cellular automata or units based on the related idea that only a few unit volumes are potentially active, that is either contain a molecule or a have a neighbouring unit containing a molecule. The advantage is that memory is not needed to store these empty units. This leads to a time and memory efficient approach for computing the successive generations of the units. The overall state of the system is determined by the content of all the units at a given time. Computing the next generation means determining the new state of the system after the application of all the local rules to each unit. This process must not depend on the order the units are examined and, ideally, each unit is treated independently of all the other units. The standard way to represent the 3-D space is to use a array of structures to address each unit that often contains only a number. Using this method, it is easy to determine the neighbourhood of a unit by a simple transformation of its coordinates, and then access the array to get the values of the neighbouring units. The major drawback is that we must store *all* the units, even the empty ones.

In our approach, we also represent the space by a three coordinate system, but we store in the computer memory *only* the active or potentially active units (i.e. those that are filled or next to filled units). This reduces the memory cost and allows us either to reduce the size of each unit to have a more accurate simulation, or to simulate a larger space.

The potentially active cells are stored in a hash table which allows a very fast access time, comparable to the access time of a 3-D array, if a good hash function is used along with an adapted strategy to resolve collisions. This low cost implementation of the state of the system can be used to reduce the time used to compute each generation if an extra cost is paid by duplicating the representation of the space: the local rules are applied to each active unit using the values from the first, *current* space and the result is stored in the second, *new* space. After all the units of the first space have been processed and the second space is complete, the second space becomes the current space and the next generation can be computed.

Since the current space is only accessed for *reading* values whilst the new space is only accessed for *writing* results, the current space can be freely accessed by multiple processes without synchronisation. The new space can be split into parts that can be computed separately on a multiprocessor with a consequent dramatic reduction in computation time. Each process requires its own part of the current space but also acts on a surrounding layer of single units in the parts treated by other processes. Since each process only accesses the part of another process at the boundary, each part can be stored locally in a multi-computer networked environment.

In the 12 by 12, 2-D example (Figure 7), process **P1** only needs to access the first 7 lines (0 to 6) of the current space to compute the first 6 lines of the new space, while process **P2** needs to access the last 7 lines (5 to 11) of the current space to compute the other half of the new space. Since there is no read/write conflict between **P1** and **P2** no synchronization is needed. This is another advantage of the inherent parallelism of this implementation.

9.7 Hyperstructure movements and reactions

Interactions *between* hyperstructures are proposed to result in a pre-divisional cell with one set of hyperstructures in one half the cell and a different set in the other half. Such sets of hyperstructures may be formed on the basis of common lipids, ions, binding proteins and/or water properties. Movements of hyperstructures are nicely illustrated by the SeqA-replication hyperstructure that, during the cell cycle, goes from a single focus to two foci that then migrate to the one-quarter and three-quarter positions (Ohsumi et al., 2001; Onogi et al., 1999). To model how interactions between hyperstructures might lead to redistribution of hyperstructures within the cell, we consider a cellular automaton model in which several hyperstructures can be represented simultaneously in a coarse-grained way (so that the units are bigger than single macromolecules).

The idea presented in this section entails providing local rules to reproduce molecular reaction and diffusion using cellular automata. The difference between our approach and typical reaction-diffusion processes is that the molecule concentration (in a specific position) is boolean: *true* if there is a set of molecules, *false* if there are none. One of the simplest systems has only one type of molecule on a 2-D grid (environment). Focusing on a particular molecule and its neighbourhood, it is clear that a unit plus the 8 adjacent units is a square of side 3 units. If we suppose that the molecule can move or stay in the same place, the molecule will have 9 possible positions (Figure 8). With cellular automata, the state of a unit depends on its neighbourhood. Thus, a local rule must be used to determine whether a unit in the 2D-grid becomes *true* (has molecules) or *false* (is empty). The idea is to invert the arrow direction in the previous figure. Thus, if an empty cell is adjacent to one filled cell, it has a probability of $1/9^{th}$ to become filled. We can apply this to any neighborhood.

Given a unit in a 2D-grid, the probability of the unit to become *true* (filled) is $p = n / 9$ where n is the number of filled units into its neighbourhood. More generally, for a *dim*-dimensional environment (a grid of dimension *dim*), the probability of one cell to become *true* is:

$$p = n / N \qquad (1)$$

where $N = 3^{dim}$. Figure 9 shows the results of this local probabilistic rule (rule 1) with a *60x60* grid at three different times.

To construct a multi-molecule hyperstructure, the next stage consists in putting together different types of molecules. In this case, the value of a unit is not a boolean but an integer included between *0* and *nb* (number of types of molecule). In this way, rule (1) becomes

$$p_0 = n_0 / N$$
$$p_1 = n_1 / N$$
$$p_2 = n_2 / N$$
$$\ldots \qquad (2)$$

$p_{nb} = n_{nb} / N$

where n_i is the number of molecules of type i into the neighborhood and $N = 3^{dim}$ into the *dim*-dimension grid. An empty cell is of type *0*.

To choose the future type of a cell among all the possibilities, we consider a real random number A bounded by *0* (included) and *1* (excluded). The decision rules are the following:

if $A \in [0, p_0[$ then the considered cell is of type *0*
if $A \in [p_0, p_0+p_1[$ then the considered cell is of type *1* (3)
...
if $A \in [p_0+p_1+...+p_{nb-1}, p_0+p_1+...+p_{nb}[$ then the considered cell is of type *nb*.

Figure 10 shows the results of this local probabilistic rules with a *60x60* grid at three different times and for two types of molecule.

To study hyperstructures containing many different molecules that can perform chemical reactions, we allow two different molecules to react to produce another type of molecule:

$$mol_i + mol_j \rightarrow mol_k \quad (4)$$

To do this, we add the following simple rule (5) to rule (3):

if the *considered cell* is of type *i* (resp. *j*) and the type chosen thanks to rule 3 is *j* (resp. *i*) then the (5) have the type *k* (according to rule 4)

Figure 11 shows the evolution of the system in a *60x60* grid at three different times, for two types of molecule and that react together according to rules (4) and (5) to produce a third type of molecule.

To observe the formation of and interaction between hyperstructures, we introduce the notion of affinity between molecules. In our example (Figure 12), molecules of type 1 are activated and can therefore bind one another. Molecules of type 2 and 3 have similar behaviours. Moreover, molecules of type 1 can react with molecules of type 2 to produce molecules of type 3. Figure 12 shows fluxes of molecules leading to the formation of a hyperstructure:

- Molecules of type 1 come from the top of the cellular automata and bind together
- Molecules of type 2 come from the bottom of the cellular automata and bind together too
- Molecules of type 1 react with molecules of type 2 to produce molecules of type 3
- Molecules of type 3 bind together and with molecules of type 1 and type 2.

10 Experimental aspects

10.1 NanoSIMS

Visualizing hyperstructures directly with conventional techniques has been difficult since it requires the co-localization of such disparate elements as proteins, mRNA, genes and lipids at the 50 nm scale. In secondary ion mass spectrometry, a section of biological material is subjected to a beam of ions that pulverizes it to release secondary ions that are filtered by mass spectrometry

to allow an image to be obtained [Thellier, 1993 #1084]. Recent developments in NanoSIMS technology are very promising since the new generation of machines provides resolution at the scale required and allows detection of isotopically marked probes to proteins and nucleic acids. This opens up the exciting possibility of studying hyperstructures by imaging simultaneously both nucleic acids and up to 10 different proteins at a resolution intermediate between light and electron microscopy.

10.2 Optical waveguide lightmode spectroscopy (OWLS)

In the case of glycolysis, we lack details of the exact abundance of proteins such as phosphoglucose isomerase**,** fructose -1,6-P2 aldolase, triose-P isomerase, glyceraldehyde 3-phosphate dehydrogenase A complex, and phosphoglycerate kinase. Although we can obtain these *via* radioactive labeling and 2-D gel electrophoresis, there are attractive, recent techniques such as those based on isotope-coded affinity tags (Gypi *et al*., 1999). More seriously, we lack details of the constants of affinity of the PTS and glycolytic enzymes. These could be obtained using OWLS in experiments with purified proteins and substrates (Ramsden, 1993). By introducing and removing the substrates, it may also prove possible in these experiments to estimate the period of time for which an enzyme remains active (i.e. has a higher affinity constant) once its substrate has gone (Ricard *et al*., 1998).

10.3 MALDI-MS and ES-MS

We are presently using sensitive techniques of mass spectrometry to explore the possibility that concomitant with overproduction of a membrane protein is a compensatory overproduction of the lipid for which it has an affinity (Arechaga et al., 2000). If this approach is successful, a semi-automated, general strategy might be developed in which bacteria are transformed with plasmids each containing a different peptide (from a random library); the idea is to obtain thousands of colonies, each containing lipids resulting from the overproduction of a particular peptide. Mass spectrometry and sequencing would then match lipids and peptides. The data would be used to try to derive consensus sequences to be used to interpret the genome and construct a 'lipidome'.

10.4 Atomic Force Microscopy (AFM) and the Langmuir-Blodgett technique

Langmuir-Blodgett monolayers of phospholipids, which assemble at the air-water interface, followed by transfer to a solid support and inspection with AFM, provide a powerful combination of techniques for studying FtsZ interaction with membranes and may constitute the beginnings of an *in vitro* division system (Alexandre et al., 2001). The characteristics of the lipids used along with the values of parameters obtained for factors that interact with FtsZ, such as calcium, GTP and other division proteins, might be used to try to construct an *in silico* model of the division process.

11. I-cell

Developing new concepts may prove essential to a full understanding of how a cell works. To test and develop such concepts, we advocate the construction of an *Integrated* or *Imaginary* cell – *I-cell* – which would undergo selection for growth and survival in a world of artificial chemistry (Dittrich & Banzhaf, 1998). The unit volumes that constitute an I-cell would be inspected at each time step and, according to the molecule(s) found, the appropriate entry would be consulted in a table containing a large number of 'biological' functions (Norris & Le Sceller, 2001). These functions would determine the interactions of the molecule with its neighbours and

also, via global functions, with distant molecules. The I-cell would be fed according to different regimes and, depending on the functions implemented, would grow and eventually divide; I-cells would be analysed after selection over several generations. Combinatorial problems would be reduced if an activity-based vision of the cell were adopted in which only a subset of constituents would be consulted at each time step; this subset would correspond to constituents that play an active role in coherent cell states via a mechanism based in part on global functions and termed competitive coherence (Norris, 1998). An I-cell might, for example, offer a way to discover the importance of a particular organising process, for example, one based on water structure or tensegrity. An I-cell might even be used to see whether new laws of complexity emerge as the number of organising processes in the system increases.

Acknowledgements

We thank Genopole and the Conseil Regional de l'Ile de France for support.

References

Alexandre, S., Cole, G., Coutard, S., *et al*. (2001). Interaction of FtsZ protein with a DPPE film. Colloids and Interfaces B in press.

Arechaga, I., Miroux, B., Karrasch, S., *et al*. (2000). Characterisation of new intracellular membranes in *Escherichia coli* accompanying large scale overproduction of the b subunit of F_1F_0 ATP synthase. FEBS Letters 482: 215-219.

Balandina, A., Claret, L., Hengge-Aronis, R., *et al*. (2001). The *Escherichia coli* histone-like protein HU regulates *rpoS* translation. Molecular Microbiology 39: 1069-1079.

Blattner, F.R., Plunkett III, G., Bloch, C.A., *et al*. (1997). The complete genome sequence of *Escherichia coli* K-12. Science 277: 1453--1462.

Bok, J. (1983). Un modèle d'auto-organisation : le principe de moindre difficulté. In L'auto-organisation. De la physique au politique. (Dumouchel, P. and Dupuy, J.-P., eds.). Paris. Seuil,

Bonnefoy, E. and Rouviere-Yaniv, J. (1992). HU, the major histone-like protein of *E. coli*, modulates the binding of IHF to *oriC*. EMBO Journal 11: 4489-4496.

Bonnefoy, E., Takahashi, M. Rouviere-Yaniv, J. (1994). DNA-binding parameters of the HU protein of *Escherichia coli* to cruciform DNA. Journal of Molecular Biology 242: 116-129.

Bouligand, Y. and Norris, V. (2001). Chromosome separation and segregation in dinoflagellates and bacteria may depend on liquid crystalline states. Biochimie 83: 187-192.

Bray, D., Levin, M.D. Morton-Firth, C.L. (1998). Receptor clustering as a cellular mechanism to control sensitivity. Nature 393: 85-88.

Buddelmeijer, N., Aarsman, M.E.G., Kolk, A.H.J., *et al*. (1998). Localisation of cell division protein FtsQ by immunofluorescence microscopy in dividing and non-dividing cells of *Escherichia coli*. Journal of Bacteriology 180: 6107-6116.

Castuma, C.E., Crooke, E. Kornberg, A. (1993). Fluid membranes with acidic domains activate DnaA, the initiator protein of replication in *Escherichia coli*. Journal of Biological Chemistry 268: 24665-24668.

Danchin, A. and Henaut, A. (1997). The map of the cell is in the chromosome. Current Opinion in Genetics and Development 7: 852-854.

Dittrich, P. and Banzhaf, W. (1998). Self-evolution in a constructive binary string system. Artificial Life 4: 203-220.

Fishov, I. (1994). Do oscillations control the bacterial cell cycle? In What is controlling Life? (Gnaiger, E., Gellerich, F.N. and Wyss, M., eds.), pp. 221-225. Innsbruck, Austria. Innsbruck University Press,

Fishov, I. and Woldringh, C. (1999). Visualization of membrane domains in *Escherichia coli*. Molecular Microbiology 32: 1166-1172.

Fralick, J.A. and Lark, K.G. (1973). Evidence for the involvement of unsaturated fatty acids in the initiation of chromosome replication in *Escherichia coli*. Journal of Molecular Biology 80: 459-475.

Gypi, S.P., Rist, B., Gerber, S.A., *et al*. (1999). Quantitative analysis of complex protein mixtures using isotope-coded affinity tags. Nature Biotechnology 17: 994-999.

Kamashev, D. and Rouviere-Yaniv, J. (2000). The histone-like protein HU binds specifically to DNA recombination and repair intermediates. EMBO Journal 19: 6527-6535.

Kauffman, S. (1996). At home in the Universe, the search for the laws of complexity., Penguin, London.

Kepes, F. and Kepes, A. (1985). Postponement of cell division by nutritional shift-up in *Escherichia coli*. Journal of General Microbiology 131: 677-685.

Ksenzenko, S.M. and Brusilow, W.S.A. (1993). Protein-lipid interactions of the proteolipid c subunit of the *Escherichia coli* proton-translocating adenosinetriphosphatase. Archives of Biochemistry and Biophysics 305: 78-83.

Le Sceller, L., Ripoll, C., Demarty, M., *et al*. (2000). Modelling bacterial hyperstructures with cellular automata. Interjournal Paper 366: http://www.interjournal.org.
Letoffe, S., Delepelaire, P. Wandersman, C. (1996). Protein secretion in gram-negative bacteria: assembly of the three components of ABC protein mediated exporters is ordered and promoted by substrate binding. EMBO Journal 15: 5804-5811.
Lewis, P.J., Thaker, S.D. Errington, J. (2000). Compartmentalization of transcription and translation in *Bacillus subtilis*. EMBO Journal 19: 710-718.
Lloyd, P.G. and Hardin, C.D. (1999). Role of microtubules in the regulation of metabolism in isolated cerebral microvessels. American Journal of Physiology 277: C1250-1262.
Mileykovskaya, E. and Dowhan, W. (2000). Visualization of phospholipid domains in *Escherichia coli* by using the cardiolipin-specific fluorescent dye 10-N-nonyl acridine orange. Journal of Bacteriology 182: 1172-1175.
Miller, C.G. (1996). Protein degradation and proteolytic modification. In Escherichia coli and Salmonella. (Neidhardt, F.C., ed.), Vol. I, pp. 938-954. Washington D.C. American Society for Microbiology,
Mitchell, C.G. (1996). Identification of a multienzyme complex of the tricarboxylic acid cycle enzymes containing citrate synthase isoenzymes from *Pseudomonas aeruginosa*. Biochemical Journal 313: 769-774.
Mowbray, J. and Moses, V. (1976). The tentative identification in *Escherichia coli* of a multi-enzyme complex with glycolytic activity. European Journal of Biochemistry 66: 25-36.
Norris, V. (1995). Hypothesis: transcriptional sensing and membrane domain formation initiate chromosome replication in *Escherichia coli*. Molecular Microbiology 15: 985-987.
Norris, V. (1998). Modelling *E. coli*: the concept of competitive coherence. Comptes Rendus de l'Academie des Sciences 321: 777-787.
Norris, V., Demarty, M., Raine, D., *et al*. (2001). Hypothesis: hyperstructures regulate initiation in *Escherichia coli* and other bacteria. Biochimie : in press.
Norris, V. and Fishov, I. (2001). Hypothesis: membrane domains and hyperstructures control bacterial division. Biochimie 83: 91-98.
Norris, V., Fralick, J. Danchin, A. (2000). A SeqA hyperstructure and its interactions direct the replication and sequestration of DNA. Molecular Microbiology 37: 696-702.
Norris, V., Gascuel, P., Guespin-Michel, J., *et al*. (1999). Metabolite-induced metabolons: the activation of transporter-enzyme complexes by substrate binding. Molecular Microbiology 31: 1592-1595.
Norris, V. and Le Sceller, L. (2001). A cellular automaton approach to modelling a bacterium. International Conference of Systemics, Cybernetics and Informatics : in press.
Norris, V. and Madsen, M.S. (1995). Autocatalytic gene expression occurs *via* transertion and membrane domain formation and underlies differentiation in bacteria: a model. Journal of Molecular Biology 253: 739-748.
Ohsumi, K., Yamazoe, M. Hiraga, S. (2001). Different localization of SeqA-bound nascent DNA clusters and MukF-MukE-MukB complex in *Escherichia coli* cells. Molecular Microbiology 40: 835-845.
Onogi, T., Niki, H., Yamazoe, M., *et al*. (1999). The assembly and migration of SeqA-Gfp fusion in living cells of *Escherichia coli*. Molecular Microbiology 31: 1775-1782.
Ouzounis, C., Casari, G., Valencia, A., *et al*. (1996). Novelties from the complete genome of *Mycoplasma genitalium*. Molecular Microbiology 20: 898-900.
Pedersen, A.G., Jensen, L.J., Brunak, S., *et al*. (2000). A DNA structural atlas for *Escherichia coli*. Journal of Molecular Biology 299: 907-930.
Petty, H.R. and Kindzelskii, A.L. (2001). Dissipative metabolic patterns respond during neutrophil transmembrane signaling. Proceedings of the National Academy of Science U.S.A. 98: 3145-3149.

Ramsden, J.J. (1993). Review of new experimental methods for investigating random sequential adsorption. J. Statist. Phys. 73: 853-877.
Raskin, D.M. and de Boer, P.A. (1999). Rapid pole-to-pole oscillation of a protein required for directing division to the middle of *Escherichia coli*. Proceedings of the National Academy of Science U.S.A. 96: 4971-4976.
Revet, B., von Wilcken-Bergmann, B., Bessert, H., *et al*. (1999). Four dimers of λ repressor bound to two suitably spaced pairs of λ operators form octamers and DNA loops over large distances. Current Biology 9: 151-154.
Ricard, J., Gontero, B., Avilan, L., *et al*. (1998). Enzymes and the supramolecular organization of the living cell. Information transfer within supramolecular edifices and imprinting effects. Cellular and Molecular Life Sciences 54: 1231-1248.
Robinson, G.W., Cho, C.H. Urquidi, J. (1999). Isobiestic points in liquid water: Further strong evidence for the two-state mixture model. Journal of Chemical Physics 111: 698-702.
Segre, D., Ben-Eli, D. Lancet, D. (2000). Compositional genomes: prebiotic information transfer in mutually catalytic noncovalent assemblies. Proceedings of the National Academy of Science U.S.A. 97: 4112-4117.
Speck, C., Weigel, C. Messer, W. (1999). ATP- and ADP-DnaA protein, a molecular switch in gene regulation. EMBO Journal 18: 6169-6176.
Stock, J. and Levit, M. (2000). Signal transduction: hair brains in bacterial chemotaxis. Current Biology 10.: R11-4.
Torshin, I. (1999). Activating oligomerization as intermediate level of signal transduction: analysis of protein-protein contacts and active sites in several glycolytic enzymes. Front. Biosci. 4: D557-570.
Ussery, D., Larsen, T.S., Wilkes, K.T., *et al*. (2001). Genome organisation and chromatin structure in *Escherichia coli*. Biochimie 83: 201-212.
Velot, C., Mixon, M.B., Teige, M., *et al*. (1997). Model of a quinary structure between Krebs TCA cycle enzymes: a model for the metabolon. Biochemistry 36: 14271-14276.
Vichniac, G.Y. (1984). Simulating physics with cellular automata. Physica D 10: 96-116.
Weigel, C., Schmidt, A., Seitz, H., *et al*. (1999). The N-terminus promotes oligomerization of the *Escherichia coli* initiator protein DnaA. Molecular Microbiology 34: 53-66.
Wiggins, P.M. (1990). Role of water in some biological processes. Microbiological Reviews 54: 432-449.
Woldringh, C.L. and Nanninga, N. (1985). Structure of the nucleoid and cytoplasm in the intact cell. In Molecular Cytology of *Escherichia coli*. (Nanninga, N., ed.), pp. 161-197. London. Academic Press.

Figure 1 (see **plate 6** at the end of the book)

Formation of a non-equilibrium hyperstructure due to changes in the affinity of its constituent enzymes for one another. Enzymes E1 can only diffuse in the plane of the membrane whilst the other enzymes, E2 to E7 diffuse in the cytoplasm. The binding of a substrate, such as a sugar, to the E1 enzymes leads to an increase their affinity for one another and their assembly into an E1 domain. On binding its substrate, each enzyme in the pathway acquires an increased affinity for the following enzyme. This results in the assembly of metabolons E1 to E7 and the assembly of the hyperstructure (here, a group of metabolons). Note that transcription of the genes encoding E1 to E7 and the simultaneous translation of the mRNA may help the assembly of the hyperstructure.

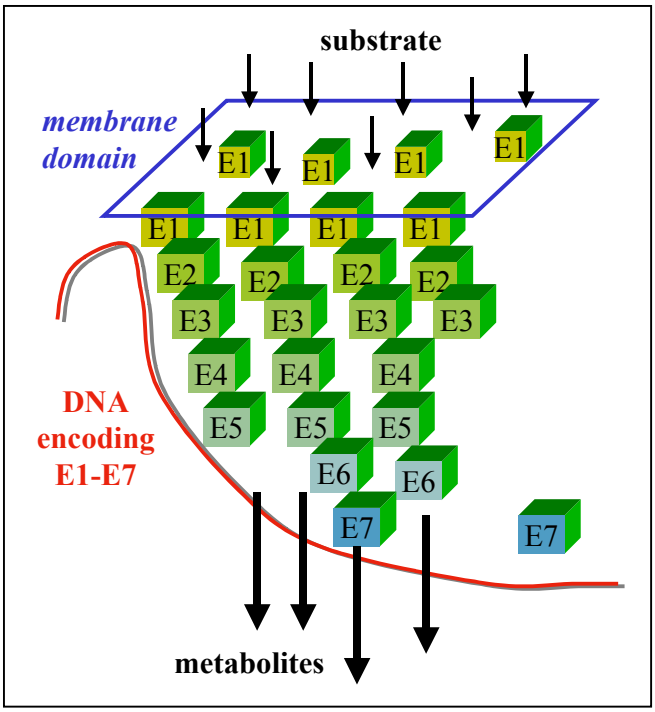

Figure 2 (see **plate 5** at the end of the book)

Horizontal links aid the assembly of a hyperstructure. Oligomeric protein E3 may bind together two identical metabolons (E1-E5 to E1-E5) or two different ones (E1-E5 to F1-F5). In the former case, E3 plays a role in the assembly of an individual hyperstructure whilst in the latter case E3 plays a role in the interaction between two different hyperstructures.

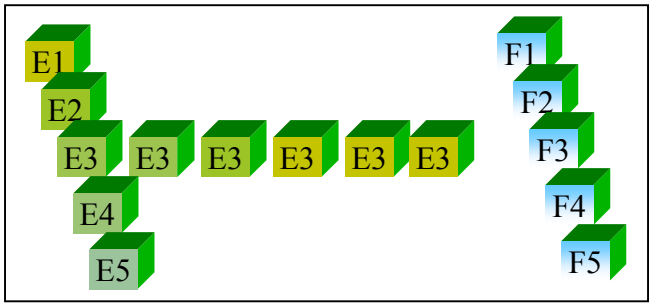

Figure 3 (see **plate 7** at the end of the book)

Local concentrations of oligomeric proteins can promote hyperstructure assembly. Protein E6 binds to its site (green) present in DNA or RNA to produce a region of the cytoplasm enriched in both E6 and its sites.

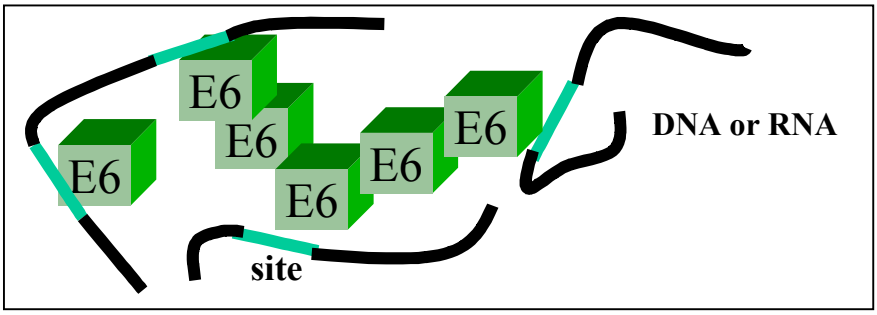

Figure 4 (see **plate 8** at the end of the book)

Transertion can nucleate hyperstructure assembly. Transertion, alias the coupled transcription, translation and insertion into and through membranes of proteins, may enrich a region of the membrane in the lipids (green) for which the proteins have an affinity. At a critical density of inserted nascent proteins, small proteolipid domains fuse into large ones and so nucleate hyperstructure assembly.

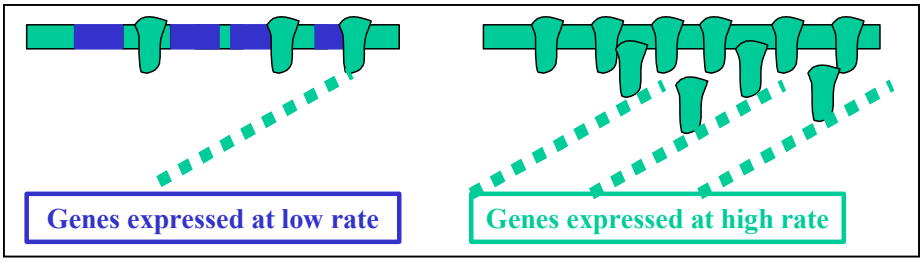

Figure 5 (see **plate 10** at the end of the book)

Cell cycle progress as a state cycle of hyperstructures. Rectangles represent non-equilibrium hyperstructures each performing one function. Blue rectangles correspond to hyperstructures with a common set of lipid (or other) preferences whilst red rectangles correspond to hyperstructures with a different set of preferences.

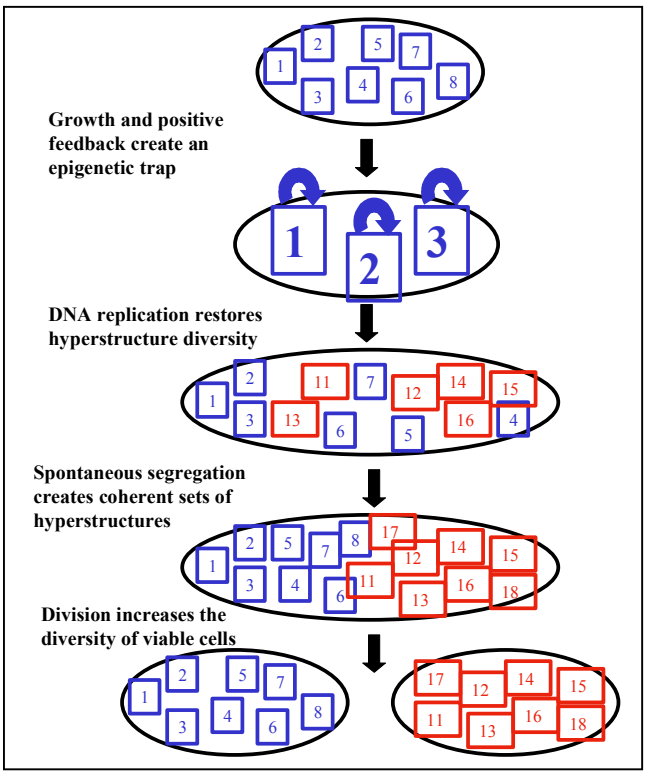

Figure 6 (see **plate 9** at the end of the book)

The spatiotemporal control of cell division by hyperstructures. The hyperstructures (the green or blue polygons) form one of two sets depending on the common preference within a set for lipids, ions, proteins etc. Each set is associated with a chromosome and is present in the future daughter cell. The division site is in the cytoplasmic membrane (thin rectangles) at the interface between these sets indicated by the arrow. Two possibilities for the structure of the division site (red arrows) which may be between the principal domains (blue and green) at either the interface or a separate, specific domain (red).

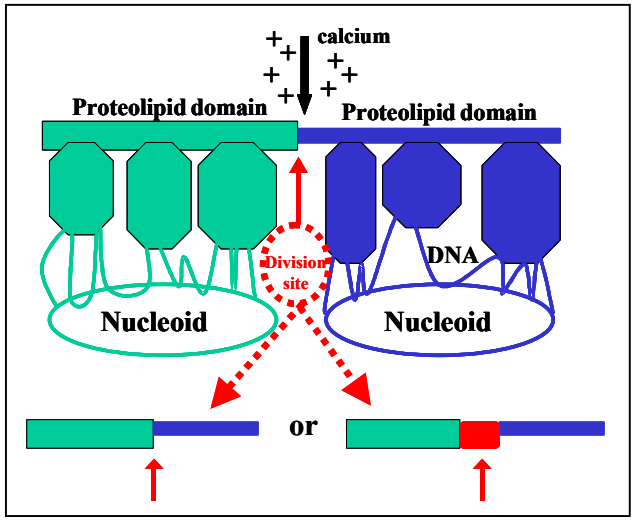

Figure 7

A two process example of parallel processing. Since each process does not need to access the space of the other one (except the boundary of the current space), each part can be stored locally in a multi-computer networked environment. The boundary of each part is the only information to be shared (i.e. transmitted between the computers).

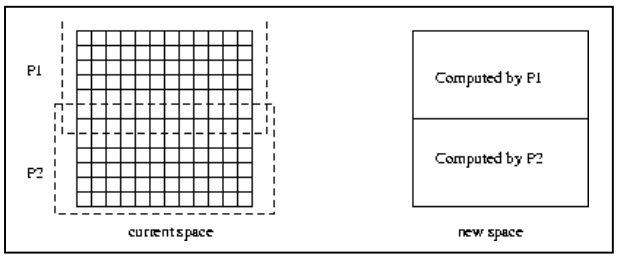

Figure 8

Movement on a 2-D grid. A molecule at time *t* can choose between 9 positions at time *t+1*. a molecule at time *t* can choose between 9 positions at time *t+1*.

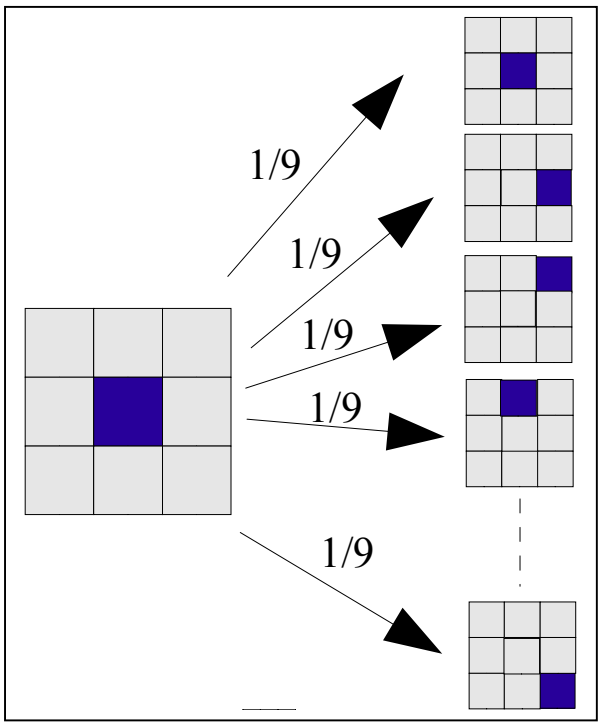

Figure 9

Diffusion in a cellular automata system. Empty units are black and filled units are yellow. States at successive times (t=0, 10 and 100) are shown.

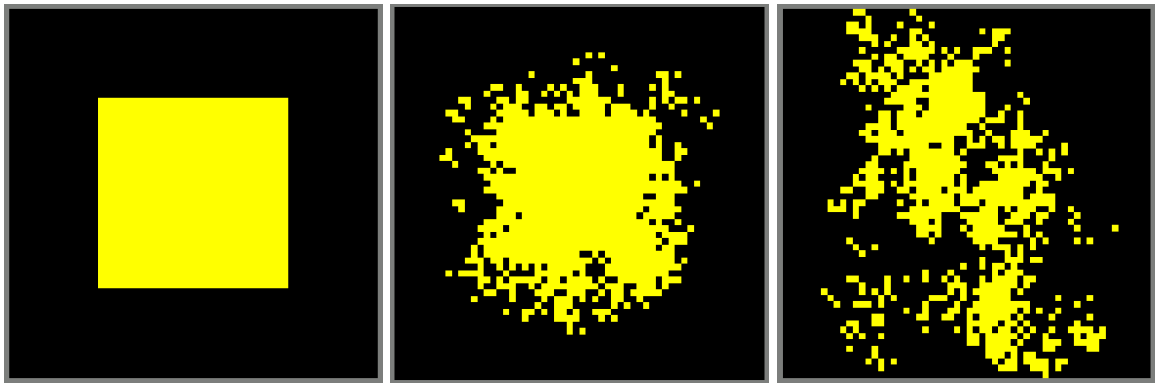

t=0 t=10 t=100

Figure 10 (see **plate 11** at the end of the book)

Diffusion of 2 types of molecule in a cellular automata system. States at successive times (t=0, 10 and 100) are shown

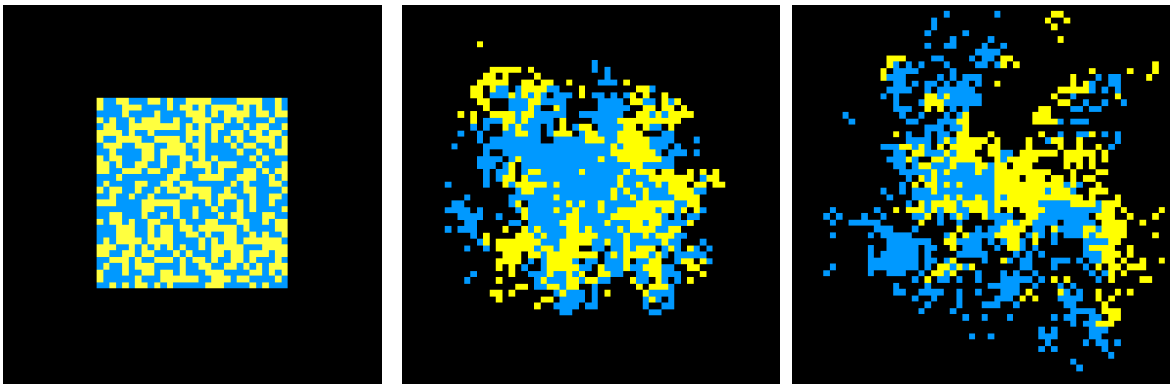

t=0 t=10 t=100

Figure 11 (see **plate 12** at the end of the book)

Diffusion of 2 substrates and a product in a cellular automata system. Molecules of type 1 and molecules of type 2 interact to produce type 3. At time t=0, there are only 2 types of molecules, type 1 (yellow) and type 2 (light blue). At time t=3, type 3 (dark blue) appears

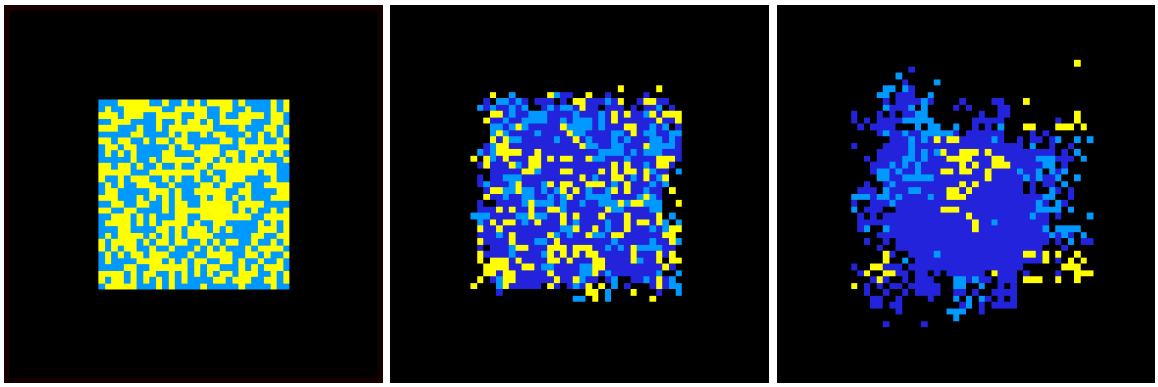

t=0 t=3 t=10

Figure 12 (see **plate 13** at the end of the book)

Formation of a hyperstructure compound with 3 types of molecules. At time t=5 and t=20, 2 simple molecular structures develop. Molecules of type 1 are at the top and molecules of type 2 are at the bottom of the cellular automata. At time t=50, the two structures meet and produce molecules of type 3. Then, at time t=100, a hyperstructure with 3 types of molecules appears.

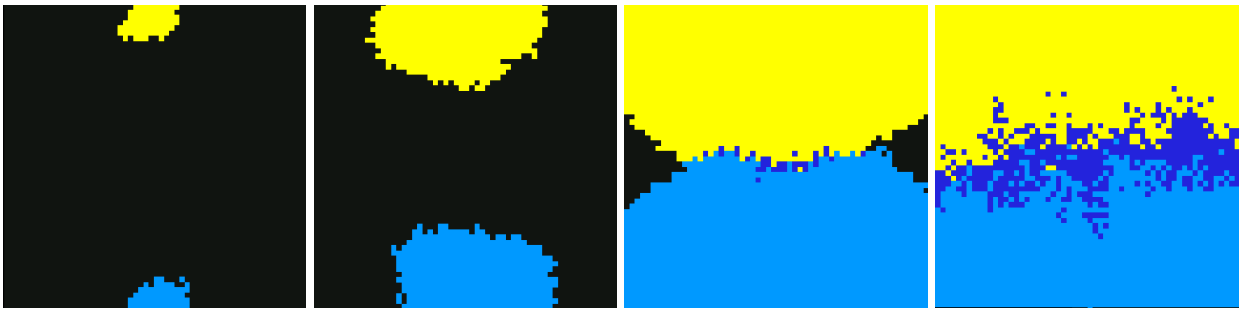

t=5 t=20 t=50 t=100

Epigenesis, multistationarity and positive feedback circuits.

Janine Guespin-Michel

Laboratoire de microbiologie du froid et groupe interdisciplinaire de Biologie Intégrative et Modélisation. Université de Rouen. F-76821 Mt St Aignan cedex ;
tel/fax (33) (0)2 35 14 66 8 4
e-mail janine.guespin@univ-roeun.fr

Résumé

L'existence de modifications épigénétiques commence à être admise en biologie, mais il n'existe pas de consensus quant à leur nature. Nous présentons ici quelques évidences concernant l'utilité d'un point de vue dynamique et de la notion de multistaionnarité, à travers un exemple pris en microbiologie. Cela permet de souligner l'importance des circuits de rétroaction positifs, et de présenter l'utilité de la méthode d'analyse logique généralisée pour les modéliser.

Mots clef **:** épigenèse, multistationnarité, circuits de retroaction, analmyse logique généralisée**.**

Abstract

Biologists now accept the existence of epigenetic modifications, but are divided as to their possible nature. Here we discus the interest of using dynamical concepts such as multistationarity, through an example in microbiology. This gives an insight into the importance of positive feedback circuits. Generalized logical analysis as a handy tool to model these circuits is presented.

Keywords : epigenesis, multistationnarity, feedback circuits, generalised logical analysis

The word epigenesis was first coined by Harvey as long ago as 1651, to describe the gradual formation of the different parts of an embryo. But a new meaning emerged when modern genetics developed the notions of genotype and phenotype. Epigenetic modifications arise and can be transmitted from a cell to its progeny in the absence of any genetic or environmental modification. They may be triggered by an environmental signal but do not disappear with this signal. This means that several stable phenotypes may arise from the same genome in the same conditions, which is equivalent in biologist's terminology to the physicist's statement that there exists multiple steady states [1]

Numerous cases of epigenetic modifications are known and epigenesis meetings are held to increase their number and try and understand their nature. However, most « epigeneticits » are interested in chemical mechanisms among which DNA methylation was most thoroughly studied. We shall see here that the use of the concepts issued from the study of non linear dynamical systems, such as multistationarity, and positive feedback circuits, may also help understanding at least some aspects of epigenesis and open quite

new prospects. Although not yet very popular, these ideas are not new however, since as early as 1949, Delbrück [2] already proposed to ascribe differentiation to a multistationarity process. And the first well established epigenetic modification that can best illustrate the interest of using the concept of multistationarity, involves the catabolism of lactose by *Escherichia coli* [3] .

Epigenesis and the lactose operon: importance of a positive feedback circuit.

The experiment was reported by Novick and Wiener in the famous journal "Proceedings of the National Academy of Sciences US" [4]. Lactose utilisation by the bacterium *E. Coli* had been studied for some time in the Pasteur Institute. It was known that lactose catabolism required both an enzyme (the β-galactosidase) that degrades lactose and a permease that facilitates its penetration into the cells. Both proteins were not synthesised by the bacteria unless lactose, designated hence as the "inducer" of this synthesis, was present in the culture medium. Novick and Wiener evidenced an epigenetic modification when the bacteria were grown in the presence of a low concentration of lactose, which was not sufficient to induce the synthesis of the two proteins. However if the cells had been previously induced (by a high concentration of lactose in the medium, but for as short as 10 minutes), they could synthesise the proteins in the presence of the low lactose concentration for (at least) 150 generations. Thus the phenotype of the same bacteria with regard to the production of β-galactosidase, was different in this culture medium (with a low concentration of lactose) depending on whether they had or not experienced during 10 min, 150 generations ago, a high concentration of lactose. This is a wonderfully simple but quite typical epigenetic modification. And the consequences are not trivial. It means that the phenotype of this extremely well known bacterium, whose genome has been fully sequenced, is still not predictible, when the bacteria are in a medium containing a low lactose concentration if the history of the culture is not known!

Now, as everybody knows, the mechanism of the induction by lactose of the synthesis of the proteins required for its metabolism was unravelled by Jacob and Monod [5], who were awarded the Nobel prize for their now famous "operon model". Fig 1 depicts the mechanism as it is established now. In the absence of lactose a negative regulator, protein LacI, which is always produced due to the constitutive expression of gene *lacI* , is active and prevents the expression (transcription followed by translation) of three genes including gene *lacZ* encoding the β-galactosidase, and *lacY*, encoding the lactose permease. In the presence of lactose, a derivative of this sugar (allolactose) has a high affinity for protein LacI and provokes an allosteric modification of this protein that looses its affinity for the promoter of the operon, which can thus be transcribed. When there is no more lactose, protein LacI resumes its active conformation, and the synthesis of the enzymes is rapidly interrupted. But how does lactose enter inside the cells? When the external concentration is high, it can diffuse through the cell wall, but this process is not sufficient at low lactose concentration. This explains why, in general, bacteria cannot be induced by low lactose concentrations.

Let us now go back to the Novick and Wiener experiment. At low lactose concentration, the cells cannot be induced, but pre-induced cells have produced a permease that allows lactose transport into the cells even at low concentration! So all that is to the epigenetic behaviour is that the permease allows the entrance of lactose that allows the

synthesis of the permease etc…From this simple fact, arise all the properties of epigenesis: the phenotype (with regard to β-galactosidase synthesis) depends on the history of the culture, a short pulse of a high concentration of lactose (or a transitory removal of lactose) suffices to change one of the phenotype into the other, and there is hysteresis, since the concentration required to induce the culture is much higher than the concentration below which the cultures is "de-induced" (fig 2).

All these properties are those of a bistable system, a non linear dynamical system with two steady states. And all these properties result from the fact that the lactose permease promotes its own synthesis under low lactose concentration, that is, **lactose permease is part of a positive feedback circuit.**

Now, if you will agree that epigenetic modifications are plenty in the living world, the main question to ask is how useful to the understanding of epigenesis are these two concepts, multistationarity and positive feedback circuits, that we have borrowed from the physicists and the engineers. But for this we shall borrow one more tool, from the mathematicians now, logical analysis.

One additional tool: logical analysis.

Another epigenetic modification was discovered shortly after the first one, and its study as a dynamical non linear system was to yield a major advance. It still involves the bacterium *E.coli*, and a virus (phage λ) endowed with a very special behaviour. When phage λ meets a population of bacteria of the species *E.coli* some of the cells are infected as with every ordinary (virulent) phage and eventually lyse, but some cells do not lyse, and become immune to a further infection by phage λ. It was shown that the phage's DNA has inserted into the bacterium genome, at a specific location. The cell has become lysogenic, and the phage's DNA is termed "prophage". A negative regulator (C_I) produced from the phage's genome is responsible for the inability of this DNA to express its lytic functions, and is positively self regulated [6], forming a positive feedback circuit . Thus, the same phage's DNA, entering the same bacteria can bestow two completely different states. Genetic studies have unravelled the genes responsible for this phenomenon (fig 3a), but not the reason of the "choice".

René Thomas was a well known geneticists working in the field of phage λ, when he became aware that logical analysis (or Boolean algebra), was likely to help solve this question. First of all, geneticists consider that genes are On or Off, and that the corresponding proteins are present or absent. This is a binary approach just as Boolean algebra is. And the reason is that the regulatory interactions between genes and proteins are steep sigmoïds in most instances. Therefore, it is possible to express the (non linear) dynamics of a regulatory system in term of Boolean equations, in which X,YZ are functions that roughly corresponds to the order given to the corresponding genes by the regulatory proteins, x, y, z..

$X_{(t+1)} = f(x_t, y_t, z_t)$, etc…

Where variables and functions have only the values 0 or 1. Fig 3b shows the Boolean functions corresponding to the (simplified) regulatory scheme of the early steps of phage λ infection. Solving these equations shows that the system has indeed two steady

states, corresponding to the regulator C_I being present or absent (respectively the prophage and the virulent phage states). It shows that a model that simulates the phage's infection as a non linear dynamical system can predict the two steady states, but does not give any new insight into the system.

The main advance was performed when Thomas took into account the fact that in the living system, when a protein regulates two genes there is no reason why it should do it at the same speed. In the synchronous Boolean approach, if a state 00 is followed by a state 11, this state is obtained in a single step. In the asynchronous analysis proposed by Thomas [7,8,9,10], state 00 is followed either by 01 or by 10, and the probability of having one or the other answer is a function of the speed with which each state is reached. If, in a population, both speeds are roughly equal, then both states will occur and the population will be heterogeneous; why one individual will reach one state rather than the other will depend on the actual speed of the reactions in this individual. Fig 3c shows the results of this asynchronous analysis in the description of the phage's infection. Now it is possible, not only to simulate the existence of two steady states, but to propose explanations amenable to experiences [11]

Thus, on the one hand a positive feedback circuit, in a non linear dynamical system, is (again) responsible for the existence of an epigenetic phenomenon; on the other hand, the utilisation of a mathematical model able to simulate this non linear dynamical model allowed the authors to propose an explanation of the choice, and new experiments to ascertain it.

Logical analysis is by no mean the only way to model non linear dynamic systems. Differential equations are most often used, and give the same qualitative results and better quantitative estimations. Asynchronised logical analysis, or the more recent generalised analysis [12,13] is most useful however when quantitative data are lacking, as it most often the case with genetical data which are mainly qualitative (see also [14,15]).

Epigenesis, feedback circuits and models.

In these two quite different examples of epigenetic behaviour, a positive feedback circuit turned out to be the "motor" of the multistationarity. From this, and many other more theoretical studies, Thomas conjectured that a positive feedback circuit could be a necessary (although not sufficient) condition for multistationarity in a non linear dynamic system [1]. This was later on partially demonstrated mathematically [16,17, 18, 19]. In addition the number of steady states does not depend on the number of elements in a circuit, but on the number of circuits in the system (n circuits give 2^n steady states).

The consequence of this statement are very important for biologists, since it means that an apparently quite complicated system may be explained by a very limited number of causes, and that feedback circuits may be of paramount importance for this [3,20]. The discovery of these feedback circuits requires analytical studies such as are routinely performed in modern biology. But once evidenced, it may be worth studying the dynamics of the system (either by generalised logical analysis, or by differential equations if possible), mainly if an epigenetic behaviour can be suspected. Thus numerous feedback circuits are already known in the regulatory nets of all living systems. But very few biologists have questioned their role or even wonder whether they really work. This comes

from the fact that this dynamic approach has long been ignored, or even denied by biologists.

Some other epigenetic modifications

But feedback circuits or epigenetic modifications are not restricted to genetic networks. Cell differentiation that occur during development of an egg to an organism can be viewed as an epigenetic modifications of the two daughter cells [21], and studies are in progress to find positive feedback circuits responsible for these modifications. Thus, Kaufman and Thomas [22] analysed the role of circuits in the evolution of lymphocytes populations, and Sanchez *et al*, [23,24] performed an analysis of such circuits during early development of the *Drosophila* embryo.

Other properties have been briefly outlined with the Novick and Wiener experiment. In this system, the bacteria "remember", after 150 generations, that they have experienced a 10min exposure to a high concentration of lactose. This has been summarised by an hysteresis curve (fig 2). An other consequence of this hysteresis, is that a very short pulse of lactose can shift the non induced population of cells growing in low lactose concentration, into an induced population, and conversely, a rather short removal of lactose may shift the induced population to the non induced state. Thus some aspects at least of memory may also be due to positive feedback circuits in the information retention by plants, as well as in memory itself [25,26] .

Finally, with phage lambda we have exemplified yet another important behaviour in biology, the heterogeneity of a population of genetically identical cells or organisms, may be of epigenetic origin and stems from a positive feedback circuit.

Thus, an important new field in functional genomics may arise. Whenever epigenesis is suspected in a biological system, it may be worth looking for the feedback circuits in which some at least of the elements of the system are involved, at all possible levels of regulation. Then models should be run to know which circuit may be responsible of the epigenetic behaviour, using either generalised logical analysis, or differential equations, if data are sufficient. Last but not least, experiments must decide [27, 28], and a good model must lend itself to experimental validation (Cf Bernot et al, this book).

Acknowledgements

I thank Dr M. Kaufman, and P. Amar for reading and discussing this manuscript.

References

1) Thomas R., On the relation between the logical structure of systems and their ability to generate multiple steady states or sustained oscillations, Springer Series in Synergies 9 (1988) 180-193.

2) Delbrück M., Unités biologiques douées de continuité génétique, Colloques internationaux du CNRS (1949).

3) Thomas R., Laws for the dynamics of regulatory networks, International Jour.

Dev. Biol. 42(1998) 479-485.

4) Novick A., Wiener, M., Enzyme induction is an all-or-none phenomenon. Proc. Natl. Acad. Sci. USA 43(1957) 553-556.

5) Jacob F. Monod, J., Genetic regulatory mechanisms in the Synthesis of Proteins J. Mol.Biol. 3 (1961) 318-356.

6) Eisen H., Brachet P., Pereiria da Silva L., Jacob F., Regulation of repressor expression in lambda, Proc.Natl.Acad.Sci.USA 66 (1967) 855-862.

7) Thomas R, Boolean formalisation of genetic control circuits, Jour. theor. Biol.42(1973) 563-585.

8) Thomas R.(ed), Kinetic logic: a Boolean approach to the analysis of complex regulatory systems, Lecture notes in Biomathematics 29, (1979) 507p

9) Thomas R., Regulatory networks seen as asynchronous automata: a logical description, Jour. theor. Biol. 153(1991) 1-23.

10) Thomas R., Bacteriohage λ : Transactivation, positive control and other odd findings, BioEssays 15 (1993) 285-289.

11) Thomas R., Van Ham P., Analyse formelle de circuits de régulation génétique: le contrôle de l'immunité chez les bactériohages lambdoïdes, Biochimie 56 (1974) 1529.

12) Snoussi E.H., Thomas R., Logical identification of all steady states: the concept of feedback loop characteristics states, Bul. Math. Biol. 57 (1993) 277-297.

13) Thomas R., Thieffry D., Kaufman M., Dynamical behaviour of biological regulatory networks.-1. Biological role of feedback loops and practical use of the concept the of the loop-characteristic state. Bul. Math. Biol. 57 (1995) 247-276.

14) Thomas R., Kaufman M., Multistationarity, the basis of cell differentiation and memory. I. Structural conditions of multistationarity and other nontrivial behaviour. Chaos 11(2001) 170-179.

15) Thomas R., Kaufman M., Multistationarity, the basis of cell differentiation and memory. II. Logical analysis of regulatory networks in terms of feedback circuits. Chaos 11 (2001) 180-195.

16) Plahte E., Mestl T., Omholt S.W., Feedback loops, stability and multistationarity in dynamical systems, J Biol Syst 3 (1995) 409-413.

17) Snoussi E.H., Necessary conditions for multistationarity and stable periodicity, J. Biol. Sys 6 (1998) 3-9.

18) Gouze J.L., Positive and negative circuits in dynamical systems, J. Biol. Syst. 6 (1998) 11-15.

19) Cinquin O., Demongeot J., Positive and negative feedback : striking a balance between necessary antagonists. J. Theor. Biol.(In the press.)

20) Thomas R., Thieffry D., Les boucles de rétroaction rouages des réseaux de régulation biologiques. Médecine/Science 11 (1995) 189-197.

21) Demongeot J., Multistationarity and cell differentiation. J.Biol.sys. 6 (1998) 1-2.

22) Kaufman M., Thomas R., Model analysis of the bases of multistationarity in the humoral immune response, J. Theor. Biol. 129 (1987) 141-162.

23) Sanchez L., van Helden J., Thieffry D., Establishment of the dorso-ventral pattern during embryonic development of *Drosophila melanogaster* : a logical analysis, J. Theor. Biol. 189 (1997) 377-389.

24) Sanchez L., Thieffry D., A logical analysis of the Drosophila Gap-gene system, J.Theor. Biol. 211 (2001) 115-141.

25) Demongeot J., Thomas R., Thellier M., A mathematical model for storage and recall functions in plants, C. R.Acad. Sci, Paris série III 323 (2000) 93-98.

26) Demongeot J., Kaufman M., Thomas R., Positive feedback circuits and memory. C. R.Acad. Sci, Paris série III 323 (2000) 69-79.

27) Guespin-Michel J.F., Les boucles de rétroaction positives, une nouvelle approche intégrée de la physiologie microbienne. Bul. société franç.mirobiol. (2000) Septembre.

28) Guepsin-Michel J.F., Kaufman M., Positive feedback circuits and adaptive regulations in bacteria, Acta biotheor. 49 (2001) 207-218.

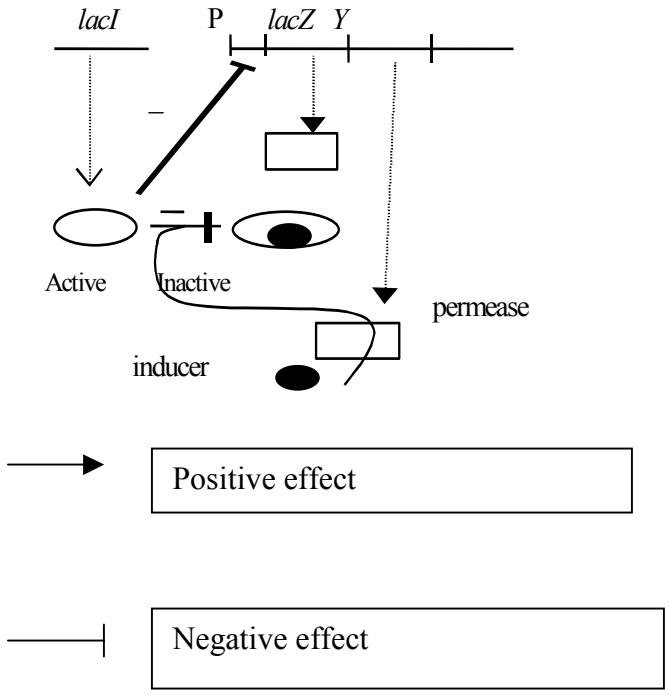

Figure 1 : the lactose operon : simplifies cartoon summarizing the regulation.

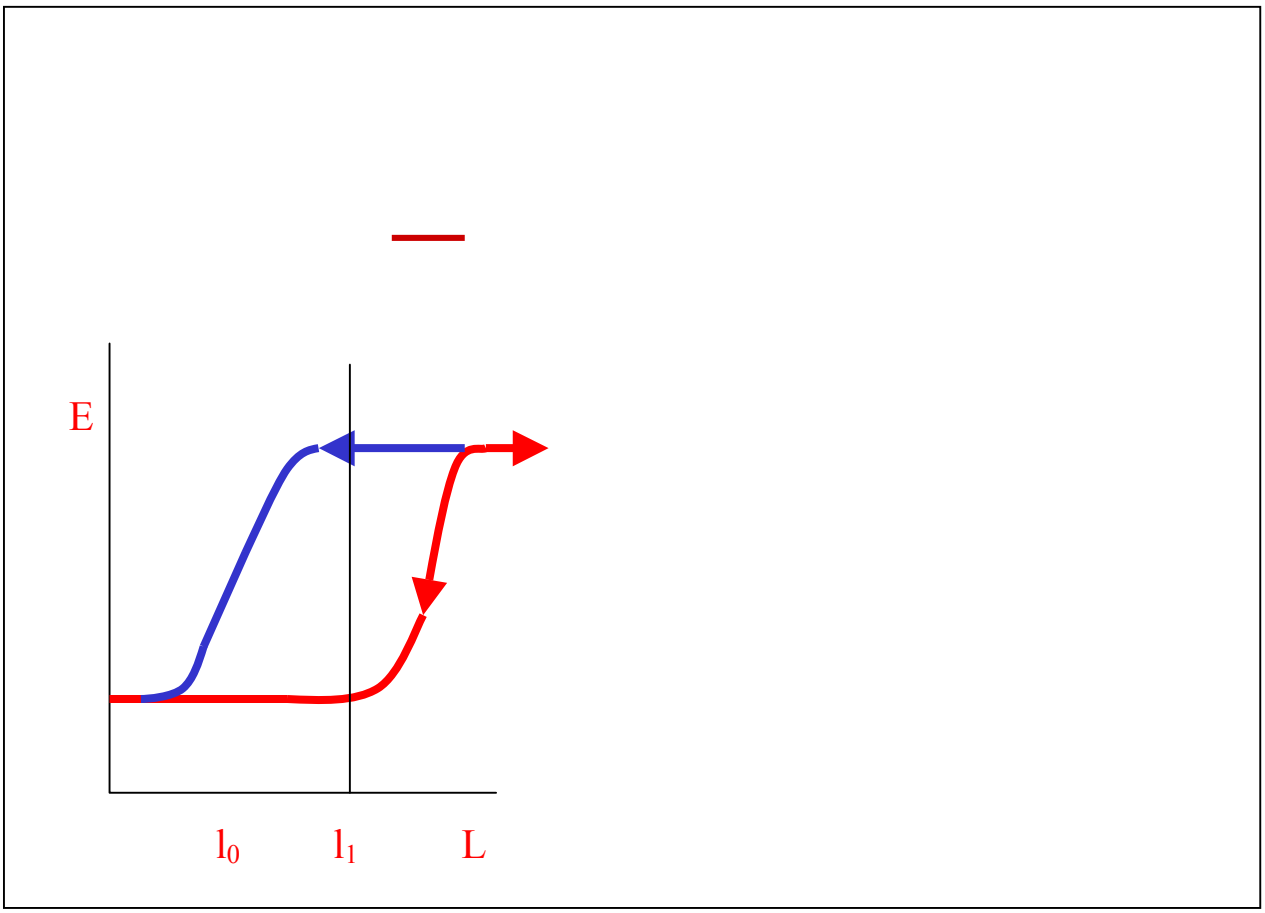

Figure 2 Hysteresis of the lactose induction curve

E specific activity of the enzyme (β-galactosidase)

λ inducer. l_0 , l_1 , L are respectively null, low and high concentrations of the inducer.

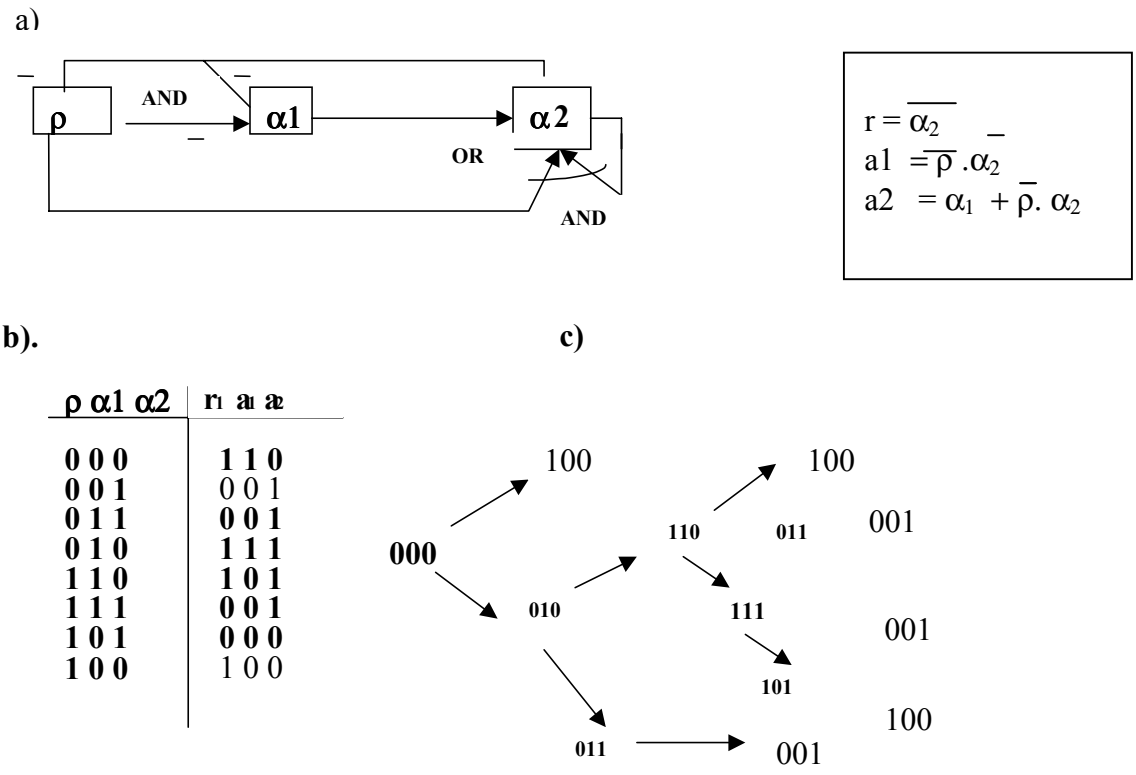

Figure 3 regulation of the early steps of phage lambda infection. (from Thomas 1979)

a) logical graph of phage lambda early regulation (simplified) and the corresponding logical equations

ρ, α1, α2 represent the products of regulatory genes cro, cII and cI respectively, and r, a1 and a2 are the functions associated, (roughly, the expression of the corresponding genes). An arrow indicates a positive regulation, whereas a negative regulation is noted as a -. AND , OR,, are the logical operations.

b) State table corresponding to the logical equation

c) Pathways in the asynchronous logical description.

Tensegrity and oscillations : exploring some constitutive and emergent features of virtual cell models

Philippe Tracqui[1], Emmanuel Promayon[1], Thomas Sauvaget[1], Vic Norris[2] and Jean-Louis Martiel[1]

[1]Laboratoire TIMC-IMAG, CNRS, Inst. A. Bonniot, 38706 La Tronche Cedex
[2]Laboratoire des Processus intégratifs cellulaires, Fac. Sciences et Techniques, Univ. Rouen, 76821 Mont-Saint-Aignan Cedex

1. Introduction

The key role of the coupling between mechanical forces and tissue growth and remodelling was suggested nearly twenty years ago (Trinkhaus, 1984), especially in the field of bone formation and remodelling. However, it is only recently that a large body of experiments highlighted the effects of physical forces such as tension, compression, gravity or shear stress at the cell level (Edwards et al., 1999; Huang and Ingber, 1999; Kaspar et al., 2000). Indeed, direct application of mechanical stresses to cultured cells can induce or modify cell differentiation, growth and migration as well as gene expression (Fujisawa et al., 1999; Wang et al., 2000; Meyer et al., 2000). However, we do not still fully understand how individual cells perceive mechanical signals and orchestrate them to produce a particular behaviour, both individually and collectively, through the control of cooperative phenomena at the cell population or tissue levels.

In some sense, the "cell challenge" is to sense all kind of signals but to generate a single, integrated response. Among these different cell signalling mechanisms, mechanotransduction, i.e. the conversion of a mechanical signal into a biological or biochemical response, has a kind of special status (Wang et al., 1993). Indeed, it already relies on the global structural characteristics of cells as opposed to biochemical events which can occur locally, for example near the cytoplasmic membrane or within an intracellular organelle. Mechanotransduction is why the development of theoretical cytomechanical model of the living cell is crucial : it provides the only way to understand how many simultaneous extracellular mechanical inputs (adhesion to extracellular matrix (ECM) proteins, junctions with other cells, …) combined with heterogeneous mechanical properties (local softening or hardening of the cytoskeleton) are integrated with other stimuli to provide a specific physiological or pathological cellular response (Lelièvre et al., 1996; Janmey, 1998).

We will briefly explore here some of these theoretical models, with special emphasis on the cell tensegrity paradigm proposed by D.E. Ingber (1993; 1997). Alternative cytomechanical models based on a simple elastic or viscoelastic continuum or stressed submembranous cortex will also be presented. Two issues will be presented. The first deals mainly with modelling the architectural properties of the cytoskeleton (CSK) as a physical basis for analysing both the mechanical properties of cells and the different way mechanical forces are transduced to yield an integrated cell response. The second is more concerned with cellular dynamics and related morphological changes since CSK remodelling is one of the intracellular factor controlling gene expression. Both presentations are based on the conviction that modelling how cells dynamically stabilise and self-organise their structure and shape is essential if we are to understand how cells sense their physical microenvironement and respond to mechanical signals through in/out bi-directional signalling pathways that connect the plasma membrane to the nucleus.

After reviewing the main aspects of both discrete and continuous mechanical models of cells, this paper ends with some propositions for testing a virtual, integrated cell model. These will be discussed in connection with the concepts, possibilities and limitations offered by research programs on computational cells such as Virtual Cell and Electronic cell.

2. Discrete mechanical cell models

2.1. Cells as tensegrity structures

Since the eighties, D. E. Ingber and coworkers have promoted and architectural view of the living cell and of larger biological entities based on the concept of tensional integrity or tensegrity, according to which the structure of cells depends on tensile forces for its integrity (Ingber, 1993 ; 1997). As explain by Ingber, this proposition draws on a close analogy with the architectural principles developed for the construction of buildings by R. B. Fuller and K. Snelson, as exemplified by geodesic domes and later discovered as underlying the organization of viral capsids.

It seems worth emphazing in this introductory paragraph that the holistic approach proposed by Ingber has deep conceptual implications. First, it again drew attention to the need for unifying principles necessary to interpret the plethora of biological data successfully collected by a reductionism that cannot explain them on its own. Second, it strengthened the view of biological systems as non-linear systems with functions that are more than the sum of its parts.

How is a tensegrity system defined? According to Ingber and Jamieson (1985) " *A tensegrity system is defined as an architectural construction that is comprised of an array of compression-resistant struts that do not physically touch one another but are interconnected by a continuous series of tension elements*". At the cell level, the tensegrity framework proposed by D. E. Ingber is based on several initial assumptions.

The first assumption is that cell shape is stabilized by an internal mechanically active structure, the cytoskeleton. This assumption excludes both theoretical models treating the cell as a viscous fluid surrounded by a membrane, as well as mechanical models treating the CSK as a passive structure. Indeed, it is well-documented that living cells (and even non-muscle cells like endothelial or fibroblasts) can generate active tension through an actomyosin filament sliding mechanism similar to the one used in the contraction of smooth muscles. This is easily visualised, either at the cell level by the wrinkling of malleable substrata by cells (Dembo et al., 1996 ; Dembo and Wang, 1999), or at the population level via measurements of isometric tension or compaction rate of viscoelastic biogels (Kolodney and Wysolmersky, 1992; Eastwood et al., 1996). This internal contraction capability creates within the cell a prestress upon which external mechanical loads are superimposed. Tensegrity cell models have thus been developed by considering elastic and contractile actin microfilaments as tension elements and microtubules as compression-resistant elements (Wang et al., 2001).

The second assumption is that forces are not transmitted continuously across the cell but rather that transfer of mechanical loads and stresses take place at points where the cell is anchored to the extracellular matrix (ECM) and to neighbouring cells. Indeed, the cell anchors itself to the ECM by physically binding CSK elements to specific focal adhesion complexes (FACs) that cluster within localized adhesion sites. Such complexes include not only transmembrane proteins, mostly integrins, but also a scaffold of actin-binding proteins (talin, vinculin, α-actinin, paxillin, …) which form a molecular bridge between the CSK and the intracellular part of the integrin. Similarly, specific cell-cell adhesions molecules (CAMs), like cadherins, selectins, cathenins, …) insure the transmembrane coupling of neighbouring cells CSK at localised junctional sites (adherens junctions, desmosomes).

Cellular architecture seen in this way defines a mechanical network that provides a physical support to biochemical signal transduction pathways and that allows mechanical signals to be propagated from mechanoreceptors on the surface (in the form of cell adhesion molecules and transmembrane receptors) to targets deep within the cell.

2.2 Qualitative behaviour of cell tensegrity models

Some basic, qualitative properties of cell tensegrity models have been illustrated by Ingber and co-workers by constructing a physical structure made of multiple wood dowels interconnected with a series of elastic springs (Ingber, 1997). This "cellular toy" has interesting properties: if it is not subjected to an external force and if not attached to a rigid surface, it has a round shape because of the internal tension. However, it can spread out and flatten along a rigid surface if an external force is applied vertically. Moreover, if the toy is attached to a flexible surface while in its flattened configuration, and if the external force is then removed, the toy contracts spontaneously and returns to the round shape characteristic of its rest state, again because of the presence of internal tension. This relaxation is accompanied by a progressive wrinkling of the flexible substratum which closely mimicks the formation of wrinkles observed when living cells are cultured on malleable substrates like silicon rubber.

Simulations of tensegrity via the construction of virtual cells may eventually prove indispensable to understanding how the cell interprets its genome. In this context, an additional and particularly interesting feature of models of cellular tensegrity is their ability to fit naturally into a structural hierarchy. One can then include within such virtual cells smaller intracellular structures with their own mechanical properties. Of course, the cell nucleus is the first candidate. The nucleus has its own internal structure, the nuclear matrix, and a body of experimental findings are consistent with the nucleus being mechanically coupled to the rest of the cell. For example, when a cell spreads on a rigid substratum, its nucleus extends in parallel, even if some delay can be observed in migrating cells. The tensegrity model explains how the nuclei of living cells can respond directly to mechanical stimuli that are applied to specific surface receptors as those involved in cell adhesion. It thus provides a basis to understand how extracellular mechanical stimuli can modify gene expression through mechanical deformations of the nucleus (Maniotis et al., 1997).

2.3. Theoretical properties of cell tensegrity models.

Different theoretical studies have been undertaken to analyse the mechanical properties of cell tensegrity models. A minimal tensegrity structure composed of 6 compressive elements (bars) and 24 extensible elements (cables) with frictionless joints has been analysed by Stamenovic et al. (1996). This study was extended by Wendling et al. (1999) who investigated wether such a pre-stressed geometric structure could account for the stiffening response observed in living cells. They showed that, under large deformations, the tensegrity structure exhibits a non-constant stiffening response which depends on the loading conditions (extension, compression or shear). They further demonstrated that, although the Young's elastic moduli of each constitutive element stays constant, the apparent elastic modulus of the overall structure, the apparent elastic modulus of the overall structure does not stay constant.

They analysed the deformation of the 30-element cell tensegrity model governed by the constitutive equation :

$$\{\mathbf{F}\} = [\mathbf{K}]\{\mathbf{u}\}$$

which relates the vector of external forces $\{\mathbf{F}\}$ to the vector $\{\mathbf{u}\}$ defined by the displacement (distance between the deformed and the reference state) of each of the 12 nodes through the rigidity matrix $[\mathbf{K}]$ of the structure (cables and bars are assumed to be linearly elastic with Young's modulus E_c and E_b respectively, with $E_b >> E_c$) . The external forces are applied at three upper nodes of the structure, while the contact of the structure with the inferior plane

occurs through three fixed nodes : this latter condition is chosen to simulate a weak cell adhesion of a round cell onto a rigid substratum.

At the unloaded (reference) state, mechanical equilibrium results from the balance between pre-stretching stress in the cables and in the bars. For the different loading conditions, the tensegrity model response is analysed by considering the apparent elasticity moduli derived from the stress-strain relation ship. With reference to continuous material, apparent elasticity modulus E_s and shear modulus G_s of the tensegrity structure have been defined as the derivative of the polynomial functions fitting the apparent normal and shear stresses to the apparent normal and shear strains respectively.

The numerical simulations of the tensegrity model response to extension and compression exhibit a non-linear mechanical response, characterised by linear relationship between the apparent elasticity modulus and the apparent strain. The modulus increases with strain during extension and is thus associated with a strain-hardening behaviour of the structure. On the contrary, a strain-softening occurs under compression, with decreasing values of the elasticity modulus as strain increases. This behaviour is qualitatively preserved when the length of the elastic elements or their pre-stress is changed by several orders of magnitude. Application of shear stresses lead to a more complex response, with initial stress-softening followed by stress-hardening.

This study illustrates how the response of the CSK of the living cell to applied stress might be a property of an integrated system and not a characteristic of individual components : even if each component of the tensegrity structure exhibits independently a linear elastic response with constant elastic moduli, the integrated response is non-linear with apparent elastic moduli that are strain-dependent. Such behaviour is related to the re-orientation of stresses which, even applied locally, are spatially distributed through the myriads of interconnected filaments composing the CSK. Evidence for such stiffening response of cells comes from several different, biological experiments. Moreover, these experiments provide additional information on the mechanical response of intracellular components such as the cell nucleus.

2.4. Simulation of virtual cell models : the example of physically based computational models

Despite the virtues of the tensegrity model, it should be noted that it cannot explains certain dynamic features of the CSK such as its remodelling. We briefly reported here a recently developed computational approach that provides an alternative way for simulating the mechanical response of virtual objects modelling living cells (Promayon et al., 2002) and that could be more extensible. This approach is inspired by the physically based computational framework proposed for simulating the respiration movements of the human trunk (Promayon et al., 1996 ; 1997). Based on algorithms operating within an object oriented programming language, this approach is able to take into consideration dynamic changes of objects properties and shapes. In this modelling framework, cells are considered as three-dimensional elastic bodies submitted to internal cohesive forces as in the tensegrity approach. In addition, external attractive forces (gravity, chemo-attraction, …) are also considered as possible control factors of the virtual cell dynamical features.

The virtual cell we have constructed within this framework is defined as a 3D incompressible object. From a computational point of view, this virtual cell is considered as an entity with its own properties (elasticity, contractility,…) and history (interactions with other cells or ECM, …). To simplify the calculations, a cell is defined by a 3D closed surface represented by a triangular mesh and its associated contour nodes.

Dynamical cell shape changes occur as a response to various forces (gravity, locally applied mechanical loads, …) applied to each node of the mesh. The dynamic of the local cell

response is then determined by the mass initially assigned to each node. Since mass-spring networks are known to be rather unstable systems, cell elasticity properties have been modelled by defining a local shape memory (Promayon et al., 1996). This means that the elastic property of a cell object is simply its ability to recover its original shape once deformed. This property is modelled by defining a local shape coordinate system in which each node of the structure is defined relatively to its neighbours by three parameters.

Some applications of this physically based computational approach are given below. First, as with tensegrity models, the mechanical response of specific cell architectures can be analysed. For example, one can simulate the effect of different intracellular organisation of the CSK which can mimic specific orientation of cell stress fibres. Figure 1 shows the simulated influence of transverse links within an elastic discrete envelope when the cell is submitted to uniaxial compression. The cell0 is defined as a strict elastic discrete envelop, with no internal links. In cell1, we considered a reinforcement of the cell architecture with horizontal elastic cross-links modelling CSK fibres. Finally, cell2's architecture includes internal diagonal elastic links connecting the apical and basal physical cell surfaces.

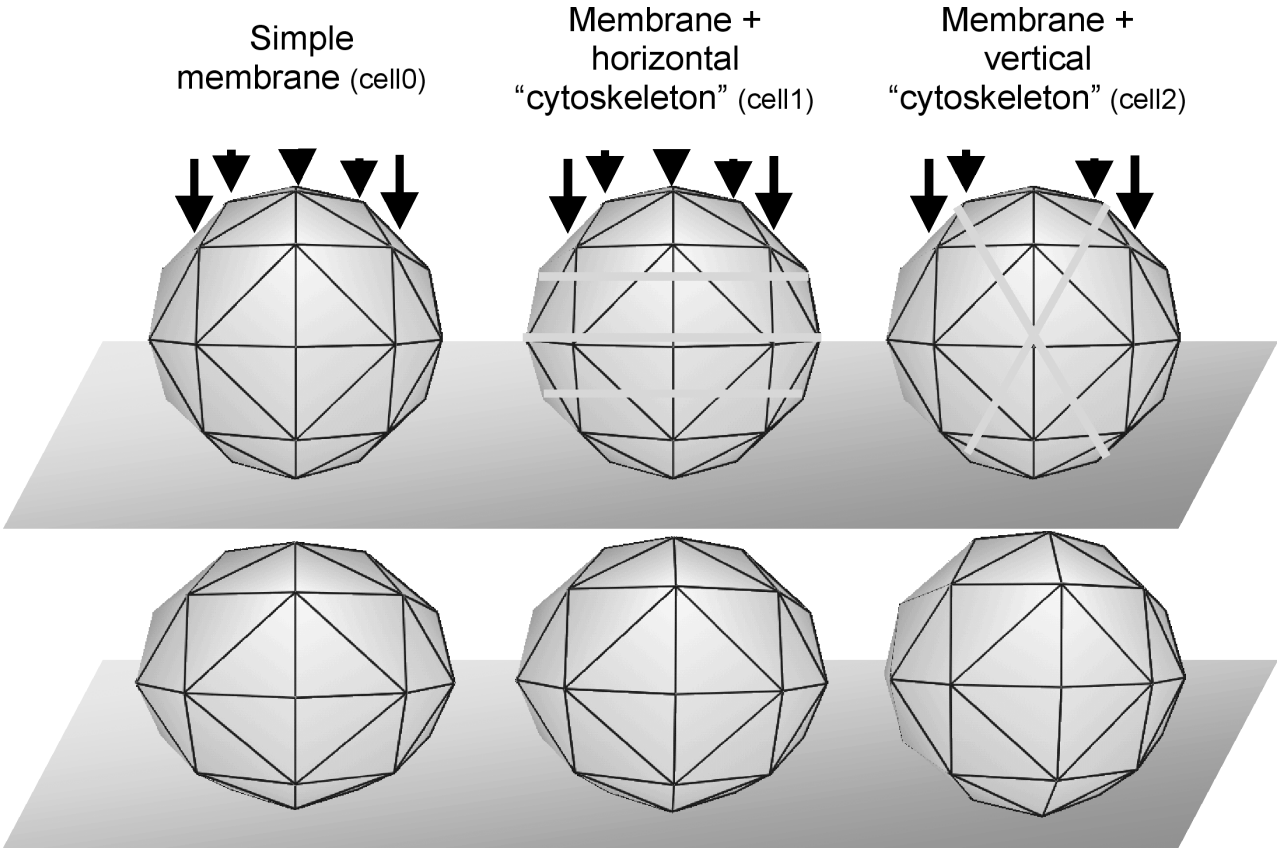

Figure 1 : Influence of the "cytoskeleton" of the virtual on the mechanical response to vertical load. Three cell types are considered: no "cytoskeleton" (cell0), horizontal links (cell1), diagonal links (cell2). The first raw presents the initial 3D shape of each cell prototype. For a given fixed value k_{elas} of the elasticity modulus of each cell object, the second raw in the figure indicates the equilibrium state which is reached when a vertical loading force F_c is applied on the 5 (cell0 and cell1) or 4 (cell2) nodes marked with arrows..

To make a closer comparison with real cells, we consider a virtual cell devoid of internal elastic links. This provides a model of living cells like human erythrocytes, where the cell membrane is entirely responsible for the elastic deformation of the cell, the inner cytoplasm being only viscous. The

relevance of this modelling approach with regard to real experiments is illustrated in figure 2 where optical tweezers experiments of Henon et al. (1999) to deform nearly spherical erythrocytes have been simulated. In the experiments, a force F is exerted on two silica microbeads which are stuck to the erythrocyte membrane in diametrical position. By slowly incrementing the distance between the two trapped beads, an increasing stress is applied to the cell membrane. To simulate this experiment, a force F_s has been locally exerted on two opposite nodes of the physical cell membrane, pulling them apart. The simulation parameters are the elasticity of the cell, i.e. k_{ela} and the modulus of F_s. Fig ZZZ shows that k_{ela} could be approximated to that the modelled cell: the real erythrocyte have the same behaviour.

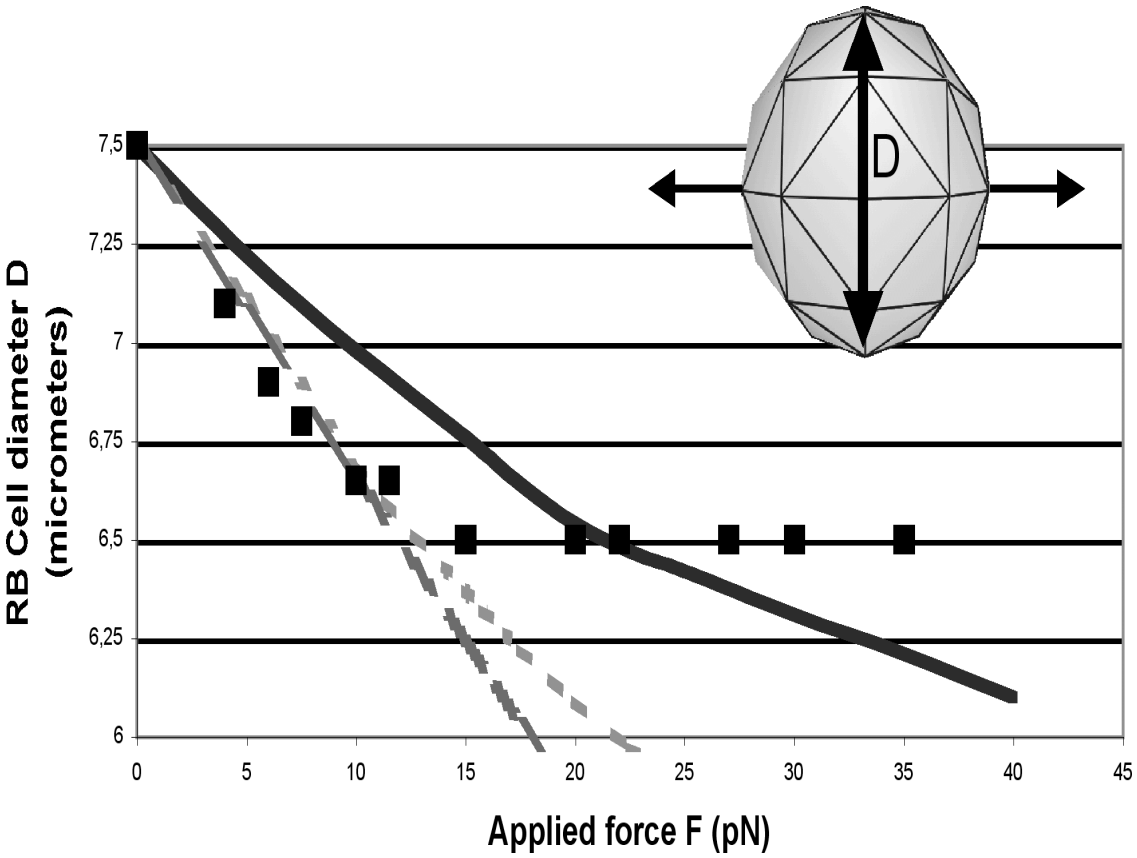

Figure 2 : Simulated virtual spherical red blood cell (RBC) suspended in an hypotonic solution. Optical tweezers double trap is simulated by exerting locally a force F_s on two opposite nodes of the cell object contour (upper insert). The variation with load of the cell object diameter D(F_s) in a plane perpendicular to the loading direction is simulated and compared to experimental data published by Henon et al. (1999) With appropriate scaling of the force, one can adjusted the parameter k_{elas} such that the experimental mechanical response of RBC can be nicely fitted in the linear elastic regime. Increasing the elasticity modulus k_{elas} induces a stiffer response which qualitatively reproduces the departure from the linear regime at larger traction forces.

The microplate experiments of Thoumine et al. (1997 ; 1999 ; 2000) can also be simulated in a similar fashion (Sauvaget, 2001) (Fig. 3). Experimentally, the adhesion of a fibroblast is realised between two glass microplates, one of them being slightly flexible. The mechanical of the cell response to stretching is measured. To qualitatively simulate these experiments, a cell object was defined as a two-region object: a virtual plama and nucleus membranes, both of them being represented by triangulated surfaces. Each node of the membrane is elastically linked to its neighbours as well as to the corresponding node in the other membrane. Microplates are modelled by two circular rigid objects attached to the apical and basal part of the external membrane, one of them being translated vertically. The corresponding shape of the virtual cell and nucleus at equilibrium is shown in figure 3 right.

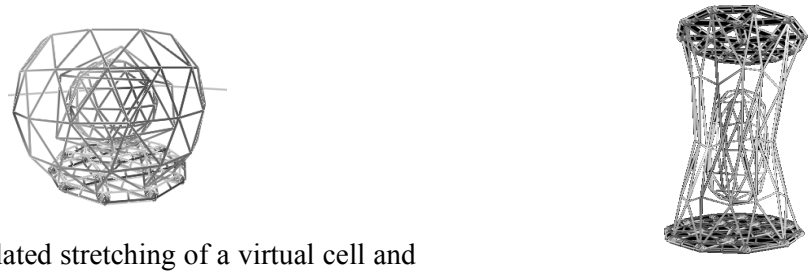

Figure 3: Simulated stretching of a virtual cell and its "nucleus" which mimics microplates experiments. Left : rest shape of the two embedded structures. Right : simulated cell and associated nucleus deformations.

For large amplitude deformations (hyperelastic behaviour), a non-linear mechanical response of the virtual cell could be observed. This property indictaes that, as observed with the cellular model of tensegrity of Ingber and col , the global mechanical behaviour of this virtual cell is not the sum of its individual component responses. Further developments are needed to analyse the theoretical properties of such a virtual cell, especially with regard to mechanical properties exhibited by continuous finite elements models. However, the simulation of the microplates experiments reported here illustrates the capability of this approach to deal with multi-scale dynamical phenomena. For example, it is also possible to simulate cell population behaviours such as tissues (figure 4) or cell interactions during cell migration (Promayon et al., 2002)

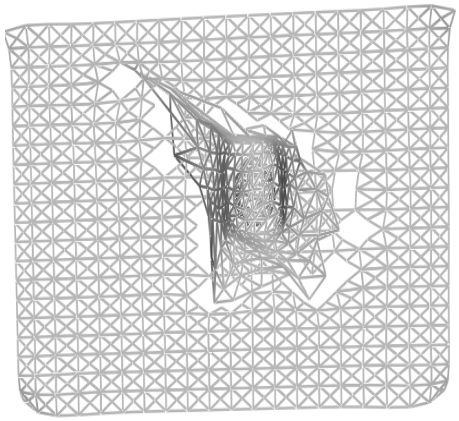

Figure 4 : Simulated contraction of an elastic substratum by a virtual adherent fibroblast linked to this extracellular film by localised "focal contacts"

3. Oscillating cellular deformations and continuous virtual cell models

The existence of a mechanical continuum within the cell means that oscillatory deformations could occur and affect gene expression. We therefore review some of the theoretical models proposed for analysing and modelling oscillations in cell shape. Each of them highlights a particular biophysical process as the central mechanism responsible for cell shape changes. Nevertheless, the common theme is that all the interactions considered are integrated into a single response, namely an oscillation of cellular protrusions.

It has been shown for a long time that living cells change their shape by extruding and remodelling different types of membrane protrusions. Filopodia are finger-like protrusions of the plasma membrane while lamellipodia are sheet-like protrusions associated with Filamentous actin (F-actin) network . It was once generally believed that the cell membrane fluctuates without any particular direction in space and without any particular coherence in time. However, recent progress in cell imagery techniques and cell images analysis has revealed the organised dynamics of cell protrusions (Germain et al., 1999). For example, Killich et al. (1994) have reported the existence of different organize patterns of morphological changes in the amoebae *Dictyostelium discoideum*. Ehrengruber et al. (1995) show that neutrophils undergo periodic cytoskeletal rearrangements that lead to cycles of shape change with period of 8-10s that is associated with sinusoidal oscillations of F-actin. Different hypotheses have been proposed to explain the formation of cellular protrusions. These hypotheses have considerable implications for our understanding of intracellular signalling and theoretical models of the types reviewed here are essential tools in the testing and refining of such hypotheses.

3.1. Cortical F-actin solation/gelation models.

In the early eighties, Oster and Perelson (1985) proposed a model of lamellipodial motion based on the physical chemistry of actomyosin gels. The model consists of a sheet of cytogel attached to the substratum by elastic tethers. The rhythmic activity of extending and retracting lamellipods is assumed to be driven by alternating phases of solation and gelation of the cortical actomyosin gel respectively. This phase transition is controlled by intracellular levels of calcium which is stored in intracellular compartments and which is released into the cytoplasm; this release is under the control of mechanisms that operate in a complex, non-linear (autocatalytic) fashion known as the calcium-induced calcium release mechanism (CICR). In Oster and Perelson's model, raising levels of free intracellular calcium concentration activate solation factors which disrupt the F-actin gel network. Factors such as gelsolin or severin can either break the actin chains themselves or break the cross-links between the chains or induce a depolymerisation of the chains. Such breakdown induces the swelling of the gel up to a point where the swelling pressure is balanced by elastic resistance of the network.

One important aspect of this non-linear process is that calcium also triggers the actomyosin contractile machinery. There is thus a defined range of calcium concentration where contraction occurs. In addition to the CICR mechanism quoted above, it is clear, regarding non-linear systems theory, that the cell has all the physical and biochemical ingredients needed to induce spontaneous self-sustained oscillations above some critical threshold. The trigger is assumed here to be an initial leak of calcium at the leading edge of the cell membrane. Leaking can be induced by the bindings of extracellular factors to membrane receptors or by a mechanical stimulus exerted at adhesion site, with associated possibly accompanied by a modification of ion channels.

3.2. Intercalation of actin monomers : the Brownian ratchet mechanism

Peskin et al. (1993) formulated a theory to account for the force generated by the polymerisation process itself when the filaments are rigid. They proposed that the addition, below the cell membrane, of G-actin monomers at the end of F-actin growing filaments could exploit the Brownian motion of any diffusing object in the front of the filament. Thus, random fluctuations of the plasma membrane would create a free sub-membrane space where this intercalation could take place (Abraham et al., 1999 ; Borisy and Svitkina, 2000). This ratchet mechanism could explain the formation of thin cell protrusions when F-actin filaments are perpendicular to the membrane surface, but it cannot satisfactorily explain the formation of lamellipodia.

Molginer and Oster (1996) extend this model by further assuming that the bending of the filament tips drives the protrusion formation. This bending mechanism would therefore provide a mechanical explanation for the appearance of lamellipodia type of protrusions. Moreover, Molginer and Oster inferred an optimal angle of 96 degrees between to two branching filaments.

3.3. Alternative to the ratchet model.

The pathogen bacterium *Listeria monocytogenes* uses actin polymerization to propel itself through the cytoplasm and the membrane of infected cells (Theriot et al, 1992; Frischknecht and Way, 2001). Experimental data show that the cell motility results from cooperation between the bacterium and the host cytoplasm proteins. The bacterium surface protein ActB controls the activity of the complex Arp2/3 that initiates actin polymerization (Welch et al., 1997). Actin dynamics is also controlled by an actin depolymerizing factor (ADF/cofilin) and capping proteins, which are in the cytoplasm host. The last two factors maintain a high level of actin monomers in the cytoplasm to achieve filament growth at the bacterium surface. In vitro studies proved that movement was possible with a limited number of proteins, including Arp2/3, ADF/cofilin and a capping protein (Loisel et al., 1999). Biophysical investigations demonstrate that the bacterium and its actin-tail are tightly bound, which rules out the ratchet model approach for this system (Gerbal et al., 2000). In addition, the same group measured the actin-tail Young modulus at a value of 103-104 Pa, a value 10 times larger than the cytoplasm rigidity. Using the framework of elasticity theory, Gerbal et al. (2000) proposed that the mechanical stresses generated at the *Listeria* cell surface are relieved at the back of the bacterium pushing the cell forwards. Their model accounted satisfactorily for the cell speed (about 0.1 $\mu m.s^{-1}$) and was extended to explain the hopping motion observed in a *Listeria* mutant

3.3. Actin polymerisation, F-actin nucleation and reaction-diffusion models

3.3.1. Some experimental data

Actin dynamics plays a major role not only in cell movement (Condeelis, 1993) but also in cell adhesion or neuron plasticity (Colicos et al., 2001; Star et al., 2002). Characterisation of actin filaments growth proved the importance of the polymerization/depolymerization balance at the filament ends and the role of proteins in inducing actin polymerization (e.g. Arp2/3), severing actin filaments (e.g. gelsolin, ADF/cofilin) or protecting the filaments ends by capping proteins (Pollard et al., 2000). Actin monomers associate to form filaments with a polarity (barbed *vs*. pointed ends). At the barbed end, subunits associate rapidly, with a low equilibrium actin monomer concentration

($C_{eq,B} = 0.08\mu M$). In contrast, the dynamics is much more slower at the pointed end but with a larger equilibrium monomer concentration ($C_{eq,P} = 0.5\mu M$, Carlier et al., 1997). At steady-state, the actin monomer concentration is:

$$C_{eq} = \frac{k_B^+ C_{eq,B} + k_P^+ C_{eq,P}}{k_B^+ + k_P^+}$$

where k_B^+ and k_P^+ are the association rate of actin monomers to the barbed (B) or pointed (P) ends. At steady-state, the growth at the barbed end is exactly compensated by the disassembly at the pointed end, a dynamical state called *treadmilling*. However, the predicted treadmilling steady-state flux (i.e. $k_B^+(C_{eq} - C_{eq,B}) = -k_P^+(C_{eq} - C_{eq,P})$) is too slow ($0.2s^{-1}$) to account for the rapid turnover observed *in vivo*. This suggests that other cellular factors affect actin dynamics, including interactions with intracellular proteins (Carlier et al, 1997a, Pollard et al., 2000), intracellular signaling (Machesky et al., 1999; Mullins, 2000) and movement generation (Borisy et al., 2000).

3.3.1. Models for actin network formation

In marked contrast with the actin dynamics complexity, models were first addressed to analyse the polymerization and fragmentation of actin filaments alone *in vitro* (Edelsetein-Keshet et al., 1998; Ermentrout et al., 1998). These models use the classical framework of kinetic differential equations without addressing the question of interactions between filaments and network formation. In the next step, actin bundle formation was considered including the kinetic approach (Edelstein-Keshet, 1998). This model was developed to account for the length distribution of actin filaments in a lamellipod (Edelstein-Keshet et al., 2001). Actin filament orientation was also studied using a Boltzmann-like equation (Geigant et al., 1998). However, these models are based on the kinetics of actin polymerization or actin filaments association without geometrical or mechanical constraints. A recent attempt to address the more complex question of actin network generation was done by Maly and Borisy (2001) who developed a model for the actin network formation as a self-organization process. They were able to account for the preferential direction of the actin filament bundle observed *in vivo*. Finally, one should mention the analysis of the actin gel formation on bead surface both experimentally and theoretically providing insight in the actin network regulation in cells (Noireaux et al., 2000).

Models for spatio-temporal F-actin interactions *in vivo* were developed by LeGuyader and Hyver (1997), who analysed the oscillatory dynamics of the cortical actomyosin ring of human lymphoblasts by interpreting it in terms of a reaction-diffusion process. They proposed a three-variable model that takes into account free and membrane-bound F-actin as well as nucleation proteins. By assuming the existence of a non-linear reaction in which the synthesis of F-actin is autocatalytic, their model generated oscillatory actin waves within a fixed area corresponding to the cell cortex. This theoretical behaviour is in agreement with the experimental work of Bornens et al. (1989) and more recent work showing that the disruption of the microtubule network by nocodazole induces cortical oscillations (Pletjushkina et al., 2001). Bornens et al. (1989) suggested that oscillating concentrations of nucleation proteins between the two poles of the cell would indeed create a polymerisation/ depolymerisation wave of actin travelling through the cell. Such behaviour was also reported during the extension of pseudopods in *Dictyostelium discoïdeum* (Vicker et al., 2000).

3.5. Protrusive dynamics due to the modulation of stress-strain relationships within the actomyosin cytogel.

The cytomechanical model of Lewis and Murray (1992) extends the solation/gelation model by considering the stress-strain relationships within the actomyosin cytogel. The cytogel is modelled as a viscoelastic continuum submitted to active stress and osmotic pressure. In addition, the sol/gel transition is controlled by the resulting strain level within the cytogel. At high strain, the gelation rate is increased, while at low strain, the solation rate increases. The model dynamics is controlled by the non-linear stress-strain relationship defining qualitatively the contractile actomyosin stress. The inhomogeneous spatial solutions generated by this model have been specifically discussed with regard to the patterned formation of microvilli at the cell surface (Murray, 1993).

3.6. Coupling of actin-dynamics with cell cortex curvature.

In a series of papers, Alt and col. (1995; 1999) proposed a modelling approach in which cell protrusions dynamics are due to the biophysical properties (viscoelasticity, contractility,...) of the cortical network of actin and myosin filaments underlying the cell membrane. This more or less dense network is able (i) to disassemble at locations where it becomes too condensed, (ii) to reassemble in cell protrusions like lamellipodia. Thus, cell protrusions mainly result from a mechanical balance between stresses acting on the cell cortex (mechanical forces generated by the actomyosin complex, tension forces due to the local membrane curvature (Raucher and Sheetz, 2000)) and associated F-actin polymerisation/ depolymerisation induced by intracellular network -free space variation in each moving protrusion.

A minimal three-variable model has therefore been developed to describe the spontaneous, self-organized, dynamics of cell deformations. This model has been used to study the spatio-temporal deformations of keratinocytes (Alt et al., 1995) as well the morphological changes in L929 fibroblasts (Stephanou et al., 2002a, Fig. 5). The model takes into account (i) the dynamics of F-actin polymerisation/depolymerisation in the cell cortex, (ii) the contractile activity generated by the actin/myosin interactions, (iii) the F-actin convection. The local amount of F-actin also determines the intensity of the resistive stress applied on the membrane as the result of CSK-cell cortex attachments. This resistive stress plus the stress induced by the cell cortex local curvature is assumed to balance the intracellular hydrostatic pressure.

The analysis of the morphological changes of adherent cells is at least a two-dimensional free-boundary problem. However, a simpler one-dimensional problem can be considered by assuming that the F-actin density as well as its convective tangential velocity is constant in the radial direction. In a cylindrical coordinate system (r,θ), the remaining variables in the cytomechanical model are thus: (i) the F-actin concentration in the cortex $a(\theta,t)$, (ii) the F-actin tangential velocity $v(\theta,t)$, (iii) the cell membrane position or the width of cell cortex annulus $L(\theta,t)$ measured from an virtual cell body delimited by an inner circle with radius R_0, with $L(\theta,t) << R_0$ (Alt and Tranquillo, 1995).

The spatio-temporal evolution of these three variables is given by a system of three partial differential equations which define respectively :

- variations of cortical F-actin concentrations, where the net rate η of actin polymerisation/depolymerisation depends on the local value of F-actin concentration relatively to the chemical equilibrium value a*.

$$\frac{\partial(L.a)}{\partial t} + \frac{\partial(L.a.v)}{\partial \theta} = \eta.L.(a^{*}-a)$$

- the balance of forces applied on the cell cortex in the radial direction. The model takes into account a viscous friction of the cell protruding over the rigid substratum, with coefficient ϕ_1, the intracellular hydrostatic pressure β_1, the resistive elastic stress of the cell CSK controlled by the elasticity coefficient $\gamma_1$and a curvature-dependent stress due to the surface tension of the cell cortex modulated by the coefficient τ_1.

$$a.\phi_1\frac{\partial L}{\partial t} = \beta_1 - \gamma_1.L.a + \frac{\partial}{\partial \theta}\left(\tau_1.a.\frac{\partial L}{\partial \theta}\right)$$

- the balance of forces in the tangential direction. It includes the frictional drag of the actin cortex moving in the viscous cytosol, with magnitude controlled by the drag coefficient ϕ_0, a viscous stress with viscosity coefficient μ and the membrane curvature induced stress with coefficient τ_0.

$$a.\phi_0.\mathrm{v} = \frac{\partial}{\partial \theta}\left[\mu_0.a.\frac{\partial v}{\partial \theta} + \sigma_0(a,a_{sat}) - \frac{\partial}{\partial \theta}\left(\tau_0.a.\frac{\partial L}{\partial \theta}\right)\right]$$

In addition, the contractile stress of the actomyosin network is modelled by the non-linear function σ_0 (a(θ,t), a_{sat}). Two mechanical states can be distinguished according to the value of the network F-actin concentration a(θ,t)). At low concentration values (a(θ,t) < a_{sat}), the contractile stress increases, while above the saturation threshold a_{sat}, the contractile stress decreases exponentially as a consequence of the network swelling. The non-linear function σ_0 (a(θ,t), a_{sat}) proposed by Alt and Tranquillo (1995) is the following:

$$\sigma_0(a,a_{sat}) = \psi_0.\, a^2.\, \exp(-a/a_{sat})$$

where the coefficient ψ_0 controls the magnitude of the contractile stress.

The existence and properties of protruding and retracting cell membrane protrusions are related to oscillatory solutions of the cytomechanical model. This theoretical analysis is performed in a standard way by looking for critical values of the model's parameters above which small random perturbations are amplified (Hopf bifurcation) until a coherent spatio-temporal pattern emerges with typical unstable modes or wave length (Fig. 5). As it may be expected intuitively, high values of the cell cortex surface tension reduce the number of cell protrusions whilst high values for the contractile efficiency of the actomyosin network contractility increase the number of oscillatory cell protrusions by favouring the destabilisation of higher unstable modes (Fig. 5 right). In an extension of this model by Stephanou et al. (2002b), the influence of extra-cellular factors on protrusivity dynamics and cell migration have been analysed.

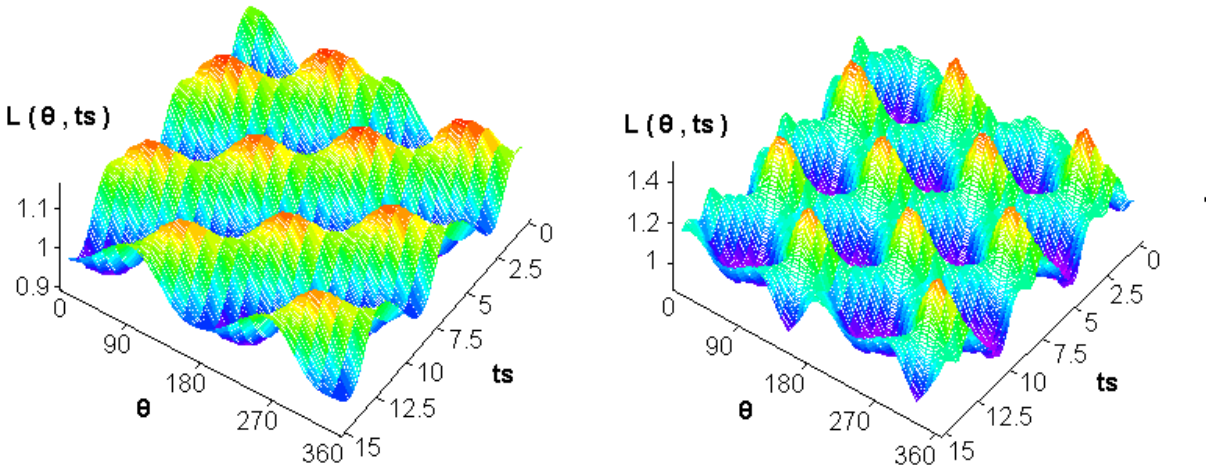

Figure 5 : Simulated evolution with time t_s of the length $L(\theta, t_s)$ of the cell protrusion along the cell periphery for different unstable spatial modes m. Left : mode m=2 corresponding to a single protrusion with apparent travelling motion around the cell body. Right : mode m=4 simulating oscillatory changes of cell shape with two protrusions alternatively occurring along to perpendicular directions. (see **plate 19** at the end of the book)

4. Artificial tensegrity

Another approach to studying the coupling between mechanical forces and cytoskeletal dynamics is to construct an *in silico* system in which populations of artificial cells containing different proteins with cytoskeletal properties are subjected to selection for resistance to hydrostatic pressure. By allowing mutations to alter the properties of the proteins and by selecting the surviving cells, it might be expected that one or more types of CSK would evolve. In essence, the idea is to explore the parameters underlying the formation of tensegrity structures by feeding artificial cells and selecting for those that evolve the best structures. In our project, the initial cell consists of a lipid membrane in the form of a monolayer and several types of proteins, the membrane is under pressure and membrane units can diffuse.

Two cases are explored:

1. The cell does not grow but there is either turnover of cellular constituents or migration of the entire cell.
2. The cell grows. The cell is fed by the random insertion of proteins and lipids.

The following rules are applied:

1. Turgor pressure results from the difference in concentration of molecules between the outside and the inside of the cell.
2. A cell is maintained until it lyses where lysing is defined as having a breach in membrane integrity that cannot be repaired within a certain period.
3. Two cells are compared and the one retained is either the one that lasts the longer or the one that maintains the higher turgor pressure or the one that can migrate.
4. Mutations are made by introducing new types of proteins.
5. Components that are used are less likely to be discarded than those that are not used (use is defined as forming part of a structure under tension or compression)

Components include:

- Membrane proteins that respond to curvature and to which other proteins can bind
- Proteins that cause filaments to branch
- Proteins that cross-link filaments
- Lipids of two types (cone and inverted cone) that form a monolayer.
- Calcium (in the form of a gradient that is higher outside the cell)

Variables include:

- Binding affinities that may depend on the tension in the system or on activation by another protein (equivalent of post-translational modification)
- Proteases

Mechanical aspects:

Turgor is calculated from the density of molecules within the cell. Individual molecules produce more turgor than those that are in the form of polymers or aggregates (molecules with no free spaces around them generate no turgor). This turgor then acts at the membrane. The membrane can deform by movement of lipids normal to its plane.

At this stage, artificial tensegrity is simply a gedanken or thought experiment Nevertheless, several testable predictions can be made. Firstly, large cells should have less problem with turgor pressure than small cells. Secondly, calcium should have an important role in strengthening the CSK to resist lysis (hence a small leak is self-repairing). Thirdly, cells that do not grow or move have a CSK parallel to the membrane whilst those that can grow or move have one that is perpendicular. Fourthly, there should be a reserve pool of lipids and cytoskeletal components near the membrane in readiness for incorporation in the membrane in time of need.

5. Discussion

This brief presentation underlines the advantage and limitations of continuous versus discrete modelling approaches to cell behaviour. Continuous models can account for a large variety of cellular dynamics including the protrusive activity which is coupled to modifications of continuous mechanical properties such as membrane tension, cell cortex viscoelasticity or mechanical stresses developed by the F-actin network.. However, a more refined description of CSK organisation, including the orientation of filaments or the formation of stress fibres, is hardly compatible with a continuous formulation, although recent models bridge the gap between mesoscopic mechanical properties of the actin cortex and a description at the molecular level (Maly et al, 2001). Models for cell dynamics, including lamelipod formation, modification of the cell architecture or cell adhesion to a substrate should incorporate actin dynamics to allow cell reshaping and motility in response to extracellular signals. Conversely, discrete tensegrity models seem to provide a more adequate description of the cell as a physical object, as evidenced by the larger number of criticisms encountered by these models compared to others.

Indeed, the tensegrity paradigm is still a matter of active controversy, as illustrated by recent papers (Ingber et al., 2000; Wang et al., 2001). For D. E. Ingber, the intransigence of the remaining critics seem to "… largely result from an overly strict definition of what tensegrity is and how it can be applied" (Ingber et al., 2000). As quoted above, the tensegrity model states that: (i) cells and tissues exhibit integrated mechanical behaviour through use of specific structural principles, namely the discontinuous-compression / continuous-tension construction submitted to a pre-existing tension or prestress (Pourati et al., 1998), and (ii) the cell has an elastic submembranous skeleton with its associated lipid bilayer which can be linked to the internal CSK depending on type of cell adhesion.

Can we propose experiments to discriminate between the models? It seems worth reporting here the different interpretations of similar experiments such as the induction of cell deformation through a direct manipulation of transmembrane receptors. According to Ingber and col., application of mechanical stresses to integrins using surface-bound micropipettes pre-coated with fibronectin induces CSK reorganisation, nucleus elongation along the tension lines as well as reorganisation within nucleoli, i.e. deep inside the nucleus (Maniotis et al., 1997). On the other hand, and as expected, such a reorganisation was not observed when similar mechanical stresses were applied to membrane receptors which are only linked to the submembranous F-actin CSK.

Opposite conclusions were drawn by Heideman and col. (1999; in Ingber et al., 2000) based on the application of similar mechanical stresses to integrin membrane receptors with glass needles treated with laminin, an ECM adhesion protein. Formation of an actin spot was observed on the cytoplasmic side of the membrane, inducing a locally high deformation of the membrane rather than a global change in cell shape. Heideman and colleagues thus conclude that the elastic cortical CSK is not connected to the internal microtubule cytoskelton, which is in complete disagreement with the fundamental tenet of tensegrity.

Analysing the argument in detail is beyond the scope of this paper. Maybe we should simply mention that Ingber's reply is that experiments showing a lack of action at a distance when pulling on the cell via integrins *before* focal adhesion formation are not valid as proofs of the failure of the tensegrity model. It is certainly clear that the tensegrity paradigm highly stimulates both theoretical and experimental work, including the development of new physical methods of quantification. For example, this has led to experiments to determine the significance of the compression of microtubules compression for cell mechanics. Ingber (Ingber et al., 2000) reported that microtubules counterbalanced approximately one-third of the total cellular prestress within a cell whose activation has been stimulated by histamine, a chemical constrictor, whilst noting that cell attachment to a rigid substratum would decrease this prestress level. Prestress within the cell can be estimated from microbeads displacement when deformable polyacrylamide gels containing small fluorescent microbeads are used as cell culture substratum, but looking for other quantification methods is the subject of current investigations.

From a theoretical point of view, a clear advantage of the tensegrity model paradigm is to provide an alternative view to cell engineering models that would only describe cell mechanical behaviour by ad hoc "data fitting" models, based for example on combination of rheological elements. Trough the cell tensegrity model, more specific questions can be addressed regarding specific cell behaviours such as strain-hardening or CSK stiffness (Volokh et al., 2000; Wendling et al., 2000), or the process of mechanotransduction. In the latter case, tensegrity-based predictions can be compared to theoretical predictions inferred from other cell models like the percolation model of Shafrir et al. (2000). This possibility of exploring various mechanistic hypotheses is a real advantage of the tensegrity model when compared to other cell simulation models such as Electronic Cell (http://e-cell.org/) or Virtual cell (http:// www.nrcam.uchc.edu/ vcell_development/ vcell_dev.html) where cytomechanical parameters are absent from the theoretical framework. That said, the dynamic remodelling of the cell is not yet taken into account in the current tensegrity model. This is one of the requirements for future modelling work in which the integration of mechanical and biochemical properties may provide an appropriate framework to simulate cells in a way that may ultimately enable a better interpretation of genomic data..

References

Abraham V. C., V. Krishnamurthi, D. L. Taylor and F. Lanni, The actin-based nanomachine at the leading edge of migrating cells, *Biophys. J.*, 77:1721-1732, 1999.

Alt W., O. Brosteanu, B. Hinz and H. W. Kaiser, Patterns of spontaneous motility in videomicrographs of human epidermal keratinocytes. *Bioch. Cell. Biol.* **73**, 441-459, 1995.

Alt W. and R. T. Tranquillo, Basic morphogenetic system modeling shape changes of migrating cells: How to explain fluctuating lamellipodial dynamics,*J.Biol.Syst*. 3 : 905-916,1995.

Alt W. and M. Dembo, Cytoplasm dynamics and cell motion: two-phase flow models, Math Biosci., 156(1-2):207-28, 1999.

Borisy, G.G. and T.M. Svitkina. Actin machinery:push-pull the envelope, *Curr. Opin. Cell Biol.* **12**:104-112, 2000.

Bornens M., M. Paintraud and C. Celati, The cortical microfilament system of lymphoblastes display a périodique oscillatory activity in the absence of microtubules : implications for cell polarity, *J. Cell Biol.,* **109** :1071-1083, 1989.

Carlier MF. and D. Pantaloni. Control of actin dynamics in cell motility. *J. Mol. Biol.* **269**:459-467, 1997.

Colicos M., Collins BE., Sailor M., and Y. Goda. Remodeling of synaptic actin induced by photoconductive stimulation. *Cell,* **107**:605-616, 2001.

Condeelis, J. Life at the leading edge: the formation of cell protrusions; *Annu. Rev. Cell. Biol*. **9**:411-444, 1993.

Dedhar S, Hannigan G E. Integrin cytoplasmic interactions and bidirectionnal transmembrane signalling *Curr Opin Cell Biol* **8** : 657-669, 1996.

Dembo M., T. Oliver, A. Ishihara and K. Jacobson, Imaging the traction stresses exerted by locomoting cells with the elastic substratum method, *Biophys. J.,* **70**:2008-2022, 1996.

Dembo M. and Y. L. Wang, Stresses at the cell-to-substrate interface during locomotion of fibroblasts, *Biophys. J.,* **76**:2307-2316, 1999.

Eastwood M, Porter R, Khan U, Mcgrouther G, Brown R. Quantitative analysis of collagen gel contractile forces generated by dermal fibroblasts and the relationship to cell morphology. J Cell Phys 166 : 33-42, 1996.

Edelstein-Keshet L. A mathematical approach to cytoskeletal assembly. *Eur. Biophys. J.* **27**:521-531, 1998.

Edelstein-Keshet L. and GB. Ermentrout. Models for the length distributions of actin filaments: I. simple polymerization and fragmentation. *Bull. Math. Biol.* **60:**449-475, 1998.

Edelstein-Keshet L. and GB. Ermentrout. A model for actin-filament length distribution in a lamellipod. *J. Math. Biol.* **43**:325-355, 2001.

Edwards Y.S., L.M. Sutherland, J.H. Power, T.E. Nicholas and A.W. Murray, Cyclic stretch induces both apoptosis and secretion in rat alveolar type II cells, *FEBS lett.* **448**(1) :127-130, 1999.

Ehrengruber M. U., T. D. Coates and D. A. Deranleau, Shape oscillations: a fundamental response of human neutrophils stimulated by chemotactic peptides?, *FEBS Lett.,* **359**:229-232, 1995.

Ermentrout GB., and L. Edelstein-Keshet L. Models for the length distributions of actin filaments: II. Polymerisation and fragmentation by gelsolin actin together. *Bull. Math. Biol.* **60:**477-503, 1998.

Frischknecht F. and M. Way. Surfing pathogens and the lessons learned for actin polymerization. *Trends Cell. Biol.* **11**:30-38, 2001.

Fujisawa T., T. Hattori, K. Takahashi, T. Kuboki, A. Yamashita and M. Takigawa, Cyclic mechanical stress induces extracellular matrix degradation in cultured chondrocytes via gene expression of matrix metalloproteinases and interleukin-1, *J. Biochem.,* **125**(5) : 966-975, 1999.

Geigant E., Ladizhansky K. and A. Mogilner. An integrodifferential model for orientational distribution of F-actin in cells. *SIAM J. Appl. Math.* **59**:787-809, 1998.

Gerbal F., Chaitkin P., Rabin Y. and J. Prost. An elastic analysis of Listeria monocytogenes propulsion. *Biophys. J.* **79**:2259-2275, 2000.

Gerbal F., Laurent V., Ott A., Carlier MF, Chaitkin P. and J. Prost. Measurement of the elasticity of the actin tail of Listeria monocytogenes. *Eur. Biophys. J.* **29**:134-140, 2000.

Germain F., A. Doisy, X. Ronot and P. Tracqui. Characterization of cell deformation and migration using a parametric estimation of image motion, *IEEE Trans. Biomed. Eng*., **46**(5), p.584-600, 1999.

Guilak F., M. Sato, C. M. Stanford and R. A. Brand, Cell mechanics, *J. Biomech*. **33**:1-2, 2000.

Heidemann S.R., S. Kaech, R.E. Buxbaum and A. Matus, Direct observation of the mechanical behaviors of the cytoskeleton in living fibroblasts, *J. Cell Biol.,* **145** :109-122, 1999.

Hénon S., G. Lenormand, A. Richert and F. Gallet, A new determination of the shear modulus of the human erythrocyte membrane using optical tweezers. *Biophys J.* **76**:1145-51, 1999.

Huang S. and D.E. Ingber, The structural and mechanical complexity of cell growth control, *Nature Cell Biol.*, **1**:E131-E138, 1999.

Ingber D. E. and J. D. Jamieson, Cells as tensegrity structures : architectural regulation of histodifferentition by physical forces transduced over basement membrane, in Gene expression during normal and malignant differentition, eds., Academic Press, pp.13-32, 1985.

Ingber D. E., Cellular tensegrity : defining new rules of biological design that govern the cytoskeleton,*J. Cell Sci.* **104**: 613-627, 1993.

Ingber D.E., Tensegrity : the architectural basis of cellular mechanotransduction, *Annu Rev Physio* **59** : 575-79, 1997.

Ingber D. E., S. R. Heideman, P. Lamoureux and R. E. Buxbaum, Opposing views on tensegrity as a structural framework for understanding cell mechanics, *J. Appl. Physiol.,* **89**:1663-1678, 2000.

Janmey P. A., The cytoskeleton and cell signaling: component localization and mechanical coupling, *Physiol. Rev.,* **78**(3):763-781, 1998.

Kaspar D., W. Seidl, C. Neidlinger-Wilke, A. Ignatius and L. Claes, Dynamic cell stretching increases human osteoblast proliferation and CICP synthesis but decreases osteocalcin synthesis and alkaline phosphatase activity, *J. Biomech*. **33**:45-51, 2000.

Killich, T., Plath, P. J., Hass, E. C., Wei, X., Bultmann, H., Rensing, L. and Vicker, M.G. Cell movement and shape are non-random and determined by intracellular, oscillatory rotating waves in dictyostelium amoebae. *Biosystems* **33** :75-87, 1994.

Kolodney M. and R.T. Wysolmersky, Isometric contraction by fibroblasts and endothelial cells in tissues cultures: a quantitative study. *J Cell Biol* **117** :73-82, 1992.

Le Guyader, H. and C. Hyver, Periodic activity of the cortical cytoskeleton of the lymphoblast: modelling by a reaction-diffusion system. *C. R. Acad. Sci. Paris*, Ser III, **320**:59-65, 1997.

Lelievre S., V. M. Weaver and M. J. Bissell. Extracellular matrix signalling from the cellular membrane skeleton to the nuclear skeleton : a model of gene regulation*, Recent Prog. Horm. Res.* 51:417-432, 1996.

Lewis M. A. and J. D. Murray, Analysis of dynamic and stationary pattern formation in the cell cortex, *J. Math. Biol.,* **31**:25-71, 1992.

Loisel TP, Boujemaa R., Pantaloni D. and MF Carlier. Reconstitution of actin-based motility of Listeria and Shigella using pure proteins. *Nature*: **401**, 613-616, 1999.

Machesky LM. And RH. Insall. Signalling to actin dynamics. *J. Cell. Biol.* **146**:267-272, 1999.

Maly IV. And GG. Borisy. Self-organization of a propulsive actin network as an evolutionary process. *Proc. Nat. Acad. Sci. USA*. **98**:11324-11329, 2001.

Maniotis A.J., K. Bojanowski and D.E. Ingber, Mechanical continuity and reversible chromosome disassembly within intact genomes removed from living cells, *J. Cell Biochem.,* **65** :114-130, 1997.

Meyer C. J., F. J. Alenghat, P. Rim, J. H. Fong, B. Fabry and D. E. Ingber, Mechanical control of cyclic AMP signalling and gene transcription through integrins, *Nature Cell Biol*., **2**:666-668, 2000.

Mogilner, A. and Oster, G., The physics of lamellipodial protrusion, *Eur. Biophys. J.* **25**:47-53, 1996.

Murray J. D., Mathematical Biology, 2nd edition, Springer Verlag, 1993.

Noireaux V., Golsteyn RM., Friederich E., Prost J., Antony C., Louvard D. and C. Sykes. Growing an actin gel on spherical surfaces. *Biophys. J.* **78**:1643-1654, 2000.

Oster, G. F. and A. S. Perelson, Cell spreading and motility: a model lamellipod, *J. Math Biol*, **21**:383-388, 1985.

Peskin, C. S., G. M. Odell and G. F. Oster (1993). Cellular motions and thermal fluctuations: the brownian ratchet, *Biophys. J.,* **65** :316-324, 1993.

Pollard TD., Blanchoin L. and RD. Mullins. Molecular mechanisms controlling actin filament dynamics in nonmuscle cells. *Annu. Rev. Biophys. Biomol. Struct*. **29**:545-576, 2000.

Pourati J., A. Maniotis, D. Spiegel, J. L. Schaffer, J. P. Butler, J. F. Fredberg, D. E. Ingber, D. Stamenovic and N. Wang, Is cytoskeletal tension a major determinant of cell deformability in adherent endothelial cells ?, *Am. J. Physiol.,* **274**:C1283-1289, 1998.

Pletjushkina O. J., Z. Rajfur, P. Pomorski, T. N. Oliver, J. M. Vasiliev and K. A. Jacobson, Induction of cortical oscillations in spreading cells by depolymerization of microtubules, *Cell Motil Cytoskeleton*, **48**:235-44, 2001.

Promayon E., Baconnier P., Puech C. Physically-based deformations constrained in displacements and volume. In Computer Graphic Forum*, vol.* 15(3), pp.155-164, 1996.

Promayon E., Baconnier P., Puech C. Physically-based model for simulating the human trunk respiration movements. Lecture notes in Computer Science, vol. 1205, pp 379-388. Springer Verlag, 1997.

Promayon E., J.L. Martiel and P. Tracqui, Physical object oriented 3d simulations of cell migration and déformations, to appear in "*Polymer and Cell Dynamics - Multiscale Modelling and Numerical Simulations*", 2002.

Raucher, D. and M.P. Sheetz (2000). Cell spreading and lamellipodial extension rate is regulated by membrane tension, *J. Cell Biol.,* **148**:127-136, 2000.

Sauvaget T., Mémoire de DEA, Univ. J. Fourier, Grenoble, 2001.

Stamenovic D, Fredberg J J, Wang N, Butler J P, Ingber D E. A microstructural approach to cytoskeletal mechanics based on tensegrity , *J Theor Biol* **181** : 125-136, 1996.

Shafrir Y., Ben-Avraham D. and G. Forgacs, Trafficking and signalling through the cytoskeleton: a specific mechanism, *J. Cell Sci.,* **113**:2747-2757, 2000.

Star E., Kwiatkowski DJ., and VN. Murthy. Rapid turnover of actin in dendritic spines and its regulation by activity. *Nature neurosci*. **5**:239-246, 2002.

Stephanou A., X. Ronot and P. Tracqui, Analysis of cell motility combining cytomechanical model simulations and an optical flow method, to appear in "*Polymer and Cell Dynamics - Multiscale Modelling and Numerical Simulations*", 2002a.

Stephanou A. and P. Tracqui, Cytomechanics of cell deformations and migration: a mathematical modelling and experimental study *C.R. Acad. Sci*., in press, 2002b.

Theriot JA, Mitchison TJ, Tilney LG and DA Portnoy. The rate of actin-based motility of intracellular L. monocytogenes equals the rate of actin polymerization. *Nature*, **357**:257-260, 1992.

Thoumine O. and A. Ott, Time scale dependent viscoelastic and contractile regimes in fibroblasts probed by microplate manipulation, *J. Cell Sci.,* **110**:2109-2116, 1997.

Thoumine O., A. Ott, O. Cardoso and J.J. Meister, Microplates: a new tool for manipulation and mechanical perturbation of individual cells, *J Biochem Biophys Methods*. **39**:47-62, 1999.

Thoumine O. and J. J. Meister, Dynamics of adhesive rupture between fibroblasts and fibronectin: microplate manipulation and deterministic model, *Eur Biophys J.,* **29**:409-419, 2000.

Trinkhaus J. P., Cells into organs. The forces that shape the embryo, 2nd edition, Prentice-Hall, Englewood, 1984.

Vicker M. G., Reaction-diffusion waves of actin filament polymerisation/depolymerization in Dictyostelium pseudopodium extension and cell locomotion, *Biophys. Chem.,* **84**:87-98, 2000.

Volokh K. Y., O. Vilnay and M. Belsky, Tensegrity architecture explains linear stiffening and predicts softening of living cells*, J. Biomech.* **33**:1543-1549, 2000.

Wang J. H. C., E. S. Grood, J. Florer and R. Wenstrup, Alignment and proliferation of MC3T3-E1 osteoblats in microgrooved silicone substrata sujected to cyclic stretching, *J. Biomech*. **33**:729-735, 2000.

Wang N, Butler J P, Ingber D E. Mechanotransduction across the cell surface and through the cytoskeleton , *Science* **260** : 1124-1127, 1993.

Wang N, K. Naruse, D. Stamenovic, J. J. Fredberg, S. M. Mijailovich, I. M. Tolic-Norrelykke, T. Polte, R. Mannix and D. E. Ingber, Mechanical behavior in living cells consistent with the tensegrity model, *Proc. Natl. Acad. Sci. USA*, **98**:7765-7770, 2001.

Welch MD, Iwamatsu A. and TJ Mitchison. Actin polymerization is induced by Arp2/3 protein complex at the surface of Listeria monocytogenes. *Nature* **385**: 265-269, 1997.

Wendling S., C. Oddou and D. Isabey, Stiffening response of a cellular tensegrity model, *J. Theor. Biol*., **196** :309-329, 1999.

Wendling S., E. Plannus, V. Laurent, L. Barbe, A. Mary, C. Oddou and D. Isabey, Role of cellular tone and microenvirnmental conditions on cytosquelette stiffness assessed by tensegrity model, *Eur. Phys. J. Appl. Phys.,* **9** :51-52, 2000.

Computational Models for Integrative and Developmental Biology

Jean-Louis Giavitto[1], Christophe Godin[2], Olivier Michel[1], Przemyslaw Prusinkiewicz[3]

[1] Laboratoire de Méthodes Informatiques, CNRS UMR 8042,
Tour Evry2, Genopole,
Université d'Evry, 523 place des terrasses de l'Agora 91000 Evry

giavitto@lami.univ-evry.fr
michel@lami.univ-evry.fr

[2] AMAP, UMR CIRAD-CNRS-INRA-Université Montpellier II,
TA 40/PS2 34398 Montpellier cedex 5, France

godin@cirad.fr

[3] Department of Computer Science,
University of Calgary
2500 University Drive N.W. Calgary, Alberta, Canada T2N 1N4

pwp@cpsc.ucalgary.ca

1 Introduction

The relation between biology and computation has a long history reviewed by Langton [LIL89]. In this paper, we classify the interactions between computer science and biology in three areas:

1. *Bioinformatics* develops the automated management and analysis of biological data.

2. *Computational Biology* looks at biological entities as information processing systems with the final goal of a better understanding of nature using computer science notions.

3. *Biological Computing* goes in the reverse direction and studies how biological techniques can help out with computational problems.

Bioinformatics consists of developing software tools to support and help the biologist in the analysis and comprehension of biological systems. A good example is the development of data-bases supporting the genome project [Kan00].

Biological Computing imports some *biological metaphors* [Pat94] to develop new way of computing and to design new algorithms. From the beginning of computer sciences, biological processes have been abstracted to produce new computational models: formal neural networks inspired by natural neurons, evolutionary algorithm inspired by Darwinian evolution (see the "Parallel Problem Solving from Nature" (PPSN) conference series), parallel computer architecture (e.g. cellular automata) inspired by biological tissues (see for example the "Information Processing in Cells and Tissues" (IPCAT) conference series), DNA computing abstracted from biochemistry [Pau98a], cooperative distributed algorithm (e.g. multi-agents) motivated by ethological behaviors or social interactions, ...

Computational Biology. Here we are mainly interested in computer modeling and simulation of biological processes. The computer simulation of a biological process implies the definition of a model sufficiently rigorous to lead to a program. With such a formal model, it is possible to systematically explore the system's behavior and sometimes to make predictions. This kind of study is part of the more general idea of *simulated experiments* (also called *in silico* experiment by biologists and numerical experiment by physicists). These experiments are required when in-vivo or in-vitro experiments are out of reach for economical, practical or ethical reasons. Note however that the simulation of a computer model is only one of its possible use: because it is formal, it is possible to reason about it and for example to infer some properties (existence of steady state, stability, phase changes, etc.) that can be checked against the natural phenomena.

More generally, formal models can have a pedagogical, normative, constructive or ideological role:

- pedagogical and heuristic: the model is used to share knowledge about a given system or to illustrate a set of complex relationships involved in a biological process.

- normative: the model is used as a reference between scientists or to compare several systems.

- constructive: the model is used as a blueprint in the design of a new biological entity. Biology has reached the point where in addition to the study of already existing natural entities, it has to design new biologicals artifacts (drug design, metabolic pathways, genetically modified organisms, ...).

- ideological: a model illustrates some biological paradigm and constraints furthermore the investigated schemes. Biology has imported a number of notions developed in computer science, for instance the notion of programs, memory, information, control, etc. [Ste88, Kel95], that have then structured biological theories.

The transfer of concepts and tools between biology and computer science is not a one-way process and often, a computing model inspired initially by a biological phenomena, leads to a formalism used later in simulation of some (other) biological processes. A good example is given by the history of cellular automata (CA): initially developed by J. Von Neuman [VN66], they abstract the idea of a tissue of cells, to investigate the notion of self-reproducing programs. The CA formalism has then been largely used in biological simulation, for example to model the growth of tumor (Eden's models) or in ecology (it has been also successful in numerous other application domains, like in physics).

The contributions of Computational biology in the area of molecular dynamics or ecological modeling, are now well established. They are largely centered around the notion of *dynamical systems*. What appears now, is that this kind of computational models can make connections between molecular mechanisms and the physiological properties of a cell. The theme

$$\text{gene expression} \longrightarrow \textit{system dynamics} \longrightarrow \text{cell physiology}$$

is an emerging paradigm [JTN00] that becomes increasingly more important as we try to integrate the exponential knowledge of all the cells components in a true understanding of the cell. However, this schema from biology to dynamical system and back to biology, has long been advocated in the more general domain of the development [Smi99, Kau95].

2 Dynamical systems

2.1 Basic definitions

Many natural phenomena can be modeled as *dynamical systems*. At any point in time, a dynamical system is characterized by its *state*. A state is represented by a set of *state variables*. For example, in the description of planetary motions around the sun, the set of state variables may represent positions and velocities of the planets. Changes of the state over time are described by a *transition function*, which determines the next state of the system (over some time increment) as a function of its previous state and, possibly, the values of external variables (input to the system). This progression of states forms a *trajectory* of the system in its *phase space* (the set of all possible states of the system).

Mathematical objects with diverse properties can be considered dynamical systems. For instance, state variables may take values from a continuous or discrete domain. Likewise, time may advance continuously or in discrete steps. Examples of dynamical systems characterized by different combinations of these features are listed in Table 1.

In simple cases, trajectories of dynamical systems may be expressed using mathematical formulas. For example, the ODE (ordinary differential equation) describing the motion of a mass on a spring has an analytical solution expressed by a sine function (linear spring, in the absence of friction and damping). In more complex cases, analytic formulas representing trajectories of the system may not exist, and the behavior of the system is best studied using computer simulations.

By their nature, simulations operate in discrete time. Models initially formulated in terms of continuous time must therefore be discretized. Strategies for discretizing time in a manner leading to efficient simulations have extensively been studied in the scope of simulation theory, *e.g.* [Kre86].

Table 1: Some formalisms used to specify dynamical systems according to the discrete or continuous nature of time and state variables.

C: continuous, D: discrete.	ODE	Iterated Mappings	Finite Automata
Time	C	D	D
State	C	C	D

Dynamical systems with apparently simple specifications may have very complex trajectories. This phenomenon is called *chaotic behavior*, *c.f.* [PJS92], and is relevant to biological systems, for example populations models [May75, May76].

2.2 Structured dynamical systems

Many biological systems are structured, which means that they can be decomposed into parts. The advancement of the state of the whole system is then viewed as the result of the advancement of the state of its parts. For example, the operation of a gene regulation network can be described in terms of the activities of individual genes.

Formally, we use the term *structured dynamical system* to denote a dynamical system divided into component subsystems (units). The set of state variables of the whole system is the Cartesian product of the sets of state variables of the component subsystems. Accordingly, the state transition function of the whole system can be described as the product of the state transition functions of these subsystems. Similarly to non-structured systems, structured dynamical systems can be defined assuming continuous or discrete state variables and time. In addition, the components can be arranged in a continuous or discrete manner in space. Some of the formalisms resulting from different combinations of these features are listed in Table 2.

Table 2: Some formalisms used to specify structured dynamical systems according to the continuous or discrete nature of space, time, and state variables of the components. The heading "Numerical Solutions" refers to explicit numerical solutions of partial differential equations and systems of coupled ordinary differential equations.

C: continuous, D: discrete.	PDE	Coupled ODE	Numerical Solutions	Cellular Automata
Space	C	D	D	D
Time	C	C	D	D
States	C	C	C	D

Time management is an important issue in the modeling and simulation of structured systems [Lyn96]. For example, state transitions may occur *synchronously* (simultaneously in all components) or *asynchronously* (in one component at a time). Furthermore, efficient simulation techniques may assume different rates of time progression in different components [Jef85].

In many cases, the transition function of each subsystem depends only on a (small) subset of the state variables of the whole system. If the components of the system are discrete (i.e., excluding partial differential equations, or PDEs), these dependencies can be depicted as a *directed graph*, with the nodes representing the subsystems and the arrows indicating the inputs to each subsystem. We say that this graph defines the *topology* of the structured dynamical system, and call *neighbors* the pairs of subsystems (directly) connected by arrows.

The topology of a structured dynamical system may reflect its *spatial organization*, in the sense that only physically close subsystems are connected. A dynamical system with this property is said to be *locally* defined. Locality is an important feature of systems that model physical reality, because physical means of information exchange ultimately have a local character (e.g., transport of signaling molecules between neighboring cells). On the other hand, physically-based models need not to be rigorously local. For example, when modeling plants, it may be convenient to assume that higher branches cast shadow on lower branches without simulating the local mechanism of light propagation through space.

When the number of components in a structured dynamical systems is large, the exhaustive listing of all connections between the components becomes impractical or infeasible. This limitation can be overcome in several ways. For example, if the components are arranged in a regular pattern, the neighbors of each component need not to be listed explicitly. This is the case of *cellular automata* (*e.g.* [TM87], in which cells are arranged in a square grid). *Group-based fields* [GM01b] are a generalization of this idea, allowing for a wider range of connection patterns. Large structures can also be defined by *simulated development*, discussed next.

2.3 Dynamical systems with a dynamic structure

A developing multicellular organism can be viewed as a dynamical system in which not only the values of state variables, but also the *set* of state variables and the state transition function change over time. These phenomena can be captured using an extension of structured dynamic systems, in which the set of subsystems and/or the topology of their connections may dynamically change. We call these systems *dynamical systems with a dynamic structure* [GM01b], or $(\mathrm{DS})^2$-systems in short.

For example, let us consider a model of a multicellular organism, defined at the level of individual cells. When a cell divides, the subsystem that represents it is replaced by two subsystems that represent the daughter cells. Furthermore, the topology of the whole system is adjusted to:

- remove connections (neighborhood relations) between the mother cell and the rest of the organism,
- create connections between the daughter cells,
- insert connections between the daughter cells and the rest of the system.

These operations make it possible to gradually create a large network of interconnected cells.

2.4 A Taxonomy of Formalisms

From a computer science (or a mathematical) point of view, the problem raised by the simulation of dynamical systems with a dynamical structure is that of the programming paradigm (or the modeling language) well fitted to the specification of such systems. For instance, the PDE formalism is not a relevant solution because it prescribes an *a priori* given set of relations between an *a priori* given set

of variables. Consequently, these two sets, which embed implicitly the structural interaction between the entities or the system parts, cannot evolve jointly with the running state of the system [Mic96, pp 6, 85], [GM01b, chapter 1].

However, there exist several formalisms that can be used. The criteria used to classify the DS formalism in section 2.1 and 2.2 are still valid and the representation of time and state can be discrete or continuous for $(DS)^2$ as for standard DS. Here we propose an additional criterion to distinguish between the topological nature of the system structure. Table 3 presents some formalisms for the discrete time case.

Table 3: Some formalisms used for the modeling of $(DS)^2$, according to the underlying topology of the state.

Topology	Multiset	Sequence	Uniform	Combinatorial
Formalism	multiset rewriting	L-systems	GBF	map L-systems, Graph-grammars, MTG, MGS

In this table, the first line gives the type of the topology used to connect the subcomponents of a system. In a *multiset*, all elements are considered to be connected to each other. In a *sequence*, elements are ordered linearly; this case includes lists and extends also to tree-like structures. *Uniform* structures represents a regular neighborhood: for example, in a rectangular lattice (Von Neumann neighborhood), each element has exactly four neighbors. *Combinatorial* structures are used to define arbitrary connections between the components.

Considering solely the type of the topology underlying the structure of a state is only a partial caracterization that does not emphasize other several important points. Let us mention some of them.

- The relationship between the components can take place in an *a priori* structure. This approach is also known as the Newtonian conception of space where phenomena take place in a predefined scene. The other approach, which has been promoted by Leibniz, considers the topology as the result of the connection between the existing entities. In this point of view, the topology results from the dynamic connection between the system elements. This distinction is found in biology with the notions of *space oriented* or *structure oriented* models. For instance, accretive growth (growth on the boundaries) is an example of a space oriented process and intercalary growth (growth from the inside) is an example of a structure oriented process.

- There are several degrees in the dynamic of the structure. In the simplest case, the type of the topology remains the same during the evolutions of the system. An example is the growth of *Anabaena* filaments (Cf. section 4.2) where the system is always described as a sequence of cells. In addition, once a cell is connected with two neighbors, these connections remain the same. On the other hand, during the development of an embryo, several domains of cells change dramatically their shapes. For instance, the neural tube is formed dorsally in the embryonic development of Vertebrates by the joining of the 2 upturned neural folds formed by the edges of the ectodermal neural plate, giving rise to the brain and spinal nerve cord. In this process, which implies cell migration, the connections of a cell change over time and the global shape changes from a sheet to a tube.

- We have assumed that the interaction between the system parts can be described by a graph. Implicitly, this implies that elements interact two by two, which is not always the case. More elaborated interaction may imply more participants (e.g. a chemical reaction between two chemicals that requires also a catalyst; or the many-to-one relation between a subsystem and its decomposition). An interaction between n participants can be modeled by an n-edge in an *hypergraph*. An alternative representation is to use a n-simplex in a *simplicial complex* [GV01]. In the last case, the dimension of the simplex is directly linked with the number of participants.

- The notion of dimension also appears in the interactions between components in the following way. Often, the components of a system have a physical nature and the logical neighborhood established by the component interaction is the same as the spatial neighborhood implied by the physical structure of the system. For example, the topology implied by the representation of the cell sub-structures is tridimensional (compartments), bidimensional (membranes) and zero-dimensional (molecules). Obviously, the interactions that must be described depend of the dimension of the invoked entities: for instance, a flow of molecules can be conceived only through a membrane boundary between two compartments, not between a filament and another molecule; conservation laws depend on the topological nature of the entities, etc. From this point of view, multiset corresponds to a trivial topology (two points are always neighbors), L-systems corresponds to one-dimensional topologies and a GBF described by n fundamental generators (cf. below, section 5) describe n-dimensional topologies.

2.5 Outline

Following table 3, the next sections and chapters presents some formalisms usable for $(\mathrm{DS})^2$ Modeling:

- Section 3 reviews the use of multisets to model biological state and multiset rewriting to specify the evolution function.

- Section 4 sketches the L-system formalism. This formalism is an effective approach for the modeling of linear and branching structure. For instance, it as largely been applied in the field of plant growing.

- Section 5 presents a general framework, instantiated in a programming language, that is able to unify several approaches by using a topological point of view.

- The chapter **??** "Cellular automata and multi-agent" in this document gives some examples of the use of the computational device in the field of biological modeling.

- "Neural networks" are a special kind of dynamical systems. A large part of the considerations presented here, apply. Their importance has motivated numerous investigations and a lot of results are available. They are presented in **??**.

3 Multiset Rewriting and the Modeling of Biological Systems

3.1 Basic Concepts

Consider a simple chemical system of two molecules types A and B. We suppose that only deterministic second-order catalytic reactions are allowed, that is: a collision of two molecules will catalyze

the formation of a specific third molecule and the two colliding molecules are regarded as catalysts. The possible reaction rules are given explicitly as follows:

$$\begin{aligned} r_1: &\quad A + A \longrightarrow A + A + B \\ r_2: &\quad A + B \longrightarrow A + B + B \\ r_3: &\quad B + B \longrightarrow B + B + A \end{aligned}$$

A simulation in which every molecule is explicitly stored and every single collision is explicitly performed can easily be implemented if the chemical reactor is abstracted as a *multiset*. Unlike a set, an element can occur several times in a multiset. In the following, we denote a multiset using braces: $\{A, C, A, D, B, C\}$ is a multiset m with elements A and C occurring twice, and elements B and D occurring only one time. To simulate the chemical reaction, we simply interpret each rule as a transformation of the multiset. For instance, the rule r_1 specifies that two molecules A taken in the multiset have to be replaced by the three molecules A, A and B. For example, if reaction r_1 occurs in m at a given time step t_0, then m is transformed in $\{A, C, A, D, B, C, B\}$ (one additional B is produced). See figure 1.

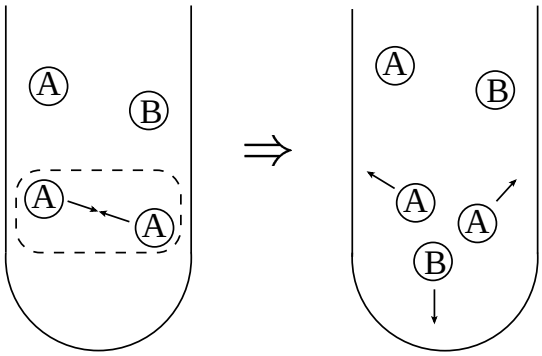

Figure 1: Illustration of one occurence of a reaction r_1 occuring in a test tube considered as a multiset of molecules.

Because several chemical reactions can occur *in parallel* (which means that several reactions involving different elements occur in the same time step), the strategy is to apply in parallel as many transformations as possible to the multiset. Such transformations are iterated to model the evolution of the state of the reactor. However, several competing rules may apply at the same time step: for instance consider a chemical reactor described by $\{A, A, B\}$ at time t_0 and subject to the two reactions r_1 and r_2. If r_1 occurs, then there is no longer A at t_0 to proceed with r_2 and vice-versa. The two reactions cannot occur together because there are not enough resources. In this case, we consider that one of the two rules is chosen in a non-deterministic manner. No assumption is made on the order on which the reactions occur.

The "+" sign that appears in the left and right hand side of the rules means that the linked molecules are present together in the chemical reactor. Thus, the left hand side of rule r_2 can also be equivalently written $B + A$. From a mathematical point of view, it is very convenient to consider $+$ as a formal commutative-associative operator used to construct multisets: a multiset $\{A, C, A, D, B, C\}$ is simply a formal sum $A + C + A + D + B + C$. The associativity and the commutativity properties are simply the expression that the elements of this last sum can be rearranged in any order. Then, rules like the r_i rules can be interpreted as rules for rewriting such formal expression. Abstractly, we can say that a chemical reaction can be modeled as a multiset rewriting system.

This modeling paradigm can be extended from this chemical example to other situations and its biological relevance is advocated in several recent papers [Man01, FMP00]. To quote[1] Fisher *et al.* [FMP00]: "A biological system is represented as a term of the form $t_1 + t_2 + \cdots + t_n$ where each term t_i represents either an entity or a message [or signal, command, information, action, etc.] addressed to an entity. [The simulation of the physical evolution of the biosystem] is achieved through term rewriting, where the left hand side of a rule typically matches an entity and a message addressed to it, and where the right hand side specifies the entity's updated state, and possibly other messages addressed to other entities. The operator $+$ that joins entities and messages is associative and commutative, achieving an ' associative commutative soup ', where entities swim around looking for messages addressed to them."

3.2 Division, Growth and Diffusion Processes

To illustrate this paradigm in a biological situation, we consider the multiplication of a mono-cellular organism in a test tube. A cell exists in one of two forms A or B. Type A and B can be used to characterize a phase of the life cycle of the cell, or as a cell polarity, etc. The division of a cell of type A produces one cell of type A and one of type B. In contrast, a cell of type B does not divide but evolves to give a cell of type A. This can be summarized by the two rules:

$$\begin{aligned} r_1 : \quad & A \longrightarrow A + B \\ r_2 : \quad & B \longrightarrow A \end{aligned}$$

Starting from a test tube with three initial cells, abstracted as a multiset $m_0 = \{A, B, B\}$, the first three evolutions are:

$$m_0 \to \{A, B, A, A\} \to \{A, B, A, B, A, B, A\} \to \{A, B, A, B, A, B, A, B, A, A, A\} \to \ldots$$

There exists several software environments that support multiset rewriting (see next paragraph). So the previous two rules *directly turn to a computer program* that simulates the growing and division processes of this hypothetic mono-cellular organism. In fact, these rules fit well the development of Anabaena, which is described more in details in the next section, if we neglect the sequential organization of the cells. However, this model admit also other interpretations. For example, Fibonacci studied (in the year 1202) about how fast rabbits could breed under some ideal circumstances. Suppose a newly-born pair of rabbits, one male, one female, are put in a field. Rabbits are able to mate after one month so that at the end of its second month a female can produce another pair of rabbits. We simplify the model assuming that rabbits never die and that a female always produces one new pair (one male, one female) every month from the second month on. We model by symbol B a newly-born pair of rabbits and by symbol A a mature pair of rabbits. Then the rule r_1 expresses that a mature pair produces a newly-born pair and survive and rule r_2 specifies the maturation of a new pair.

The simulation of this process can be used to determine, for example, the relative ratio of A and B types in a population after some time. However, as mentioned in the introduction, the use of a formal model is not restricted to simulation and can be used to prove formal properties of the system without looking at the results of the simulation (e.g.: Fibonacci was able to prove that the ratio between B and A converges to the golden section as the time goes).

In the previous examples, each entity (a molecule, a cell or a pair of rabbits) is represented as an element of a multiset. In addition, the multiset structure allows objects to interact in a rather unstructured way, in the sense that an interaction between two objects is enabled simply by virtue of

[1] with adaptations in the terminology, brackets are our comments

both being present in the multiset. In other word, there is no *localization* of the entities. Here is an example of another approach, where multiset rewriting is used in another way to take into account a geometric information. The problem is to model the diffusion of a set of particles on a line. The line is discretized as a sequence of small boxes, indexed by a natural integer, each containing zero or many particles. At each time step, a particle can choose to stay in the same box, or to jump to a neighboring box, with the same probability. See figure 2. The state of a particle is the index of the box where it resides. The entire state of the system is represented as a multiset of indices. The evolution of the system is then specified as three rules:

$$\begin{aligned} r_1 : &\quad n \longrightarrow n \\ r_2 : &\quad n \longrightarrow n-1 \\ r_3 : &\quad n \longrightarrow n+1 \end{aligned}$$

where n is an integer and the operations "$+$" and "$-$" that appear in the right hand side are the usual arithmetic operators. Rule r_1 specifies the behavior of a particle that stay in the same box; rule r_2 corresponds to a particle that jumps to the box at the left; and rule r_3 defines a particle jumping to the right. Another solution is to factorize the three rules into one:

$$r : \quad n \longrightarrow n + \text{Random}(-1, 0, 1)$$

where the function Random$(\dots)$ returns randomly one of its arguments. In the case of three competing rules, we must assume that there is some fairness in the choice of the rules r_1 to r_3 to be applied, i.e., they have the same probability of being chosen. If there is more chance to stay in a box than to leave it, then the underlying formalism must be able to express some finer control over the rule application. As a matter of fact, specifying an application strategy of the rules that respect the symmetries of the system can be very difficult.

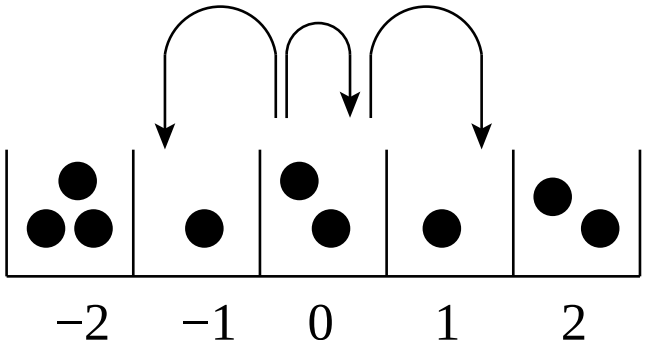

Figure 2: Diffusion of a particle along a line

3.3 Applications, Theories and Tools for Multiset Rewriting

Multiset rewriting has inspired several applications leading to the emergence of a new field: *Artificial Chemistry*. The home page [Dit00] and reference [DZB00] are a good introduction to this new area. There is a growing body of applications in artificial life, chemical and biological modeling, information processing and optimization. More specifically, Artificial Chemistry has been advocated as a productive framework for the study of pre-biotic and bio-chemical evolution, and for the study of the evolution of organization in general.

Multiset rewriting has also been used to extend other formalisms. For example, a multiset of L-systems is used to model an ecosystem (a multiset) of individual plants (modeled using L-system), see [LP02].

From the computer science point of view, the use of the chemical metaphor as a *computing model* has been investigated by Gamma [BM86, BCM87] in the middle of the eighties. A good review of the research done about Gamma can be found in [BFM01]. The CHemical Abstract Machine (CHAM) formalism extends these ideas with a focus on the expression of semantic of non deterministic processes [BB90]. The CHAM is an elaboration on the original Gamma formalism introducing the notion of sub-solution enclosed in a membrane. It is shown that models of algebraic process calculi can be defined in a very natural way using a CHAM: the fact that concurrency (between rule application) is a primitive built-in notion makes proof far easier than in the usual process semantics. The motivations of Gamma and the CHAM are the development of a formalism to support the specification and the programming of parallel and non deterministic programs. Multiset rewriting lies at the core of the formalism.

From the point of view of *term rewriting* [DJ90], multiset rewriting is the special case where the operators considered are both associative and commutative. In this domain, the perspective is more logical and directed towards the concepts of rewriting calculus and rewriting logic. The applications considered are the design of theorem provers, logic programming languages, constraint solvers and decision procedures. Several frameworks provide efficient and expressive environments to apply rewrite rules following dedicated strategies. It is worth mentioning ELAN [ela02] and MAUDE [mau02].

At last but not least, in the domain of formal language theory and computational complexity, P systems [Pau98b, Pau00] are a new distributed parallel computing model based on the notion of a membrane structure. This paradigm extends standard multiset rewriting introducing the notion of membrane. A membrane structure is a nesting of compartments represented, e.g, by a Venn diagram without intersection and with a unique superset: the skin. Objects are placed in the regions defined by the membranes and evolve following various transformations: an object can evolve into another object, can pass through a membrane or dissolve its containing membrane. In the initial definition of the P systems, each region defined by a membrane corresponds to a multiset of atomic objects which can evolve following evolution rules very similar to Gamma's (the right hand side of each rule is augmented to specify the destination of the results of the reaction). The membrane structure enables the specification of some localization of the processes. For an example, see section 5. Several alternatives have been devised and a region can be equipped with various computational mechanisms: string rewriting, splicing systems (DNA computing), etc. From the calculability point of view, several variants of such computing devices can compute all recursively enumerable sets of natural numbers. When an enhanced parallelism is provided, by means of membrane division (and, in certain variants where one works with string-objects, by means of object replication), NP-complete problems can be solved in linear time (of course, making use of an exponential space).

4 L-systems

4.1 Basic notions

L-systems were introduced in 1968 in the landmark paper by A. Lindenmayer, *Mathematical models for cellular interaction in development* [Lin68]. They provide a well developed and flexible tool for modeling and simulating a restricted but biologically important class of dynamic systems with a

dynamic structure: linear and branching structures.

Originally, Lindenmayer described his formalism in terms of cellular automata, in which — in contrast to the standard definition — the cells could divide. Subsequently he observed that L-systems can be formulated in a simpler and more elegant manner in terms of formal language theory [Lin71]. That theory was originally proposed by Chomsky [Cho56, Cho57] to describe the syntax of natural languages. Its fundamental notion is that of a (generative) *grammar*, which consists of *productions* or *rewriting rules*. In general, a production replaces a symbol by zero, one, or several new symbols. They may represent words in a sentence, as in the original interpretation by Chomsky, but they also may represent cells or other components of a living organism, as was proposed by Lindenmayer. The use of related formalisms in the description of such apparently distant notions as languages and biological structures may seem surprising at first. In fact, it reflect the common dynamic nature of sentences under construction and developing organisms.

Applications of L-systems to modeling have an extensive literature, last reviewed in [Pru98] and [Pru99]. Below we outline one variant, called *parametric L-systems* [Han92, PH90, PL90] Within this formalism, the individual subsystems are called *modules*. Each module is represented by a symbol (letter) with optional parameters. This letter and parameters jointly characterize the module's state. For instance, the letter may represent a cell type, while the parameters may represent quantitative attributes of the cell, such as its dimensions and concentrations of chemicals that it contains.

The assumption that the organism forms a filament makes it possible to represent it at any moment of time as a string of modules, called a *parametric word*. For example, the string

$$A(2.5)B(3.14, 0.2)CA(1.3) \tag{1}$$

may represent an organism that consists of four cells. The first cell has type A and is characterized by one parameter, the value of which is equal to 2.5. The remaining symbols have an analogous interpretation.

An L-system model describes the development of the entire structure by operating on individual modules. A production specifies the fate of a unit over a given time interval as a function of its current state and, optionally, the states of its neighbors. For example, the production

$$A(x) < B(y, z) > C \rightarrow CB(x + y, z/2) \tag{2}$$

operates on a module B that appears in the *context* of a module A to its left and module C to its right. The left and right contexts are separated from the *strict predecessor* B by the metasymbols (i.e., the symbols that do not represent modules) $<$ and $>$, respectively. In this example, module B divides into a module C and a new module B. The arithmetic expressions in the production's successor determine new parameter values. Hence, when applied to string (1), production (2) will yield the string

$$A(2.5)CB(5.64, 0.1)CA(1.3). \tag{3}$$

Simultaneous application of productions to all modules advances the state of the whole structure. If the set of module types is finite, the corresponding finite set of productions provides a mechanism for advancing the state of the entire structure independently of its size (the number of modules).

4.2 A sample model

We will illustrate the notion of genetic L-systems by constructing a model of heterocyst differentiation in a growing filament of the cyanobacterium *Anabaena*. The following description is adapted from [HP96].

The cells of *Anabaena* are organized into filaments which consist of sequences of *vegetative cells* separated by *heterocysts*. The vegetative cells divide into two cells of unequal length and, in some cases, differentiate into heterocysts which do not further divide. The organism maintains an approximately constant spacing between heterocysts: whenever the distance between two heterocysts becomes too large due to the division and elongation of vegetative cells, a new heterocyst emerges.

What mechanisms is responsible for the differentiation of heterocysts and the maintenance of the approximately constant spacing between them? Baker and Herman [BH70, BH72] (see also [dL87, HR75, Lin74] proposed the following simulation model. The heterocysts produce a substance that diffuses along the filament and is used by the vegetative cells. This substance inhibits the differentiation of vegetative cells into heterocysts. When its level in a cell drops below a threshold value, the cell detects that it is no longer inhibited and differentiates into a heterocyst.

Although the model of Baker and Herman is capable of reproducing the observed pattern of heterocyst spacing, it is very sensitive to parameter values. Small changes in these values easily result in filaments with pairs of heterocysts appearing almost simultaneously, close to each other. This is not surprising, considering the operation of the model. The gradient of the concentration of the inhibitor may be too small near the middle of a sequence of vegetative cells to precisely define the point in which a new heterocyst should differentiate. Consequently, the threshold value may be reached almost simultaneously by several neighboring cells, resulting in the differentiation of two or more heterocysts close to each other.

The above model can be improved assuming that the prospective heterocysts compete until one "wins" and suppresses the differentiation of its neighbors. This "interactive" model was originally proposed by Wilcox *et al* [WMS73]. It can be formalized using the framework of the *activator-inhibitor* class of reaction-diffusion models [Mei82]. In addition to the substance that inhibits the differentiation, the cells are assumed to carry a substance called the activator. The concentration of the activator is the criterion that distinguishes the vegetative cells (low concentration) from the heterocysts (high concentration). The activator and inhibitor are antagonistic substances: the production of the activator is suppressed by the inhibitor unless the concentration of the inhibitor is low. In that case, production of the activator drastically increases through an autocatalytic process (an increased concentration of the activator promotes its own further production). High concentration of the activator also promotes the production of the inhibitor, which diffuses to the neighboring cells. This establishes a ground for competition in which activator-producing cells attempt to suppress production of the activator in the neighboring cells. For proper values of parameters that control this process, only individual, widely spaced cells are able to maintain the high-activation state.

An L-system implementation of these mechanisms (a variant of the L-system from [HP96]) is given below.

$$
\begin{array}{ll}
\omega : & M(0.5, 0.1, 200, \text{right})M(0.5, 0.1, 100, \text{right})M(0.5, 0.1, 100, \text{right}) \\
p_1 : & M(s_l, a_l, h_l, p_l) < M(s, a, h, p) > M(s_r, a_r, h_r, p_r) : \\
 & \quad s < s_{max} \,\&\, a < a_{th} \rightarrow M(s', a', h', p) \\
p_2 : & M(s_l, a_l, h_l, p_l) < M(s, a, h, p) > M(s_r, a_r, h_r, p_r) : \\
 & \quad s \geq s_{max} \,\&\, a < a_{th} \,\&\, p = \text{left} \rightarrow \\
 & \quad M(ks', a', h', \text{left})M((1-k)s', a', h', \text{right}) \\
p_3 : & M(s_l, a_l, h_l, p_l) < M(s, a, h, p) > M(s_r, a_r, h_r, p_r) : \\
 & \quad s \geq s_{max} \,\&\, a < a_{th} \,\&\, p = \text{right} \rightarrow \\
 & \quad M((1-k)s', a', h', \text{left})M(ks', a', h', \text{right}) \\
p_4 : & M(s_l, a_l, h_l, p_l) < M(s, a, h, p) > M(s_r, a_r, h_r, p_r) : \\
 & \quad a \geq a_{th} \rightarrow M(s, a', h', p)
\end{array}
$$

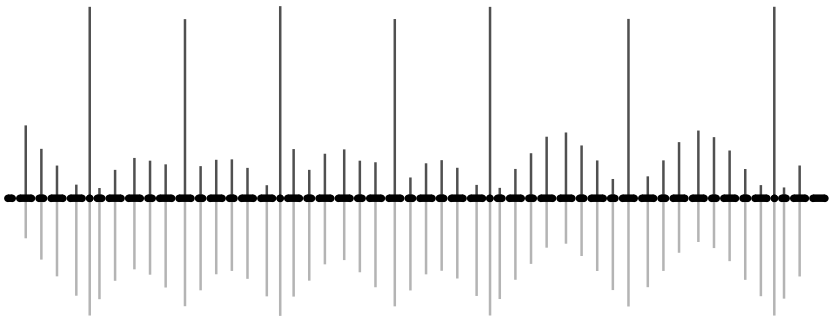

Figure 3: Fragment of a simulated filament of *Anabaena*. Vertical lines indicate the concentrations of the activator and inhibitor (above and below the cells, respectively). Notice the sharp peaks of the activator concentration that define the heterocysts, and high levels of the inhibitor concentration in the neighboring vegetative, which prevent their differentiation. The parameters used in the simulation were: $\rho = 3$, $\kappa = 0.001$, $a_0 = 0.01$, $\mu = 0.1$, $h_0 = 0.001$, $\nu = 0.45$, $D_h = 0.004$, $a_{th} = 1$, $k = 0.38196$, $s_{max} = 1$, $r = 0.002$, and $w = 0.001$.

where

$$\begin{aligned} s' &= s(1 + r\Delta t), \\ a' &= a + \left(\frac{\rho}{h}(\frac{a^2}{1+\kappa a^2} + a_0) - \mu a\right)\Delta t, \\ h' &= h + \left(\rho(\frac{a^2}{1+\kappa a^2} + h_0) - \nu h + D_h\frac{h_l + h_r - h}{sw}\right)\Delta t. \end{aligned}$$

The cells are specified as modules M, where parameter s stands for cell length, a is the concentration of the activator, h is the concentration of the inhibitor, and p denotes polarity, which plays a role during cell division. All productions are context-sensitive to capture diffusion of the activator and inhibitor. It is assumed that the main barrier for the diffusion are cell walls of width w. Production p_1 characterizes growth of vegetative cells ($a < a_{th}$), controlled by the growth rate r. A cell that reaches the maximum length of s_{max} divides into two unequal daughter cells, with the lengths controlled by constant $k < 0.5$. The respective positions of the longer and shorter cells depends on the polarity p of the mother cell, as described by productions p_2 and p_3. Increase of the concentration of the activator a to or above the threshold value a_{th} indicates the emergence of a heterocyst. According to production p_4, a heterocyst does not further elongate or divide. The equations for s', a', and h' govern the exponential elongation of the cells and the activator-inhibitor interactions [Mei82].

The operation of the model is illustrated in Figure 3. The vertical lines indicate the concentrations of the activator (above the filament) and inhibitor (below the filament) associated with each cell.

It is interesting from the historical perspective that the interactive model of Wilcox *et al.* [WMS73] and its subsequent L-system implementation [HP96] predicted the essential structure of the gene regulation network that controls the development of *Anabaena* filaments in nature [Ada00]. The activator corresponds to the protein HetR, which plays a key role in the maintenance of the heterocyst state, whereas the inhibitor corresponds to the protein PatS (or a fragment of it), which diffuses across the filament and maintains the spacing between the heterocysts. The character of interactions captured by the simulation model is consistent with the postulated structure of the gene regulation network, in which HetR upregulates its own production as well as the production of PatS, whereas PatS downregulates production of HetR.

We believe that models of similar nature, integrating the action of genes into developmental models of multicellular structures, will become more widely used in the future, offering insights into

developmental processes that are difficult to obtain through observations and qualitative reasoning alone.

5 The MGS Approach

5.1 Motivations and Background

The previous examples of formalisms do not fully address issues of structural interactions between entities or system parts because of the *lack of topological organization*. The need to represent more structured organizations (than sequence or multiset) of entities and their interactions has been already stressed [FMP00] and motivates several extensions of rewriting (see for one example amongst others [BH00]). However, a general drawback with these extensions is that they work with a fixed topology of entities, and it is not obvious at all how to extend this to systems where the relationships between entities are drastically changing. This is precisely one of the main motivations of the MGS research project[2].

MGS is aimed at the representation and manipulation of local transformations of entities structured by *abstract topologies* [GM01b, GM02]. A set of entities organized by an abstract topology is called a *topological collection*. Topological means here that each collection type defines a neighborhood relation specifying both the notion of *locality* and the notion of *sub-collection*. The collection types can range in MGS from totally unstructured with sets and multisets to more structured with sequences and GBFs [GMS95, Mic96, GM01a] (other topologies are currently under development and include Voronoï partitions and arbitrary combinatorial neighborhoods).

The *global transformation* of a topological collection C consists in the parallel application of a set of *local transformations*. A local transformation is specified by a rewriting rule r that specifies the change of a sub-collection. A rewrite rule r:

1. selects a sub-collection A in C,
2. computes a new collection B as a function f of A and its neighbors,
3. and specifies the insertion of B in place of A into C.

These steps are summarized in figures 4 and 5. The topology of B depends on f and can be different from the topology of A. For example, a set in a sequence can be replaced by a sequence. Moreover, the topological structure of C can be changed through the application of transformations. These features enables the modeling of $(\text{DS})^2$: states of a DS are represented by collections and transformations are used to model transition functions on these structured states.

As a programming language based on topological concepts, MGS integrates the idea of topological collections and their transformations into a general high-level functional programming language: topological collections are just new kinds of values and transformations are functions acting on collections. The approach is purely declarative: operators acting on values combine values to give new values, they do not act by side-effect.

[2] MGS is the acronym of "*(encore) un Modèle Géneral de Simulation (de système dynamique)*" (yet another General Model for the Simulation of dynamical systems). The MGS home page is located at url `www.lami.univ-evry.fr/mgs` where additional informations are available.

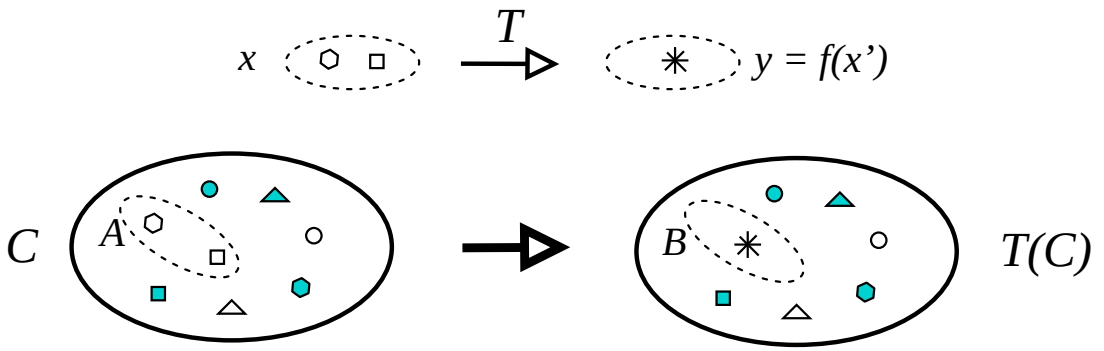

Figure 4: A basic transformation of a topological collection. Collection C is of some kind (set, sequence, array, cyclic grid, tree, term, etc). A rule T specifies that a sub-collection A of C has to be substituted by a collection B computed from A. The right hand side of the rule is computed from the sub-collection matched by the left hand side x and its possible neighbors x' in the collection C.

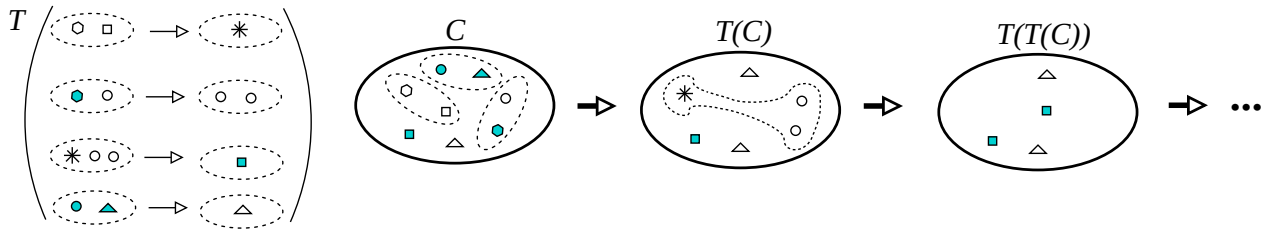

Figure 5: Transformation and iteration of a transformation. A transformation T is a set of basic transformations applied synchronously to make one evolution step. The basic transformations do not interact together. A transformation is then iterated to build the successive states of the system.

5.2 Biological Examples in MGS

In this subsection, we sketch several examples in various domains to exemplify the versatility of the MGS formalism.

The Eden Model

We start with a simple model of growth sometimes called the Eden model (specifically, a type B Eden model) [Ede58]. The model has been used since the 1960's as a model for such things as tumor growth and growth of cities. In this model, a 2D space is partitioned in empty or occupied cells (we use the white-space character and the C letter). We start with only one occupied cell. At each step, occupied cells with an empty neighbor are selected, and the corresponding empty cell is made occupied.

The corresponding MGS model starts by defining the 2D partition using a *group based field* (GBF in short). A GBF is an extension of the notion of array, where the elements are indexed by the elements of a group, called the *shape* of the GBF [GMS95, GM01a]. This kind of collection can be used to describe uniform and regular topologies. For example:

```
gbf Grid2 = < north, east >
```

defines a shape called *Grid2*, corresponding to the Von Neuman neighborhood in a classical array (a cell above, below, left or right – not diagonal). The two names `north` and `east` refer to the direc-

tions that can be followed to reach the neighbors of an element. These directions are the *generators* of the underlying group structure. The list of the generators can be completed by giving equations that constraint the displacement in the shape:

```
gbf Hexagon = < east, north, northeast ;
                east + north = northeast >
```

defines an hexagonal lattice that tiles the plane, see. figure 6. Each cell has six neighbors (following the three generators and their inverses). The equation `east + north = northeast` specifies that a move following `northeast` is the same has a move to `east` followed by a move to `north`.

The Eden's aggregation process is simply described as the following transformation:

```
trans Eden = {
    x,y / (x = "C") & (y = " ")  ⇒  x,"C";
}
```

the keyword `trans` introduce the rules of a transformation. A rule takes the following form:

$$pattern \Rightarrow expression$$

where *pattern* in the left hand side of the rule matches a sub-collection A of the collection C on which the transformation is applied. The sub-collection A is substituted in C by the collection B computed by the *expression* in the right hand side of the rule. Here, the pattern "`x,y`" filters an element y neighbor of an element x such that the value of x is occupied and the value of y is empty. The conditions on the elements matched are given by the expression after the "`/`" operator and the comma operator "`,`" means that x and y must be neighbors. The right hand side specifies that the couple `x,y` matched by the left hand side must be replaced by a couple `x,"C"`.

The transformation *Eden* defines a function that can then be applied to compute the evolution of some initial state. One of the advantages of the `MGS` approach, is that this transformation can apply indifferently on grid or hexagonal lattices (or *any* other collection kind). The meaning of the neighborhood operator "`,`" in the pattern of a rule depends on the collection on which the transformation is applied.

It is interesting to compare transformations on GBFs with the genuine cellular automata (CA) formalism (see the corresponding chapter). There are several differences. The notion of GBF extends the usual square grid of CA to more general Cayley graphs. The pattern in a rule may match arbitrary domain, not only one cell as it is usually the case for CA. Moreover, the value of a cell can be arbitrary complex (even another GBF) and is not restricted to take a value in a finite set.

Restriction Enzymes

This example shows the ability to nest different topologies to achieve the modeling of a biological organization. We want to represent the action of a set of restriction enzymes on the DNA. The DNA structure is simplified as a sequence of letters `A`, `C`, `T` and `G`. The DNA strings are collected in a multiset. Thus we have to manipulate a multiset of sequences (this kind of nested structures has been proved useful in other areas, e.g. [LP02]).

A restriction enzyme is represented as a rule that splits the DNA strings; for instance a rule like:

```
EcoRI =  x+ as X,
         (cut+ as CUT / CUT = "G","A","A","T","T","C"),
         y+ as Y
      ⇒ (X, "G")::("A","A","T","T","C", Y)::seq:()
```

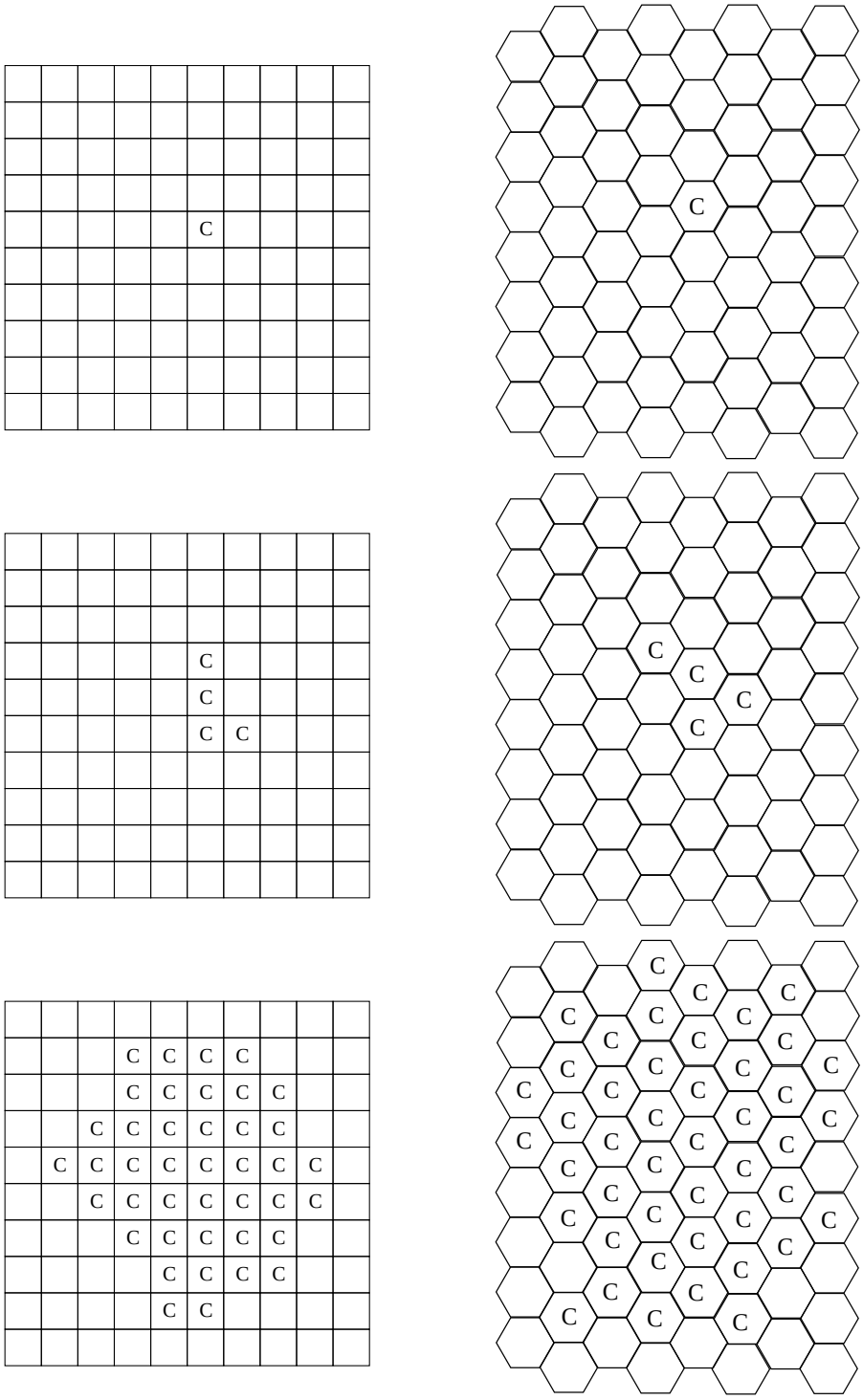

Figure 6: Eden's model on a grid and on an hexagonal mesh (initial state, and states after the 3 and the 7 time steps). The same transformation is used for both cases.

corresponds to the *EcoRI* restriction enzyme with recognition sequence G^AATTC (the point of cleavage is marked with ^). The x+ pattern filters the part of the DNA string before the recognition sequence and the result is named X (the + operator denotes repetition of neighbors). Identically, Y names the part of the string after the recognition sequence. The right hand side of the rule constructs

the two resulting parts as a sequence of two sequences (the `::` operator indicates the construction of a nested sequence).

We assume that all restrictions enzyme rules are collected into one transformation. We need an additional rule, called `Void` for specifying that a DNA string without recognition sequence must be inserted as such:

```
trans Restriction = {
    EcoRI = ...;
    ...;
    Void = x+ as X ={flat=false}=> X
}
```

The attribute "`flat=false`" in the body of the arrow of rule `Void` indicates that the X (which is a sequence) must be inserted in the resulting multiset as one single entity. This contrasts with the rule `EcoRi` whose right hand side computes a sequence of elements to be inserted in the enclosing multiset.

The transformation *Restriction* can then be applied to the DNA strings floating in a multiset using the simple transformation:

```
trans Apply = { dna ⇒ Restriction(dna) }
```

A Localized Signaling Network

At last but not least, we want to sketch the modeling of a spatially distributed biochemical network in `MGS`. We rely on a model proposed by A. E. Bugrim [Bug00]. The example focuses on a small signaling network that consists of cAMP and calcium signaling. See figure 7 for a more complete description.

The corresponding topological structure mimics the spatial organization of the cell using nested multisets, see figure 8. The `MGS` declarations:

```
collection Volume = bag;
collection Membrane = bag;
collection Environment = Volume;
collection Plasma = Membrane;
collection Cytosol = Volume;
collection EndoRetic = Membrane;
```

are used to introduce some new kinds of multisets (the `bag` keyword). This kinds are used here mainly do describe the hierarchy of localization and compartments and can be used, if necessary, to discriminate between multisets.

The main part of the corresponding `MGS` program consists in defining the ontology of this application domain: there exists several molecules, each have a name; some exists in two state: active or inactive; some are characterized as receptors; etc. Such ontology is described in `MGS` using *subtyping*. These subtypes are then used in pattern-matching to select entities with or without some properties. For example, a molecule is described as a record having or not some fields. Record type in `MGS` may specify the presence or the absence of a field, or the value of a specific field. For instance:

```
state Molecule = {name};
state Activity = {activation};
```

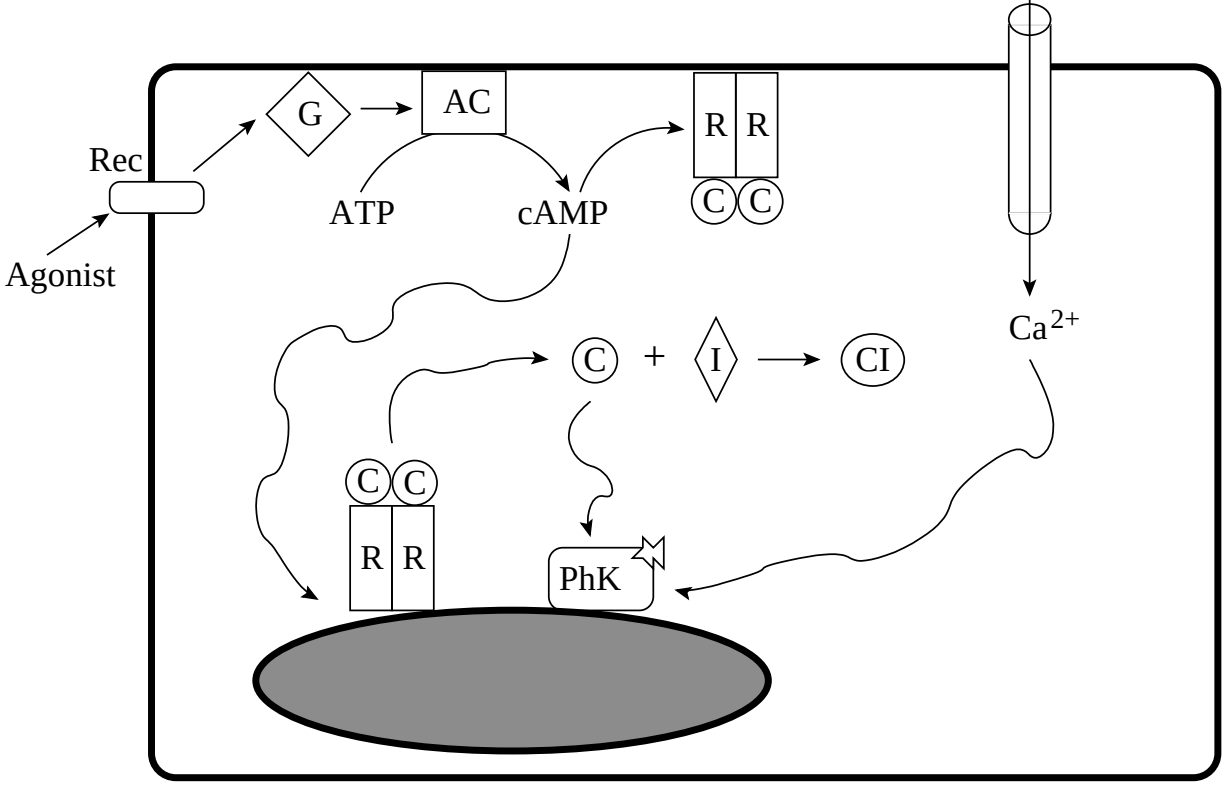

Figure 7: *cAMP and calcium signaling pathways* (this schema is reprinted from [Bug00]). The different components of the two pathways are localized at various places within the cell.
The first steps of the cAMP pathway occur at the plasma membrane, starting with the activation of adrenegric receptors. Then, the cAMP molecules bind to a regulatory sub-unit of the protein kinase A, with the effect of dissociating a catalytic sub-unit C. The localization of PKA depends of a family of anchoring proteins AKAPs that target this kinase to different compartments. In this example, two localizations are considered: the plasma membrane and an internal compartment (e.g., nucleus or ER).
The calcium pathway starts by the activation of a channel in the plasma membrane. The fraction of PhK associated to the internal compartment is the target of both pathways. A possible inhibitor I of PKA is also considered.

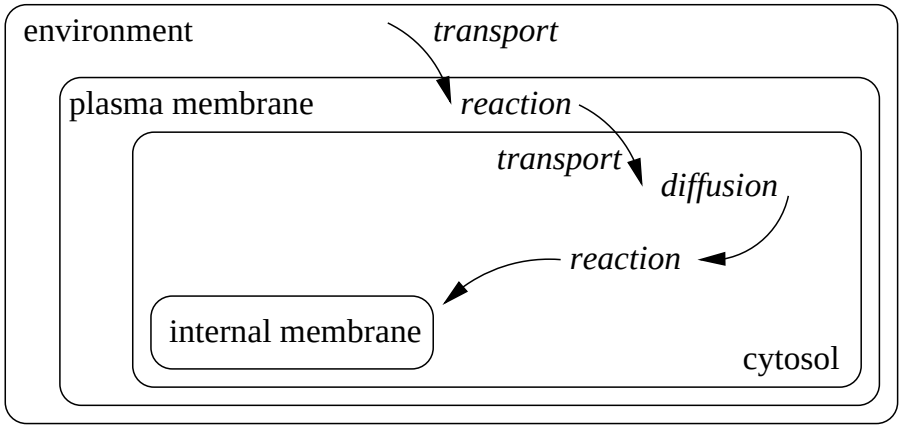

Figure 8: The reaction, diffusion and transport processes described in figure 7 are modeled as multiset transformations taking place in a nest of multisets. This is reminiscent of the P system approach, see section 3.

```
state Activated = {activation = 1};
state Inactivated = {activation = 0};
state ATP = Molecule + {name = "atp"};
```

define five record types. The record type declaration is introduced by the keyword `state`. *Molecule* is the type of any record having at least a field named `name`. *Activated* is the type of a record having at least a field named `activation` and with value `1`. This type is a subtype of *Activity* which only requires the presence of the field `activation`. The type *ATP* corresponds to a molecule named `"atp"`.

Three kinds of transformations are used to define the processes of the Bugrim's model. The first class corresponds to some ancillary transformations. For example

```
trans ActivateReceptor = { r:Receptor → r + {activation=1} }
```

is a rule that updates to `1` the field `activation` of an entity r of type *Receptor*. This kind of transformations is triggered by a rule of the sole transformation of the second class. This transformation summarize all the rule corresponding of the description of the biochemistry (they are about 10 reactions in this pathway):

```
trans Biochemistry = {
    R1 = a:ActiveAgonist, p:Plasma
        ⇒ a+{activation=0},ActivateReceptor(p);
    ...
}
```

For example, rule `R1` specifies that an active agonist and a plasma membrane interact to inactivate the agonist and to transform the plasma with transformation *ActivateReceptor* (this transformation turn on all the activation fields of the receptors anchored in the plasma membrane).

There is also only one transformation in the last class of transformations. It is used to thread the biochemistry rules amongst the nested multisets:

```
fun Run(x) = Thread(Biochemistry(x));
trans Thread = {
    p:Membrane ⇒ Run(p);
    c:Volume ⇒ Run(c);
}
```

The transformation *Thread* applies the function *Run* to each entity of type *Membrane* or *Volume* found in the collection argument. The function *Run* consists in running the biochemistry transformation and then iterating the threading.

The complete `MGS` program is approximatively 150 line long, including the building of the initial system state. It describes 40 molecules in diverse states, uses of 5 auxiliary transformation to define 10 chemical interactions.

6 Multiscale graphs

The previous formalisms have been used to model the changes of structure that arise throughout time. However, biological structures may change also due to a change in the scale of observations.

On the one hand, plants appear as complex structures due to the intrication of many sub-structures at various levels of detail. On the other hand, plants are essentially spatially and temporally periodic structures which gives an overall impression of simplicity. In such a paradoxical situation, the question arises: what mathematical formalisms and what tools are necessary to model plants at several scales ?

In this chapter, we analyse how biological systems, such as plants, can be formally represented with combinatorial formalisms (see section 2). We particularly analyze how this formalism must be designed in order to account for a new dimension, namely the scale dimension. We then briefly describe the types of mathematical and computational tools that must be developed in this context.

6.1 Plants as modular organisms

The growth of a plant can be depicted as the result of two growth processes. This *apical growth process* gives the plant the ability to develop in one direction. During their activity, shoot meristems can give birth to distinct embryogenic cellular areas (always associated with corresponding leaves), called axillary or lateral meristems. This defines the *branching process*. Plants make branching structures if the meristems located at leaf axils enter an apical growth process. Using the branching process, plants can develop shoots in more than one direction. The overall *growth process* is thus the combination of both the apical growth process and the branching process. Growth is a fundamentally repetitive process which creates various forms of patterns repeated as "modules" throughout the plant structure ([HRW86], [Bar91]). Figure 9 illustrates different types of modules that can be observed on plants.

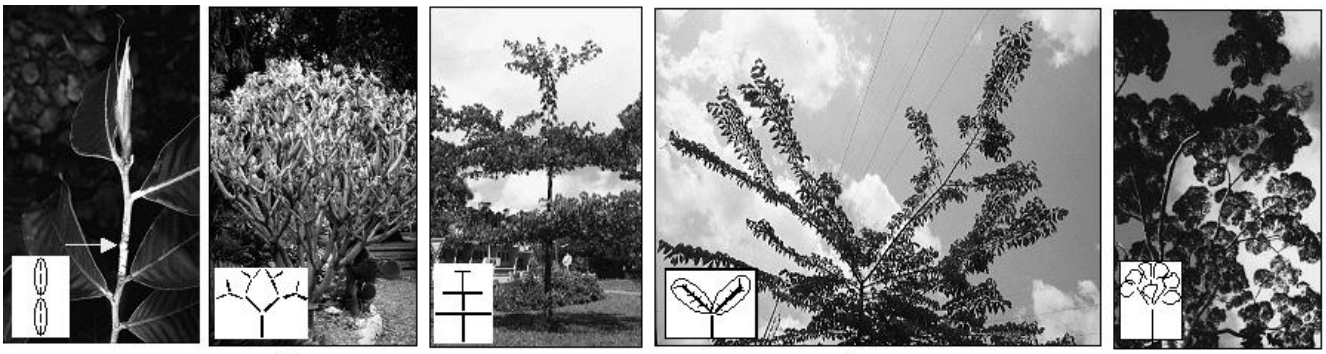

Figure 9: Different types of modularity in plants. a. nodes b. axes c. whorls d. branching systems e. crownlets

For a given type of module, the plant can be split-up into a set of modules of this type. This defines a particular plant modularity. A plant modularity, is caracterised by the type of modules considered and their adjacency within the plant. This information can be represented by a *directed graph*.

A directed graph is defined by a set of objects, called vertices, and a binary relation between these vertices. The binary relation defines a set of ordered pair of vertices, called edges. In plant representations, vertices represent botanical entities and edges adjacency between these entities. Edges are always directed from oldest entities to youngest ones. Given an edge (a, b), we say that a is a *father* of b and b is a *son* of a. Directed graphs representing plants have tree-like structures : every vertex, except one, called the root, has exactly one father vertex. Morevover, in order to identify the different axes of a given plant, two types of connections are distinguished : an entity can either precede (type '$<$') or bear (type '+') another entity (Figure 10). In order to describe different characteristics of

plant entities, vertices can have attributes, e.g. length, diameter, spatial location, leaf area, number of flowers, type of branched entities, *etc*.

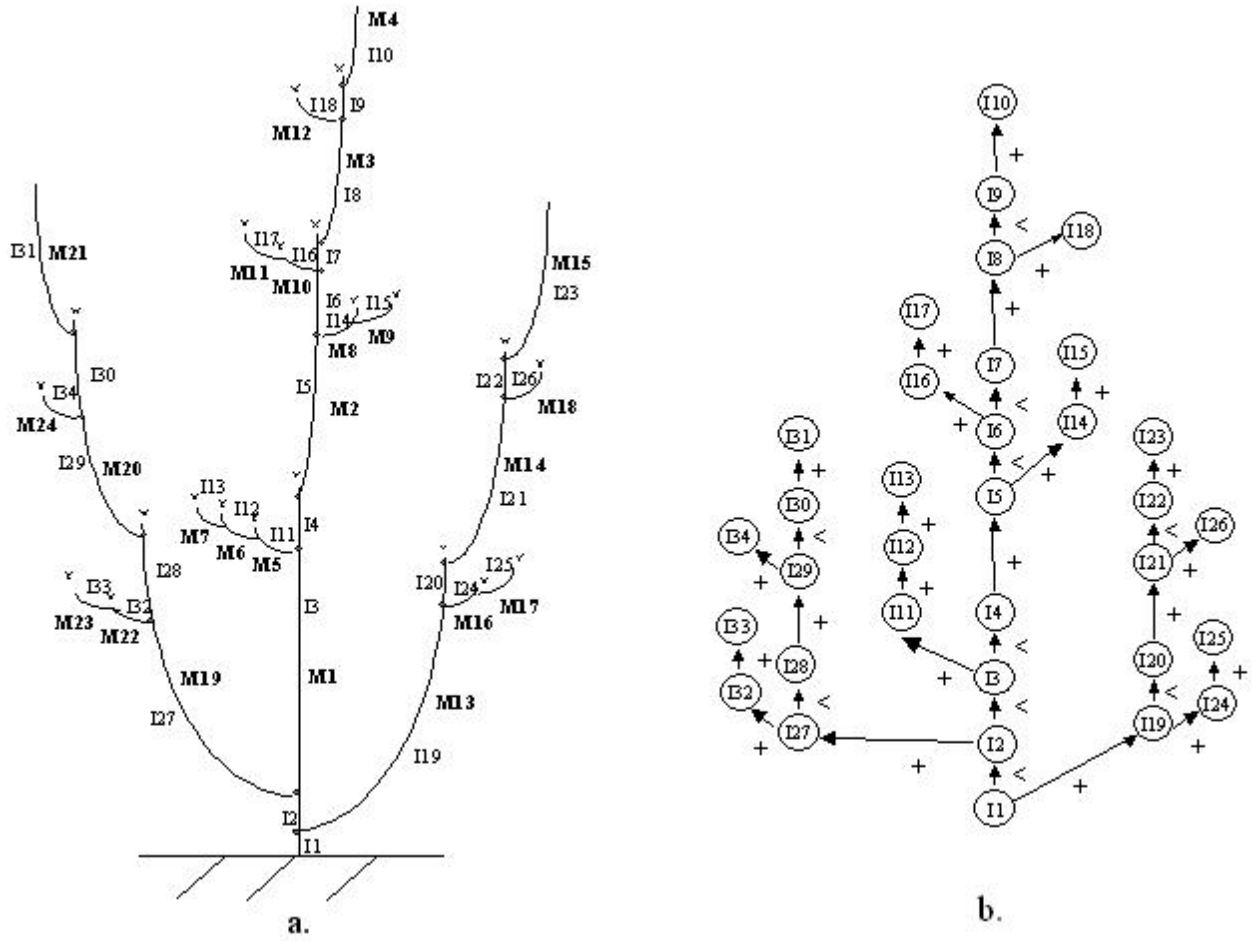

Figure 10: a. A tree b. The tree graph representation of its topology (at node scale)

6.2 Multiscale representations

Many modularities can exist on a single individual. Several types of modularity, stemming from either natural or artificial decomposition of the plant into modules, can exist within a single individual at the same time. For above-ground systems, at least the nodal (the plant is a set of leaves) and the axial modularity (the plant is a set of axes) coexist. If, in addition, the plant reiterates, a modularity by reiteration is superimposed on the previous ones. Thus, there always exist two or three types of modularities expressed in a plant simultaneously. There can be more, depending on the number of regular fluctuations that characterize the plant growth. This is the case, for example, for plants containing growth unit or annual shoot modules. These types of module can exist simultaneously in a plant, such as in apricot tree, evergreen oak or Aleppo pine. For a single plant, there is thus the theoretical possibility of finding numerous types of modularity, each one corresponding to a particular topological interpretation of the plant.

The existence of several modularities on the same plant can be illustrated by *Vochysia guyanensis* [San92]. For this plant, the number of modularities stemming from natural decomposition is relatively high. The highest scale corresponds to the description of the topological structure in terms of

internodes. At a lower scale, the rhythmic elongation of stems produces an alternate sequence of cataphylls and developed leaves which enables the observer to define growth unit modules (11.a). The final stopping of stem elongation, due to the death of their apical meristem, makes it possible to group growth units into axes (11.a). The architectural unit of the young tree consists of a stack of such axes (11.b). The plant continues its development by reiterating its architectural unit. The resulting topological structure is described in terms of reiterated complexes. Eventually, at the lowest scale, the crown of the adult tree is a set of crownlets, each of them made of reiterated complexes (11.c). The plant can thus be represented by a specific topological structure for each possible scale. The set of these topological structures defined at every scale and their relations characterizes the overall topological structure of the plant, *i.e. multiscale topological structure* of the plant.

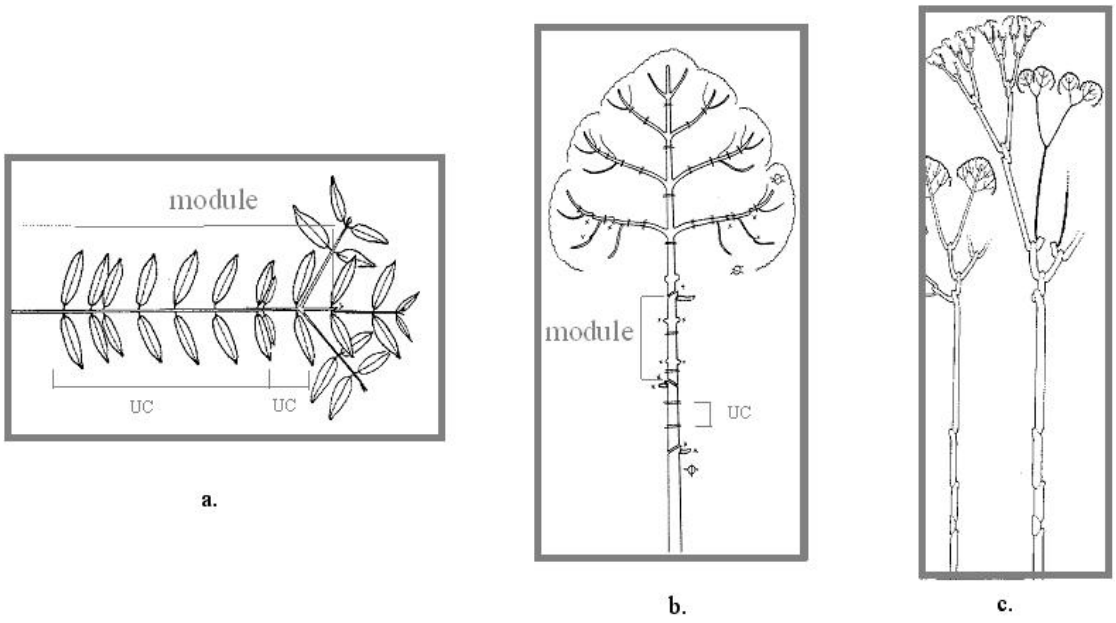

Figure 11: Nested modularities: a. nodes, growth units and axes. b. Architectural unit c. crowlets.

To formally represent the multi-modular structure of plants, extension od directed graphs, called multiscale tree graphs (MTGs) [GC98], are used. The MTG formalism has been designed in order to enable users to express both the modularity and the multiscale nature of plant structures. Each scale of analysis corresponds to a modular structure which can be formally represented by a tree graph. Entities at one scale are decomposed into entities at finer scales. For instance, internodes of Figure 10.a can be grouped into growth units, leading to a more macroscopic description of the plant topology (Figure 12).

A MTG integrates in a homogeneous framework the different tree graphs corresponding to plant descriptions at different scales (Figure 13.a). Vertices at one scale are composed of vertices at a higher scale. If an entity a is composed of n entities $x_1, x_2, ..., x_n$, for every $i \in [1, n]$, a is called the *complex* of x_i, and x_i is a *component* of a. The complex of any entity x_i is denoted $\pi(x_i)$. If the scale of a is defined by the integer s, then for every $i \in [1, n]$, the scale of x_i is $s + 1$. The most macroscopic scale s_0 consists of a single vertex, representing the entire plant, and by convention has value 0. In order to maintain coherence between the different tree graph representations of a same individual, MTGs must respect the following consistency constraint : if there exists an edge (x, y) in the tree graph representing the plant structure at scale $s + 1$, and if the complexes of x and y are different, then there necessarily exists a corresponding edge $(\pi(x), \pi(y))$ between these complexes in the tree

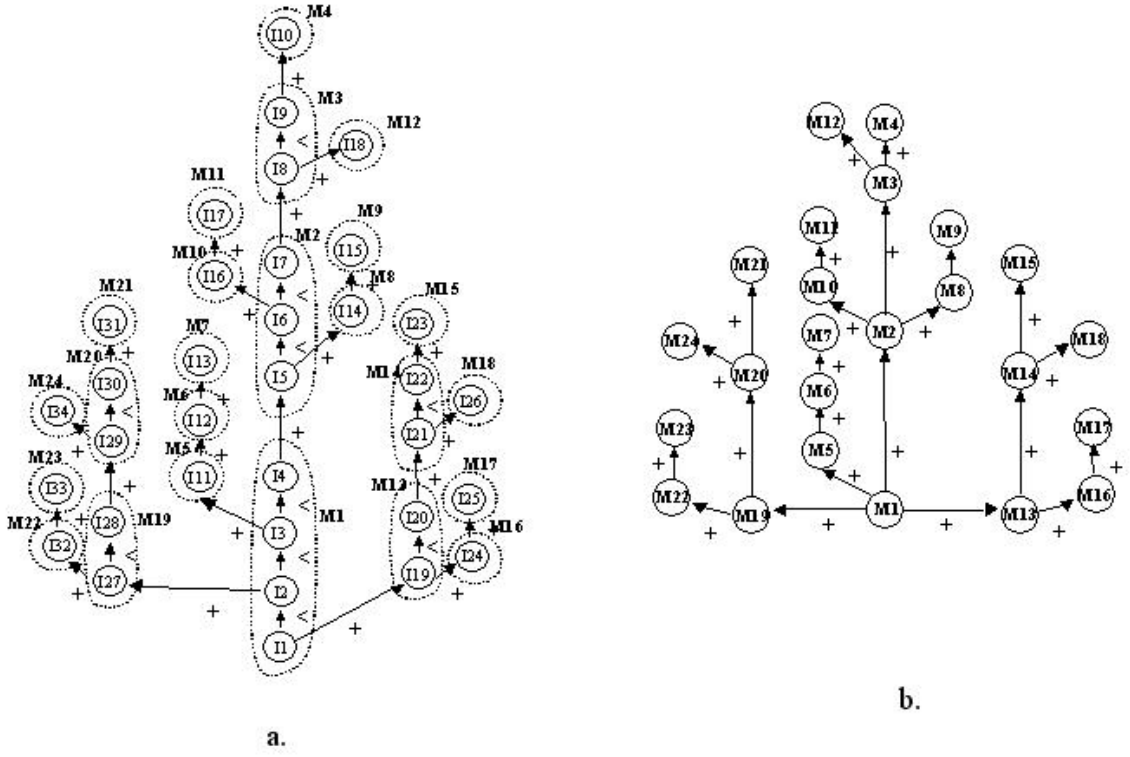

Figure 12: a. Partitionning graph of Figure 10 into growth units (M). b. Topology of the plant at scale M.

graph representing the plant at scale s (Figure 13.b) This expresses that the connection between two macroentities results from the connection between two of their components.

6.3 Space of modularities

From a structural point of view, the relative position of two modularities in a plant can be of two types.

- Firstly, one modularity is a refinement of the other (Figure 14.a). For example, a topological structure represented in terms of growth units can be refined by considering the plant decomposition in terms of internodes. Each growth unit is considered as a set of internodes. Similarly, the axis structure of a plant can be interpreted as a refinement of the plant description in terms of branching systems, since each branching system can be decomposed into a set of axes. Hence, one modularity is a refinement of another if each module of the second can be decomposed into a set of modules of the first and, reciprocally, each module of the first modularity is a part of a module of the second. These modularities correspond to two topological structures representing the plant at two different *scales*. The highest scale corresponds to the finest modularity, while the lowest scale corresponds to the coarsest modularity. Within a plant representation, the scale of internodes is higher than the scale of growth units which is itself higher than the scale of axes.

- Secondly, the two modularities are not a refinement of eachother : they are overlapping (Figure 14.b). This is the case if at least one module of one modularity shares a common part with one module of the second modularity, whereas there is no inclusion of one into the other. Let us

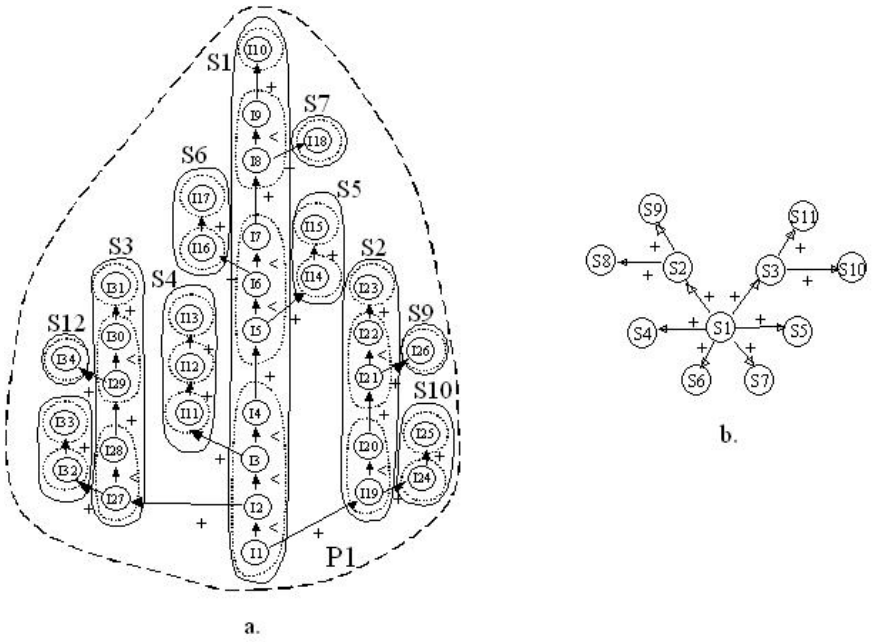

Figure 13: a. Multiscale graph corresponding to tree of Figure 10. b. corresponding topology at S module scale.

consider for example the topological structure of an apple tree in terms of both annual shoots and axes (14.b). At the beginning of the vegetative period, the apical meristem of some branches produces short shoots terminated by a flower, called ”bourse”[CL95]. During a second phase of the vegetative period, a vegetative shoot may develop on some bourses. These are called ”bourse shoots”. A bourse shoot is part of the same annual shoot as the bourse, since it is created during the same vegetative period. Therefore, some annual shoots are made of a bourse bearing a bourse shoot. Such an annual shoot is thus straddling two axes : on one side the axis terminated by the bourse and on the other side, the axis which begins with the bourse shoot. Reciprocally, each axis is straddling two annual shoots. The modularities corresponding respectively to axes and annual shoots determine two topological interpretations of the plant which are not a refinement of eachother.

The different types of modularities that can be identified within a given plant define different topological structures. These modularities are *comparable* if they are refinements of each other. The refinement relation expresses the existence of a decomposition relation between the modules of the coarsest modularity and those of the finest. In the opposite case, modularities are *incomparable*, i.e. none of them is a refinement of the other. No decomposition relation exists between the modules of both modularities since they overlap.

Now, if we consider a graph g and different partitionning of the vertices of this graph, representing different modularities (Figure 15.a). Let us assume that each modularity is represented by a square element (Figure 15.b), and an edge is drawn from modulatities A to modularity B whenever A is a refinement of B. The graph obtained from this process is a lattice :

Let g be a tree graph. Let $L(g)$ be the set of all partitions on g, such that the induced macroscopic graph (quotient graph) is a tree graph.

$L(g)$ is a lattice

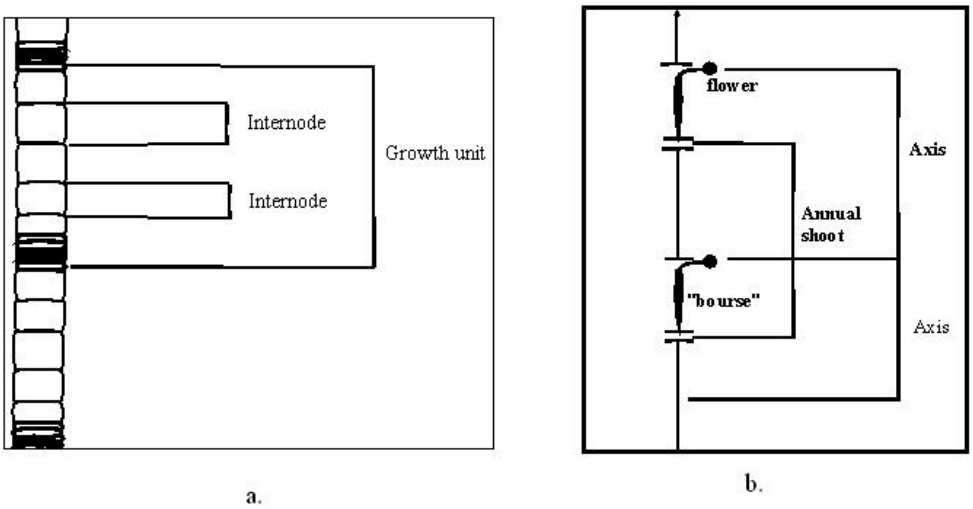

Figure 14: a. nested modularities. b. overlapping modularities

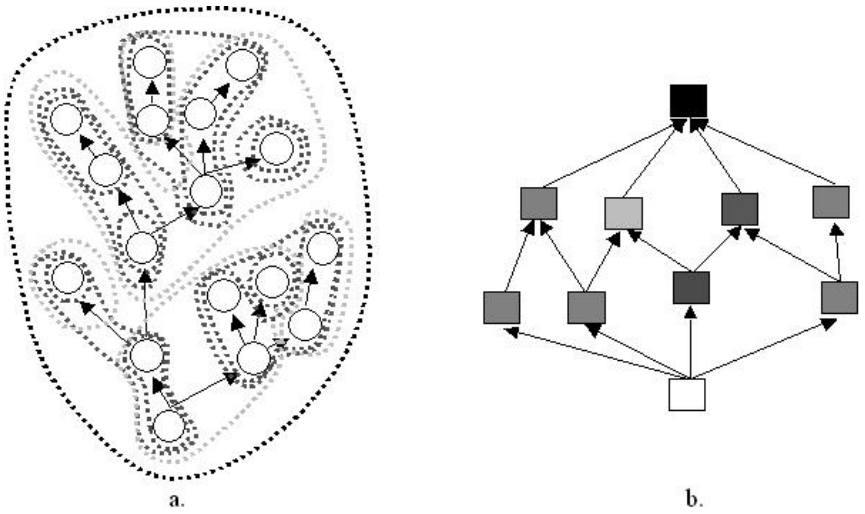

Figure 15: a. a general MTG. b. its corresponding modularity graph.

This proposition characterizes the space of all modularities that can be potentially defined on a given individual by a remarkable algebraic property : it is a sublattice of the partition lattice (the set of all subsets of a set). A multiscale graph is associated with only a subset of this sublattice. This subset corresponds to the set of modularities that are actually taken into consideration by the observer in the plant description. Multiscale graphs are thus a model of the observer's subjective interpretation of the plant.

6.4 Growing multiscale structures

From a temporal point of view, the analysis of the relations between the different types of modularities is a delicate issue. Indeed, whereas the growth of a topological structure at a given scale seems to be a relatively clear phenomenon, the simultaneous growth of different topological structures representing a given individual, at different scales, raises the problem of understanding how these growth processes are linked to each other [GC98]. Figure 16 illustrates such a problem.

Consider an adult tree bearing a well hierarchized crown (16, date t_1). At a subsequent date t_2, a

possible development of the crown may preserve the original hierarchy of branches. Another possible development is that one of the branches starts to compete with the trunk, yielding a reiterated complex (16 dates t_1 and t_2). This phenomenon can be interpreted in terms of MTGs (lower part of 16) if we assume that a component can belong to different complex entities throughout time.

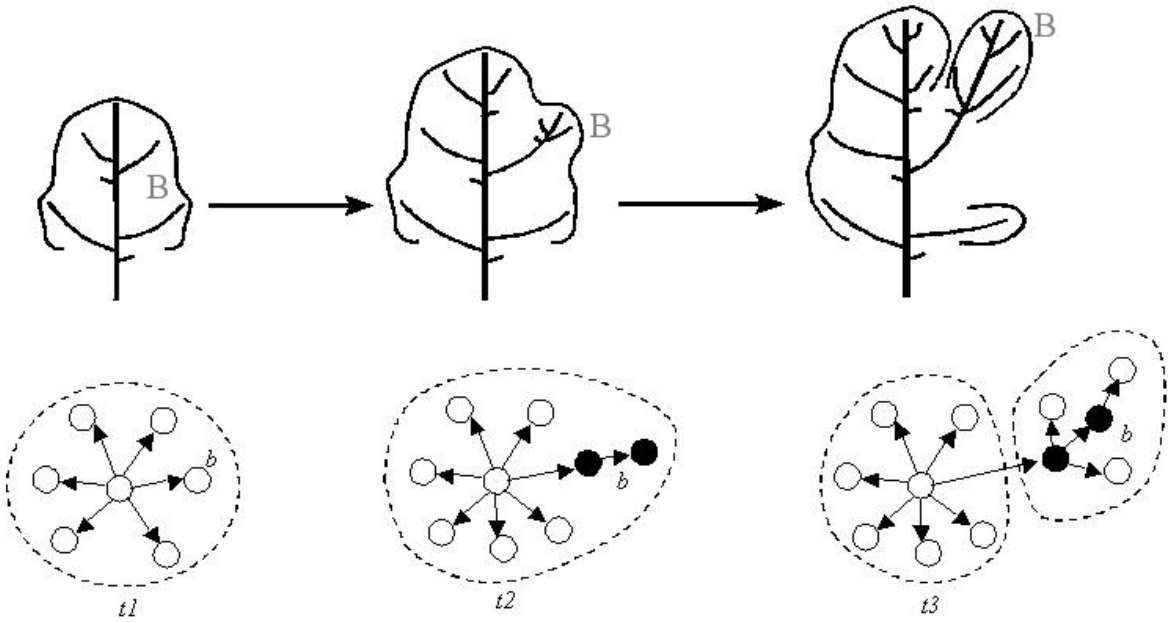

Figure 16: a. (upper part) reiterated complex is produced througout time. b. (lower part) Corresponding MTG interpretation

The growth of a multiscale structure illustrates an important aspect of the model : rather than an objective plant topological structure, defined once and for all, a time-varying multiscale graph actually represents the plant topological structure as a subjective object depending on the observer's goals, knowledge and means of observation.

6.5 Handling plant architecture databases

Multiscale tree graphs are currently used as the backbone of a general methodology for measuring and analyzing plant topological structures, implemented in the AMAPmod software [GGC99]. Real plants are encoded by the observer using a specific coding language designed for this purpose. The multiscale plant topological structure can then be loaded into the computer. A set of dedicated tools, gathered in the AMAPmod software, enable the user to access these virtual plants and to explore them. They provide users with a methodology and corresponding tools to measure plants, create plant databases, analyse information extracted from these databases. This methodology can be depicted as follows (Figure 17).

Multiscale representation of plant architectures are described from either field observations or plant growth simulation programs, using a dedicated encoding language. The resulting database can then be analysed with various statistical analysis tools (e.g. [GBCC01]). Plants can be graphically reconstructed at different scales and vizualised in 3 dimensions. Various types of data can be extracted and analysed with different viewpoints. Different families of probabilistic or stochastic models are provided in the system. These models are intended to be used as advanced statistical analysis tools for exploring in greater depth the information contained in the database. All these tools are available

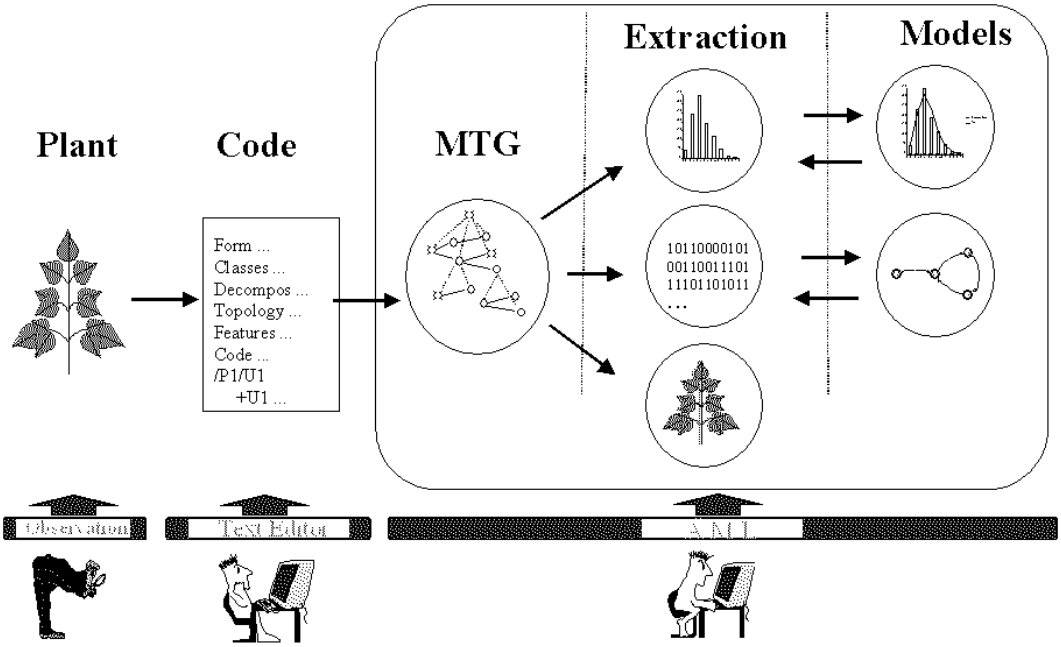

Figure 17: Synopsis of the AMAPmod system.

through a querying language called AML (AMAPmod Modelling Language) which enables the user to work on various objects, i.e. multiscale representation of plants, samples of data or models. AML provides the user with a homogeneous language-based interface to load, display, save, analyse or transform each type of object.

References

[Ada00] D. G. Adams. Heterocyst formation in cyanobacteria. *Current Opinoin in Microbiology*, 3:618–624, 2000.

[Bar91] D. Barthlmy. Levels of organization and repetition phenomena in seed plants. *Acta Biotheoretica*, 39:309–323, 1991.

[BB90] G. Berry and G. Boudol. The chemical abstract machine. In *Conf. Record 17th ACM Symp. on Principles of Programmming Languages, POPL'90, San Francisco, CA, USA, 17–19 Jan. 1990*, pages 81–94. ACM Press, New York, 1990.

[BCM87] J. P. Banatre, A. Coutant, and Daniel Le Metayer. Parallel machines for multiset transformation and their programming style. Technical Report RR-0759, Inria, 1987.

[BFM01] Jean-Pierre Banâtre, Pascal Fradet, and Daniel Le Métayer. Gamma and the chemical reaction model: Fifteen years after. *Lecture Notes in Computer Science*, 2235:17–??, 2001.

[BH70] R. Baker and G. T. Herman. CELIA — a cellular linear iterative array simulator. In *Proceedings of the Fourth Conference on Applications of Simulation* (9–11 December 1970), pages 64–73, 1970.

[BH72] R. Baker and G. T. Herman. Simulation of organisms using a developmental model, parts I and II. *International Journal of Bio-Medical Computing*, 3:201–215 and 251–267, 1972.

[BH00] Ronald Brown and Anne Heyworth. Using rewriting systems to compute left kan extensions and induced actions of categories. *Journal of Symbolic Computation*, 29(1):5–31, January 2000.

[BM86] J. P. Banatre and Daniel Le Metayer. A new computational model and its discipline of programming. Technical Report RR-0566, Inria, 1986.

[Bug00] A. Bugrim. A logic-based approach for computational analysis of spatially distributed biochemical networks. In *ISMB 2000*, San Diego California, August 2000.

[Cho56] N. Chomsky. Three models for the description of language. *IRE Trans. on Information Theory*, 2(3):113–124, 1956.

[Cho57] N. Chomsky, editor. *Syntactic structures*. Mouton & Co., The Hague, 1957.

[CL95] E. Costes and P. L. Lauri. Processus de croissance en relation avec la ramification sylleptique et la floraison chez pommier. In J. Bouchon, editor, *Architecture des Arbres Fruitiers et Forestiers*, volume 74, pages 41–50, Montpellier, France, 1995. INRA Editions.

[Dit00] P. Dittrich. Artificial chemistry page, 2000. `http://ls11-www.cs.uni-dortmund.de/achem`.

[DJ90] N. Dershowitz and J.-P. Jouannaud. *Handbook of Theoretical Computer Science*, volume B, chapter Rewrite systems, pages 244–320. Elsevier Science, 1990.

[dL87] C. G. de Koster and A. Lindenmayer. Discrete and continuous models for heterocyst differentiation in growing filaments of blue-green bacteria. *Acta Biotheoretica*, 36:249–273, 1987.

[DZB00] P. Dittrich, Jens Ziegler, and Wolfgang Banzhaf. Artificial chemistries - a review. *Artificial Life*, 2000. (to be submitted, available from the authors).

[Ede58] M. Eden. In H. P. Yockey, editor, *Symposium on Information Theory in Biology*, page 359, New York, 1958. Pergamon Press.

[ela02] Elan home page, 2002. `http://www.loria.fr/equipes/protheo/SOFTWARES/ELAN/`.

[FMP00] Michael Fisher, Grant Malcolm, and Raymond Paton. Spatio-logical processes in intracellular signalling. *BioSystems*, 55:83–92, 2000.

[GBCC01] Y. Gudon, D. Barthlmy, Y. Caraglio, and E. Costes. Pattern analysis in branching and axillary flowering sequences. *Journal of Theoretical Biology*, 212:481–520, 2001.

[GC98] C. Godin and Y. Caraglio. A multiscale model of plant topological structures. *Journal of Theoretical Biology*, 191:1–46, 1998.

[GGC99] C. Godin, Y. Gudon, and E. Costes. Exploration of plant architecture databases with the AMAPmod software illustrated on an apple-tree hybrid family. *Agronomie*, 19(03-avr):163–184, 1999.

[GM01a] J.-L. Giavitto and O. Michel. Declarative definition of group indexed data structures and approximation of their domains. In *Proceedings of the 3nd International ACM SIGPLAN Conference on Principles and Practice of Declarative Programming (PPDP-01)*. ACM Press, September 2001.

[GM01b] J.-L. Giavitto and O. Michel. MGS: A programming language for the transformation of topological collections. Research Report 61-2001, CNRS - Université d'Evry Val d'Esonne, Evry, France, 2001.

[GM02] J.-L. Giavitto and O. Michel. The topological structures of membrane computing. *Fundamenta Informaticae*, 49:107–129, 2002.

[GMS95] J.-L. Giavitto, O. Michel, and J.-P. Sansonnet. Group based fields. In I. Takayasu, R. H. Jr. Halstead, and C. Queinnec, editors, *Parallel Symbolic Languages and Systems (International Workshop PSLS'95)*, volume 1068 of *Lecture Notes in Computer Sciences*, pages 209–215, Beaune (France), 2–4 October 1995. Springer-Verlag.

[GV01] J.-L. Giavitto and E. Valencia. *Diagrammatic Representation and Reasonning*, chapter A Topological Framework for Modeling Diagrammatic Reasoning Tasks. Springer-Verlag, 2001.

[Han92] J. S. Hanan. *Parametric L-systems and their application to the modelling and visualization of plants*. PhD thesis, University of Regina, June 1992.

[HP96] M. Hammel and P. Prusinkiewicz. Visualization of developmental processes by extrusion in space-time. In *Proceedings of Graphics Interface '96*, pages 246–258, 1996.

[HR75] G. T. Herman and G. Rozenberg. *Developmental systems and languages.* North-Holland, Amsterdam, 1975.

[HRW86] J. L. Harper, B. R. Rosen, and J. White. *The growth and form of modular organisms*. The Royal Society, "London, UK", 1986.

[Jef85] D. Jefferson. Virtual time. *ACM Transactions on Programming Languages and Systems*, 7(3):404–425, July 1985.

[JTN00] K. Chen J.J. Tyson, M.T. Borisuk and B. Novak. *Computational Modeling of Genetic and Biochemical Networks*, chapter Analysis of Complex Dynamics in Cell Cycle Regulation, pages 287–306. MIT Press, 2000.

[Kan00] Minoru Kanehisa. *Post-genome informatics*. Oxford University Press, 2000. ISBN 0-19-850326-1.

[Kau95] S Kaufman. *The Origins of Order: Self-Organization and Selection in Evolution*. Oxford University Press, 1995.

[Kel95] Evelyn Fox Kelle. *Refiguring Life: Metaphors of Twentieth-century Biology*. Columbia University Press, 1995.

[Kre86] W. Kreutzer. *System simulation: Programming styles and languages*. Addison-Wesley, Sydney, 1986.

[LIL89] C. Langton, L. In, and C. Langton. Artificial life, 1989.

[Lin68] A. Lindenmayer. Mathematical models for cellular interaction in development, Parts I and II. *Journal of Theoretical Biology*, 18:280–315, 1968.

[Lin71] A. Lindenmayer. Developmental systems without cellular interaction, their languages and grammars. *Journal of Theoretical Biology*, 30:455–484, 1971.

[Lin74] A. Lindenmayer. Adding continuous components to L-systems. In G. Rozenberg and A. Salomaa, editors, *L Systems*, Lecture Notes in Computer Science 15, pages 53–68. Springer-Verlag, Berlin, 1974.

[LP02] Brendav Lane and Przemek Prusinkiewicz. Specifying spatial distributions for multilevel models of plant communities. In *proc. of Graphics Interface 2002*, 2002.

[Lyn96] N. A. Lynch. *Distributed algorithms*. Morgan Kauffman, Los Altos, CA, 1996.

[Man01] Vincenzo Manca. Logical string rewriting. *Theoretical Computer Science*, 264:25–51, 2001.

[mau02] Maude home page, 2002. `http://maude.csl.sri.com/`.

[May75] R. M. May. Biological population models obeying difference equations: Stable points, stalbe cycles, and chaos. *Journal of Theoretical Biology*, 51:511–524, 1975.

[May76] R. M. May. Simple mathematical models with very complicated dynamics. *Nature*, 261:459–467, 1976.

[Mei82] H. Meinhardt. *Models of biological pattern formation*. Academic Press, New York, 1982.

[Mic96] O. Michel. *Reprsentations dynamiques de l'espace dans un langage dclaratif de simulation*. PhD thesis, Universit de Paris-Sud, centre d'Orsay, December 1996. N°4596, (in french).

[Pat94] Ray Paton, editor. *Computing With Biological Metaphors*. Chapman & Hall, 1994.

[Pau98a] Gheorge Paun, editor. *Computing with Bio-Molecules: Theory and Experiments*. Springer, 1998.

[Pau98b] Gheorghe Paun. Computing with membranes. Technical Report TUCS-TR-208, TUCS - Turku Centre for Computer Science, November 11 1998.

[Pau00] G. Paun. From cells to computers: Computing with membranes (p systems). In *Workshop on Grammar Systems*, Bad Ischl, austria, July 2000.

[PH90] P. Prusinkiewicz and J. Hanan. Visualization of botanical structures and processes using parametric L-systems. In D. Thalmann, editor, *Scientific visualization and graphics simulation*, pages 183–201. J. Wiley & Sons, Chichester, 1990.

[PJS92] H.-O. Peitgen, H. J urgens, and D. Saupe, editors. *Chaos and fractals. New frontiers of science*. Springer-Verlag, New York, 1992.

[PL90] P. Prusinkiewicz and A. Lindenmayer. *The algorithmic beauty of plants*. Springer-Verlag, New York, 1990. With J. S. Hanan, F. D. Fracchia, D. R. Fowler, M. J. M. de Boer, and L. Mercer.

[Pru98] P. Prusinkiewicz. Modeling of spatial structure and development of plants: a review. *Scientia Horticulturae*, 74:113–149, 1998.

[Pru99] P. Prusinkiewicz. A look at the visual modeling of plants using L-systems. *Agronomie*, 19:211–224, 1999.

[San92] E. Sanoja. *Essai d'application de l'architecture vgtale la systmatique. L'exemple de la famille des Vochysiaceae*. PhD thesis, USTL Montpellier France, 1992.

[Smi99] John Maynard Smith. *Shaping Life: Genes, Embryos and Evolution*. Yale University Press, 1999.

[Ste88] Isabelle Stengers. *D'une science l'autre. Les concepts nomades*. Le Seuil, 1988.

[TM87] T. Toffoli and N. Margolus. *Cellular automata machines: a new environment for modeling*. MIT Press, Cambridge, 1987.

[VN66] J. Von Neumann. *Theory of Self-Reproducing Automata*. Univ. of Illinois Press, 1966.

[WMS73] M. Wilcox, G. J. Mitchison, and R. J. Smith. Pattern formation in the blue-green alga, *Anabaena*. I. Basic mechanisms. *Journal of Cell Science*, 12:707–723, 1973.

Cellular Automata, Reaction-Diffusion and Multiagents Systems for Artificial Cell Modeling

Abdallah Zemirline[1], Pascal Ballet[1], Lionel Marcé[1], Patrick Amar[2,3], Gilles Bernot[2], Franck Delaplace[2], Jean-Louis Giavitto[2], Olivier Michel[2], Jean-Marc Delosme[2], Roberto Incitti[4], Paul Bourgine[5], Christophe Godin[6], François Képès[7] , Philippe Tracqui[8], Vic Norris[9], Janine Guespin[9], Maurice Demarty[9], Camille Ripoll[9]

[1] *EA2215, Département d'Informatique, Université de Bretagne Occidentale, Brest*

[2] *Laboratoire de Méthodes Informatiques, CNRS UMR 8042, Université d'Evry, 91025 Evry*

[3] *Laboratoire de Recherche en Informatique, CNRS UMR 8623, Université Paris-Sud, Orsay*

[4] Institut des Hautes Études Scientifiques, Bures, France & genopole®, Evry, France

[5] *CREA - Ecole Polytechnique*

[6] *UMR Cirad/Inra modélisation des plantes, TA40/PSII, Montpellier*

[7] *Atelier de Génomique Cognitive CNRS ESA8071/genopole, Evry*

[8] *Lab. TIMC-IMAG, Equipe DynaCell , CNRS UMR, 5525, Faculté de Médecine, La Tronche*

[9] *Laboratoire des Processus Intégratifs Cellulaires, UPRESA CNRS 6037, Faculté des Sciences & Techniques , Université de Rouen, 76821, Mont-Saint-Aignan France*

Introduction

Objectives of the simulation

Simulation is the experiment on a model. A model represents a simplification of a real phenomenon. Only certain relevant parameters are taken into account and numerous others are untidy. The simulation of a model has sense only if its behavior is close to the real phenomenon, that is, if it can approach reality. So, by changing the parameter values of the model, the simulation allows to infer what would take place in reality under the influence of similar actions.

The simulation has various objectives. First, when the model is validated by the real experiment, the simulation allows to make numerous and accelerated experiments, with a very accurate parameter control. Secondly, if the model is incomplete or insufficient, the simulation allows to test hypotheses. In that case, it participates in the settling of the model. Numerous fields of research and industry use the simulation, either for the model development, for the product settling or either for the forecast of complex phenomena. Aeronautics, motorcar, economy, chemistry, meteorology, astrophysics, cosmology, nuclear physics or more recently biology use it frequently.

Simulation and biology

The in-vitro experiment, constitutes for biology the most wide-spread type of simulation. Cells are taken apart from an organism, then are studied outside, generally in a test tube. Around the beginning of the 20th century, Michaelis and Menten described the biochemical phenomenon of enzymatic reaction using differential equations. So, mathematical models became an alternative to in-vivo or in-vitro experiments. This is the start of the computational biology. Several biological fields of research use the mathematical tool to describe or explain their phenomenon. For example, in 1966 the first mathematical model describing an immune phenomenon was developed [HEG66]. A few years later, by 1970 , the

immune models based on differential equations became more complex. In 1974, Jerne [JER74] described his model of the idiotypic network. His model is highly non linear and no simple analytical solution can be found. The use of the numeric computation then became a necessity. At the same time, data processing evolves, both from the point of view of the calculation power and from the languages of development. Several paradigms appear like artificial life, cellular automata, reaction-diffusion system, object programming or multi-agents system. Thus, it becomes possible to model and to simulate biological mechanisms not by using differential equations only.

Today, data processing is a useful tool for biology and for the alive world exploration. We are convinced, and this course tries to show it, that the study of living cells can be made partially by means of computer, that is in-silico (also called in machina or in-virtuo). We will see how we can connect together different computational systems to build an artificial cell. Each system describes a level of detail for the cell (Table 1):

- reaction-diffusion system allows to model the lower granularity of the cell, that is ionic and small molecules (from Angstrom to nanometer)
- cellular automata represents the macromolecular level (few nanometers). Macro molecules are the basic components of hyperstructures
- multiagents system will be used to model the hyperstructure level (several nanometers).
- reaction-diffusion system could be used again to model some tissue morphogenesis. Perhaps, it could be use to model intra-cellular membrane too.

Biological Level	***Dimension***	***Model***
Ionic / Small molecules	10^{-10} m	Reaction - Diffusion System
Macromolecules	10^{-9} m	Cellular Automata
Hyperstructures & membranes	10^{-8} to 10^{-7} m	Multiagents System
Membrane & Tissues	10^{-7} m to 10^{-5} m	Reaction - Diffusion System

Table 1: different possible levels of granularity for an integrated artificial cell modeling

Before the description of the different approaches, we will see a short state-of-the-art in software tools aiming to simulate intra-cellular mechanisms. First, we will see the global objectives thanks to the Microbial Cell Project, then we will focus on two advanced software applications: electronic cell and virtual-cell.

Advanced applications

Principle

An advanced application in cell simulation offers software tools to model, simulate and interpret results. It must be used by biologists without any programming and it offers an intuitive interface. An advanced application must point out its own limitations, the robustness of the model parameters, the link between the model and the simulation and the results accuracy. An advanced application is integrated when it combines different means of modeling together.

We will see two applications that are integrated and advanced: e-cell [ECE01] and v-cell [VCE01]. They are based on a differential equation model (see example of Equation 1). The first one (e-cell) includes settled metabolic pathways which could be coupled with an

hypothetic biologist pathway model. The second one (v-cell) uses images (from microscopy) to put the simulation into the « real » image.

Integrated Project: Microbial Cell Project

From Notice 01-21; Advanced Modeling and Simulation of Biological Systems [MCP01]

" SUMMARY (January 2001): The Offices of Advanced Scientific Computing Research (ASCR) and Biological and Environmental Research (OBER) of the Office of Science (SC), U.S. Department of Energy, hereby announce interest in receiving applications for grants in support of computational modeling and simulation of biological systems.
The goal of this program is to enable the use of terascale computers to explore fundamental biological processes and predict the behavior of a broad range of protein interactions and molecular pathways in prokaryotic microbes of importance to DOE. This goal will be achieved through the creation of scientific simulation codes that are high performance, scalable to hundreds of nodes and thousands of processors, and able to evolve over time and be ported to future generations of high performance computers. The research efforts being sought under this Program Notice will take advantage of extensive information inferred from the complete DNA sequence, such as the genetics and the biochemical processes available for a well-characterized prokaryotic microbe; for example, Escherichia coli (E. coli). This notice encourages applications from the disciplines of applied mathematics and computer science in partnership with microbiology, molecular biology, biochemistry and structural and computational biology to combine information available on a well characterized prokaryotic microbe with advanced mathematics and computer science to enable this new understanding. This announcement is being issued in parallel with Program Notice 01-20, the Microbial Cell Project. Together, they represent a planned first step in an ambitious effort to understand the functions of the proteins in a prokaryotic microbial cell, to understand their interactions as they form pathways that carry out DOE-relevant activities, and to eventually build predictive models for microbial activities that address DOE mission needs.

Different goals of the project:
Goal 1: Identify and Characterize the Molecular Machines of Life -- the Multiprotein Complexes that Execute Cellular Functions and Govern Cell Form
Goal 2: Characterize Gene Regulatory Networks
Goal 3: Characterize the Functional Repertoire of Complex Microbial Communities in Their Natural Environments at the Molecular Level
Goal 4: Develop the Computational Methods and Capabilities to Advance Understanding of complex Biological Systems and Predict Their Behavior:

Category	Research Goal
Sequencing Informatics	➥Automated microbial genome assembly ➥Laboratory Information Management Systems (LIMS)
Sequence Annotation	➥Consistent gene finding, especially for translation start ➥Identification of operon and regulon regions ➥Promoter and ribosome binding-site recognition ➥Repressor and activator-site prediction
Structural Annotation	➥High-throughput automated protein-fold recognition ➥Comparative protein modeling from structure homologs ➥Modeling geometry of complexes from component proteins
Functional Annotation	➥Computational support for protein identification, post-translational modification, and expression ➥Protein-function inference from sequence homology, fold type, protein interactions, and expression

Category	Research Goal
	➓Methods for large-scale comparison of genome sequences ➓Mass spectrometry LIMS and analysis algorithms ➓Image analysis of protein interactions and dynamics
New Databases	➓Environmental microbial populations ➓Protein complexes and interactions ➓Protein expression and post-translational modification
Data Integration	➓Tools interoperation and database integration ➓Tools for multigene, multigenome comparisons ➓Automated linkage of gene/protein/function catalog to phylogenetic, structural, and metabolic relationships
Microbial Ecology Support	➓Statistical methods for analyzing environmental sampling ➓Sequence- and expression-data analysis from heterogeneous samples ➓Pathway inference from known pathways to new organisms and communities
Modeling and Simulations	➓Molecular simulations of protein function and macromolecular interactions ➓Development of computational tools for modeling biochemical pathways and cell processes ➓Implementation of computational tools ➓Structural modeling of protein variants ➓Computational tools for modeling complex microbial communities
Visualization	➓Methods for hierarchical display of biological data: (System level > Pathway > Multiprotein machines > Proteins > mRNA > Gene) ➓Displays of interspecies comparisons ➓Visualization by functional pathways (e.g., DNA repair, protein synthesis, cell-cycle control)

Technology Needs

The Human Genome Project taught that evolutionary improvement in existing technologies (e.g., DNA sequencing) can have a revolutionary impact on science. The systems approach taken by the Genomes to Life program dictates that existing technologies must evolve to a high-throughput capability. In addition, revolutionary technologies need to be developed, incorporating new modes of robotics and automation as well as advanced information and computing technologies. The following is a list of some key high-throughput technologies.

DNA, RNA, Protein, Protein Machine, and Functional Analyses and Imaging

· High-throughput identification of the components of protein complexes; mass spectrometry, new chip-based analyses, and capture assays
· Parallel, comparative, high-throughput identification of DNA fragments among microbial communities and for community characterization
· Whole-cell imaging; novel imaging technologies, including magnetic resonance optical, confocal,
· soft X-ray, and electron microscopy; and new approaches for in vivo mapping of spatial proximity
· New technologies for mapping contact surfaces between proteins involved in complexes or molecular machines (e.g., FRET and neutron scattering)

· Functional assays; development of novel technologies and approaches for defining the functions of genes from uncultured microorganisms

Sampling and Sample Production

· Approaches for recovering RNA and high-molecular-weight DNA from environmental samples and for isolating single cells of uncultured microorganisms
· Advances in separation techniques, including new techniques to capture targeted proteins, and high-affinity ligands for all gene products
· Improved approaches for studying proteins that are hard to crystallize (e.g., membrane proteins)

Informatics, Modeling, and Simulation

· Algorithms for genome assembly and annotation and for bioinformatics to measure protein expression and interactions
· Standardized formats, databases, and visualization methods for complex biological data sets, including expression profiles and protein-protein interaction data
· Molecular modeling methods for long-timescale, low-energy macromolecular interactions and for prediction of chemical reaction paths in enzyme active sites
· Methods for automated collection and integration of biological data for cell-level metabolic network analysis or pathway modeling; improved methods for simulation, analysis, and visualization of complex biological pathways; and methods for prediction of emergent functional capabilities of microbial communities. ”

Advanced Application: Electronic Cell

This application is able to process differential equations that model a molecular transformation (A + E -> A' + E), a complex formation (A + B -> AB), a dissociation (AB -> A + B) and an enzymatic reaction (A + B + E -> C + D + E) (Figure 1).

$$\nu_1 S_1 + \nu_2 S_2 + \cdots \rightarrow \nu_j S_j + \cdots + \nu_n S_n \quad (3)$$

$$v = k \cdot \prod_{i}^{j-1} [S_i]^{\nu_i} \quad (4)$$

$$v = \frac{V_f \cdot [S]}{K_s \frac{(1+\frac{[A]}{K_A}+\frac{[I]}{K_i})}{(1+\frac{b[A]}{\beta K_A}+\frac{a[I]}{\alpha K_i})} + [S]\frac{(1+\frac{[A]}{\beta K_A}+\frac{[I]}{\alpha K_i})}{(1+\frac{b[A]}{\beta K_A}+\frac{a[I]}{\alpha K_i})}} \quad (5)$$

$$\{S_1, S_2, \cdots, S_n\}$$

1)

$$\frac{dS_1}{dt} = f_1(S_1, S_2, ..., S_n)$$
$$\frac{dS_2}{dt} = f_2(S_1, S_2, ..., S_n)$$
$$\cdots$$
$$\frac{dS_n}{dt} = f_n(S_1, S_2, ..., S_n)$$

2)

Figure 1: *(1) concentrations in one compartment - (2) interactions(3) balance reaction - (4) speed of non enzymatic reactions (5) speed of Michaelis-Menten reaction*

Moreover, e-cell allows the grouping of molecules in compartments. Also, the molecules can be transported from one compartment to another (Figure 2).

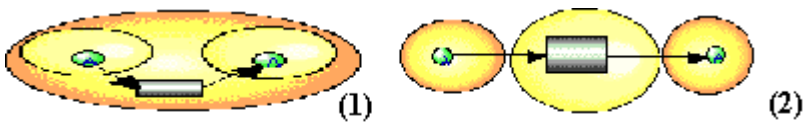

Figure 2: *(1) molecule transportation into the same compartment (2) molecule transportation between two compartments*

There are six metabolic pathways included into the system : nucleotide biosynthesis, phospholipid biosynthesis, amino acid biosynthesis, energy metabolism and gene expression System. Like this, the biologist can coupled its own metabolic pathway models to the whole system (Figure 3).

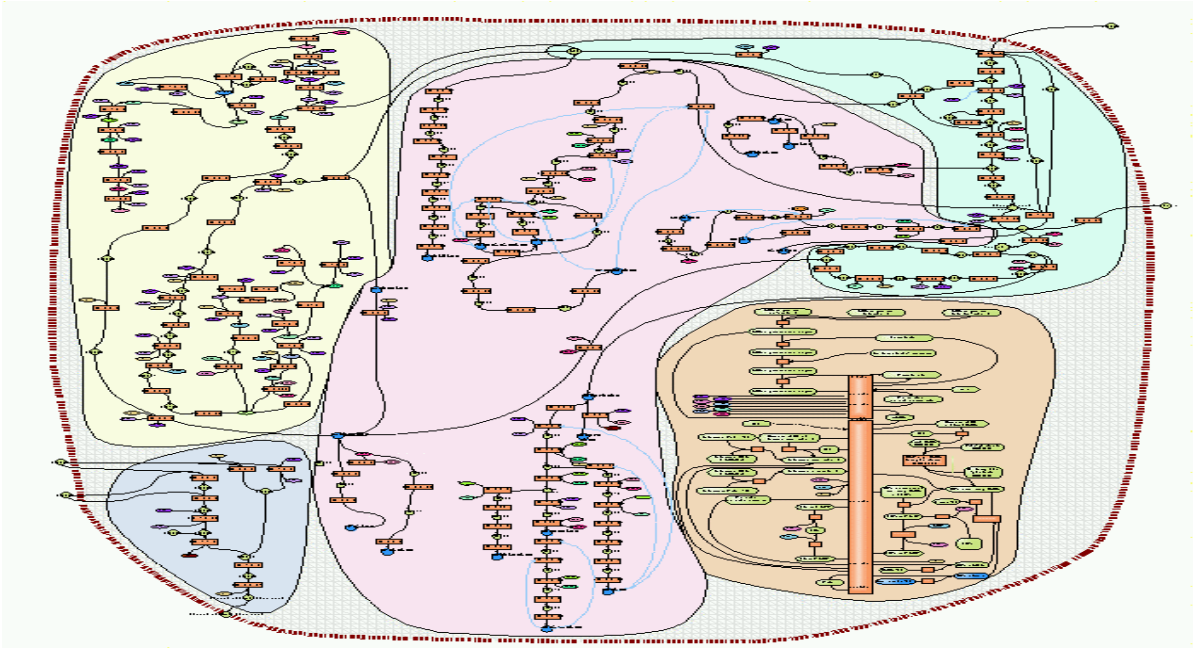

Figure 3: *pre-existing metabolic pathways in e-cell.*

The molecules, reactions and compartments are describe in a text file called “rule file”. The e-cell system analyzes this file (the source code looks like C or C++) and allows a dynamic simulation of the molecule concentrations (Figure 4).

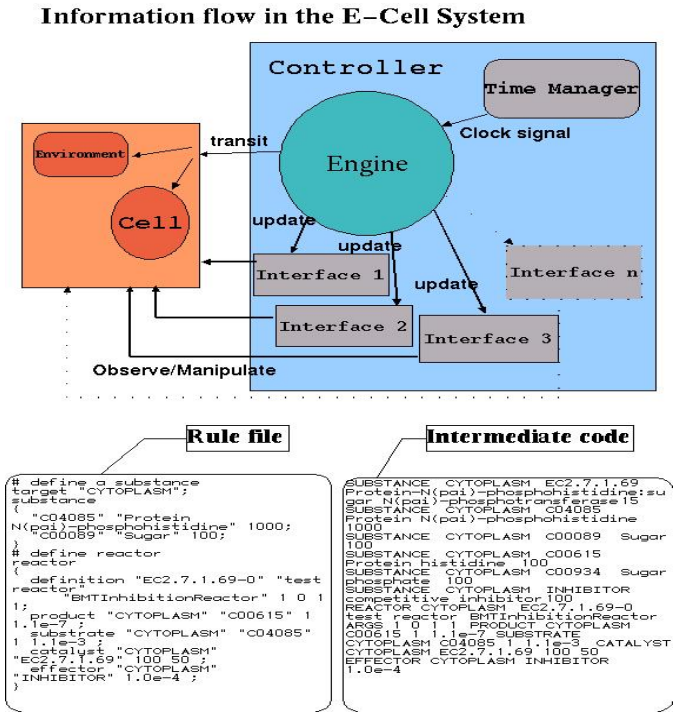

Figure 4: *Information flow in the E-Cell System.*

The interface permits the control and the observation of the system (Figure 5).

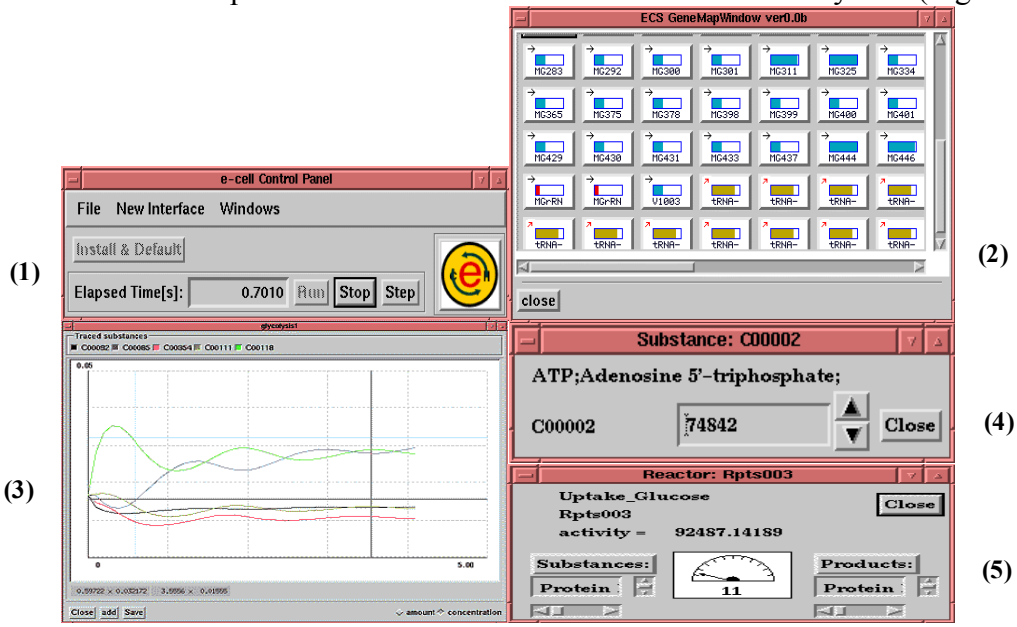

Figure 5: *1) Simulator control, 2) switches for gene expression (on / off) 3) curves of molecule concentrations - 4) one molecule information, 5) activity of the molecular reactions.*

Advanced Application: Virtual Cell

From the Virtual Cell web site [VCE01].

Introduction

NRCAM (National Ressource for Cell Analysis and Modeling, USA) has created a remote user modeling and simulation environment utilizing Java's Remote Method Invocation (RMI). Users can create biological models of various types and run simulations on a remote server. A transparent general purpose solver is used to translate the initial biological description into a set of concise mathematical problems. The generated results are stored on the remote server and can be reviewed in the software and/or exported in a variety of popular formats.

The Virtual Cell software is decomposed into three main components:

1. Modeling Framework
2. Mathematics Framework
3. WWW Interface-
   Biological Oriented Interface
   Integrated Math Editor

1. The modeling framework represents the physiological models of the virtual cell and allows for persistence and database support.

2. The mathematics framework transparently solves an important class of mathematical problems encountered in the cellular modeling.

3. The WWW accessible graphical user interface provides access to the technology mentioned above. The user interface has been developed using Java 2 Applets.

The biologically oriented user interface allows experimentalists to create models, define cellular geometry, specify simulations, and analyze simulation results. There is a Math Editor component which has been integrated within the biological interface. The design of the biological to mathematical mapping allows for separate use of biological and math components, and includes automatic mathematical simplification using pseudo-steady approximations and mass conservation relationships. This allows for direct specification of mathematical problems, performing simulations and analysis on those systems. Equations may still be generated automatically from the biological interface. The stand alone mathematics user interface is also a tool for modeling reaction-diffusion systems.

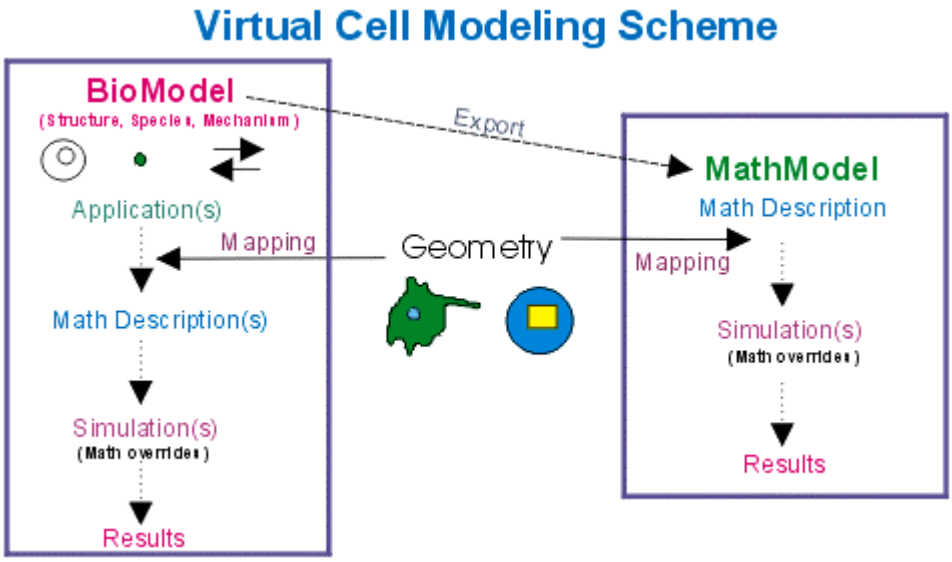

Different steps needed to develop a simulation

1. The **BioModel** contains all the necessary information needed to define the biological model, i.e. species, compartments, reactions, fluxes:

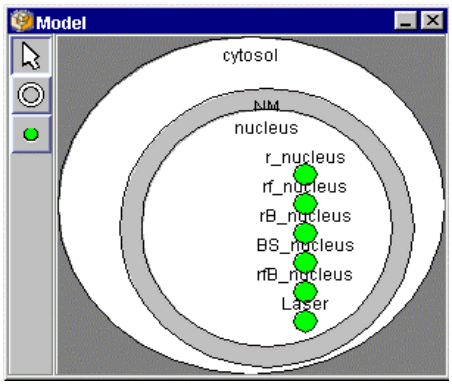

2. The Geometry Editor is the main workspace for creating geometries. Create new Geometries from uploaded experimental images or from analytically defined Geometries. The Geometry Database displays the Geometries and any associated files, i.e. BioModels, math models. The following snapshot shows the Virtual Cell Geometry interface:

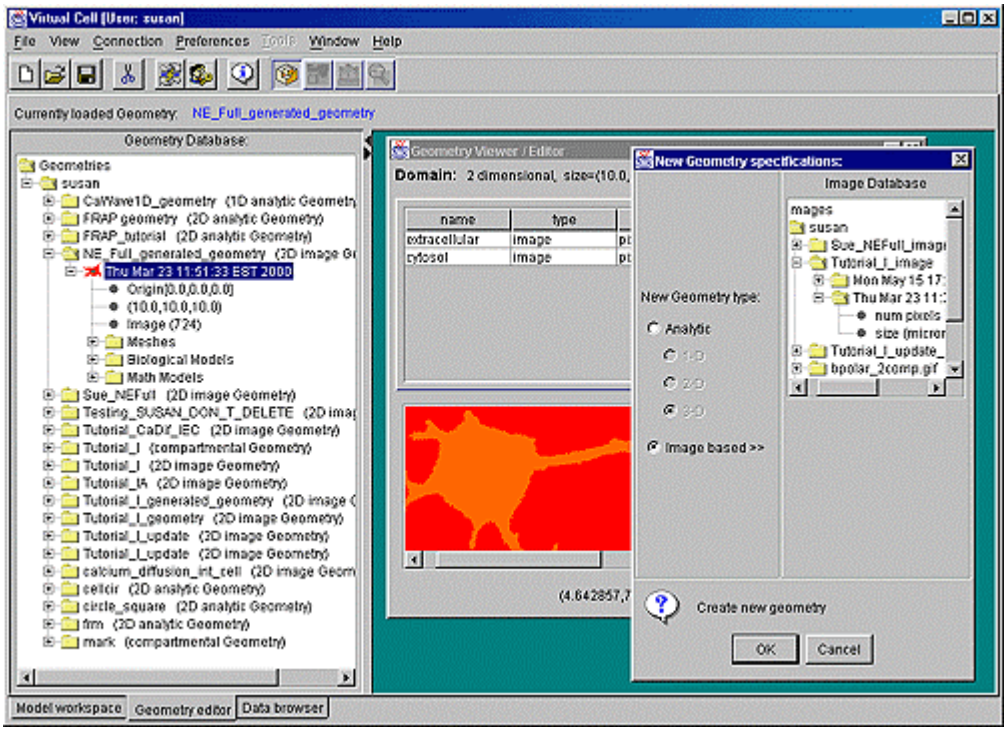

To determine a geometry, it is possible to use a segmented experimental image:

from a photo 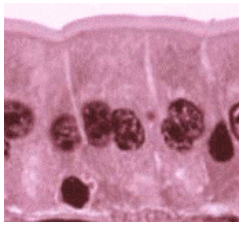 to a segmented image  where the simulation will take place.

3. The **Application** establishes the relationship between the BioModel and Geometry:

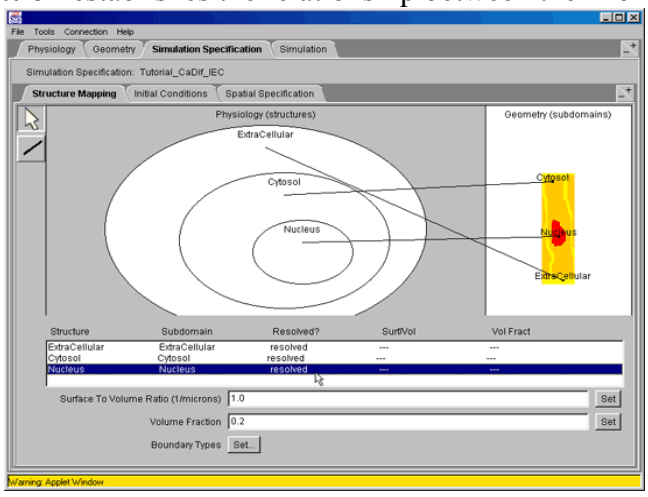

4. Creation of the mathematical code according to the Virtual Cell Math Description Language, VCMDL, in the Math Workspace. VCMDL is a declarative mathematics language, which has been developed to concisely describe the class of mathematical systems that are encountered in the Virtual Cell project. This language defines parameters, independent variables, differential/algebraic systems defined over a complex geometry including

discontinuous solutions and membrane boundaries and the description of the task to perform on such a system:

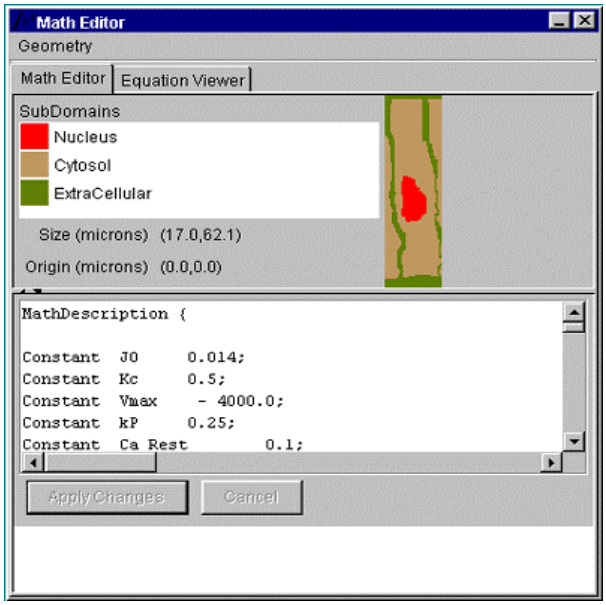

Currently six integration methods are available to solve differential equations:
- Forward Euler (first order)
- Runge-Kutta (second order)
- Runge-Kutta (fourth order)
- Adams-Moulton (fifth order)
- Runge-Kutta-Fehlberg (fifth order)
- LSODA (Variable order, Variable Time Step)

5. Run **Simulations** for Compartmental and Spatial models:

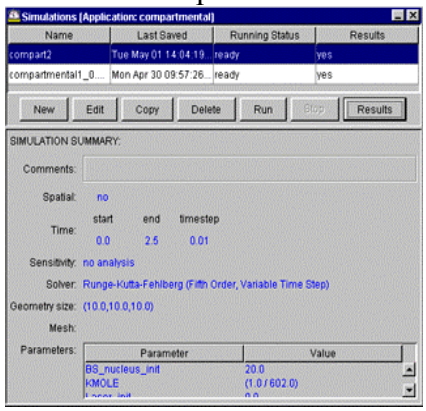

6. View **Results** for Spatial and Compartmental simulations:

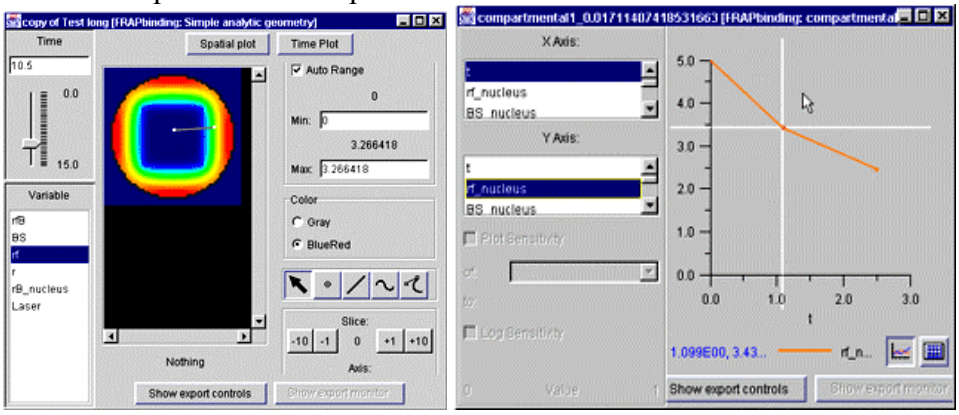

After these brief descriptions of advanced applications, it possible to say that one of the main problem of these applications is that they represent a cell like a “soupe” where spatial structuration and mechanical aspect are neglected. We think that these aspects are essential to understand the whole cell functioning. That why, the next chapters will introduce computational approaches that could be used to get a more realistic representation of a cell: reaction-diffusion systems, cellular automata and multiagents systems.

Reaction-diffusion

Principles

In his article of 1952 " The chemical bases of the morphogenesis ", Turing proposes a mathematical theory of the interaction between cells via chemical substances [TUR52]. He shows that its system can express stable states and proposes it as a possible mechanism of development of cellular configuration (multi-cellular organisms) in forming. A reaction-diffusion system shows how two or more chemical species diffusing on a n-dimensional space and reacting with one another can form many stable, cyclic or chaotic patterns. These patterns are formerly used to describe signals in multi-cellular organisms to control their growth. This model is the source of developments as those of Meinhardt [MEI82] onto the forming of biologic patterns, of Linen [LIN88] on the chimiotactism, Bard [BAR81] on the generation of zebra fur, Murray [MUR81] on the forming of pattern in the wings of butterflies or De Boer [DEB89] on the cellular division.

The basic form of a diffusion-reaction system involves two chemical species that diffuse in one or more dimensions and react together according to the following equations:

$$\frac{\partial a}{\partial t} = F(a,b) + D_a \nabla^2 a$$
$$\frac{\partial b}{\partial t} = G(a,b) + D_b \nabla^2 b$$

where a and b represent the concentration of two chemical species. The first equation indicates that the variation of the a concentration during the time depends on a function F of the local concentrations of a and b plus the diffusion of a from places nearby. The constant D_a indicates how fast a is diffusing (D_a is bounded by 0 and 1). The Laplacian ∇^2 determines how a is diffusing according to the nearby concentration of a. For example, if nearby places have lower concentrations, ∇^2 will be negative and a will diffuse away from its location.

To simulate this system, we have to digitize the different terms of the equations. The diffusion term becomes $D_a\ (a_{i+1} + a_{i-1} - 2a_i)$ and the reaction term depends on chemical equations.

Let us go with a one-dimensional example from Turing:

$$\Delta a_i = s\ (16 - a_i b_i) + D_a\ (a_{i+1} + a_{i-1} - 2a_i)$$
$$\Delta b_i = s\ (a_i b_i - b_i - \beta_i) + D_b\ (b_{i+1} + b_{i-1} - 2b_i)$$

Here, the system is described using discrete equations. a_i is the concentration of a at the position i. a_i is the “cell” number i among cells putted linearly.

The neighbours of a_i are a_{i-1} and a_{i+1}. The different parameters have the following values :

$i \in [0, 500[$ to get 500 cells
$D_a = 2^{-2}$ for molecule a diffusion
$D_b = 2^{-4}$ for molecule b diffusion
$s = 2^{-10}$ to control the balance between reaction and diffusion
$\beta_i = 12 \pm 0.25$ for irregularities in chemical concentration along the cells.

The figure 6 shows the evolution of the system up to 35000 iterations. We notice the formation of distinct peaks and valleys around step 10 000. If we increase the value of *s* the peaks and valleys become larger. For different values of β_i , peaks and valleys are not at the same place, but are roughly similar.

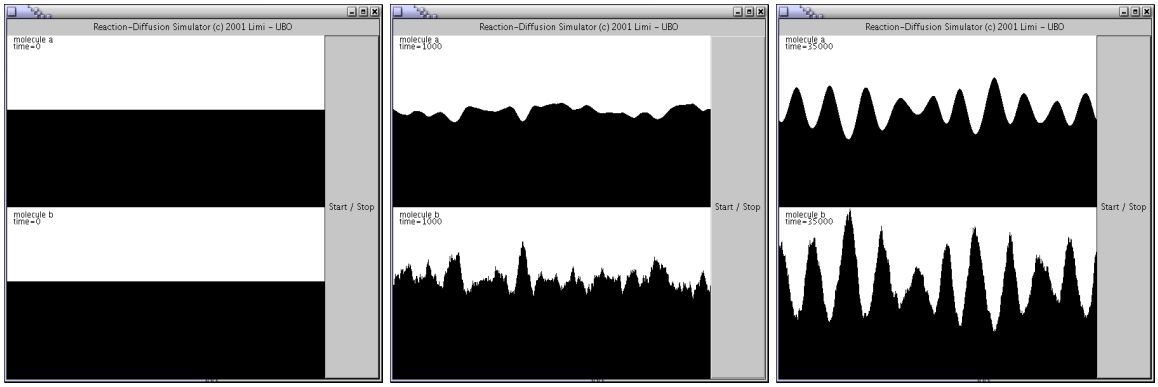

t = 0 t = 1000 t = 35000

Figure 6: evolution of the system at 0, 1000 and 35000 iterations. In *x* there are the indexes of the different cells (from 0 to 360) and in *y* there is the concentration of each cell : a_i at the top and b_i at the bottom. We can see the formation of pic and valleys.

A 2 or 3 dimensional reaction-diffusion system is more attractive for a cellular modeling. For example, it could be viewed as a multi-cellular tissue morphogenesis or as a membrane formation system. For example, using the Brusselator system (Figure 7), we can obtain tubular patterns. They could be used to describe the forming of a tubular network in a cell (see the F. Kepes & Al course in this book).

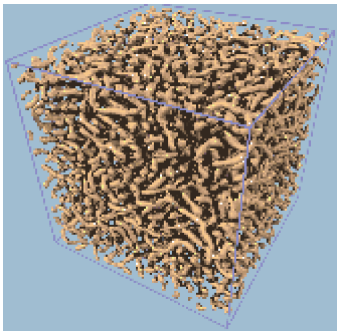

Figure 7: tubular patterns obtained thanks the Brusselator system [DEC99].
(see **plate 14** at the endof the book)

An other example of the reaction-diffusion systems is the “chemical flower” [BOI01] (Figure 8).

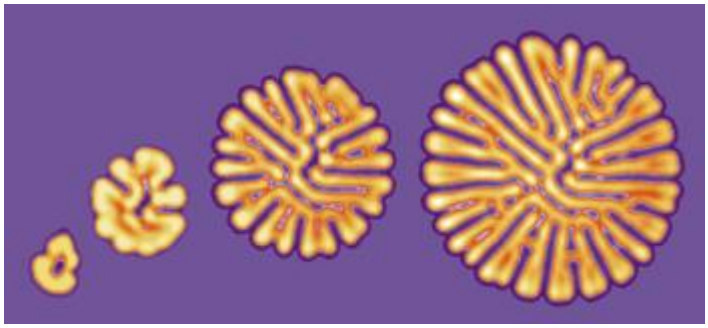

Figure 8: four stages of evolution of a chemical flower made using the Brusselator. We notice a Turing-like patterns formation. (see **plate 15** at the end of the book)

Inside a real cell, there are many concurrent and interacting processes. Thus, a multi-models approach seems to be adapted for cellular simulation in absence of unified theory. For instance, we can imagine that the reaction-diffusion matrix could be an environment for entities like agents representing hyperstructures. Moreover, these agents could represents nucleation centers or skeletons for the reaction-diffusion process.

So, before the descriprion of hyperstrucure, let us deal with an interesting related field of research: cellular automata. For our artificial cell, the cellular automata approach is used to model discrete molecules. These molecules are the basic shape of an hyperstructure. Into the next section, we will introduce the cellular automata concept which is used for the basis of hyperstructure forming.

Cellular Automata

Principles

From the theoretical point of view, Cellular Automata (CA) were introduced in the late 1940´s by John von Neumann [VNE66]. Before going further, let us clarify the functioning of a cellular machine on a simple but very rich example.

A cellular machine is represented by a *n* dimensional matrix which contains integer values. Each value (at the (i,j) position for in 2D) depends on the values of its direct neighbors (at the (i ± 1, j ± 1) positions). According to these dependancies (rules) and the matrix at time *t*, the matrix at time t+1 is generated.

The most popular 2D cellular automata is the John Conway's game of life [GAR70]. Here are the basic rules of this cellular automata :

For a space (a matrix element) that is “populated” (value is 1) :
Each cell with one or no neighbors dies, as if by loneliness.
Each cell with four or more neighbors dies, as if by overpopulation.
Each cell with two or three neighbors survives.
For a space that is 'empty' or “unpopulated” (value is 0) :
Each cell with three neighbors becomes populated.

These operations are repeated as often as necessary to observe the evolutions of the matrix configuration and its patterns. This cellular automata is very rich in interesting patterns. We show four of the simplest ones (Figure 9). Every pattern seems to have its own “life” and generally are called boat, oscillator or glider.

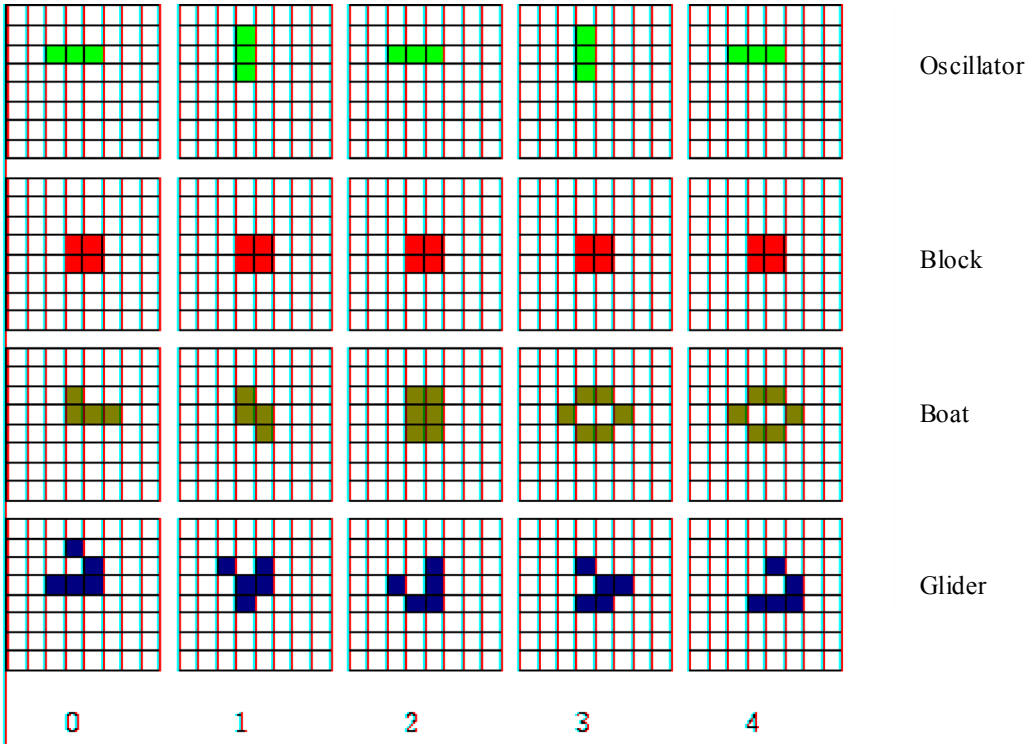

Figure 9: *Examples of patterns in the game of life*

More theoretically, "cellular automata are discrete dynamical systems and are often described as a counterpart to partial differential equations, which have the ability to describe continuous dynamical systems. The meaning of discrete is that, space time and properties of the automaton can have only a finite number of states. The basic idea is to describe a complex system by simulating interaction of cells following easy rules. Thus, macromolecules and their interactions between one another are locally defined to allow the emergence of hyperstructures. In other words:

We do not describe a complex system with global equations, but let the complexity emerge from interaction between simple individual rules.

Practically, the essential properties of a CA are:

- a regular n-dimensional lattice, where each cell of this lattice has a specific state,
- a dynamical behavior, described by neighborhood rules. These rules describe the state of a cell for the next time step [SCH99].

Cellular automata can be mathematically formalized (Equation 2). Therefore, some properties could be found *a priori* like *symmetry*, *reversible rules*, *ising model*, *non-ergodicity* or *period doubling* " [VIC84].

(1) $L=\{(i,j) \mid i,j \in N, 0 \leq i < n, 0 \leq j < m\}$ **(2)** $N_{ij} = \{(k,l) \in L \mid |k-i| \leq 1 \text{ and } | l - j | \ 1 \}$

(3) $z_{i\,j}(t+1) = \{ 1, \text{if } (z_{i-1\,j}(t) + z_{i\,j-1}(t) + z_{i\,j}(t)) = C \text{ else } 0\}$

Equation 2: L is a *m.n* matrix, *N* is the neighborhood definition and *z* is the rule of cell evolution.

Wolfram divides the cellular automata into 4 classes [WOL84]:

- **Class 1** - limit points (Evolves to homogeneous state)
- **Class 2** - limit cycle (Evolves to simple separated periodic structures)
- **Class 3** - chaotic - "strange" attractor (Yields chaotic aperiodic patterns)

Class 4 - more complex behavior (Yields complex pattern of localized structures)

Many applications using cellular automata have been developed. An interesting choice for this course is a cellular automata modeling an artificial immune system.

« A Computer Model of Cellular Interactions in the Immune System» F. Celada and P. Seiden [CEL92b].

F Celada and P. Seiden have developed since 1992 a simulator (*ImmSim*) allowing to study the humoral answer. The purpose of this cellular machine is to reproduce immune phenomena occurring within the lymphatic ganglions. It consists of a set of compartments arranged in a bidimensionnel grid. Each compartment can have various "values" according to what it represents (Figure 10). It can be the representation of a molecule or a cell. The modeled cells are B-cells, memory B-cells, plasmocytes, T-cells and antigen presenting cells. The modeled molecules are the molecules of antigens and antibodies. Each cell has a receptor which is represented by a string of binary characters allowing a variety of the molecular diversity. Each of the entities is initially placed at random on the grid. Then, the interactions between nearby entities are estimated (the interactions are probabilistic and depend on the equivalence of both involved receptors. Then, the interactions become possible only for the entities being on the same compartment (it is about a modification of the rules of the cellular machines: here a compartment changes of state according to the entities which it contains). Finally, the entities can move from a compartment into another. This sequence is repeated as often as necessary.

The simulator of Celada and Seiden was used in 1997 to check a theory on the paradox about the rhumatoide factor [STE97]. The simulation confirms the theory according to which the rhumatoide factor is auto-regulated without adding a pathologic entity in the immune system.

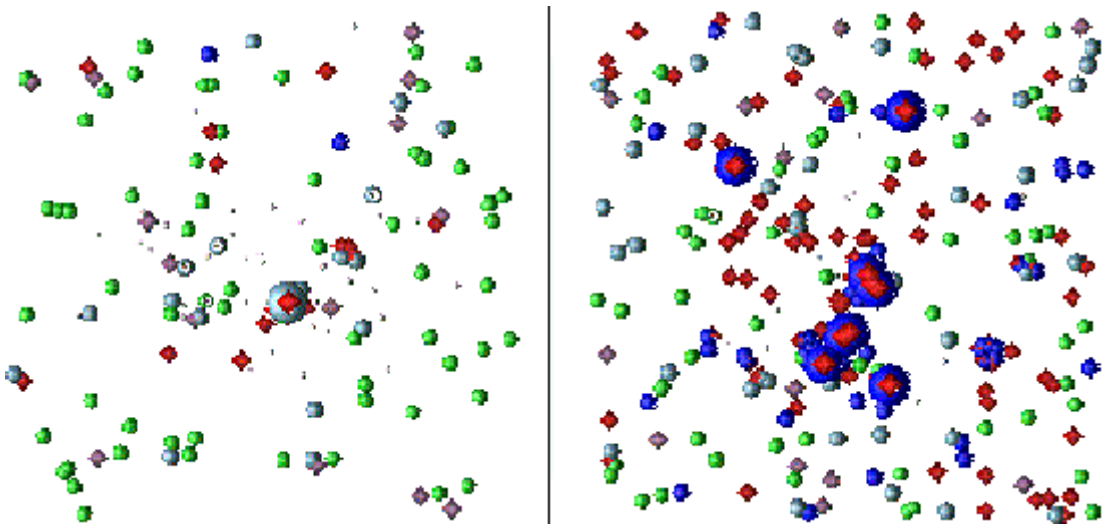

Figure 10: *Simulation of humoral answer at two different times. At the left, we observe the beginning of a immune response and at the right we see a clonal expansion of B-cells. B-cells are in blue, T in red, macrophages in green and antigens in gray [CEL92a] (see* ***plate 16*** *at the end of the book)*

This example shows that cellular automata are relevant to model and simulate cellular and molecular phenomenon. In this book, there is a description of a cellular automata for hyperstructure modeling by Vic Norris & Al.

However, many biological mechanisms are not easily modeled using this approach. For example, to allow hyperstructure to move, a multiagent approach seems to be more relevant. The aim of such systems is to gather different basic cells of a cellular automata into a single and interacting entity named “agent”. Thus, a single entity compound with several molecular units could be used to describe the moving of an hyperstructure and their interactions. So, it allows the emergence of new complex structures.

Multiagents Systems

Principles

In nature, numerous collective systems are able to carry out difficult tasks into dynamic and varied environments without any piloting nor external control like central coordination [BON94]. We notice it with ant colonies, swarms of wasps or the immune system. The researche in the field of Multiagents Systems has two major objectives. The first one concerns the theoretical and experimental analysis of the mechanisms of auto-organization which take place when several autonomous entities interact. The second focuses onthe realization of distributed systems able to carry out complex tasks by cooperation and interaction [FER95].

This approach favours the local description, where the decisions are not taken by a global observer/controller which has the synthesis of the system, but by each of the system components. These components, called agents (Figure 11), have only a partial vision of their environment in which they evolve. Each agent has a cycle of execution during which it begins by perceiving its local environment by means of sensors. Then, according to the information resulting from the environment and according to its internal state, it takes one or several decisions. A decision can modify the internal state of the agent, its behavior or its morphology. A decision changes the environment as well because an agent is able to act locally around it. For example the paws of an ant modify the position of the agent, its mandibles change the environment by taking or by putting down an object and, thanks to its pheromones, the ant changes its environment (and thus, its own future behavior and its congeners').

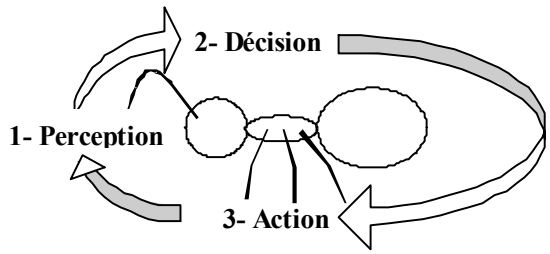

Figure 11: *Cycle perception, decision, action of an agent*

An agent having superior intellectual abilities is called cognitive agent. A simple and basic agent is called a reactive agent. The limit between reactive and cognitive agents is not clearly established. The most used criterion is the environment representation used by an agent. An agent is said reactive if it does not have, or has only in a rudimentary way, a representation of its environment. On the contrary, an agent is said cognitive if it is able to

represent its environment and to make a map in order to plan its actions. The agents we use for our works are exclusively reactive because they do not have any representation of their environment and are unable to plan their decision.

In spite of these limits, the collective, that is all the agents, has the possibility of making sensible/interesting decisions up to a certain limit. For example, ants build their hill on their own without any coordinator. Moreover, the immune system is able to defend an organism against numerous pathogenic factors without the help of a superior system. To sum up, these systems give evidence of a good adaptability, stability and robustness of this reactive and local approach.

In spite of all these advantages, the reactive multiagent systems are not entirely reliable. For the immune system, cancers or auto-immune diseases proove it. As for the coagulation system, haemophilia or thromboses show us their limits. During these dysfunctions, the cells assume to make relevant decisions to assure the maintening of organisms whereas an outside observation shows that they do not.

From a computer point of view, the multiagent system paradigm comes from the problem of the collective intelligence and from the emergence of structures by interactions [PES97]. Thus, the purpose is to create computer systems constituted of simple software elements having the ability to resolve one or few simple problems. For J. Ferber, the objective is to give birth to computer systems able to evolve by interaction, adaptation and self-replication based on agents and working in physically distributed universes. With this kind of system, only the collective can, thanks to the multiple interactions between agents, lead to a solution. This qualitative break between the individual abilities and the collective potential is called emergence.

The study of this emergence is difficult because the conventional logic does not allow to explain the observed qualitative break. Different descriptive and theoretical works [PES97] were led but without a mathematical formalization of the phenomena. However, the experimental characterization of the emergence is possible. Indeed, a qualitative change can be observed to point out strong differences in the potential of the collective with regards to the individual one. We notice such phenomenon even if all the entities have exactly the same abilities. One of the simplest illustration corresponds to the simulation of the ant sorting [DEN91]. Thanks to the same basic behavior, a population of artificial ants manages to sort out its brood. The brood represents the larvas of ants which are differentiated according to their stage of growth.

What it is necessary to note above all, it is that this sorting intervenes only if the number of artificial ants is important enough. In other words, a single ant is unable to sort out on its own whereas several ants can. Here, the heaps made by ants allow to characterize the phenomenon of emergence. The emergence is one of the key of the agent approach. However, the systems where the emergence is really used remain marginal. Indeed, no rule of evident causality exists between the individual behavior and the collective one.

The multiagent approach seems to be particularly adapted to the modeling and to the simulation of molecular and cellular phenomenon for different reasons. First, the notions of environment, autonomous entities, spatial distribution, distribution of roles are essential in biology and for a multiagent system. Second, interaction and cooperation are central both in biology and in the multiagent concepts. These similarities make the multiagent approach a natural bridge between the world of biology and that of computer simulation.

The next section will describe the development of a multiagent system for hyperstrucure modeling.

Applications

To represent basic hyperstructure phenomena inside a cell, the model must take into account the aggregation and dissociation of molecular complexes. It must be computationally efficient to simulate numerous (> 10^4) interacting molecules and extensive enough to include enhanced phenomenon like dynamic molecular shapes, simplified molecular flows or electromagnetic fields.
We propose such a system with the following properties:
A molecule is represented by:

- a deformable shape located into a 3D grid
- a specific behavior according to the difference of chemical species

The shape of a molecule represented by an agent (a molecule-agent) is based on a continuous 3D shape or a dicrete 3D shape. To be efficiently simulated, a shape must be divided in many elementary cubes (Figure 12-b) that represents an approximation of the original shape (Figure 12-a).

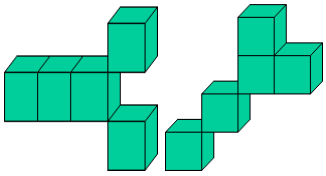

(a) (b)

Figure 12: *the left shape (a) is the original shape and the right one (b) is an approximation after a simple rotation.*

An agent has receptors into its shape to get information from its local environment (Figure 13-a). According to a local observation and its internal state, it takes decisions (Figure 13-b).

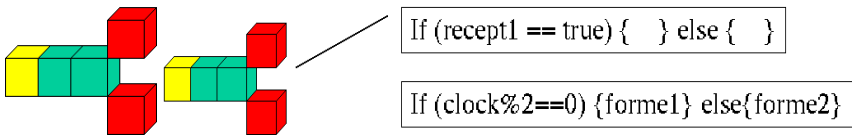

(a) (b)

Figure 13: *the shape has receptors to allow an agent to get information from its local environment (a). According to this information and its internal state, an agent can take decisions (binding, activating, moving, creating a deformation...) (b)*

The figure 14 shows a binding/separation of two agents to create hyperstructures and the figure 15 represents a molecule activation.

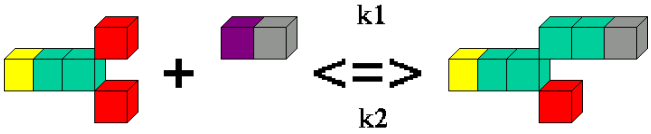

Figure 14: binding a separation of two agents.

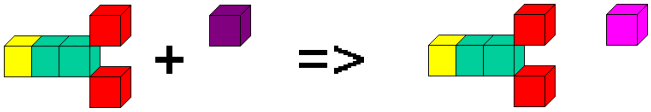

Figure 14: activation of a single molecule.

The original shape can have two types of deformation:

- with internal constraints: Original Shape + Constraints -> New Original Shape -> New Cube based Shape -> Shape possible into the environment ? -> If it is, acceptance of the new Original Shape, else cancelation.
- With external constraints: Cube based Shape + Constraints -> Deformation forces applied to the Original Shape -> New Original Shape -> New Cube based Shape -> Possible into the environment ? -> If yes, acceptance of the new Original, else cancelation.

Example of the transformation Original Shape -> Cube based Shape:

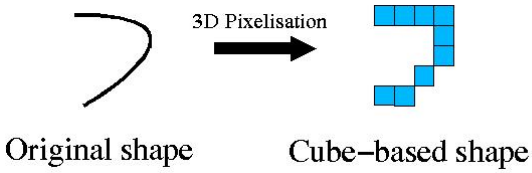

Example of a deformation coming from internal constraints

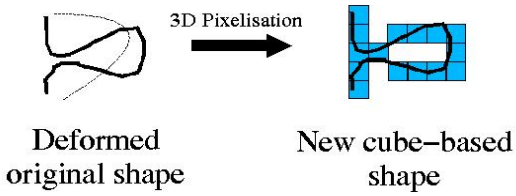

Example of a deformation coming from external constraints

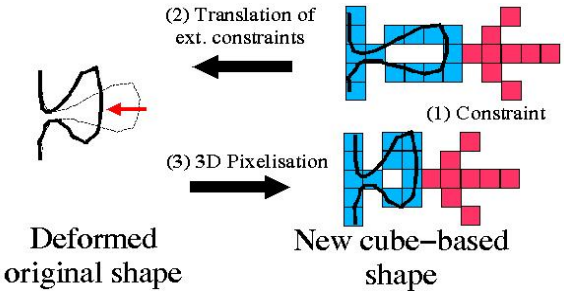

The basic behavior can modify the Original Shape of the molecule (internal or external deformation), the position of the molecule-agent (x, y, z, rx, ry, rz) according to its local environment (a molecule agent looks for 6 translations, 6 rotations and no move).
More accurately, it calculates different stabilities for each choice and only one of those is applied. The specific behavior can be any type of algorithms.

The molecule-agents live into an environment which is a set of 3D-grids. Each 3D-grid contains data shared by the agent-molecules and a molecule-agent can read data around itself to make decisions. For example, it can read into the grid the identification of each molecule-agent to *decide* if they can bind together. It can also take into account an electromagnetic and other type of fields.

An important part is the visualization of the 3D-matrix containing the hyperstructures. That is why, we have developed a 3D viewer to explore the in-silico environment (Figure 16).

A classical 3D plotter is used to draw the simulation results and a basic simulation controller is included (play, pause, stop).

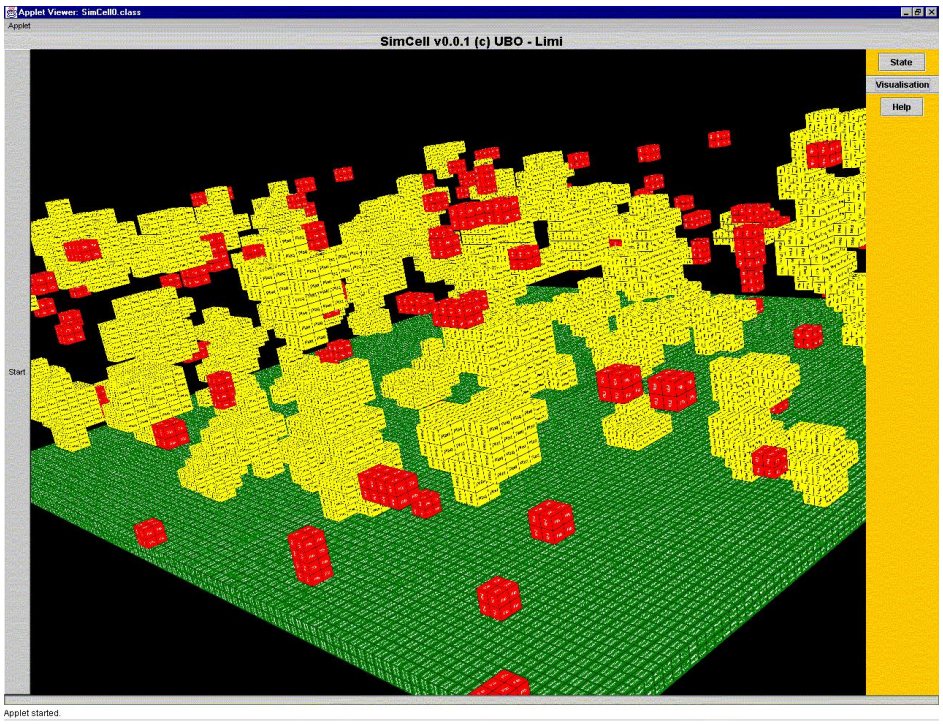

Figure 16: *3D viewer of our hyperstructure simulator. (see **plate 18** at the end of the book)*

We have seen three possible approaches to model different cellular levels / systems. The next chapter explains how a reaction-diffusion system can be merged with a multiagent system into a multi-cellular simulator.

Example of an integrated application

From « A Simulation Testbed for the Study of Multicellular Development: the Multiple Mechanisms of Morphogenesis », Kurt Fleisher and Alan Barr [FLE94].

This paper presents a simulation framework and computational testbed to study multi-cellular pattern formation. The approach combines several developmental mechanisms (chemical, mechanical, genetic and electrical) known to be important for biological pattern formation. The mechanisms are present in an environment containing discrete cells which are able to move independently (cell migration). Experience with the testbed indicates that the interactions between the developmental mechanisms are important in determining multicellular and developmental patterns.

Each simulated cell has an artificial genome whose expression is dependent only upon its internal state and its local environment. The changes of each cell's state and of the environment are determined by piecewise continuous differential equations. The current two-dimensional simulation exhibits a variety of multicellular behaviors, including cell migration, cell differentiation, gradient following, clustering, lateral inhibition and neurite outgrowth.

The next table summaries the modeling framework:

Modeling Framework (abstraction)	*Testbed (implementation)*
Discrete cells (allows cell migration)	
- cell geometry	- 2D circles
- cell substructures	- none
-growth cones	- modeled as small cells
- neurites	- path of growth cone and communication link between cell and growth cone
Genetic / Cell lineage	
- genetic control of cell operations	- Parallel Oes w/conditions
- inherit state from parent cell	- yes
- control over orientation of cell divisions	- yes
- asymmetric cell division	- not implemented yet
Extracellular environments	
- chemical	- 2D reaction-diffusion grid
- mechanical	- mechanical barriers, viscous drag
Cell-cell interactions	
- mechanical	- collisions and adhesion between cells
- chemical (membrane, proteins)	- adhesion and contact recognition
- electrical (gap function, synapse)	- not implemented yet
Cell-environment interactions	
- chemical	- emit, absorb, sense values in grid
- mechanical	- cell-environment collisions and adhesion

Table 1: the modeling framework and its implementation.

Detailed implementation:

Cell: A cell is modeled as a geometric shape (currently a circle, with optional neurites) with a given response to applied forces, as well as an array of cell state variables.

Continuous cell behaviors: Cells exhibit several continuous behaviors, determined by the cell behavior functions

- attempt to move in some direction (may be limited by collision, adhesion or drag)
- attempt to grow in size
- emit or absorb chemical from the environment
- change amount of particular proteins in the membrane (eg. Cell adhesion proteins, which mediate how much this cell will adhere to another cell)

Discontinuous cell behaviors (events): The cell provides functions which determine the timing of the following events. An event is a discontinuty in the solution, which stops the solver and may create or destroy data structures. The timing of events is determined by cell behavior functions:

- split (cell division)
- die
- emit neurite with growth cone

Cell state variables: An array of variables which loosely represent the amounts of proteins within the cell. The values of these variables affect the cell's movements, the timing of events and the cell's interaction with the environment.

Environment: All the simulated cells interact within a single global environment. The environment contains diffusing, reacting chemicals, as well as physical barriers. Within the simulation, cells access information about their environment locally through an array of local environment variables.

Local environment variables: An array of variables which represent the local environment of a cell. The values available to the cell as a function of time and they depend on the extracellular environment. Since each cell is in a different location, in general the local environment of two cells will differ. These variations can then lead to different behavior for the cells, even though their genomes"may be identical.

The figure 17 shows an example of the development of a multicellular system using the Fleischer's simulator:

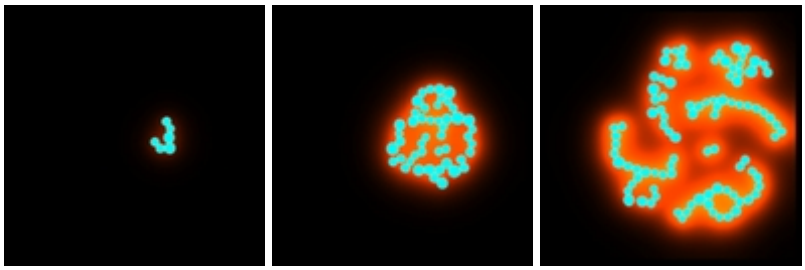

Figure 17: *Multicellular growth (discrete cells in blue (light)) and reaction-diffusion molecules in red (dark)) into a 2D environment (black). Three states of evolution of the same simulation are shown here. [FLE95] (see* ***plate 17*** *at the end of the book)*

Conclusion

The field of cell simulators is quickly growing. Many applications or projects are launched or ready to start. They aim to treate the numerous data (numerous in size and diversity) coming from the high scale molecular biology to help biologists on the living cell understanding. We have seen three major modelers/simulators available for biologists to compute cell mechanisms and see some of their principal drawbacks: they do not include spatial and mechanical phenomenon nor self-organized molecular structures (like hyperstructures or membranes). Then, to avoid these drawbacks, we introduce, according to the granularity level of cell modeling, different approaches that could be used: reaction-diffusion systems for ionic/atomic descriptions, cellular automata for small molecules representation and multiagents systems for membrane or hyperstructures modeling. One of the problem is to merge these different approaches into an integrated cell system. Thus, we have seen how a recent application couple a multiagents system and a reaction-diffusion system.
The next step will be the design of multi-levels models to develop a realistic integrated cell software system.

References

[BAR81] Bard, *A model for generating aspects of zebra and other mammalian coat patterns*, J. Theor. Biol., 93 : 501-531, 1981.

[BOI01]Boissonade J, **De Kepper P**., 2001: Morphogénèse Chimique, modes de croissance atypiques, http://www.crpp.u-bordeaux.fr/MC2_morphochim_main.html

[BON94] E. Bonabeau, *Robotique Collective*, Intelligence Collective, Hermes pages 181-202, 1994.

[CEL92a] Franco Celada et Philip E. Seiden, *A model for simulating cognate recognition and response in the immune system*, Journal of Theorical Biology, volume 158, pages 329-357, 1992.

[CEL92b] Franco Celada et Philip E. Seiden, *A computer model of cellular interactions in the immune system*, Immunology Today, volume 13, pages 56-62, 1992.

[GAR70] Martin Gardner, Mathematical Games - The fantastic combinations of John Conway's new solitaire game Life, Scientific American, October 1970, pp 120-123.

[DEB89] M.J.M. de Boer, *Analysis and computer generation of division patterns in cell layers using developmental algorithms*, rapport de thèse de doctorat, Université d'Utrecht, soutenue le 20 novembre 1989.

[DEN91] J-L. Deneubourg, S. Goss, A. Sendova-Franks, C. Detrain et L. Chretien, *The Dynamics of Collective Sorting Robot-like Ants and Ant-Like Robots*, From Animals to Animats, pages 356-363, MIT Press, 1991.

[ECE01] Electronic Cell, http://www.e-cell.org

[FER95] J. Ferber, *Les systèmes Multiagents*, InterEdition, Paris, 1995.

[FLE94] Kurt Fleisher et Alan H. Barr, *A simulation testbed for the study of multicellular development :the multiple mechanisms of morphogenesis*, Artificial Life III, Ed C. G. Langton, SFI Studies in the Sciences of Complexity, Proc. Vol. XVII, Addison-Wesley, pages 389-417, 1994.

[FLE95] Kurt W. Fleischer, *A Multiple-Mechanism Developmental Model for Defining Self-Organizing Geometric Structures*, California Institute of Technology, rapport de thèse, 1995.

[DEC99] Luc Decker, *Modèles de Structures Aléatoires de Type Réaction-Diffusion*, thèse de doctorat présentée à l'École Nationale Supérieure des Mines de Paris, 1999. Web: http://www.oragenet.org/decker/these

[HEG66] J.S. Hege et G. Cole, *A mathematical model relating circulating antibodies and antibody forming cells*, Journal of Immunology, V.97, pages 34-40, 1966.

[JER74] Jerne, N.K., Towards a network theory of the immune system, Ann. Immunol. (Institut Pasteur), 125C, 373, 1974.

[LIN88] C. C. Lin and L. A. Segel, *Mathematics applied to deterministic problems in the natural sciences*, Philadelphia, PA : SIAM, 1988.

[MCP01] The Microbial Cell Project, http://microbialcellproject.org

[MEI82] Hans Meinhardt, *Models of biological pattern formation*, Londre : Academic Press, 1982.

[MUR81] J. D. Murray, *On pattern formation mechanisms for Lepidoptera wing pattern and mammalian coat marking*, Phil. Trans. Roy. Soc. (B) 295 : 473-496, 1981.

[PES97] S. Pesty, E. Batar, C. Brassac, L. Delépine, M.P. Gleizes, P. Glize, O. Labbani, C. Lenay, P. Marcenac, L. Magnin, J.P. Muller, J. Quinqueton et P. Vidal, *Emergence et SMA*, Intelligence Artificielle et systèmes Multi-Agents, pages 323-341, 5e journées francophones, JFIADSMA 1997.

[SCH99] Alexander Schatten, Cellular Automata, Digital Worlds, 1999. Web: http://www.ifs.tuwien.ac.at/~aschatt/info/ca/ca.html

[STE97] Jeffrey J. Stewart, Harvey Agosto, Samuel Litwin, J. Douglas Welsh, Mark Shlomchik, Martin Weigert et Philip E. Seiden, *A solution of the rheumatoid factor paradox*, The Journal of Immunology, Volume 159, pages 1728-1738, 1997.
[TUR52] A.M. Turing, *The chemical basis of morphogenesis,* Philos. Trans. Roy. Soc. London B237: 37-72, 1952.
[TUR] Greg Turk, Generating Textures on Arbitrary Surfaces using Reaction-Diffusion,
[VNE66] John von Neumann, Theory of Self-Reproducing Automata, University of Illinois Press, Champain, IL, 1966.
[VCE01] Virtual Cell, http://www.nrcam.uchc.edu
[VIC84] Vichniac G.Y., 1984: Physical modeling, containing *symmetry* properties, *reversible rules*, *Ising model*, *non-ergodicity and order parameters*, *period doubling.*
[WOL84] Wolfram S., 1984: *universality* and *complexity* in CA´s, the *classification* of one-dimensional automata into four classes and their properties.

Neural Networks

Abdallah Zemirline[1], Pascal Ballet[1], Lionel Marcé[1], Patrick Amar[2,3], Gilles Bernot[2], Franck Delaplace[2], Jean-Louis Giavitto[2], Olivier Michel[2], Jean-Marc Delosme[2], Roberto Incitti[4], Paul Bourgine[5], Christophe Godin[6], François Képès[7] , Philippe Tracqui[8], Vic Norris[9], Janine Guespin[9], Maurice Demarty[9], Camille Ripoll[9]

[1] *EA2215, Département d'Informatique, Université de Bretagne Occidentale, Brest*

[2] *Laboratoire de Méthodes Informatiques, CNRS UMR 8042, Université d'Evry, 91025 Evry*

[3] *Laboratoire de Recherche en Informatique, CNRS UMR 8623, Université Paris-Sud, Orsay*

[4] Institut des Hautes Études Scientifiques, Bures, France & genopole®, Evry, France

[5] *CREA - Ecole Polytechnique*

[6] *UMR Cirad/Inra modélisation des plantes, TA40/PSII, Montpellier*

[7] *Atelier de Génomique Cognitive CNRS ESA8071/genopole, Evry*

[8] *Lab. TIMC-IMAG, Equipe DynaCell , CNRS UMR, 5525, Faculté de Médecine, La Tronche*

[9] *Laboratoire des Processus Intégratifs Cellulaires, UPRESA CNRS 6037, Faculté des Sciences & Techniques , Université de Rouen, 76821, Mont-Saint-Aignan France*

The development of neural networks had initially as objective the modeling information processing and learning in the brain, in order to understand how a population of interconnected biological neurons performs a cerebral function. Now, neural networks are used in several practical applications, in various fields including computational molecular biology [23, 24], and the artificial neurons are quite remote from biological neurons.

1. Biological neural networks

A neuron [22] is a nervous cell having a cytoplasm body and several cytoplasm extensions (axons and dendrites) that allow it to dispatch (axons) and to receive (dendrites) signals. The exchanged information by two neurons is accomplished by means of electrical signals, which are the result of potassium-sodium ion exchanges. The electrical signal exchanges are made at the level of the synapses, which link the axons of neurons to the dendrites of other neurons. A neuron may have 1 000 to 10 000 synapses and can receive information from 1 000 other neurons. Besides, although the synapses are often constituted between axons of cells and dendrites of other cells, there are other types of synaptic junctions : between axon and axon, between dendrite and dendrite, between axon and cellular body. The human brain may contain until 10^{11} neurons.

The complexity of biological neural networks (BNNs) is very variable. There are some BNNs like the ganglions that are constituted of heaps of neurons, as there exist sophisticated BNNs like the complex BNNs of the neocortex. These ones are able to modify their functioning and even their structures as well as they are capable of computing, memorizing and learning. Memorizing and learning of the BNNs are made by means of some modifications at the synaptic level. The synapses may modulate their activity, as exciting or inhibiting a neuron, and in this way to let possible the writing of an information in a memory area. In 1949, Hebb [2] made the hypothesis that the abilities of BNNs are the result of the self-organization of their connections : The efficiency of a synapse increases when the neurons that it connects are at the same time either all active or all inactive; otherwise the efficiency lessens.

2. Artificial neural networks
2.1. Neural network models

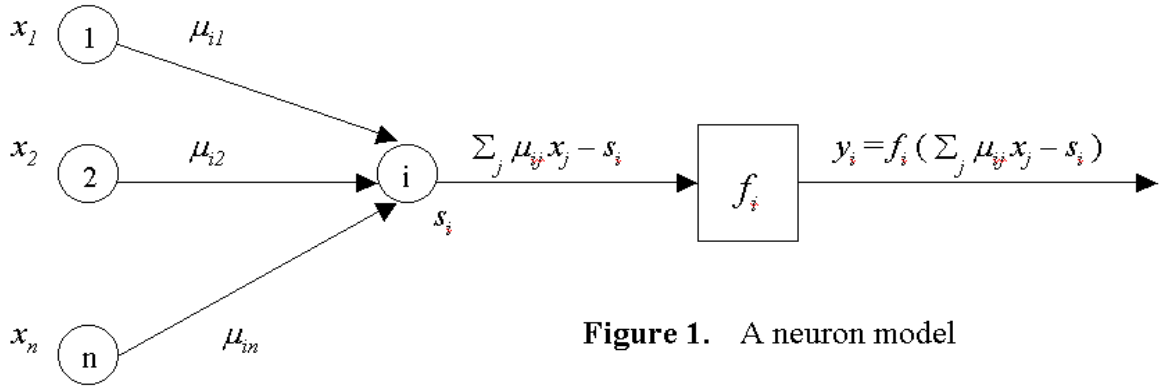

Figure 1. A neuron model

An *artificial neural network* (ANN) can be described as a set of interconnected units evolving in time and operating in parallel; the units represent axons and dendrites and each connection (*j*,*i*) from unit *j* to unit *i* has a *weight* μ_{ij} that modulates the influence of unit *j* on unit *i*. Thus, an ANN is a weight-directed graph in which to each node *i* are associated a *bias* or *threshold* s_i and a *transfer function* f_i, so that unit *i* will produce an output y_i of the form : $y_i = f_i(\sum_j \mu_{ij} x_j - s_i)$, where x_j is the *j*th input of this unit and $\sum_j \mu_{ij} x_j$ is the sum of all its weighted inputs. If this sum is greater than the threshold s_i, unit *i* is activated for producing the output y_i; otherwise unit *i* is in an inactive state (Figure 1). The parameters μ_{ij} and s_i can be adjusted so that the neural network produces some desired behavior. Namely, the neural network can be trained to achieve some particular job by adjusting the weight and bias parameters.

The transfer functions widely used are nonlinear, smooth, increasing and bounded such as sigmoid functions (so called from their "S" shape). However, sometimes the transfer function is linear like the identity function. When $f_i(x) = 1$ if $x > 0$ and $f_i(x) = 0$ otherwise, unit *i* is called a *threshold gate*. As threshold functions are discontinuous, they are often replaced by sigmoidal transfer functions that are continuous and differentiable, such as $f(x) = arctan(x)$ and $f(x) = tanh(x)$, or by other transfer functions such as $f(x) = 1 / (1 + e^{-x})$.

One drawback of this neuron model appeared when it was used to describe what electro-chemical triggering phenomena takes place at the active cell membranes of biological neurons. It was noticed that the description of signal transformations in complicated neural networks needs an analysis computationally too heavy. Whereat T. Kohonen [13] suggested the following simple nonlinear dynamic model for a neuron (Figure 2) :

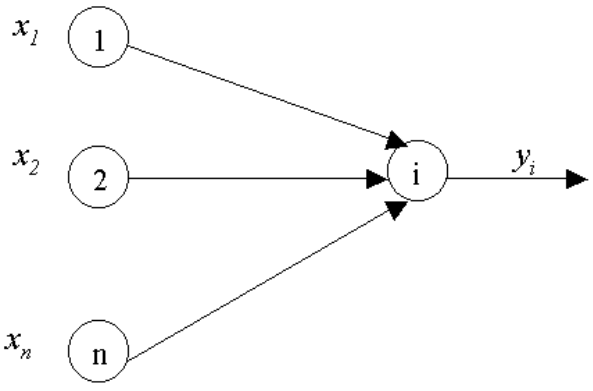

$$dy_i / dt = I_i - \gamma(y_i), \quad y_i \geq 0 \qquad (1)$$

Figure 2. A nonlinear dynamic neuron model

In Figure 2, the x_j and y_i are nonnegative scalar variables, the input activation I_i is some function of the x_j and of some internal parameters. The function $\gamma(y_i)$ is the leakage term, a nonlinear function of output activity. In order to guarantee good stability in feedback networks γ must be convex (i.e., its second derivative with respect to y_i must be positive). The leakage term $\gamma(y_i)$ takes in account all different losses and dead-time effects in the neuron, as a progressive function of activity.

2.2. Network architectures

Usually, three important architectures are considered for the ANNs : *layered* architecture, *feedforward* architecture and *recurrent* or *feedback* architecture. A *recurrent* architecture contains directed cycles; therefore, the signal paths can return to a same node. The feedback ANNs are difficult to implement. A *feedforward* architecture is devoid of directed cycles, thus the signal paths never return to a same node. A *layered* architecture is an architecture where the units are partitioned into classes, called *layers*, and where the connectivity patterns are defined between the classes.

Besides, the unit set is partitioned into *visible* units (those in contact with the external world such as *input* and *output units*) and *hidden* units. Often, the input units are grouped in an *input layer* and the output units in an *output layer*. A *hidden layer* is constituted of hidden units.

2.3. Three main categories of ANNs

It is customary to distinguish three categories of ANNs : *adaptive signal transfer networks*, *state transfer networks*, and *competitive-learning* or *self-organizing networks*.

The *signal transfer networks* have their output signals depending uniquely on input signals. These are often layered feedforward networks such as the *multilayer Perceptron* [3], the *Madaline* [4], the feedforward network in which learning is defined by means of an *error propagation algorithm* [5], and the *radial-basis-function networks* [6].

The *state transfer networks* are recurrent ANNs in which the feedbacks and nonlinearities are very strong so that the activity state quickly converges to one of its equilibrium points (attractors). Indeed, input information sets the initial activity state and once the network is in operation the output is fed back as the input until the network output will settle on one of its stable values. Typical representatives of these ANNs are the *Hopfield network* [7] and the *Boltzmann machine* [8].

The cells of the *competitive-learning* or *self-organizing networks*, which generally receive identical input information, compete in their activities by means of lateral interactions. Each cell or cell group is sensitized to a different domain of vectorial input signal values, and acts as a decoder of that domain [9, 10]. Besides, both of the *adaptive-resonance-theory models* of Grossberg and Carpenter [11,12] and the *Self-Organizing Maps* of T. Kohonen [14] belong of course to this category.

2.4. Phases of development of neural models

Three phases of development of models in ANN theory are distinguished : *memoryless* models, *adaptive* models and *plasticity-control* models

Memoryless Models : In this first modeling phase, which starts with the classical *McCulloch-Pitts* network [1], the transfer properties of the network were assumed fixed. And when feedback connections were added, such as in some interconnected networks [3] and also in some state transfer models [7, 8], only the relaxation of activity distributions was considered. There, the dynamic state equation is written as : $dA/dt = f(I, A)$; where signal activity A is a function of location, I is the external input acting on the same locations, and f is a general function of I and A, and of location.

Adaptive Models : These models take in account the *adaptation* and *memory* properties that result from parametric changes in the network. The equations, which describe the adaptive signal-transfer

circuits, are : $dA/dt = f(I, A, M)$, $dM/dt = g(I, A, M)$; where : M denotes the set of system parameters (M may be a function of location and represent an adaptive bias), and f and g are general functions of I, A, and M . These equations were used in the first endeavors to model emergence of feature sensitive cells and elementary forms of self-organizing mappings.

Plasticity-Control Models : T. Kohonen [14, 15] was not convinced that a model with adaptive connectivity parameters is accurate enough to capture all aspects of self-organization, such as, for instance, the learning rate of a synaptic connection, which is called *plasticity* in neurophysiology. And in 1993, he [15] advanced the idea that the *plasticity* should be described and controlled by a third group of state variables called P and wrote the system equations as :

$dA/dt = f(I, A, M)$, $dM/dt = g(I, A, M, P)$, $dP/dt = h(I, A, M, P)$; where f, g, and h are general functions and where P does not take part in the control of activity A.

3. Learning and Evolution

A*daptation* refers to a control of parameters in order to optimize some performance measure, or to a behavioral modification that depends on experiences and that improves the performance of a system. In classical ANNs *adaptation* is called *learning* or also *training*. Besides, in *evolution*, *adaptation* is the adjusting of species to environment by natural selection or by behavioral change. Hence in *evolutionary artificial neural networks* (EANNs), which are a special class of ANNs, *adaptation* is called *evolution*. Thus, in ANNs *adaptation* takes two fundamental forms : *Learning* and *Evolution*.

3.1. Learning

Following the Hebb's assumption and in order that the ANNs may develop an associative memory, it is necessary that the efficiency of the connections, which link the artificial neurons, may be computed. Since the fifties, several rules appeared, especially the Perceptron rule [3] and the Widrow-Hoff learning rule [4]. These rules put the ANN on a supervised learning, which can be summarized as follows: After having presented to the input units what it must be memorized, the ANN answer is scanned. Since the correct answer is known then it is attempted to reduce the gap between these two answers by acting on the efficiencies of the connections that link the artificial neurons, more particularly on the thresholds s_i and the weights μ_{ij}. When these efficiencies stabilize, the learning phase ends.

More generally, Learning in ANNs can roughly be partitioned onto *supervised*, *unsupervised*, and *reinforcement learning* :

Supervised learning makes a direct comparison between the current output of an ANN and the correct output, which is known. This comparison is often made by means of a minimization of an error function such as the total mean square error between the actual output and the desired output. In order to minimize this error, a gradient descent-based optimization algorithm such as backpropagation [4] can then be used to adjust connection weights in the ANN interactively. *Reinforcement learning* is a special case of supervised learning where the only known information is whether or not the current output is correct (the desired output is unknown). In this learning mode adaptive changes of the parameters due to reward or punishment depend on the final outcome of a whole sequence of behaviour.

Unsupervised learning works only on the correlations among input data; there is not any other information for learning. It is without a priory knowledge about the classification of samples.

Sect. 3.1.2. describes the Perceptron learning algorithm. Sect. 3.1.3. is devoted to *competitive-learning* networks and to an *unsupervised learning* which is used to get a representation of high-dimensional nonlinearly related data items in a illustrative two-dimensional display [14].

Finally, notice that the essence of a learning algorithm is certainly its learning rule (i.e., for example, a weight-updating rule which determines how the signals should modify the adaptive connection input weights or other parameters of the neurons in learning) and that its correctness needs to make clear what the ANN submitted to learning is supposed to do (for instance, its function is associative memory or detection of elementary patterns).

3.1.1. Some Learning Laws

3.1.1.1 Hebb's Law

Consider first the simplest classical learning law for neurons like the one defined in Figure 1. If the ANNs made of such neurons are supposed to reflect simple *memory effects,* especially those of *associative* or *content-addressable memory,* a model law that describes changes in the connections is based on *Hebb's hypothesis* [2] :

> "When an axon of cell *A* is near enough to excite a cell *B* and repeatedly or persistently takes part in firing it, some growth process or metabolic change takes place in one or both cells, such that *A's* efficiency, as one of the cells firing *B,* is increased"

This means that the weight μ_{ij} is varying according to $d\mu_{ij} / dt = \alpha y_i x_j$ (2) ;
where x_j is the *j*th input (the presynaptic "activity") of unit *i*, y_i is the output of unit *i* (the postsynaptic "activity"), and α is a scalar parameter named *learning-rate factor.* This law, generally called *Hebb's law,* has given rise to some elementary associative memory models, named *correlation matrix memories* [16-18]. In vector form, it can be written as :

$dm_i / dt = \alpha y_i x$ (2') ; where $m_i = (\mu_{i1}, \ldots, \mu_{in})^T$; $y_i = \sum_j \mu_{ij} x_j = m_i^T x = x^T m_i$; $x^T = (x_1, \ldots, x_n)$ and n the number of inputs of each unit.

Notice that with this law the associative memory function is omitted. Moreover, as *feature-sensitive cells* have central roles in the classification functions both at the input layers of the neural networks, as weIl as inside them, some modifications of Hebb's law were considered : the *perceptron* learning law, the *Riccati* learning law, and the *principal-component-analyzer* (*PCA*) law.

3.1.1.2. Perceptron Learning Law

The perceptron learning rule is a modified form of Hebb's learning law. It was proposed by F. Rosenblatt [3] in the late 1950s. It is the following : $dm_i / dt = \alpha (y_i^c - y_i) x$ (3) ;
where y_i^c is the desired output (i.e., the correct output).
This rule is also known as back-propagation rule, LMS (least mean squares) rule, or as delta rule.

3.1.1.3. The Widrow-Hoff Learning Law

This law, which stems from Widrow [4] , was introduced for multilayer feedforward networks. It can be also written as (3) and where the least mean of square error criterion is applied and the optimization is performed by Robbins-Monro stochastic approximation.

3.1.1.4. The Riccati-Type Learning Law

A major revision [14] made to Hebb's law introduces a *scalar-valued plasticity-control function P* that may depend on many factors (activities, diffuse chemical control, etc …) and that shall have a time-dependent *sampling effect* on the *learning* of the signals x_j. On the other hand, it was assumed that the weights μ_{ij} are affected proportionally to x_j. In this way, the first term of the learning equation is written as $P\, x_j$, where *P* is a general functional that describes the effect of activity in the surroundings of neuron *i*.

The second major revision is inclusion of an "active forgetting" term that guarantees that the μ_{ij} remains finite. This involves the introduction of a scalar-valued *forgetting rate functional Q*, which is some function of synaptic activities of neuron *i*. Therefore, the equation, which describes a kind of "active learning and forgetting" and where the plasticity control *P* affects the total learning rate, is the following : $d\mu_{ij} / dt = P\,(x_j - Q\,\mu_{ij})$. In this equation, *P* can be seen as describing extracellular effects and *Q* intracellular effects. Moreover, it seems proper to assume that the "active forgetting" effect at synapse *j* is proportional to $\sum_k \mu_{ik} x_k$, where the sum extends over the whole

cell, including synapse j itself. Then the latter equation can be written as the Ricatti-type equation :

$d\mu_{ij} / dt = P\,(x_j - \mu_{ij} \sum_k \mu_{ik} x_k)$; or in vector form with $\alpha = P$ and $\beta = P\,Q$ as

$$dm_i / dt = \alpha\, x - \beta\, m_i \mathrm{m}_i^T x \qquad (4) \quad .$$

3.1.1.5. The PCA-Type Learning Law

This learning law, which was introduced by E. Oja [19], is analogous to (4), except that its right-hand side is multiplied by the expression $y_i = \sum_j \mu_{ij} x_j = x^T m_i$.

The differential equation of this law is the following : $dm_i / dt = \alpha y_i x - \beta y_i^{\,2} m_i$ or

$$dm_i / dt = \alpha x^T m_i\, x - \beta\, (\mathrm{m}_i^T x\, x^T m_i)\, m_i \qquad (5) .$$

3.1.2. Perceptron Learning Algorithm [3] [5] [20]

The perceptron learning algorithm obeys perceptron learning rule (3). It applies to feedforward neural networks where the neuron model is the one of Figure 1. Training patterns x are presented to the neural network; the output y_i is computed. Then the weights μ_{ij} are modified according to :

$$m_i(t + 1) = m_i(t) + \alpha\,(y_i^c - y_i)\, x \quad \text{where } m_i = (\mu_{i1}, \ldots, \mu_{in})^T.$$

Hereafter, the single-layer perceptron learning algorithm and the back-propagation perceptron learning algorithm are described.

1) A single-layer perceptron neural network comprises one or more artificial neuron in parallel. Like in Figure 1 each neuron has n inputs and one output. The <u>perceptron learning algorithm for a single-layer perceptron neural network</u> is the following :

(0) Initialize the weights μ_j and threshold s to small random numbers; $t = 0$;

(1) Present an input vector $x = (x_1, \ldots, x_n)^T = x(t)$ and the desired output y^c, (where n is the number of input units), and calculate the output $y = y\,(t)$ according to

$y = f(\sum_j \mu_j x_j - s)$, where f is a given transfer function

(f can be the sigmoid function : $f(x) = 1 / (1 + e^{-x})$);

(2) Update the weights μ_j according to : $\mu_j(t + 1) = \mu_j(t) + \alpha\,(y^c(t) - y\,(t))\, x_j(t)$

$j = 1, \ldots, n$; where $0.0 < \alpha < 1.0$) ; $t = t + 1$;

(3) Repeat steps (1) and (2) until the iteration error is less than a user-specified error threshold or a predetermined number of iterations have been completed.

2) <u>Multi-layer Perceptron Learning Algorithm, or Back-Propagation Learning Algorithm</u> :

The algorithm for multi-layer perceptron learning is based on the back-propagation rule (3) and on a gradient descent in error space. The error is defined as

$$E = \sum_p E_p \qquad (6)$$

Where

$$E_p = (\sum_i (y_i^c - y_i)^2) / 2 \qquad (7)$$

where y_i is the actual output and y_i^c is the desired output and where the sum is over the output units of the network.

A change of weights can be made according to the gradient of the error :

$$\Delta\mu = - \alpha \nabla E \qquad (8)$$

where α is a constant scaling and ∇ is the gradient operator. The weight change for the connection from unit j to unit i, of this error gradient can be written as :

$$\Delta\mu_{ij} = - \alpha \nabla_{ij} E = - \partial E / \partial \mu_{ij} \qquad (9)$$

But

$$\partial E / \partial \mu_{ij} = (\partial E / \partial y_j)\, (\partial y_j / \partial z)\, (\partial z / \partial \mu_{ij}) \qquad (10)$$

with

$$z = \sum_k \mu_{kj}\, y_k \,.$$

Hence

$$z / \partial \mu_{ij} = \partial \sum_k \mu_{kj}\, y_k / \partial \mu_{ij} = \sum_k \partial\, (\mu_{kj}\, y_k) / \partial \mu_{ij} = \sum_k ((\partial \mu_{kj} / \partial \mu_{ij})\; y_k + \mu_{kj}\, (\partial y_k / \partial \mu_{ij})) \qquad (11)\,.$$

Examining the first partial derivative, notice that $\partial \mu_{kj} / \partial \mu_{ij}$ is zero unless $k = i$. And examining the second partial derivative $\partial y_k / \partial \mu_{ij}$ for observing that if μ_{kj} is not zero then there exists a connection from unit k to unit j, which implies that $\partial y_k / \partial \mu_{ij}$ must be zero, otherwise the network would not be feedforward. Therefore, we get from (11) : $\partial z / \partial \mu_{ij} = y_i$ (12)

We now consider the middle partial derivative of (10) : $\partial y_j / \partial z$. Since $y_j = f(z)$ then $f(z) = 1 / (1 + e^{-z})$ would imply that $\partial y_j / \partial z = \partial\, (1 + e^{-z})^{-1} / \partial z = (1 + e^{-z})^{-2}\, e^{-z}$ $= (1 - y_j)\; y_j$. In this way : $\partial y_j / \partial z = (1 - y_j)\; y_j$ (13)

Now, return to the first derivative of (10) : $\partial E / \partial y_j$ And recall that $E = \sum_p E_p$ and

$E_p = (\sum_i (y_i^c - y_i)^2) / 2$ where the sum is over the output units of the network.

Two cases can be distinguished : j is an output unit ; j is not an output unit.

- If j is an output unit then the derivative $\partial E / \partial y_j$ can be computed as :

$$\partial E / \partial y_j = \partial (\sum_i (y_i^c - y_i)^2) / 2 / \partial y_j = \sum_i (y_i^c - y_i)\, \partial (y_i^c - y_i) / \partial y_j = -(y_j^c - y_j) \qquad (14)$$

- If j is not an output unit then we need to rely on the chain rule, applied over the units k connected to unit j :

$$\partial E / \partial y_j = \sum_k (\partial E / \partial y_k)\; (\partial y_k / \partial z)\, \mu_{kj} \qquad (15)$$

where : $\partial y_k / \partial z$ is given by (13) and $\partial E / \partial y_k$ is computed recursively.

We are now in position to describe the back-propagation learning algorithm :

(0) Initialize the weights μ_{ij} and threshold s to small random values; $t = 0$;
Present an input vector $x = (x_1, \ldots, x_n)^T$ and a target output y^c
where n is the number of input units and m the number of output units y^c;
(x and y^c represent the patterns to be associated) ;

(1) Calculate the actual output : Each layer calculates $y^k = f(\sum_j \mu_{ij} x_j - s)$;
(where f is defined by : $f(z) = 1 / (1 + e^{-z})$)
This is then passes this to the next layer as an input. The final layer outputs value y^v .

(2) Adapts weights : Starting from the output y^v and working backwards, do
$\mu_{ij}(t + 1) = \mu_{ij}(t) + \alpha y^v E_j$; where E_j is an error term corresponding to the input x_j of node j ;
such that : for output units : $E_j = \sigma y^v (1 - y^v) (y^c - y^v)$
for hidden units : $E_j = \sigma y^v (1 - y^v) \sum_k^q E_k \mu_{kj}$ where the sum is over all the q nodes in the layer above node j .
(σ is the steepness parameter in the sigmoidal function)

3.1.3. The Self-Organizing Map (SOM) algorithm [14] [21]

The SOM algorithm, which stems from Kohonen [14], deals with the competitive learning and self-organizing networks. It operates as a nonparametric *regression* which involves fitting a

number of reference vectors to the distribution of vectorial input samples (In *regression* some simple mathematical function is fitted to the distribution of sample values). The reference vectors m_i are considered here to approximate the probability distribution of the input signals x and are also used to define the nodes of a kind of "hypothetical elastic network". Indeed, the distribution of the vectors m_i should reflect the probability distribution of the input signals x, which is not given explicitly but only through the sample of vectors x.

Given an ANN constituted of N neurons, where to every node (neuron) i , $i = 1, \dots, N$, is associated a weight-vector $m_i = (\mu_{i1}, \dots, \mu_{in})^T \in \mathbb{R}^n$. Between the units of the ANN there exists a set C, possibly empty, $C \subseteq \{1, \dots, N\}^2$ of neighborhood connections supposed unweighted and symetric. Besides, from the connection set C, construct a two-dimensional grid G, having N nodes, so that two nodes i, j are neighbors in G if and only if $(i,j) \in C$. Let $x = (x_1, \dots, x_n)^T \in \mathbb{R}^n$ be an input vector supposed connected to each neuron i, via the weight-vector $m_i = (\mu_{i1}, \dots, \mu_{in})^T$. Vector x is compared with all the m_i in some metric, the euclidean metric for instance, in order to determine a node $c \in \{1, \dots, N\}$ such that $\|x - m_c\| = \min\{\|x - m_i\| ; i = 1, \dots, N\}$; unit c is called the *winner*. In this grid, a decaying topological neighborhood $N_c = \{ i \in \{1, \dots, N\}; (c,i) \in C\}$ of node c is defined such that $c \in N_c(t)$ for every t and $N_c(t + 1)$ is strictly contained in $N_c(t)$; where t = 0, 1, 2, … is the discrete time coordinate (see Figure 3). During learning at time t, those nodes of the grid that are in N_c(t) will activate each other to learn something from the same input x.

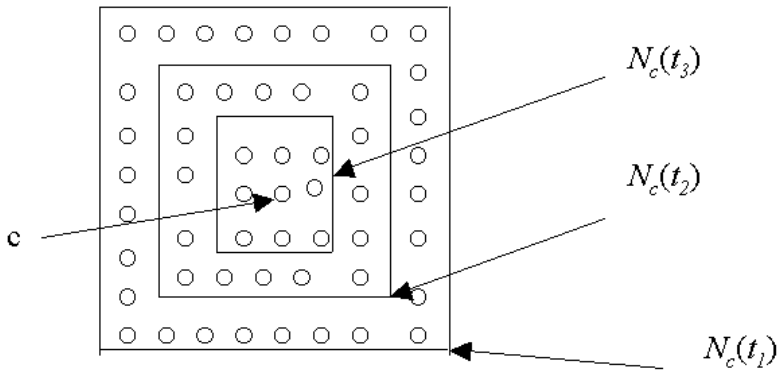

An example of topological neighborhood

Figure 3.

Indeed, the following learning process is proposed in [14] :

$m_i(0)$ is arbitrary; and for t = 0, 1, 2, …

$$m_i(t + 1) = m_i(t) + h_{ci}(t) \, (x(t) - m_i(t)) \qquad (16)$$

where $h_{ci}(t)$ must $\to 0$ when $t \to \infty$; otherwise the sequence $(m_i(t))_{t \geq 0}$ does not converge. The form of $h_{ci}(t)$ and its average width characterize the "stiffness" of the elastic surface defined by the points m_i of $\mathbb{R}^n$.

Frequently, $h_{ci}(t)$ is taken equal to 0 if $i \notin N_c(t)$ and $h_{ci}(t) = \alpha(t)$ if $i \in N_c(t)$. $\alpha(t)$ is called a *learning-rate factor* and is such that $0 < \alpha(t) < 1$. Furthermore, both $\alpha(t)$ and the radius of $N_c(t)$ are decreasing monotonically in time.

Another choice for $h_{ci}(t)$ which widely occurs is the following :

$$h_{ci}(t) = \alpha(t) \, exp \, (- \|r_c - r_i\|^2 / 2 \, \sigma^2(t)) \qquad (17)$$

where : $\alpha(t)$ is another valued learning rate factor ;

r_c and r_i *belong to* $\mathbb{R}^2$ and are respectively the location vectors of nodes c and i in the grid ; $\sigma(t)$ denotes the width of $N_c(t)$.

The <u>self-organizing feature map algorithm</u> is the following, where *Nit* is a predetermined number of iterations to be completed :

(0) Initialize the ANN to contain N units. Each unit i has n entries and an associated reference vector $m_i = (\mu_{i1}, \ldots, \mu_{in})^T \in \mathbb{R}^n$ chosen randomly ;

Initialize the connection set C to form a rectangular or a squared grid G ; $t = 0$;

(1) While ($t < Nit$) do

(1.1) Generate at random an input signal $x \in \mathbb{R}^n$ according to a continuous probability density function $p(\xi)$, $\xi \in \mathbb{R}^n$;

(1.2) Determine a unit $c \in \{1, \ldots, N\}$ such that
$\|x - m_c\| = \min\{\|x - m_i\| ; i = 1, \ldots, N\}$;
and consider the topological neighborhood $N_c(t)$;

(1.3) Adapt each unit $i \in N_c(t)$ according to (16) and (17) ; $t = t + 1$;

End while

3.2. Evolution

Evolutionary artificial neural networks (EANNs) denote a special class of ANNs, where another form of adaptation, called *evolution* and distinct from learning, takes a prominent part. This evolutionary approach of adaptation applies *evolutionary algorithms* to ANNs for evolving weight training, evolution of architectures, evolution of learning rules, evolution of input features, etc.

3.2.1. Evolutionary algorithms

An *evolutionary algorithm* (EA) refers to a population-based stochastic search algorithm inspired by natural evolution. Three mechanisms drive natural evolution (*reproduction*, *mutation* and *selection*) by acting on the chromosomes containing the genetic information of the individual (the genotype), rather than on the individual itself (the phenotype) : By the *reproduction* mechanism new individuals are introduced into a population, these offspring chromosomes inherit from their both parents a mixture of genetic information (*crossover*). The *mutation* process brings small changes into the inherited chromosomes. And the *selection* mechanism allows only the fittest individuals (the best adapted to their environment) to survive and reproduce.

To solve a problem by means of an EA makes use of a metaphor of natural evolution : All the possible solutions constitute a population living in an environment that is the problem itself. The phenotype of each individual (each candidate solution) is encoded in some manner into its genome (genotype). The adaptability of each individual is measured by means of a *fitness function*. And the natural evolutionary mechanisms are modeled by appropriate genetic operators. Starting from an initial population and by applying genetic operators to introduce progressively "niece genetic material" into the successive populations, an EA produces step by step better solutions to the problem.

The EAs comprise several types : evolution strategies [25, 26], evolutionary programming [27, 28, 29], and genetic algoritms [30, 31]. All proceed as follows :

(0) t = 0; Generate the initial population G(0) at random;
(1) While (termination criterion is not satisfied) do
(1.1) Evaluate each individual of G(t);
(1.2) From G(t) select parents P(t) based on their fitness in G(t);
(1.3) Apply genetic operators to P(t) to generate offspring which constitute G(t + 1);
(1.4) t = t + 1;
End while.

3.2.2. The Evolution of Connection Weights

Most learning algorithms, such as backpropagation [5], are based on gradient descent. This use of gradient descent let these algorithms have drawbacks : They are often incapable of finding a global minimum of the error function and get trapped in local minima. One way to overcome these shortcomings is to formulate the training process as the evolution of connection weights in the environment defined by the architecture and the associated learning rule. Indeed, EAs can be used in the evolution to find a near-optimal set of connection weights globally. Unlike the case in gradient-descent-based learning algorithms, the fitness (or error) function of an ANN does not have to be differentiable or even continuous.

The evolutionary approach to weight training in EANNs comprises two phases.

The first phase deals with the choice of a representation of connection weights, either the binary representation or the real-number representation. In a binary representation, each connection weight is represented by a number of bits with a given length; then the concatenation of all the connection weights of the network encodes the ANN in the chromosome. In a real number representation, each connection weight is represented by a real number; in this way each individual (i.e., ANN) in an evolving population is encoded by a real vector.

The second phase is the evolutionary process simulated by an EA, in which genetic operators such as crossover and mutation have to be decided in conjunction with the representation scheme. The evolution stops when the fitness is greater than a predefined value (i.e., the training error is smaller than a certain value) or the population has converged.

A typical cycle of the evolution of connection weights is the following [32] :

(1) Decode each individual (genotype) in the current generation into a set of connection weights and construct with the weights a corresponding ANN.
(2) Evaluate each ANN by computing its total mean square error between actual and target outputs. The fitness of an individual is determined by the error. The higher the error, the lower the fitness. The optimal mapping from the error to the fitness is problem dependent. A regularization term may be included in the fitness function to penalize large weights.
(3) Select parents for reproduction based on their fitness.
(4) Apply genetic operators, such as crossover and/or mutation, to parents to generate offspring, which form the next generation.

3.2.3. The Evolution of Architectures

The architecture of an ANN includes its topological structure (connectivity, and the transfer function of each node in the ANN). Architecture design is crucial in the successful application of ANNs because the architecture has significant impact on a network's information processing capabilities.

Like in the evolution of connection weights, two major phases involved in the evolution of architectures are the genotype representation scheme of architectures and the EA used to evolve ANN architectures. Encoding an ANN architecture implies deciding how much information about this architecture should be encoded in the chromosome. At one extreme, all the details, i.e., every connection and node of an architecture can be specified by the chromosome; this kind of representation scheme is called *direct encoding*. At the other extreme, only the most important parameters of an architecture, such as the number of hidden layers and hidden nodes in each layer are encoded; more details about the architecture are left to the training process to decide; this kind of representation scheme is called *indirect encoding*. The indirect encoding is used in order to reduce the length of the genotypical representation of architectures.

After a representation scheme has been chosen, the evolution of architectures can progress according to the cycle shown hereafter; the cycle stops when a satisfactory ANN is found [32].

(1) Decode each individual in the current generation into an architecture. If the indirect encoding scheme is used, further detail of the architecture is specified by some developmental rules or a training process.
(2) Train each ANN with the decoded architecture by a predefined learning rule (some parameters of the learning rule could be evolved during training) starting from different sets of random initial connection weights and, if any, learning rule parameters.
(3) Compute the fitness of each individual (encoded architecture) according to the above training result and other performance criteria such as the complexity of the architecture.
(4) Select parents from the current generation based on their fitness.
(5) Apply search operators to the parents and generate offspring which form the next generation.

An example of the direct encoding of a feedback ANN is the following (Figure 4) :

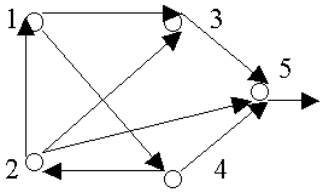

architecture

0 0 1 1 0
1 0 1 0 1
0 0 0 0 1
0 1 0 0 1
0 0 0 0 0

connectivity matrix

Figure 4.

00110 10101 00001 01001 00000

binary representation

3.2.4. The Evolution of Learning Rules

Designing an efficient learning rule is very difficult when there is little prior knowledge about the ANN's architecture, which is often the case in practice. Besides, what is often expected from an ANN is its ability to adjust its learning rule adaptively according to the task to be performed and also to its architecture. These two reasons, and certainly several others, let the evolution of learning rules be introduced into ANNs in order to learn their learning rules.

But, as the evolution of learning rules has to work on the dynamic behavior of an ANN, then one key issue is how to encode the dynamic behavior of a learning rule into static chromosomes. The answer to this requires the two following assumptions :
(i) Weight-updating depends only on local information such as the current connection weight, the activation of the input node, the activation of the output node, etc;
(ii) The learning rule in an ANN is the same for all its connections.

Thus, a learning rule can be expressed by the function [9'] :

$$\Delta w(t) = \sum_{k=1}^{n} \sum_{i_1, i_2, \ldots, i_k=1}^{n} \left(\theta_{i_1, i_2, \ldots, i_k} \prod_{j=1}^{k} x_{i_j}(t-1) \right) \qquad (18)$$

where t is the time, $\Delta w(t)$ is the weight change, x_1 , x_2 , … , x_n are local variables, and the θ's are real-valued coefficients witch will be determined by evolution.
In this way, the evolution of learning rules amounts to the evolution of real-valued vectors of θ's.

On the other hand, the evolution of learning rules raises three questions [32] :
(i) determination of a subset of terms described in Eq. (18) ;
(ii) representation of their coefficients as chromosomes;
(iii) the EA used to evolve these chromosomes.

The answers to these issues lead to the following cycle of the evolution of learning rules [32] :

(1) Decode each individual in the current generation into a learning rule.
(2) Construct a set of ANNs with randomly generated architectures and initial connection weights, and train them using the decoded learning rule.

(3) Compute the fitness of each individual (encoded learning rule) according to the average training result.
(4) Select parents from the current generation according to their fitness.
(5) Apply genetic operators to the parents and generate offspring which form the next generation.

3.2.5. Conclusion

Thus, evolution can be used in ANNs at several levels. The evolution of connection weights is quite competitive with regard to the gradient-based training algorithms. It can be also used to find quickly an efficient architecture as well as an efficient learning rule according to some architecture and to the task to be performed.

Furthermore, as it was noticed in [32], in many practical problems, the possible inputs to an ANN can be quite large. (There may be some redundancy among different inputs; a large number of inputs to an ANN increase its size and thus require more training data and longer training times). Preprocessing is often needed to reduce the number of inputs to an ANN. Given a large set of potential inputs, finding a subset, which has the fewest number of features but the performance of the ANN using this subset is no worse than that of the ANN using the whole input set, is not trivial. However, this problem can be implemented using a binary chromosome whose length is the same as the total number of input features; each bit in the chromosome corresponds to a feature : "1" indicates presence of a feature, while "0" indicates absence of the feature. The evaluation of an individual is carried out by training an ANN with these inputs and using the result to calculate its fitness value.

References

[1] W.S. McCulloch, W.A. Pitts, Bull. Math. Biophys. 5, 115, (1943).
[2] D. Hebb, *Organization of Behaviour*, Wiley, N.Y. (1949).
[3] F. Rosenblatt, *Principles of Neurodynamics : Perceptrons and the Theory of the Brain Mechanisms*, Spartan Books, Washington D.C. (1961).
[4] B. Widrow, In *Self-Organizing Systems 1962*, ed. by M. Yovits, G. Jacobi, G. Goldstein, Spartan Books, Washington D.C., 435, (1962).
[5] D.E. Rumelhart, G.E. Hinton, R.J. Williams, *Learning internal representations by error propagation*, in Parallel Distributed Processing, D. E. Rumelhart and J.L. McClelland eds, Vol. 1, *chap. 8,* MIT Press, Cambridge, MA, 318-362, (1986).
[6] T. Poggio, F. Girosi, Science 247, 978, (1982).
[7] J. Hopfield, Proc. Natl. Acad. Sci. USA 79, 2554, (1982).
[8] D. Ackley, G. Hinton, T. Sejnowski, Cognitive Science 9, p 147, (1985).
[9] R. Didday, Math. Biosci. 30, 169, (1976).
[10] S. Amari, M.A. Arbib, In Systems Neuroscience, ed. by J. Metzler, Academic N.Y., p 119, (1977)
[11] G. Carpenter, S. Grossberg, Computer 21, 77, (1988).
[12] G. Carpenter, S. Grossberg, Neural Networks 3, 129, (1990).
[13] T. Kohonen, Neural Networks 1, 3, (1988).
[14] T. Kohonen, *Self-Organizing Maps*, 2nd ed. Springer-Verlag, (1997).
[15] T. Kohonen, Neural Networks 6, 895, (1993).
[16] T. Kohonen, IEEE Trans. C-21, 353, (1972).
[17] K. Nakano, J. Nagumo, in Advance Papers, 2nd Int. Joint Conf. On Artificial Intelligence (The British Computer Society, London, UK 1971) p 101.
[18] J. Anderson, Math. Biosci. 14, 197, (1972).
[19] E. Oja, J. Math. Biol. 15, 267, (1982).
[20] F. Corbett, *Web Applets for Interactive Tutorials on Artificial Neural Learning,* Computer Engineering, University of Manitoba, Canada.
[21] B. Fritzke, *Some competitive Learning methods, Self-organizing Feature Map,*

http://www.neuroinformatik.ruhr-uni-bochum.de
[22] S. W. Kuffler, J. C. Nicholls, *From Neuron to Brain : A cellular approach to the Function of the Nervous System,* Sinauer Associates Inc. Publishers, (1976).
[23] P. Baldi, S. Brunak, *Bioinformatic, The machine learning approach*, MIT Press, (1998).
[24] J. M. Renders, *Algorithmes génétiques et réseaux de neurones*, Hermes, (1995).
[25] H.-P. Schwefel, *Numerical Optimization of Computer Models*, J. Wiley & Sons, (1981).
[26] H.-P. Schwefel, *Evolution and Optimum Seeking,* J. Wiley & Sons, (1995).
[27] L. J. Fogel, A. J. Owens, M. J. Walsh, *Artificial Intelligence Through Simulated Evolution*, J. Wiley & Sons, (1966).
[28] D. B. Fogel, *System Identification Through Simulated Evolution: A Machine Learning Approach to Modeling*, Ginn Press, (1991).
[29] D. B. Fogel, *Evolutionary Computation: Towards a New Philosophy of Machine Intelligence*, IEEE Press, (1995).
[30] J. H. Holland, *Adaptation in Natural and Artificial Systems*, The University of Michigan Press, (1975).
[31] D. E. Goldberg, *Genetic Algorithms in Search, Optimization, and Machine Learning*, Addison-Wesley, (1989).
[32] X. Yao, *Evolving Artificial Neural Networks*, Proceedings of the IEEE, 87 (9), 1423-1447, (1999).
[33] X. Yao, *Evolutionary artificial neural networks*, in Encyclopedia of Computer Science and Technology (A. Kent and J. G. Williams, eds.), vol. 33, 137-170, NY 10016 : M. Dekker Inc., (1995).